Lloyd Harold
03-16 70

United States Department of Agriculture

A.R.S. & S.C.S.

Watershed Modeling Workshop

March 16, 17 & 18, 1970

Tucson, Arizona

Pt. II


United States
Department of
Agriculture
NATIONAL
AGRICULTURAL
LIBRARY
Advancing Access to
Global Information for
Agriculture

WATERSHEDS AND HYDROLOGIC MODELS IN THE SOUTHEAST[1]

John C. Stephens[2]

INTRODUCTION

Watershed hydrology research in the Southern Branch is focalized at the Southeast Watershed Research Center (SEWRC), Athens, Ga. This Center was authorized by Congress in October 1965. Its general mission is to identify and characterize the elements that control the flow and quality of water from agricultural watersheds in the southeast.

Our specific mission is to provide research information to support the Department's operation programs in watershed engineering, as carried out principally by the Soil Conservation Service. We knew that it was the wish of the Soil Conservation Service, and we believed it was the intent of Congress, for us to direct our first studies to the Southern Coastal Plains region. Studies toward this end are now being conducted on experimental watersheds as shown in figure 1. All are in the coastal plains and so located as to give a fair sampling of physical conditions in this large region. The upper Little River watershed near Tifton, Ga. is the major research watershed, and additional watersheds in Florida and North Carolina are considered to be satellites of the Center. The research watersheds in Mississippi, under study by the USDA Sedimental Laboratory, are discussed in a separate presentation. Data from Hurricane Creek watershed in south Georgia, obtained from a SCS evaluation study, have been analyzed by the Center.

1/ Contribution from the Southern Branch, Soil and Water Conservation Research Division, Agricultural Research Service, USDA. For presentation at the ARS-SCS Workshop on Watershed Modeling; Tucson, Ariz. March 16-19, 1970.

2/ Research Investigations Leader, Watershed Engineering, and Director, Southeast Watershed Research Center, ARS-SWC, Athens, Ga.

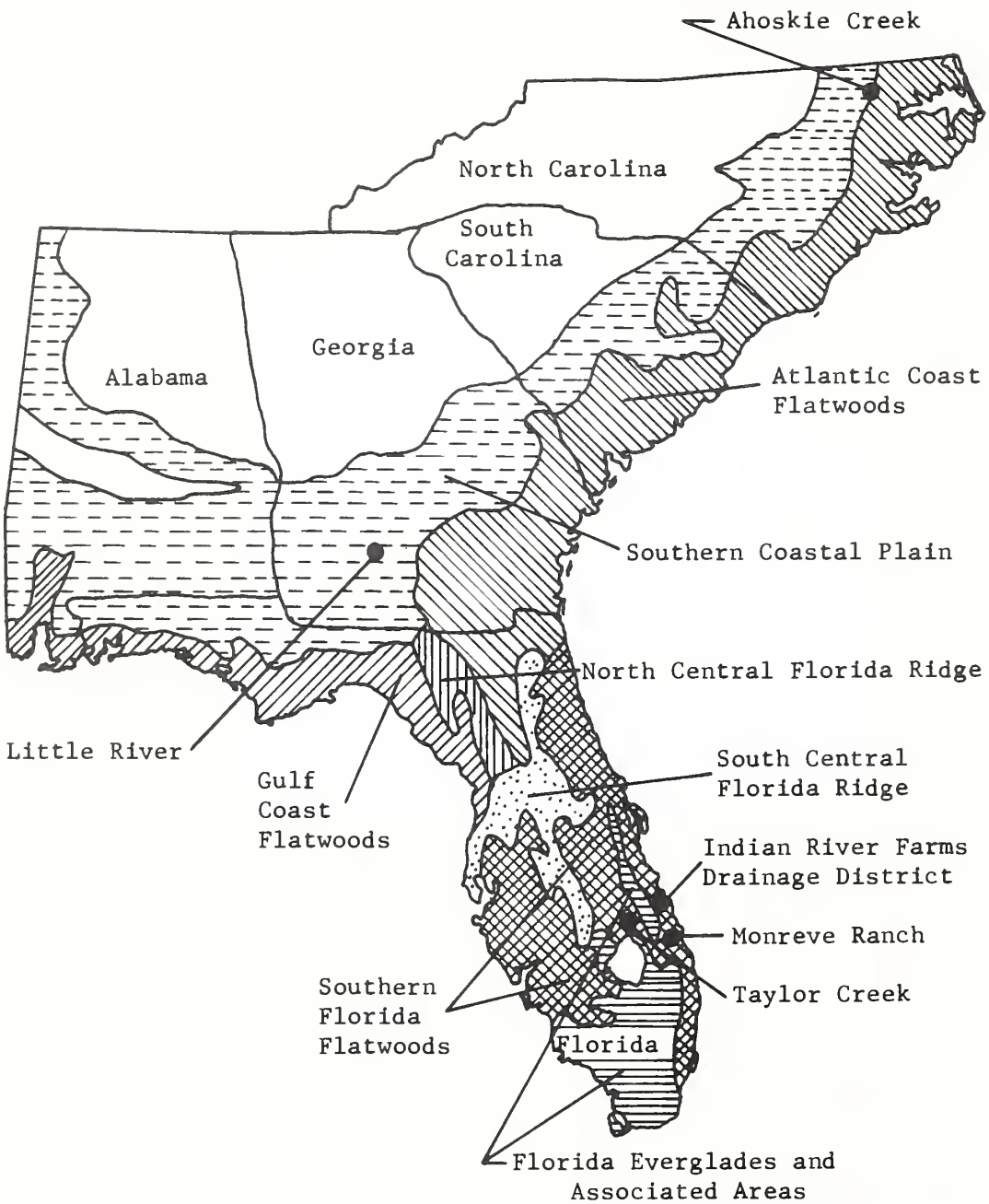

Figure 1. Location of experimental watersheds in relation to major land resource areas.

WATERSHED DESCRIPTIONS

Little River Experimental Watershed

This watershed, near Tifton, Georgia, was chosen because it is well suited to yield data for a regional hydrologic research program. Although no watershed is entirely typical of the Southern Coastal Plains Land Resource Area, this one is fairly representative of a large area. It presents a good example of coastal plains farming practices. Soils, geology, and land use are reasonably alike, yet offer some variations. Also, the stream system allows flow measurements to be made at reasonable cost, and the loss of surface water to deep seepage is relatively insignificant. Present instrumentation is directed toward studies in the broad area of precipitation, runoff, hydrogeology, and water balance.

Precipitation

Precipitation is measured with a network of 55 Fischer-Porter digital raingages. Each gage has an electronic timer and punches out accumulative rainfall at 5-minute intervals. Gages are spaced 1½ miles center-to-center on the upper 20-square-mile basin and a 3-square mile urban watershed. Gages in the remaining portion of the watershed are spaced on 3-mile centers.

The gages have been operating for a little over two years. Electronic data processing techniques for compiling this mass of rainfall information in usable form have just been completed. A more detailed description of the precipitation studies will be released in another ARS 41 publication.

Runoff Measurement

Eighteen streamflow measuring sites have been selected for instrumentation. Streams flow through the area in such a manner that runoff can be measured in parallel and in tandem. Drainage areas range from about 1 to 145 square miles. Watersheds are studied both individually and collectively.

Four of these sites, I, J, K, and M, were instrumented in 1967; two sites, F and O, in 1968; and U--an urban site--was completed, and approximately one-half of site B fin-

ished, in 1969. Site B, draining 125 square miles, is scheduled for completion in 1970. All stage recorders are the digital type with electronic times set for 5-minute punch-outs. The map, figure 2, shows the stream-flow and precipitation gaging stations.

Major construction at each site includes a broad-crested, 1 on 10 V-notch, concrete weir atop a sheet steel piling cutoff. Guide walls, a concrete protective apron, and a stilling well and recorder shelter combination set on wood piling complete the structure. A footbridge is provided for high-flow measurement.

Since weirs are submerged frequently in these low-gradient streams, both upstream and downstream stages are recorded to compute flow. The first analyses of stage-discharge relationships, however, indicate that tailwater elevations are so closely dependent on headwater flow that upstream stage alone may be used to determine discharge, even under considerable submergence--at least, for flows encountered to date.

Urban Hydrology

A 3.2-square-mile watershed, adjacent to the northwest urban limits of Tifton, which is changing from agricultural to urban use, was instrumented in late 1969 for intensive study. With the rapid increase, region-wide, in conversion of land from agricultural to urban development, it is apparent that there is a corresponding increase in the need for information on the effects of urbanization on the hydrologic behavior of a watershed.

Ahoskie Creek Experimental Watershed

One of the satellite watersheds under study is a 57-square-mile drainage area near Ahoskie, North Carolina. These studies are cooperative with the N.C. Division of Water Resources, University of North Carolina, State Agricultural Experiment Station, and Soil Conservation Service.

Ten raingages have been in operation since July 1964. Four streamgaging sites measure runoff from drainage areas ranging from 2.6 to 57 square miles. Stage recorders are operated by the U. S. Geological Survey under arrangements with SCS--an example of cooperative activities by different agencies.

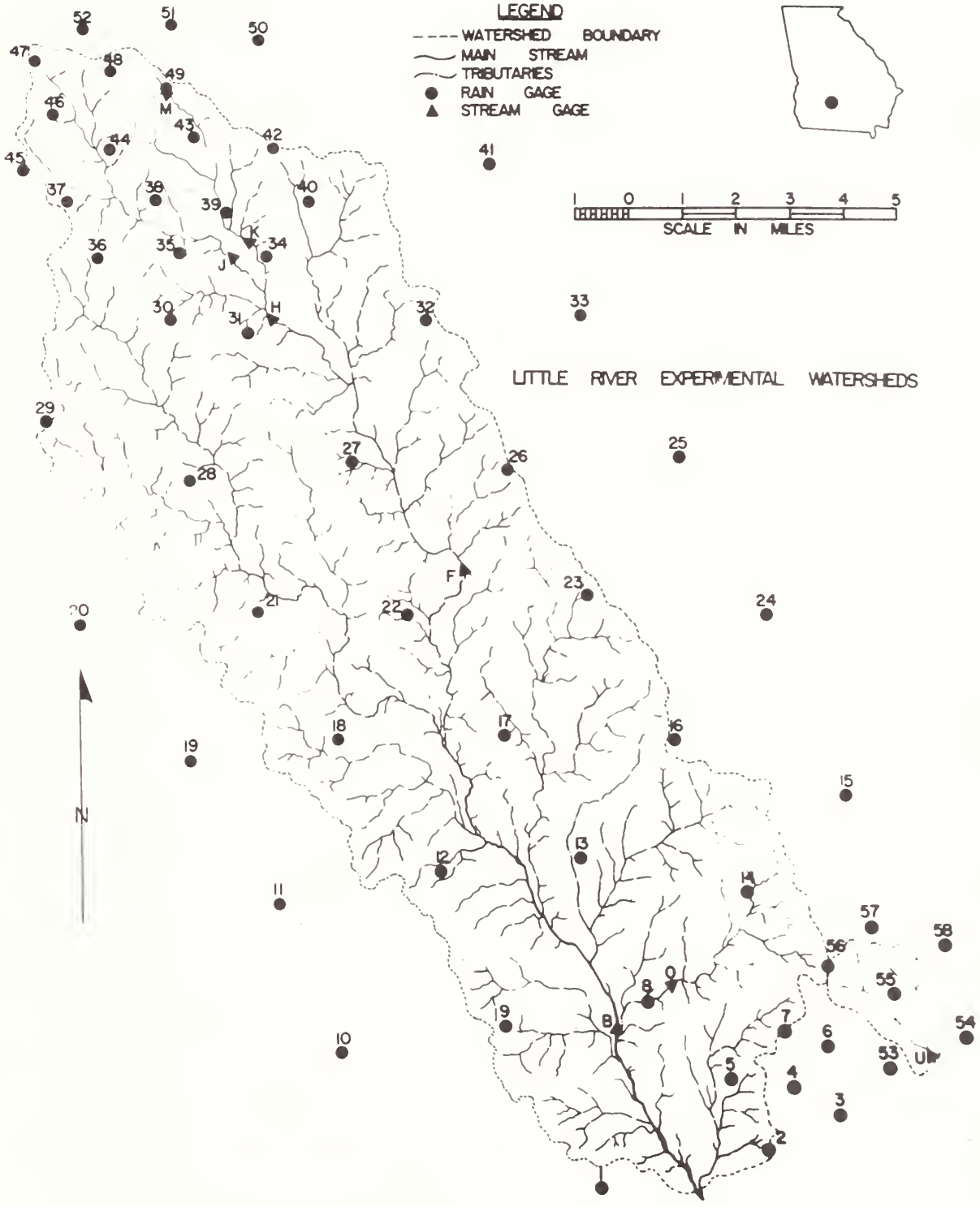

Figure 2. Little River experimental watershed, showing stream flow and precipitation gaging stations in 1970.

Also, eight groundwater wells have been installed and equipped with stage recorders. The Southeast Watershed Research Center began geological investigations on Ahoskie Creek in 1966. Electric logs were made on all wells.

Pigeon Roost Creek Watershed, Mississippi

Extensive studies have been underway for several years on the 117-square-mile Pigeon Roost Creek watershed near Oxford, Miss. Data are acquired by the USDA Sedimentation Laboratory, primarily in connection with sedimentation studies. However, the hydrologic records collected on this watershed will be analyzed later by the Southeast Watershed Research Center as needed to regionalize the studies. These studies are discussed in a separate workshop paper by A. J. Bowie.

Florida Watersheds

Precipitation and runoff are measured on three experimental watersheds in the Southern Florida Flatwoods Land Resource Area. In addition to rainfall and runoff studies, measurements are made of phreatic groundwater on the 98.7-square-mile Taylor Creek watershed, artesian heads on the 78-square-mile Indian River Farms Drainage District watershed, and irrigation water pumped into Monreve Ranch watershed from St. Lucie Canal. Records of other hydrologic data such as temperature and pan evaporation are also obtained.

Portions of this work are cooperative with the Weather Bureau, Soil Conservation Service, Federal Aviation Agency, and Central and Southern Florida Flood Control District.

Hurricane Creek, Georgia

Precipitation and discharge in the 150-square-mile Hurricane Creek basin, in the flatwoods of Georgia, were measured by the U. S. Geological Servey under agreement with the Soil Conservation Service for the period Oct. 1, 1956-Sept. 30, 1960. Other data germane to hydrologic studies have been obtained. These include maximum and minimum temperatures, pan evaporation, and solar radiation.

The North Carolina, Mississippi, and Florida experimental watersheds have been described in detail in other Department publications (1).

HYDROLOGIC MODELS OF WATERSHEDS

A prime purpose of experimental watersheds is to measure and evaluate the change in streamflow regimes caused by systematic variations in land use, or physical characteristics, or both. From a cause-and-effect study of experimental watersheds, one should then be able to predict the hydrologic response of ungaged watersheds; and, if necessary, transfer conclusions from small watersheds to complete river basins.

A successful method of attaining these objectives has been by analogy, or modeling. In watershed modeling one develops a mental picture of the anatomy of a watershed and how it functions. One's concept is naturally based on known physical laws and astute field observations. The magnitude of the forces that generate the hydrologic response of the watershed are then evaluated from the measured input-output values derived from the experimental studies. That is to say, empirical values are determined that can be substituted into one's conceptual analog, after the analog has been transformed by mathematical and modern-logic symbolism into a working model. This model can be manipulated to predict results.

Since models are born in the mind of the originator, usually by induction, and then amplified by observation and deductive reasoning, it should be apparent they are only substitutes for the real world. Models are of necessity limited by the designer's background and available information. In watershed hydrology they are an oversimplification of complex phenomena. Models, nevertheless, have resulted in some very successful methods of prediction. As long as their limitations are kept in mind--viz., they are not the real world--then models are possibly the most useful tool we have. But when any model, no matter how complex or efficient, is consistently used as a surrogate for the real world, the advance of our scientific knowledge will come to a halt.

As outlined by Bross (2), models have several advantages. They provide a reference frame for consideration of the problem, and they open up and clarify the problems of abstraction. The model-maker may thereby decide which real world attribute is to be incorporated into the model. For example, we may be interested only in peak flows and can than eliminate several complex, but relatively irrevalent,

parts of the system. Symbolic models also offer advantages in communications between scientists. They allow concise statements of the problem which can be published. And last, but not least, models frequently provide the cheapest way to predict satisfactory, but not necessarily precise, design criteria for watershed developments.

Bross also points out that models have drawbacks: "A mathematically feasible model may require gross oversimplification." There is no guarantee that a model that works well for one watershed will give satisfactory predictions for watersheds located in different land resource areas. In fact, the breakdown of models developed for the Piedmont region in predicting runoff results for the coastal plains region give considerable impetus to the establishment of the Southeast Watershed Research Center. Models are also subject to the limitations in symbolic language manipulation. But the gravest danger, as Bross emphasized, in the use of models is that . . . "some scientists become so devoted to their model (especially if it is a brain child) that they will insist that this model is the real world."

It should be remembered that a model is neither true nor false. The standard for comparing models is utility; i.e., successful prediction. Thus, models and mules are similar in that both are to be valued for what they can do, and not for their beauty. At least that's the way mules were valued on Alabama farms during my generation. And, for my money, the simplest model that will do the job required is preferred to a more sophisticated model of intellectual beauty.

One more bit of philosophy concerning the role of models--again from Bross--is that great imagination and insight are required for the creation of models, but this is only half of the story. "The mere creation of models is not enough; they must survive exacting tests, they must meet the pragmatic criterion, they must work. This brings us back to data. The test of the model involves data from the real world; without adequate data the construction of models is a mathematical pastime. . . . progress in science is based on this constant interplay between model and data."

The ideal situation in watershed research, it seems to me, will be attained by a judicious balancing between the two

processes, model-making and data collection. It should be borne in mind that good models will be displaced by better models, but, in the words of Karl Terzazhi, . . . "The results of conscientious observations in the field will remain as a permanent asset of inestimable value to the profession." Thus we can defend experimental watersheds that derive data from the real world against the academicians who depend primarily upon the output from sophisticated models.

RESEARCH CENTER WATERSHED MODELS

A basic concept for our watershed models is that for infinite time,

$$\text{inflow} = \text{outflow}$$

and for finite time,

$$\text{inflow} = \text{outflow} \pm \text{storage change}.$$

For relatively long time intervals the storage changes are usually compensating and are ignored. As discrete time periods become shorter, the importance of considering storage changes becomes increasingly significant in predictions.

The general form for the water balance equation is usually:

$$Q = P - E \pm \Delta S - s$$

where Q = runoff
P = precipitation
E = evaporation
ΔS = storage change
s = seepage outflow

This equation is an oversimplification, of course, and neglects such elements as condensation (dew), as well as possible inflow from outside the basin. Also, for other than long-term evaluations, subset equations to compute ΔS for surface water, soil moisture in the phreatic zone, and groundwater must be evaluated separately for usable predictions.

The schematic diagram we are using to provide a framework in considering hydrologic problems of Southern Coastal Plains watersheds is shown in figure 3. This diagram is similar to the one prepared by the Northwest Watershed Research Center,

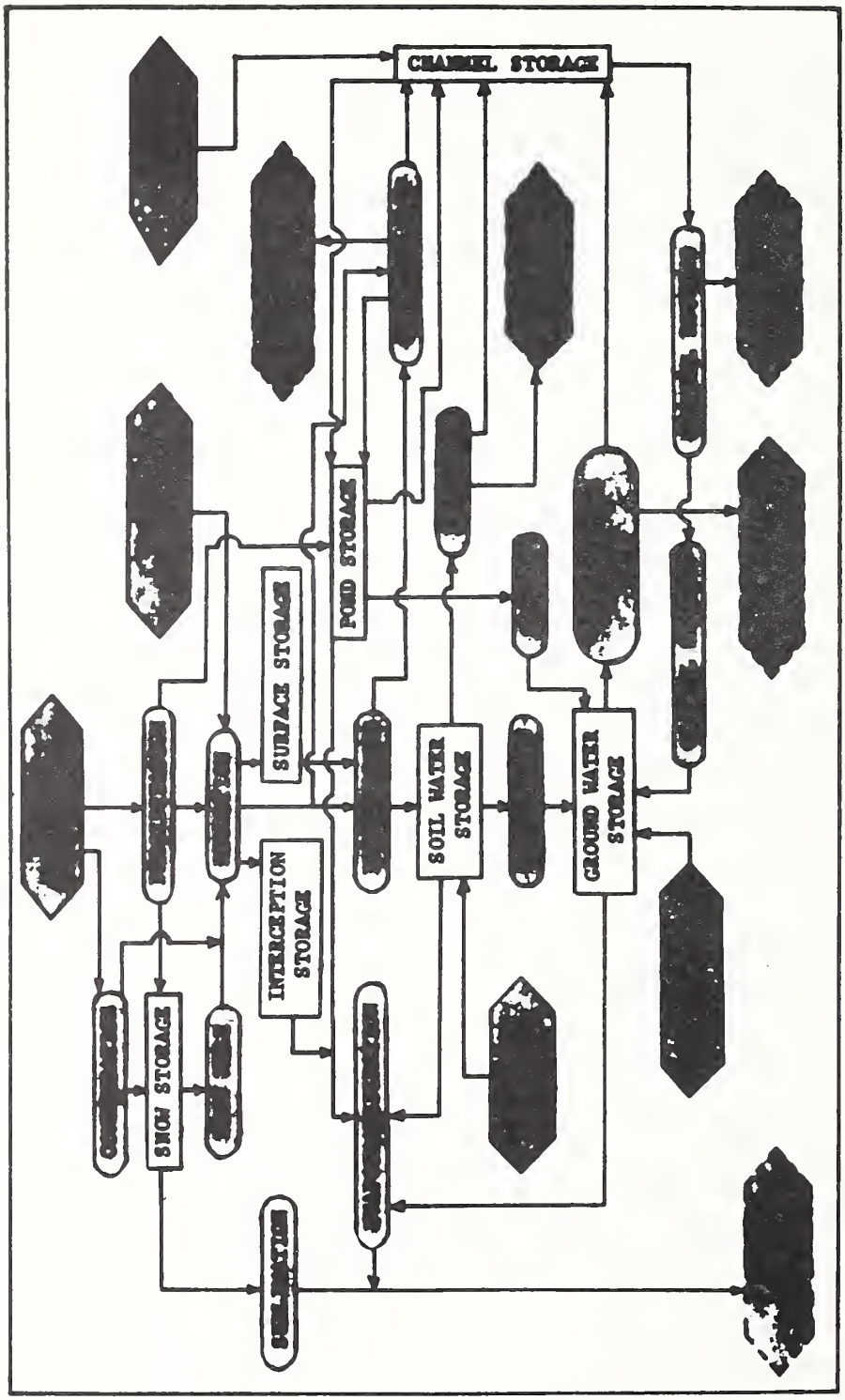

Figure 3. Schematic diagram, or verbal model, of the water balance for coastal plains basins.

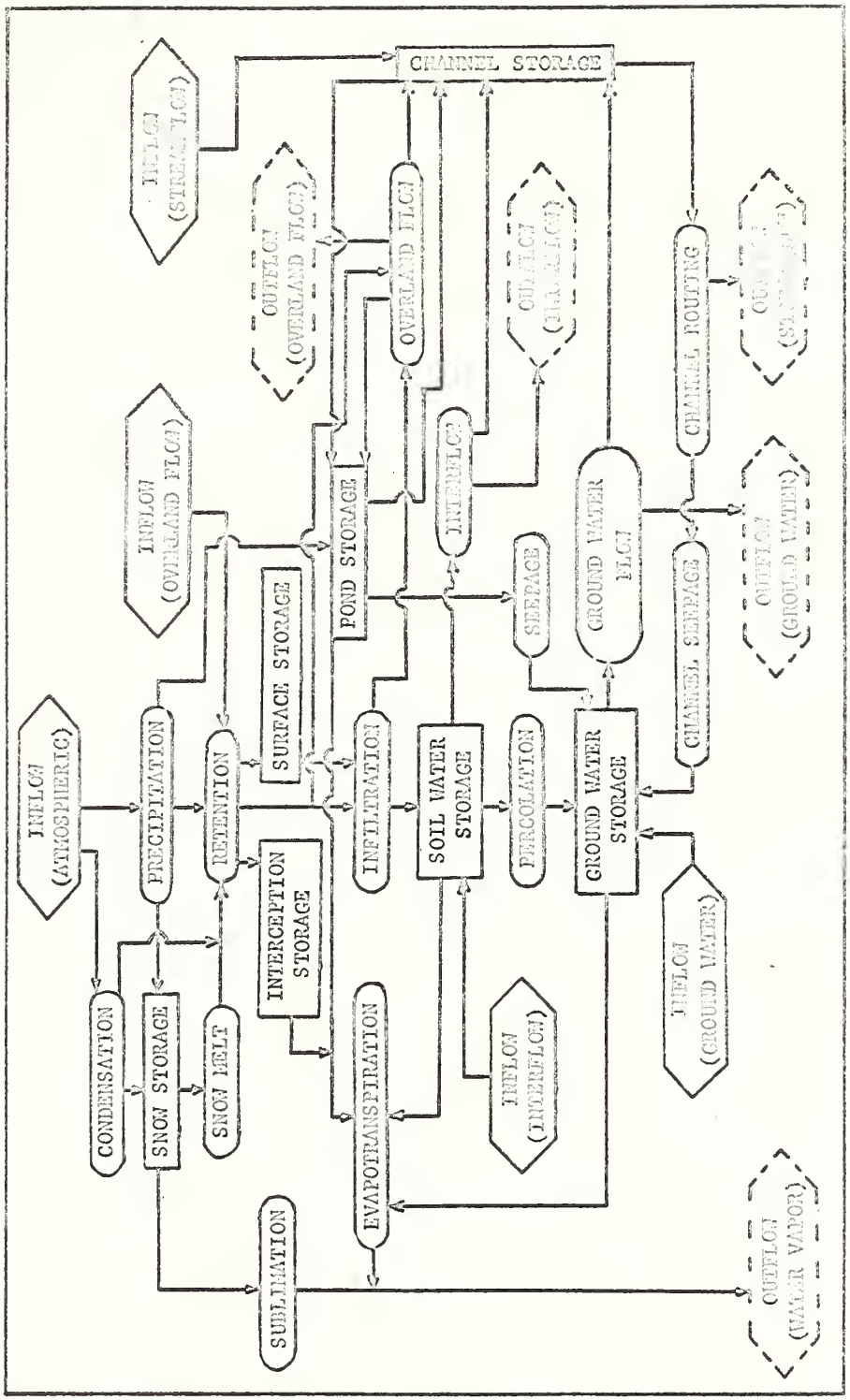

Figure 3. Schematic diagram, or verbal model, of the water balance for coastal plains basins.

but has been slightly modified to better suit our regional conditions.

This somewhat complex model is still an abbreviated simulation of the hydrologic processes that take place in actual watersheds. For example, the feedbacks, trade-offs, and other interplays that take place between the factors shown are seldom linear. As yet, we don't know how to handle them. And even if we did, the difficulty and expense in the mathematical manipulation might not be worth the effort. This was certainly the case in the past when we were compelled to use mechanical methods to capture, process, and analyze data. But with the advent of electronic gadgets to capture the information in the field, and EDP machines to put out reams of mathematical computations, we feel we are justified in taking a non-linear approach, as discussed by Snyder in "The Parametric Approach to Watershed Modeling."

Fortunately, for many practical purposes, we are able to abstract only a few of the properties or elements from the subject model, and concentrate our attention on some of the simpler phenomena that can be used to predict results that are usable and significantly accurate. In other words, while not elegant, they work.

For classification purposes I have arbitrarily divided schemes for predicting the runoff regime into two classes: peak rates and water yields. For further simplication, peak rates are considered to be flows that do not exceed 24 hours.

Peak Rate Predictions

Literally scores of emperical formulas have been developed in the past century to estimate peak discharges from relatively small drainage basins. The Handbook of Culvert and Drainage Practice (3) lists 20 empirical formulas, designed to estimate discharge capacities for small channels. These are applicable only to the particular localities for which they were developed. Most of the formulas have the general form (4):

$$q = CAI\left(\frac{S}{A}\right)^{x}$$

where q is peak discharge in cfs, C is a coefficient, depending on climate and watershed conditions, A is drainage area in acres, I is average rainfall intensity in inches/

hours, S is the slope of the drainage basin in ft./1,000 ft., and x an exponent. While these formulas are models and involve cause-and-effect relations, the results attained are markedly effected by subjective choices of the coefficients selected by the user. Since they were developed for small drainage areas and, in addition, are subject to personal bias, they are not considered especially suitable for evaluation by the Research Center.

Stochastic Models

To obtain objective design flows, a stochastic approach has been used. Such methods leave much to be desired since samples are usually too small to give a high degree of confidence. The actual probability distribution of sampled events is not known, which really requires use of Chebyshev's theorm to guarantee that the accuracy bounds on the percent of measurements will be within standard deviations of the average. Also, there's no assurance that past watershed conditions will be representative of the future. Because of their objectivity, however, we have used them to estimate design flows in combination with other models. Each then serves as a check on the other, and if they are reasonably close in predicting peak flows, we then feel more secure in our design estimates.

For example, in estimating the design flows for gaging stations in Little River experimental watershed, a combination of flood frequency curves from coastal plain streams, which appeared to be similar to streams within the experimental watershed, and the values obtained by the Cypress Creek formula were used. First, flood frequency curves for four gage sites were prepared using the SCS adaptation of the Hazen method. The second step involved the preparation of curves of "C" values in the Cypress Creek equation versus return periods, as described by the writer and Mills in ARS 41-95 (5). The third step was to reduce the flood frequency return values from the four watersheds of various size to a common base for comparison. This was done by using the basic Cypress Creek equation:

$$C = \frac{q}{A5/6}$$

where q = discharge rate, cu.ft./second
C = a coefficient (representing discharge rate for one square mile)
A = drainage area, sq. miles.

All values were then plotted on a probability graph showing the values of C versus flood return periods, as shown in figure 4. Since the structures were designed to optimize measurements up to the 25-year flood, with additional freeboard to pass the 100-year flood without structural damage, we felt safe in choosing a design value of C = 120 for the 25-year flood. Figure 4 shows that values of C for the 25-year return period ranged from about 98 to 120 for three of the watersheds. A low value of 64 on the fourth watershed was ignored--largely because the geology indicated that deep seepage losses occurred from the Big Indian Creek watershed. The Cypress Creek model indicated a mean C value of 100. The selected value of 120 is approximately one standard deviation above the mean value given by the Cypress Creek model.

Regional flood frequency model.--Essentially the regional flood frequency method, developed by the USGS, applies statistical theory to past flood records of selected stream basins to define: (a) curves relating the mean annual ($Q_{2.33}$) index flood to basin characteristics, and (b) composite curves relating discharge, expressed as a dimensionless ratio, to other recurrence intervals for streams in certain areas. That is, specific stream records are grouped together and generalized to represent the flood regime for broad related hydrologic areas. These areas are defined on a broadscale pattern and are generally related to major physiographic provinces and land resource areas. It is not uncommon, however, for them to cut across the lesser geomorphological units.

This method has the disadvantage of all stochastic models, but since it combines a large number of flow records it is usually statistically better than single stream records; especially for estimating peak flows from ungaged streams in an analogous hydrologic area. These data are published for the Southeast in a number of water supply papers (6, 7, 8). For the coastal plains the number of records available from small watersheds is relatively few and the quality poor, so that we use this procedure mostly as a check on predictions derived from other models.

Cypress Creek Model

One model of flood peak relationships is expressed by the equation:

$$q = C' \cdot A^{x} \cdot B^{y} \cdot C^{z} \ldots N^{n}$$

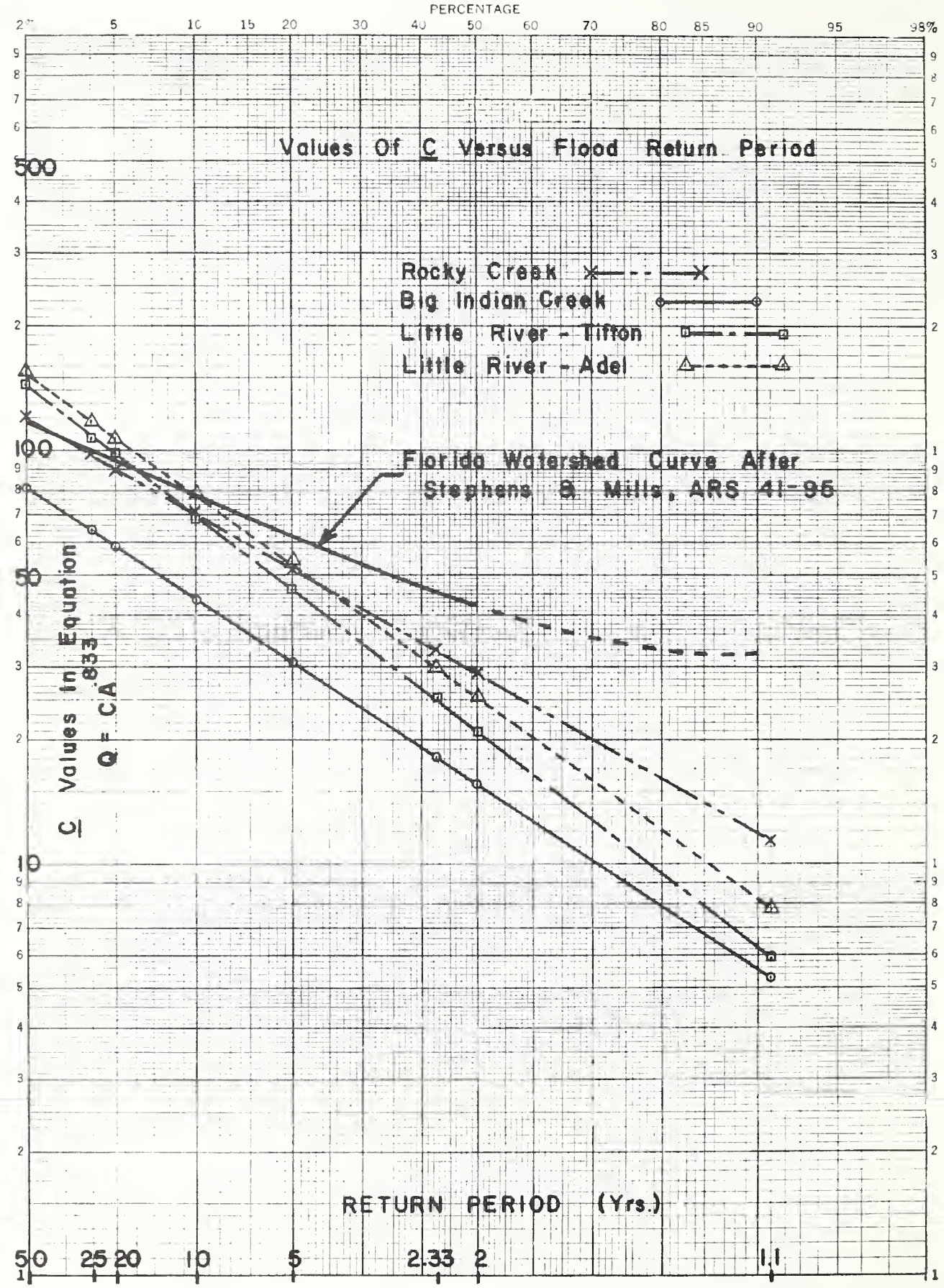
PERCENTAGE
2% 5 10 15 20 30 40 50 60 70 80 85 90 95 98%
Values Of C Versus Flood Return Period
Rocky Creek
Big Indian Creek
Little River - Tifton
Little River - Adel
Florida Watershed Curve After
Stephens & Mills, ARS 41-95
C Values in Equation
Q = CA^.833
500
100
50
10
RETURN PERIOD (Yrs.)
50 25 20 10 5 2.33 2 1.1

where q is peak flow rate, C' a coefficient depending upon return frequency, and A, B, C ... N are measurable characteristics of the basin, and where the effects of the basin characteristics are the exponents x, y, z ... n.

The dominant, and often the only readily obtainable, basin characteristic is size. In this case the flood-flow equation may be expressed as $q = CM^x$. This equation is similar to the Cypress Creek formula, $q = CM^{5/6}$, where q is the average runoff rate in cubic feet per second for the 24-hour period of greatest runoff for a storm event; M is drainge area in square miles; and C is a coefficient based on rainfall frequency and topography. To use the general equation, $q = CM^x$, however, values must be determined for the exponent x and the coefficient C.

To establish M^x relations, the equation $q = CM^x$ was analyzed graphically by plotting on logarithmic paper maximum 24-hour average runoff rates against watershed areas for the 10 maximum annual storms of record for watershed W-1 (1951-60) and the 5 maximum annual storms for watersheds W-2 and W-3 (1956-60).

The following resultant equations were obtained:

$$q = 131\ M^{0.83}$$
$$q = 115\ M^{0.79}$$
$$q = 97\ M^{0.63}$$

which corresponded to storms of about 50-, 10-, and 2-year frequencies, respectively. Most of these storms lasted about 24 hours. The best fit of the regression line was $q = 131\ M^{0.83}$. Although the exponents decreased for smaller storms, the exponent 5/6 (0.83) will produce safe design values and we recommend its use.

Values of the coefficient C in the Cypress Creek formula were then computed from annual maximum 24-hour average runoff rates for the three watersheds using the formula, $C = q/M^{5/6}$.

Figure 5 shows these C values plotted as functions of excess rainfall for all major storms. Based on 20 runoff events, and computed by the method of least squares, the regression equation is $C = 16.39 + 14.75\ Pe$, where Pe is excess rainfall (inches) for the individual storm

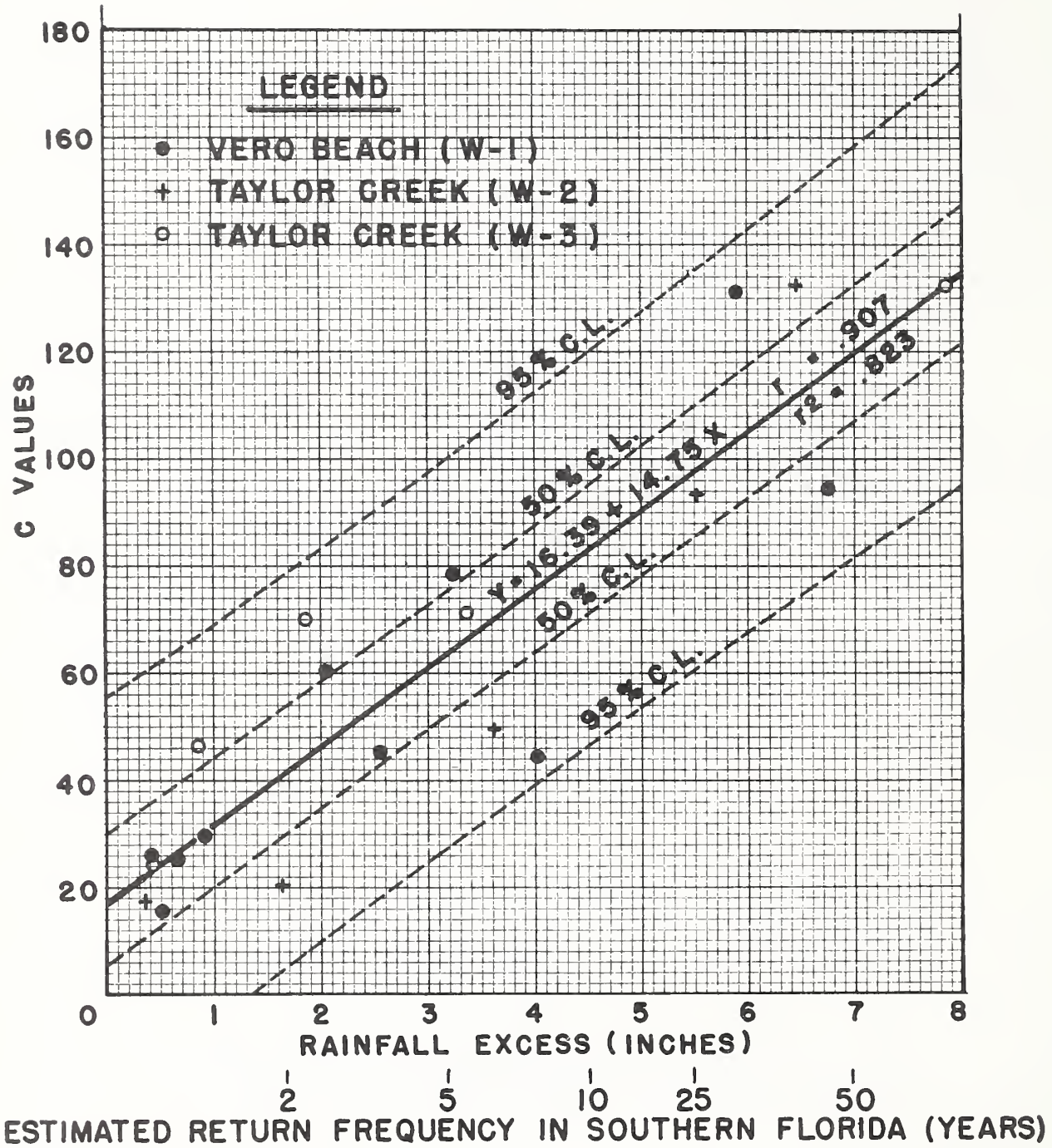

Figure 5. Values of C in the Cypress Creek formula $a = CM^{5/6}$ versus excess rainfall for three experimental watersheds in southern Florida.

periods. The correlation coefficient r, the coefficient of determination r^2, and the 50- and 95-percent confidence limits were computed and are shown in figure 5.

To determine these values from experimental watershed data, we first had to obtain rainfall excess amounts for storm events on the watersheds before we could get satisfactory relationships between rainfall and runoff. The moisture budget method was applied to the 30-day period prior to each storm event to obtain these amounts.

In this method the water table was assumed to be at ground surface with 5 inches of evaporable water in storage 30 days prior to storm runoff. Though not strictly true, error in this assumption was usually negligible over a 30-day period. Storm rainfall excess was obtained by subtracting the computed water storage available in the soil at the beginning of the storm event from the total measured storm rainfall. Infiltration rates were not limiting.

The estimated return frequency of excess rainfall was derived from the relation of excess rainfall to total storm rainfall, and the statistical frequency of the latter. These excess rainfall frequencies are essentially the return frequencies of 24-hour rainfall amounts, minus about 3 inches for soil storage.

Instantaneous peak versus 24-hour-average flows.--The Cypress Creek formula estimates 24-hour-average maximum flows and is used primarily for design of drainage works. For design of bridges, spillways, and other structures, one needs to estimate instantaneous peaks.

The amount the instantaneous peak-flow rate exceeds the maximum 24-hour-average flow rate depends on watershed size and storm intensity. For large watersheds and high-volume storms the two rates differ little, but the spread is larger as watershed size and 24-hour storm intensities decrease. The effect of watershed size for the four south Florida experimental watersheds, ranging from 6 to 98 sq. miles in area, is given by the equation, $q_i/q_{24} = 2.11 \otimes A^{-0.135}$, where q_i/q_{24} is the ratio of the instantaneous flood peak to maximum 24-hour-average runoff rate, and A is drainage area in square miles. Thus, the ratio, q_i/q_{24}, is 2.11, 1.55, and 1.14 for basins of 1, 10, and 100 square miles in area, respectively.

Unit Hydrograph Models

A commonly used model for estimating storm runoff is the unit hydrograph. It was originally developed for use in hydrologic regions where surface runoff could ostensibly be separated from base flow and interflow by hydrograph inspection. The resultant surface-runoff graph was then modified to show the effect of fictitious uniform storm rainfall over the basin. The final resulting storm hydrograph was then linearly reduced along the y-axis (runoff rate)--holding the x-axis (time) constant--to show the runoff volume from 1 inch of so-called effective rainfall. By linear methods the storm hydrographs of similar type, but higher intensity, storms could be estimated. For example, if the 24-hour unit hydrograph shows a peak rate of 300 cfs, then an effective rainfall of 6 inches should give a peak rate of 1,800 cfs.

In spite of the simplicity of the model and the fact that it is not mathematically consistent, the unit hydrograph model has yielded satisfactory results in selected regions for many years. However, in the region of the Southern Coastal Plains it is extremely difficult to separate surface runoff from interflow and base flow. It was, nevertheless, decided to try and develop unit hydrographs for southern Florida using data from the experimental watersheds.

Two runoff events, occurring on October 12-24, 1956 and June 17-26, 1959, on both watersheds W-1 and W-2, were selected. Primary considerations in selecting storm events were high rates of runoff and isolation from other rainfall events. Runoff for the Oct. 1956 event could be related to one 24-hour period of excess rainfall. Runoff hydrographs for the June 1959 event were altered slightly by subtracting hydrographs for small amounts of excess rainfall before and after the principal 24-hour excess rainfall period.

The development of these unit hydrographs required the extraction of base flows (slow flows) to obtain the runoff hydrographs of rapid and intermedial flow associated with the selected events. The average upper limits of base flow are 350 cfs for watershed W-1 and 333 cfs for W-2. Because the selected events were isolated from other rainfall events, flow rates at the beginning of the events were lower than these average limits. The

volume of base flow was obtained graphically by assuming the base flow rate increased uniformly from the beginning of the event until it reached the upper limit of base flow at the time of peak flow. This upper limit of base flow was then assumed to continue for the remainder of the hydrograph. All flow below the limit of base flow was subtracted from the storm runoff hydrograph. The flow volume remaining under the hydrograph was classified as rapid and intermedial runoff.

The unit hydrographs for watersheds W-1 and W-2 were constructed for both storms from the respective hydrographs of rapid and intermedial flow. The ordinates of the unit hydrograph (inches per hour) were proportioned according to the ratio of the unit hydrograph runoff volume (1 inch) to the rapid and intermedial runoff volume. The unit hydrographs for both storms were then graphically combined by averaging ordinates and smoothing curves to obtain a representative 24-hour unit hydrograph for each watershed. These unit hydrographs, shown in figure 6, can be used as runoff distribution graphs of excess rainfall on watersheds W-1 and W-2 for 24-hour storms.

Comparison of flows computed by the Cypress Creek model versus the unit hydrograph model.--As a check, flow rates computed by the Cypress Creek model were compared with those computed by the unit hydrograph models shown in figure 6.

Base flow was first added to the unit hydrograph models and then peak flow rates scaled by the q_i/q_{24} ratio to give proper correspondence between the two methods. Results for the 24-hour-maximum flow rates showing C values when basin size is adjusted according to the 5/6 power factor is:

Rainfall Excess (In.)	C Values: Cypress Creek Model	C Values: Unit Hydrograph Model for W-1	C Values: Unit Hydrograph Model for W-2
1	32.0	35.2	29.7
2	46.2	56.2	45.1
4	76.0	98.3	75.8
6	105.0	140.3	106.4

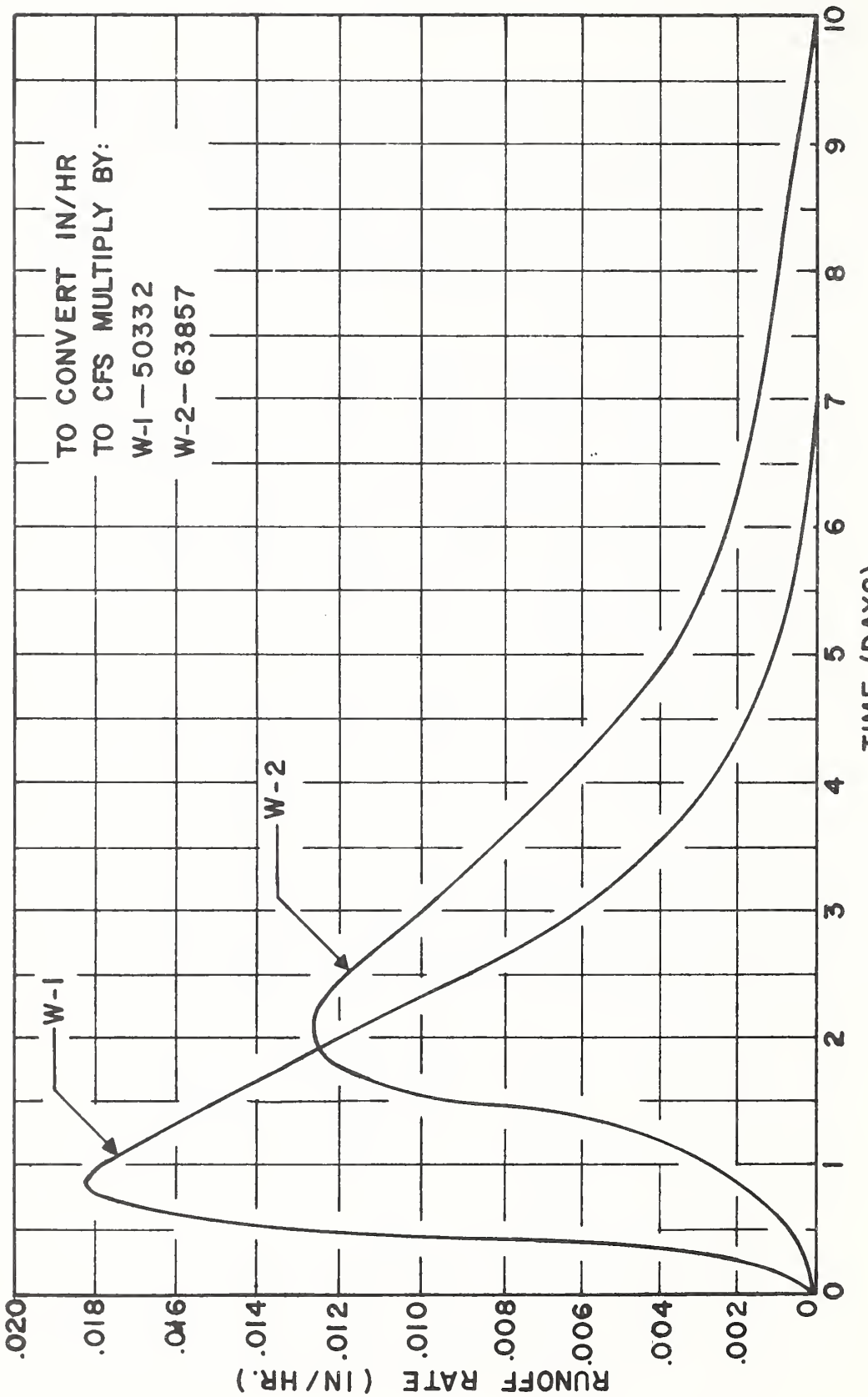

Figure 6. Twenty-four-hour unit hydrographs, watersheds W-1 and W-2. Each curve is the graphic average of two storms.

It is of interest to note that C values for W-2, the undeveloped watershed, are almost the same for both methods. Values of C for W-1, the watershed with a dense network of drainage channels, is somewhat higher than either. It is logical that peak flows should be higher for the better developed drainage system. However, when values of C for W-1 are subjected to statistical tests, or plotted on figure 5, it is found that they are not significantly different from the other two models at the 95% level, at least for return flood frequencies of less than 50 years.

The Cypress Creek model was developed from a greater number of events than the subject unit hydrographs, and also the coefficient of determination, r^2, indicates that basin size alone is associated with 82% of the variability in peak flows; therefore, at this time we still recommend use of the Cypress Creek model. One intuitively feels, however, when more data have been collected and analyzed, that differences in flood peaks will be significantly correlated with other watershed characteristics.

Non-linear Models

Most hydrologists admit that linear models do not represent the real world. Yet they have been used almost exclusively because of their simplicity and our ignorance of how to analyze data and express the findings in a non-linear form to better represent real world conditions.

As related by Willard Snyder in another paper at this workshop, the Southeast Watershed Research Center has made some progress in developing non-linear models. The basic concept is that small watersheds have inherent characteristics such as shape, soils, drainage systems, geology, etc., that are relatively invariant, which effect rainfall-runoff relations in a consistent manner. For watersheds this function is roughly triangular in graphic form. It has been termed the characteristic function. The watershed's runoff regime is further influenced by its wetness state, which includes groundwater, soil moisture, and channel conditions. The wetness state of the watershed has been termed the state function and varies with the parameter A as indicated by the equation,

$$f(t) = Ae^{-At}$$

where t is time and f(t) is the state function.

In the non-linear model the unit hydrograph is not held constant. It is generated for each element of effective rain (all rain that eventually contributes to streamflow). The term unit response is substituted for unit hydrograph, since no attempt is made to separate various types of flow such as overland runoff.

By convolution of the characteristic function with the state function, unit response functions are generated, which vary throughout the storm.

Verification of the non-linear model was tried by operating on ten selected storms by a computer program developed by Snyder, which performed the two-stage convolution and optimized parameters for the characteristic and state functions. In most cases the fit of the predicted storm hydrographs, computed by the non-linear technique, were close to the observed hydrographs.

One physical feature that would be expected to influence the derived characteristic functions is watershed size, since area under the function curve represents one inch of runoff. To eliminate this effect of watershed size, ordinates of the characteristic functions were divided by the respective watershed areas.

Characteristic functions derived from southeastern watersheds were compared visually. Although not exactly coincident, these curves for different storms on a watershed were found to be relatively similar for all watersheds, except NC W-A1. This similarity was especially evident when a comparison was made between characteristic functions for the different watersheds. There was much greater difference in the functions for different watersheds than for different storms on the same watershed, indicating that the characteristic function does reflect watershed physical characteristics as hypothesized.

Figure 7 is a comparison of the characteristic functions. These curves indicate very definitely that the Mississippi watershed is more flashy than the other watersheds. Also, two of the Ahoskie Creek watersheds seem to be slightly more flashy than the Florida watersheds.

Watershed NC W-A1, which is the one outstanding exception in regard to similarity of characteristic functions for different storms, is somewhat larger in size than the

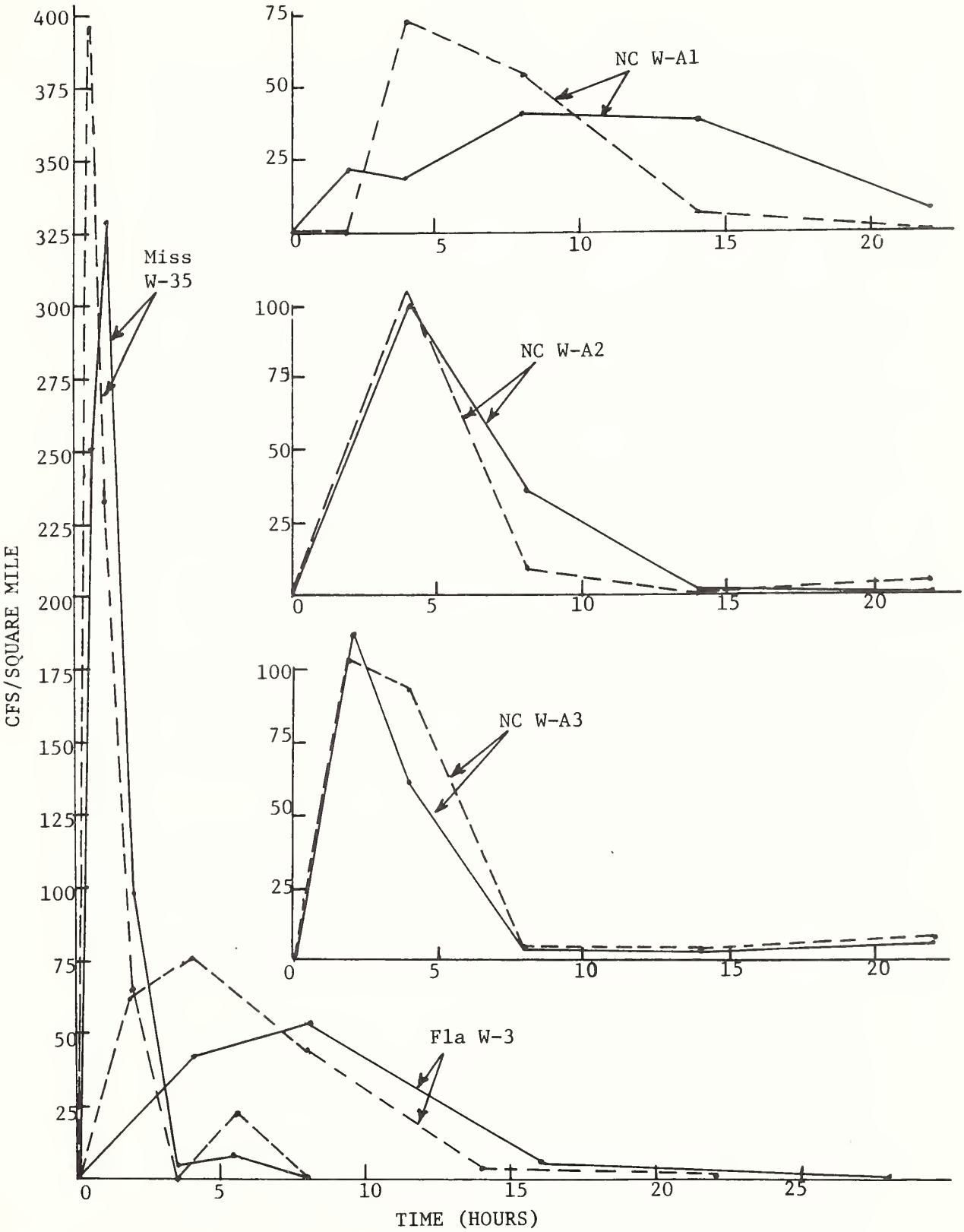

Figure 7. Comparison of characteristic functions derived from rainfall-runoff events that occurred on watersheds in the Southern Coastal Plains Province.

other watersheds. Thus, variation in contributing area for long and short duration storms may have caused the difference in characteristic functions. The long duration storm on this watershed caused a lower, more drawn-out characteristic function than the shorter duration storm. Although not as pronounced as with NC W-A1, this same relation seemed to be in evidence for the storms on the Florida and Mississippi watersheds where there was a significant difference in duration of storms compared. This would suggest that the drainage area varies for storms of different duration.

Interpretation of characteristic function shapes, contributing area, and watershed physical features should follow this preliminary work in development and testing of the two-stage convolution technique. This will involve more detailed investigations of watershed characteristics and application of the analysis technique to other watersheds and storm situations.

FOR PREDICTING WATER YIELDS

Annual Runoff

Linear Regression

Johnstone and Cross (9) describe three simple mathematical forms of the relationship of annual runoff as a function of annual precipitation. We have found the formula, $Q = b(P - a)$ to be the most suitable form to express the relationship for our watersheds.

This model--where Q is runoff, P is precipitation, b is percentage, and a is a constant in inches--is a straight line passing to the right of the origin and having a slope of less than 45°. This simple concept signifies that a relatively constant amount of rainfall will be lost to evaporation and seepage, and most of the remainder becomes runoff. It does, however, allow for the loss to increase with the precipitation.

Coefficients for this equation, and graphical results, have been compiled for our experimental watersheds, which have records long enough to be meaningful. The plotted results are almost a necessity in comprehending cause-and-effect relations between annual rainfall and runoff.

Figure 8 illustrates the technique for the Ahoskie Creek

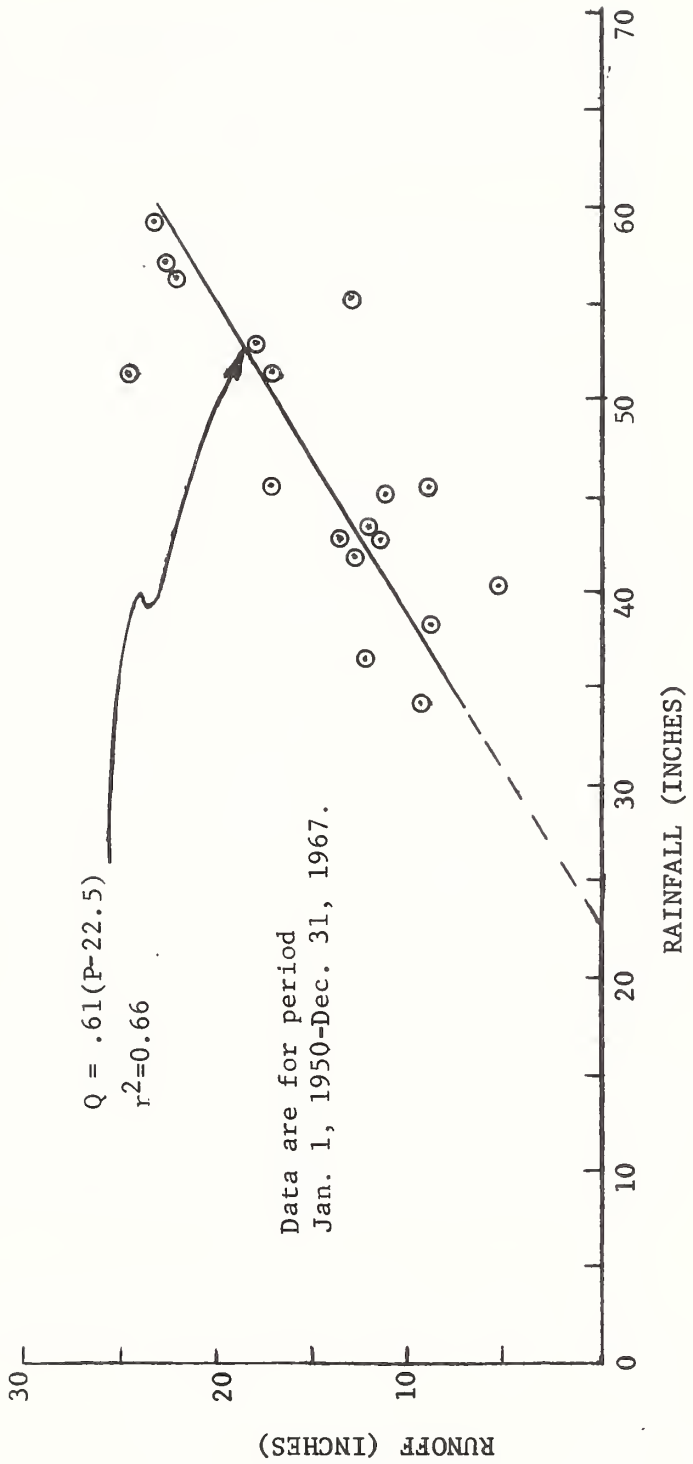

Figure 8. Annual rainfall-runoff relationship for Ahoskie Creek watershed, NC W-A1.

basin, NC W-A1, for a 17-year period. The scatter for this watershed was the worst of those we compiled. The coefficients of determination, r^2, ranged from about 0.66 for Ahoskie Creek to about 0.89 for the south Florida watersheds. Model coefficients for the individual coastal plan watersheds were:

Ahoskie Creek, N.C. (NC W-A1),	Q = 0.61(P - 22.5)
Hurricane Creek, near Alma, Ga.,	Q = 0.50(P - 25.0)
Taylor Creek, Fla. (W-2),	Q = 0.97(P - 35.0)
" " " (W-3),	Q = 0.83(P - 35.0)

If one considers the a-coefficient value to primarily represent evaporation losses, the results are consistent for expected increases in ET losses with increases in latitudes from Florida to North Carolina. The b values, or slope of the regression lines, are more difficult to explain; although we have been able to rationalize those shown for the different watersheds. As a first approximation these equations can be used to predict annual runoff for similar land resource areas. However, this model assumes that a straight line is an acceptable form to depict the precipitation-runoff relation. This is not completely logical; especially insofar as the lower values of rainfall are concerned. In extremely dry years such curves bend to the left of the sketched position. When annual rainfalls drop below 40 inches in Florida and 35 inches in Georgia and North Carolina, runoff is usually between 2 and 5 inches. These small volumes are not predictable.

Cumulative Curves

Such models are sometimes used to show relationship changes between two functions. We have attempted to ascertain what changes in rainfall-runoff relations occur with altered watershed conditions, such as shifts in land use, using cumulative curves of annual rainfall versus runoff. But with minor success. Unless watershed conditions are changed enormously, the static (error) factor in the model commonly masks out the effects of land use changes.

To illustrate, in order to detect changes in the annual runoff/rainfall ratio for Ahoskie Creek, NC W-A1, during the 18-year period (1950-67), a double mass plotting of rainfall and runoff was made. See figure 9.

Enlarged channelization of Ahoskie Creek streams was begun in 1962 and completed in 1964. The work was done by SCS under a PL 566 authorization. The cumulate curve, figure 9, shows that

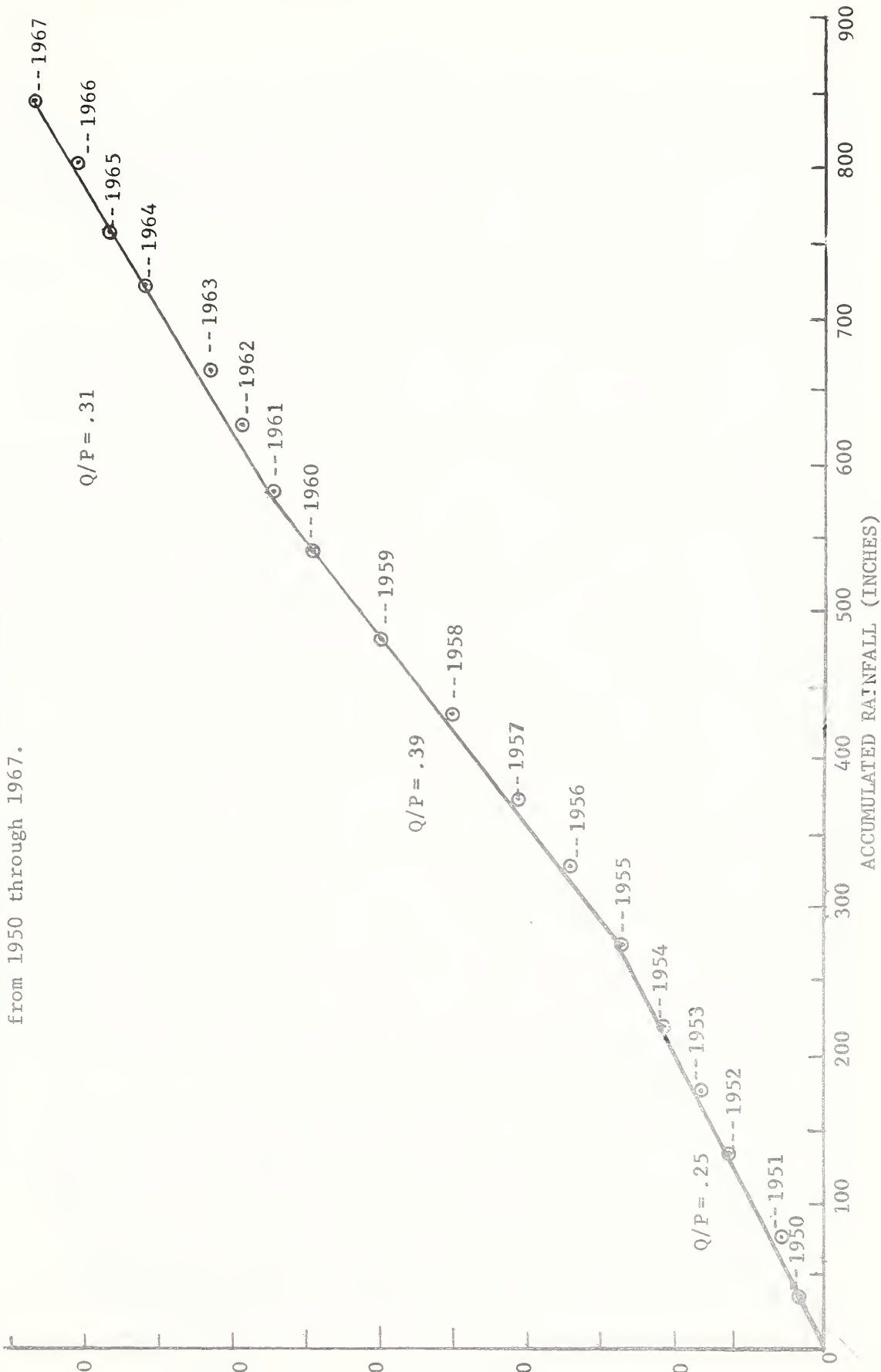

Figure 9. Double-mass curve showing changes in Q/P ratio for Ahoskie Creek watershed, W-A1, from 1950 through 1967.

the 18 years can be divided into three distinct periods of about equal lengths. These periods seem to represent cyclic weather patterns, however, rather than changes in basin conditions due to the watershed protection and flood prevention program.

Monthly Runoff

A model for predicting monthly runoff was developed for the Florida watersheds using monthly rainfall and USWB evaporation pan records as input. This method is detailed in ARS 41-152 (10).

Essentially, monthly evaporation losses (ET_w) for the Florida W-2 experimental watershed were computed from the water balance equation previously discussed; viz., $Q = P - E \pm \Delta S - s$. The monthly ET_w values were divided by the corresponding monthly USWB evaporation pan (E_p) values. The resulting ratios, ET_w/E_p, were then plotted as a function of correlative monthly rainfall. The maximum value of ET_w/E_p was about 0.78, which is the pan coefficient for watershed evaporation when soil water is not limited.

Seasonal differences in ET_w/E_p were found when the ratios were related to monthly rainfall. Various seasonal combinations were examined. In theory the relationships should be different for each month in accord with evaporative demands set by solar radiation. For practical predictive use the ET_w/E_p ratios observed during the cooler months of November, December, January, and February, as contrasted with ratios during the rest of the year, were sufficient.

Figure 10 shows the plotting of these two curves, which we have termed water-use curves. They indicate that rainfalls exceeding 3 inches per month during the winter season provided enough moisture to satisfy maximum ET_w demands. However, maximum ET during the warmer months required about 6 inches of monthly rainfall.

This accounting procedure for the water budget can be used in reverse to estimate runoff for ungaged watersheds in similar land resource areas. However, the change in basin storage (ΔS) must be estimated. The accuracy of the monthly runoff estimates will depend to a large extent on the accuracy of these (ΔS) estimates. Also, since the water-use curves reflect the statistical mode of rainfall distribution and amount, the model tends to overpredict runoff for dry years

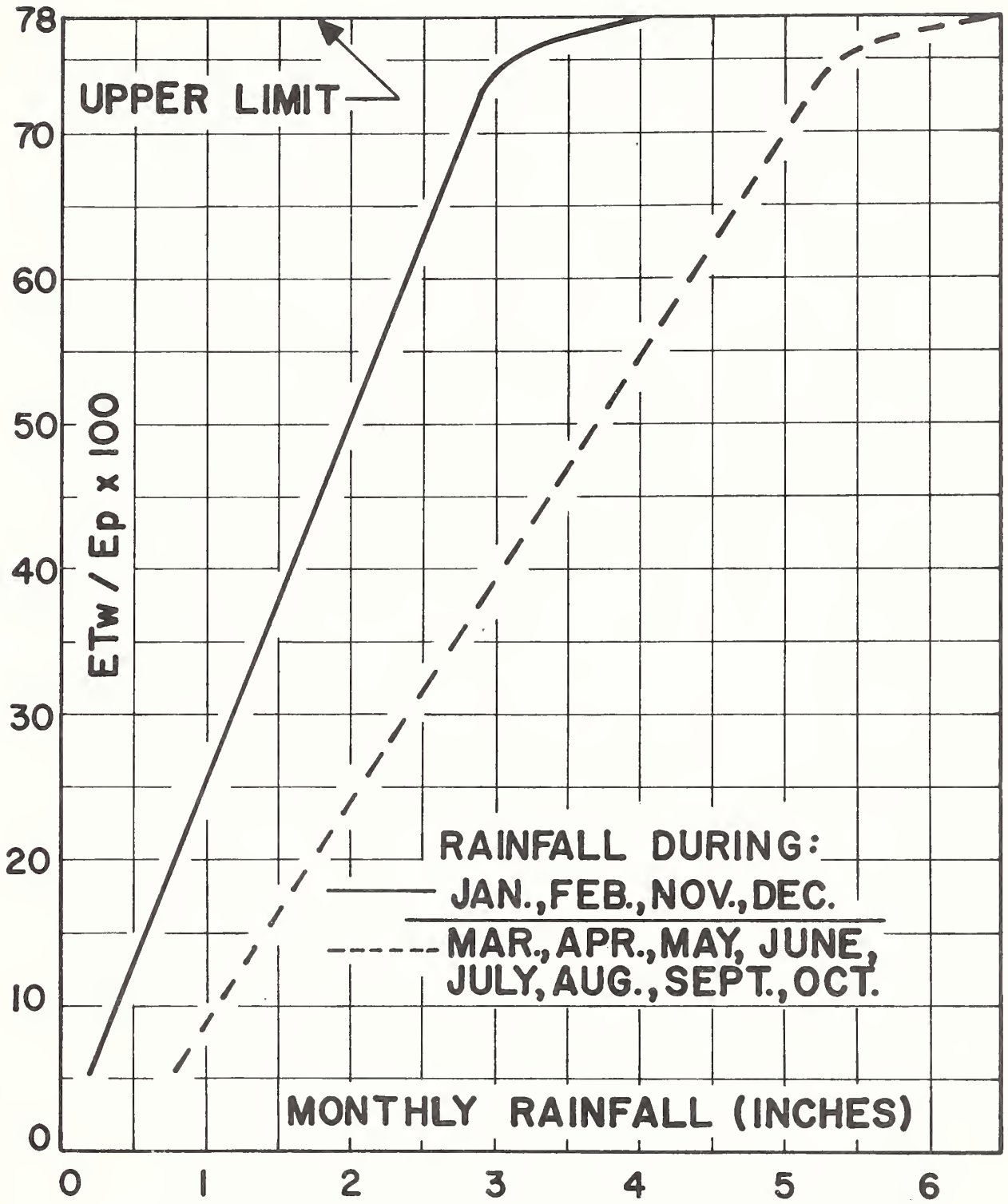

Figure 10. Seasonal water-use curves for typical coastal plain watersheds in central and southern Florida as determined by monthly rainfall.

and underpredict for wet years. In Florida an empirical correction factor was developed to be applied when the annual rainfall differs appreciably from the mean of 56 inches annually. This correction factor amounts to 25% of the total rainfall, above or below the 56-inch average. That is, for a year with rainfall of 44 inches, the model overpredicts runoff by 3 inches annually.

Figure 11 shows the cumulative plotting of measured runoff against runoff computed by this method. Measured runoff differed from computed runoff by 0.98 inch after a 7-year period (1955-62). Since we have, in reality, only fed back the data in reverse order from which the model was derived, the close correspondence shown in figure 11 is not necessarily evidence that the model will be useful in different situations.

Recently Asmussen and Thomas[3] used the water-use curves in computing the water balance for a 68-acre farm watershed near Tifton, Ga. Here, all inflows and outflows from the area were measured, except evapotranspiration. Changes in groundwater storage were established using wells equipped with both recording and non-recording gages. Evapotranspiration losses were computed using the subject water-use curve. The residual unmeasured element was taken to be changes in soil moisture in the vadose zone, and is shown in the last column in Table 1, which shows the other pertinent elements in the water balance equation.

Total results for the period are excellent. Results for shorter periods are realistic except in those cases where groundwater measurements were made during, or immediately after, heavy rainfalls. These unbalances, which are seen in the (ΔWs) column for 3/7/68, and between 5/16/68 and 6/13/68 are ascribed to the Lisse effect. This indicates that air was trapped in the sandy soils above the base of the impervious aquiclude and the layer of infiltrating water attempting to settle to the true water table. The groundwater wells thus gave higher than actual readings, which resulted in excess computed volumes of groundwater stored. When the Lisse effect occurs, then several days are required for levels measured in groundwater wells to

---

3/ Personal communication; Loris E. Asmussen, Geologist, ARS-SWC, Tifton, Ga.

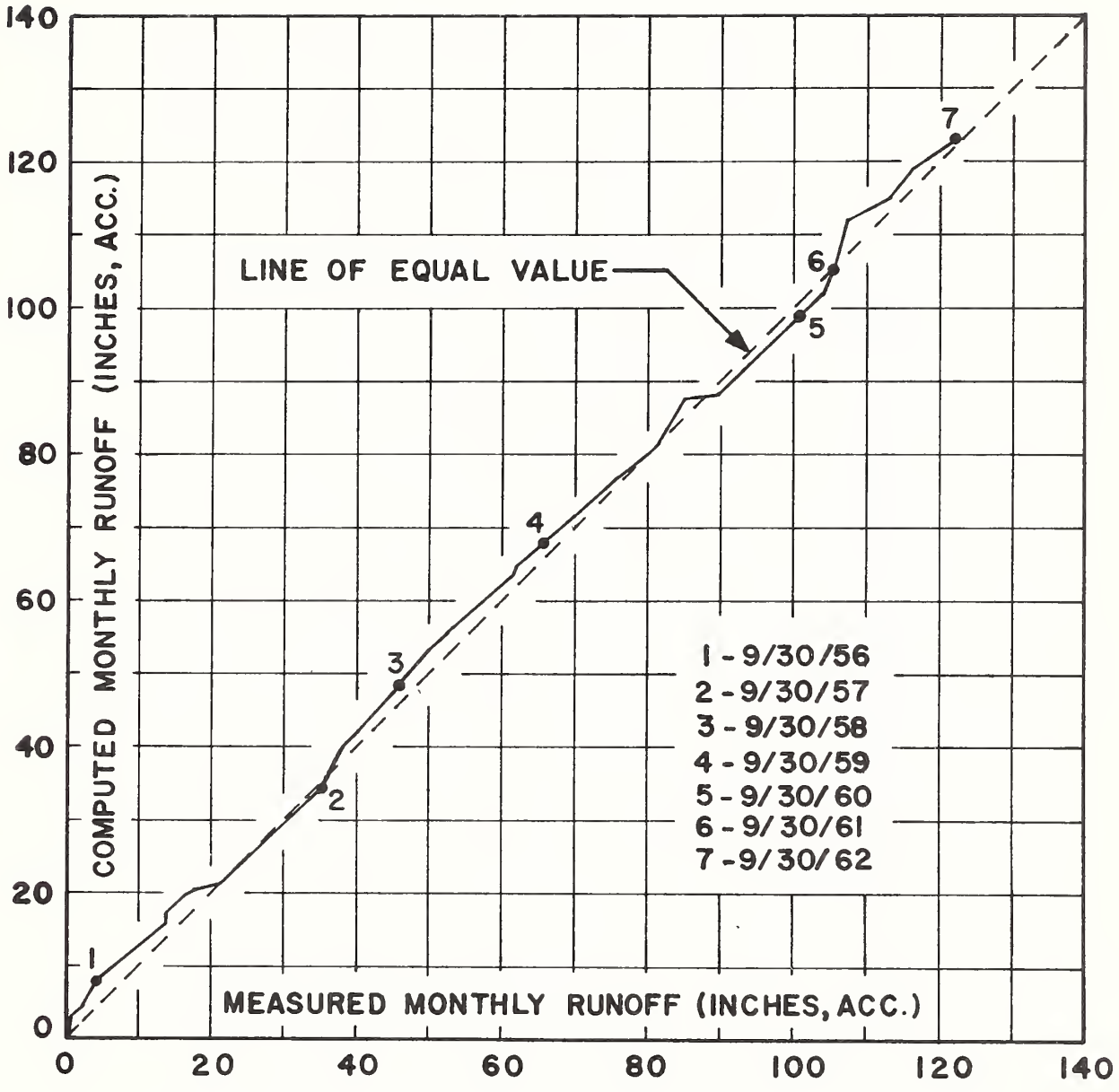

Figure 11. Measured runoff plotted against runoff computed by the water-use curve, watershed W-2.

Table 1. Water balance for Walker Pond watershed

Beginning & Ending Dates	Gains to Watershed		Losses from Watershed		Ground-water Movement	Vol. of Groundwater		Vadose Water (Ws)
	Rainfall	Irrigation	ET_{w-2}	Weir Flow		Stored*	Change	
1967								
10/12-11/16	1.85		1.41		0.09	2.63	0.48	0.05
11/16-12/14	2.72		1.12		trace	3.11	0.88	0.72
1968								
12/14-1/18	2.47		0.57		0.02	3.99	4.72	- 2.80
1/18-2/16	0.84		0.45		0.01	8.71	1.02	- 0.62
2/16-3/7	1.06				trace	9.73	1.11	
3/7-3/14	3.95		2.42	0.04	-0.14	10.83	11.70	-10.40
3/14-3/22	0.10			trace	-0.08	22.53	3.50	
3/22-4/18	0.40	0.04	0.82	0.05	-0.07	26.03	- 6.50	2.52
4/18-5/16	1.24	0.07	2.37	trace	-0.01	19.53	- 7.89	6.82
5/16-6/13	9.16		6.55	0.48	-0.16	11.64	11.83	- 9.86
6/13-7/18	3 60		3.72	0.09	0.05**	23.47	- 8.68	8.47
7/18-8/15	2.35		1.99	0.01	0.06**	14.79	- 4.92	5.27
8/15-9/12	4.58		2.73	0.08	0.07**	9.87	0.58	1.19
Total:	34.32	0.11	24.15	0.75	-0.34		7.83	1.36

* At beginning of period.
** Groundwater gains not part of watershed water balance.

reflect the correct position of the groundwater table. With the exception of the periods influenced by the Lisse effect, the water balance is good. This indicates that the water-use curves can be utilized in other watersheds in the coastal plains.

5-Day Runoff

The 5-day, or pentad, period is used at the Southeast Watershed Research Center instead of the 7-day, or weekly, period for water yield studies. We have found this to be distinctly advantageous. The pentad system allows successive years of record to keep in step with the solar year; whereas the weekly intervals vary with each year. Thus the solstice and equinox occur timewise on the same pentad unit consistently, which is not true for weekly units. Since water yields are a close function of solar energy, the advantages of the pentad system are obvious.

To illustrate, the non-linear method of computing water yield retains the two-stage convolution concept given by W. M. Snyder in another paper at this workshop. It was only necessary to change the scale of time from short-term to long-term (5-day), and some details of numeric procedures to produce the results shown in figure 9 of Snyder's paper. This figure shows the predicted annual water yields --by pentad unit--for experimental watersheds in Florida and Mississippi.

Incidentally, in the study of rainfall in Florida, we have noticed there is apparently a rhythmic cycle when precipitation volumes are grouped by 5-day intervals. Whether or not such cyclic tendencies are statistically reliable will require additional records and further analyses.

Daily Runoff

A recent joint undertaking by the Central and Southern Florida Flood Control District, USDA Hydrograph Laboratory, and a Southeast Watershed Research Center satellite station (Everglades Project) has produced some interesting and favorable results stemming from a model application[4]. The

---

4/ Personal communication from L. E. Lindahl, Systems Engineer, FCD, West Palm Beach, Fla.

purpose of the joint investigations was threefold:

1. Develop a modeling technique for south Florida watersheds that demonstrated a good potential for successful application to major portions of the 15,500-sq.-mile Central and Southern Florida Flood Control District.

2. Test the ARS-USDA Hydrograph Laboratory's model in southeast coastal and flatwoods watersheds.

3. Examine how well present and past data collection and analyses support the required inputs to a model.

The location and documentation of Taylor Creek watershed (Fla. W-2), previously described, satisfied the criteria for all three purposes. Basin vegetation includes improved and unimproved pasture, virgin forest, and marshes. Slopes are essentially flat, ranging from 0 to 2 percent. Based on 49 years of record at Lake Okeechobee Hurricane Gate #6, mean annual rainfall for the area is 46.22 inches. Major soil types include Leon, Immokalee, and Plummer fine sands.

The fundamental principles of the model are for the most part the same as those of the USDA Hydrograph Laboratory's model. Selective tailoring of the general model to better fit local conditions was done, but there were no significant departures from the hydrologic principles forwarded through publications and discussions with the Hydrograph Lab. Data for the Taylor Creek experimental watershed were supplied by the Everglades Project, Plantation Field Laboratory, (USDA-ARS), and used in developing model parameters. These inputs, together with the model, rewritten for an IBM 1130, were used in simulating the hydrologic response of the 98-sq.-mile basin.

To test the model response, Taylor Creek records for the periods of October 1 through November 15, 1956, and March 15 through July 4, 1959, were used. These periods represent 46 and 127 days, respectively.

The October 1-November 15, 1956 period of record includes a rainfall storm of approximately 1 in 100-year frequency followed by a 137-day recession. The major portion of the rainfall occurred between October 13-16 with 9.98 inches per hour. This provides an excellent check on the model's capability to simulate hydrologic response to extreme con-

ditions of rainfall with an almost uninterrupted recession. A graphical comparison of historical and simulated record is shown in figure 12.

The March 15-July 4, 1959 period of record includes a cycle of hydrologic conditions. The cycle begins with a rainfall period from March 16 to March 23 with a maximum rainfall amount of 1.92 inches and maximum intensity of 0.22 inch per hour occurring on March 19; then, an 82-day period of scattered rainfall amounting to 11.71 inches; then, a rainfall period from June 15 to June 22 with a maximum rainfall of 3.71 inches and maximum intensity of 3.00 inches per hour occurring on June 18. A graphic comparison of historical and simulated records for this period is shown in figure 13.

The following is a summary of recorded and simulated results:

	1956	
Item	Recorded	Simulation
ET	--	2.34 inches
Yield	9.90 inches	9.97 inches
Time of Peak	Midnight,10/16	Midnight,10/16
Peak Flow	6930 cfs	6700 cfs

	1959	
Item	Recorded	Simulation
ET	--	14.75 inches
Yield	13.70 inches	14.70 inches
Time of Peak	--	--
Peak Flow	1300/4450	1230/4340

With the successful calibration of the model for Taylor Creek conditions, FCD engineers have begun application of the Hydrograph Lab. model to the Kissimmee River basin. If results turn out as expected, the engineers will apply the model to the upper St. Johns River basin and possibly to the entire 17,000-sq.-mile Florida Flood Control District. The intent of the District is to use such a model as an aid in making water management decisions.

REFERENCES

(1) Hydrologic Data for Experimental Watersheds in the United States (1956-59, 1960-61, and 1962). USDA-ARS Misc. Pub. Nos. 945, 994, and 1070; Wash., D.C., Nov. 1963, May 1965, and June 1968.

(2) Bross, I. D. J. Models. Design for Decision; The McMillan Co., 1953.

(3) Anonymous. Rainfall and Runoff. Handbook of Culvert and Drainage Practice, Chapter 5, 2nd Ed., Armco Culvert Mfgrs. Assoc. (Published by R. R. Donnelly & Son) Chicago, Ill. 1941.

(4) Jens, W. J. and M. B. McPherson. Hydrology of Suburban Area. Handbook of Applied Hydrology, Sect. 20, Ven Te Chow Ed.; McGraw Hill; New York. 1964.

(5) Stephens, J. C. and W. C. Mills. Using the Cypress Creek Formula to Estimate Runoff Rates in the Southern Coastal Plain and Adjacent Flatwoods Land Resource Area. ARS 41-95, ARS-USDA. Feb. 1965.

(6) Speer, Paul R. and Charles R. Gamble. Magnitude and Frequency of Floods in the United States. Part 2-A. South Atlantic Slope Basins, James River to Savannah River. USGS Water-Supply Paper 1673. Wash., D. C. 1964.

(7) Barnes, Harry H. and Harold G. Golden. Magnitude and Frequency of Floods in the United States. Part 2-B. South Atlantic Slope and Eastern Gulf of Mexico Basins, Ogeechee River to Pearl River. USGS Water-Supply Paper 1674. Wash., D. C. 1966.

(8) Patterson, James L. Magnitude and Frequency of Floods in the United States. Part 7. Lower Mississippi River Basin. USGS Water-Supply Paper 1681. Wash., D. C. 1964.

(9) Johnstone, D. and W. P. Cross. Elementary Relationships Between Precipitation and Runoff. Elements of Applied Hydrology, Chapter 4; The Ronald Press Co., New York. 1949.

(10) Speir, W. H.,W. C. Mills, and J. C. Stephens. Hydrology of Three Experimental Watersheds in Florida. USDA-ARS 41-152. Nov. 1969.

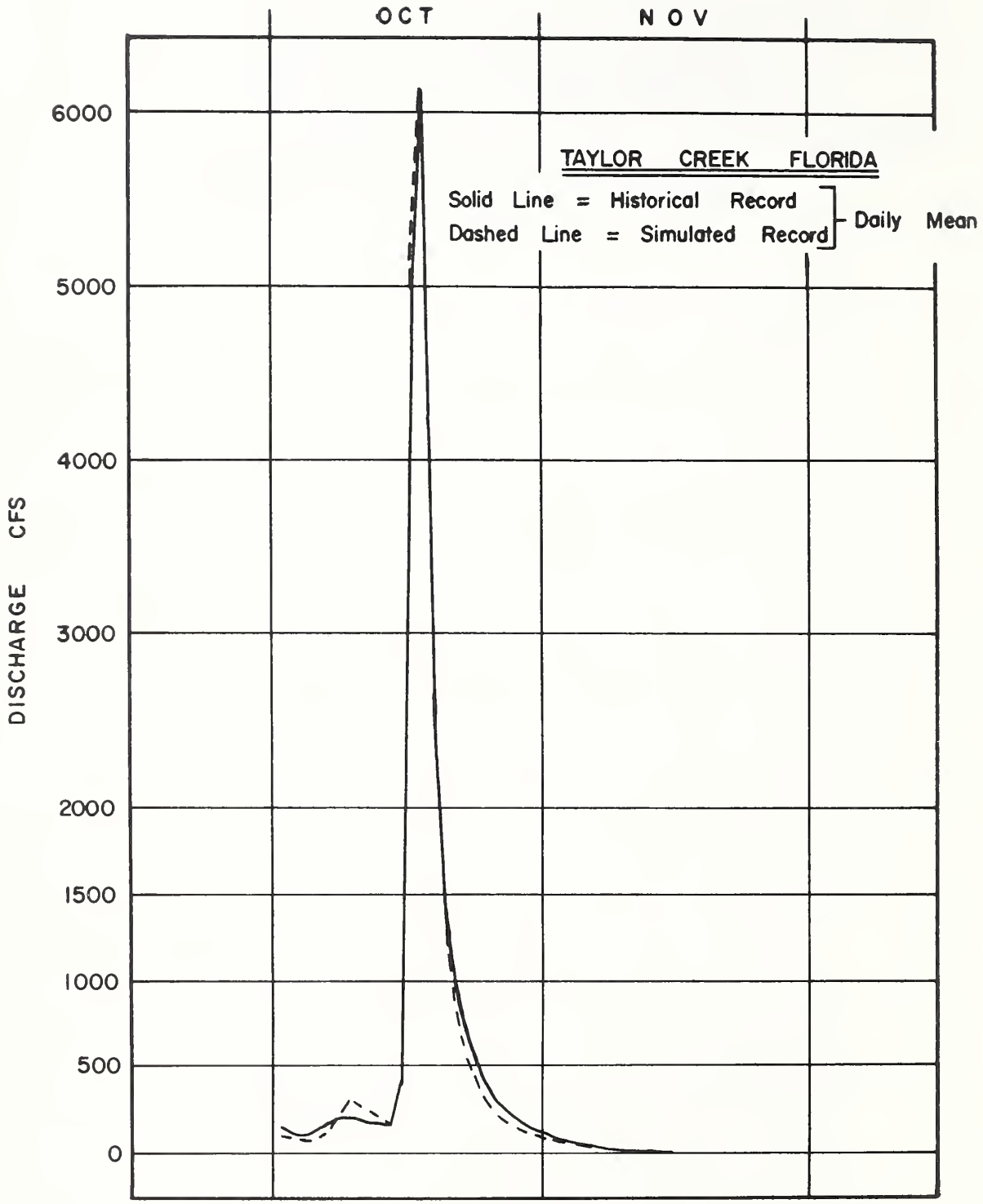
OCT
NOV
6000
5000
4000
3000
2000
1500
1000
500
0
DISCHARGE CFS
TAYLOR CREEK FLORIDA
Solid Line = Historical Record
Dashed Line = Simulated Record
Daily Mean

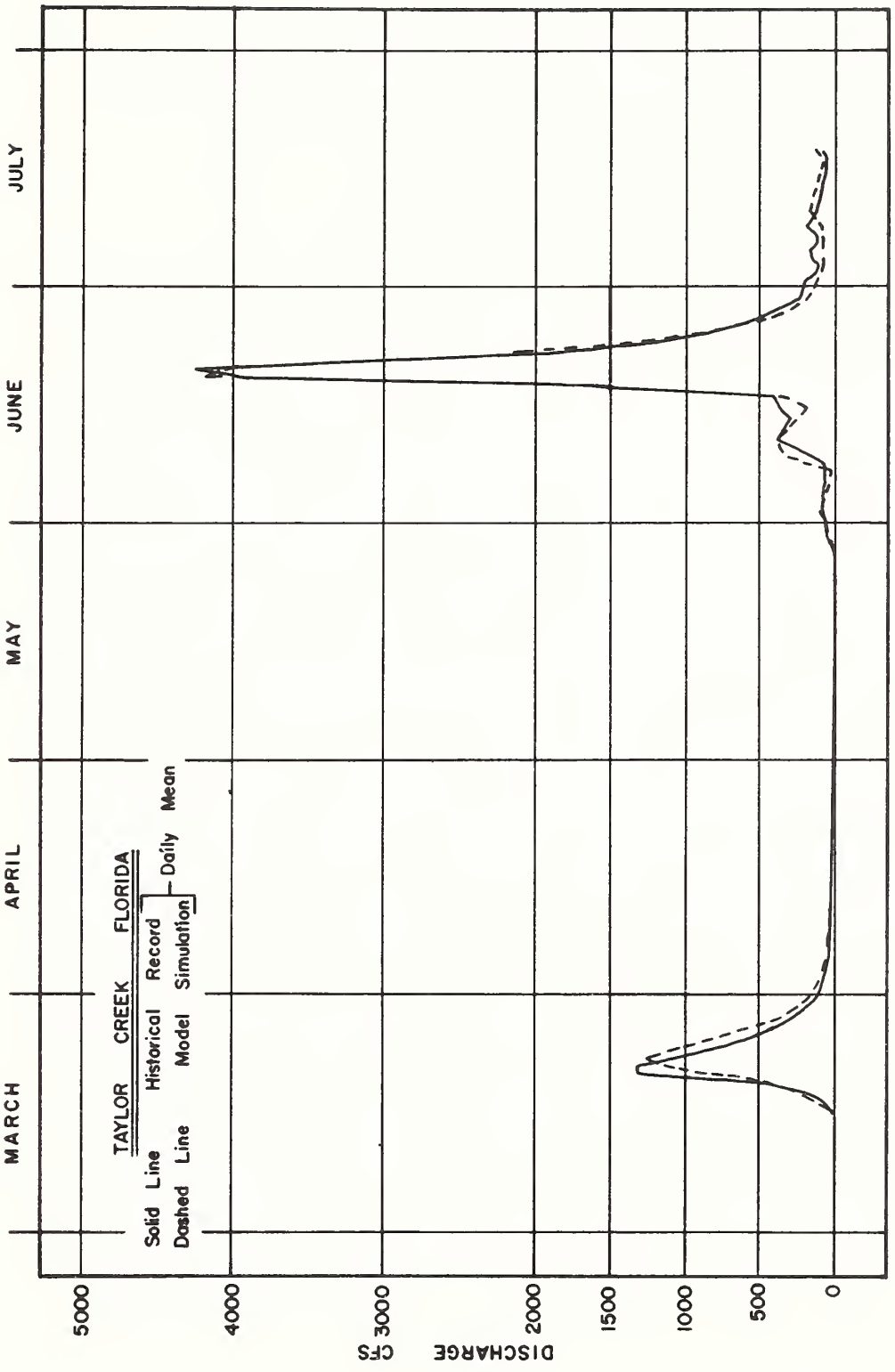
TAYLOR CREEK FLORIDA
Solid Line Historical Record
Dashed Line Model Simulation
Daily Mean
MARCH
APRIL
MAY
JUNE
JULY
DISCHARGE CFS
5000
4000
3000
2000
1500
1000
500
0

SEDIMENT YIELD INVESTIGATIONS IN A COMPLEX WATERSHED 1/

By

Andrew J. Bowie 2/

INTRODUCTION

The sedimentation research project in the Pigeon Roost Creek Watershed, located in north Mississippi, was initiated by the Agricultural Research Service during the latter part of 1956, with the actual data collection beginning in January 1957. The experimental watersheds in the Pigeon Roost Creek drainage basin provided the necessary conditions for studying the critical sedimentation problems associated with that section. The soils throughout most of the area were developed from thin loess of silty material. This material is usually less than 4 feet thick and overlies various kinds of Coastal Plains material. Once erosion has cut through the upper layer of loess, the underlying material is eroded very rapidly.

Because the soils are highly erodible, channel instability is a serious problem. The erosion processes have produced quantities of sand that have filled some channels, sanded valleys, damaged reservoirs, and caused floods. The erosion and sedimentation problems in the drainage basin are considered representative of many of the conditions found in many areas of the Southeast. With this consideration, the Soil

---

1/ Contribution from the USDA Sedimentation Laboratory, Southern Branch, Soil and Water Conservation Research Division, Agricultural Research Service, U.S. Department of Agriculture, Oxford, Mississippi, in cooperation with the University of Mississippi and the Mississippi Agricultural Experiment Station.

2/ Research Hydraulic Engineer, USDA Sedimentation Laboratory, Agricultural Research Service, Soil and Water Conservation Research Division, U.S. Department of Agriculture, Oxford, Mississippi.

and Water Division of the Agricultural Research Service selected a 117-square mile complex watershed located in the upper drainage area of the Pigeon Roost Creek Basin for extensive and detailed studies of sedimentation processes and the factors affecting stream channel equilibrium.

WATERSHED DESCRIPTION

The Pigeon Roost Creek Watershed lies in the North Central Hills region of the East Gulf Coast physiographic section of the Coastal Plain province. Figure 1 shows that the watershed is shaped similar to the State of South Carolina with the major East-West axis approximately 15 miles long and with an average width of about 8 miles. Approximately 90 percent of the drainage within the corporate limits of the City of Holly Springs is included within the watershed (1). 3/

The topographic elevation ranges from approximately 300 feet at Gaging Station 34 (Figure 1) to 640 feet near the east and southeast boundary of the watershed. The surface features consist of broad flat flood plains with both natural and dredged channels and rolling severely dissected interfluvial areas.

Approximately 22 percent of the total watershed has slopes under 2 percent with 24 percent in the 2 to 5 percent range. For the remainder of the area, 8 percent is in the 5 to 8 percent range, 10 percent in the 8 to 12 percent range, 19 percent in the 12 to 17 percent range, and 17 percent greater than 17 percent slope. In general, the land is severely eroded with gullies prevalent throughout the basin (1).

Although the percentage varies from subwatershed to subwatershed, about 23.3 percent of the total area is in cultivation and 1.2 percent in bare gullies. The remainder of the area is 17.4 percent idle, 16.6 percent pasture, 40.4 percent forest, and 1.1 percent urban, (2).

3/ Numbers in parentheses refer to References.

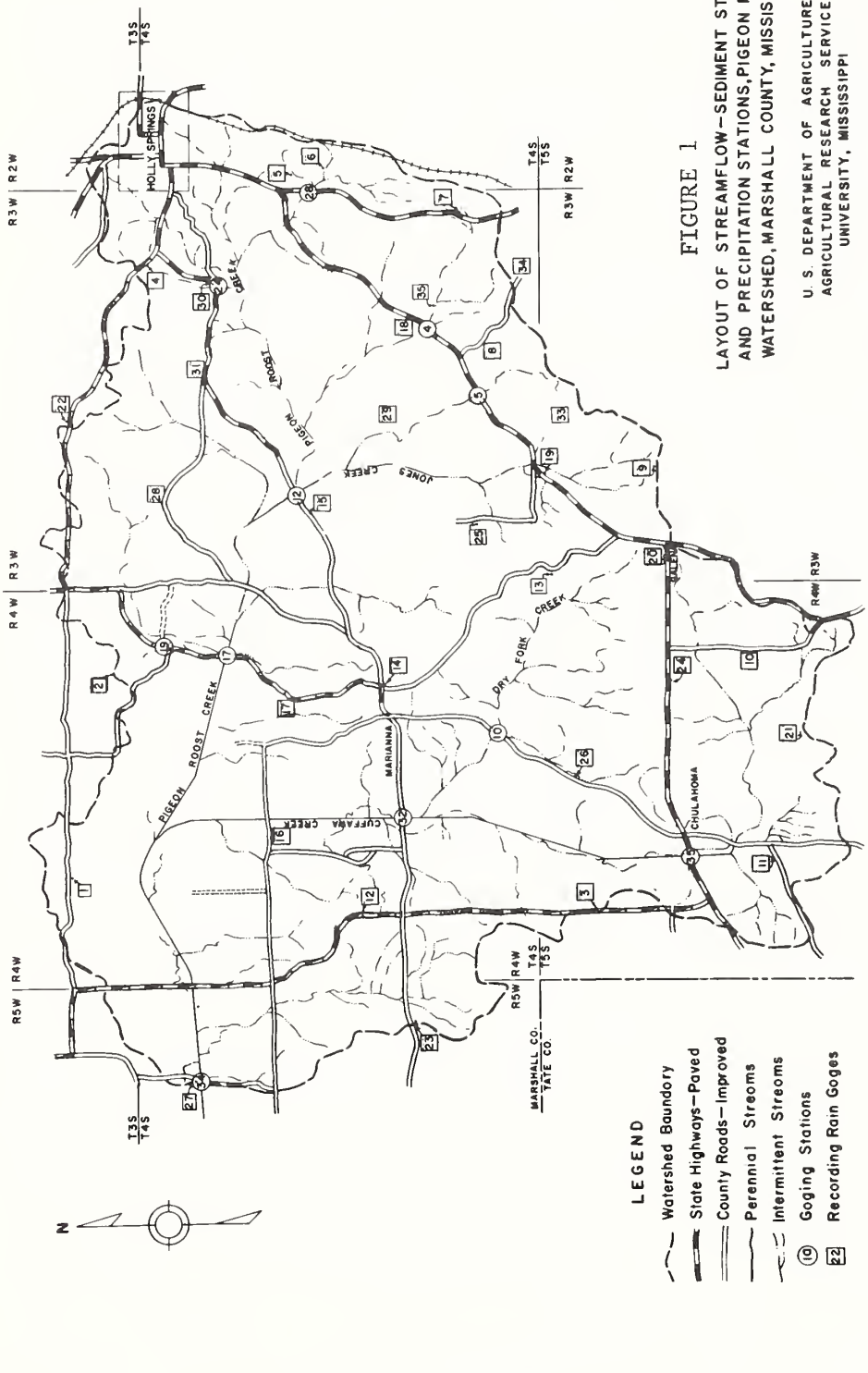

FIGURE 1

LAYOUT OF STREAMFLOW—SEDIMENT STATIONS AND PRECIPITATION STATIONS, PIGEON ROOST WATERSHED, MARSHALL COUNTY, MISSISSIPPI

U. S. DEPARTMENT OF AGRICULTURE
AGRICULTURAL RESEARCH SERVICE
UNIVERSITY, MISSISSIPPI

Cooperating Agencies— University of Mississippi
Mississippi State University

OCTOBER 1965

FIELD INSTALLATION

The original field installation for the sediment yield investigations in the Pigeon Roost Creek Watershed consisted of 12 sediment sampling and streamflow gaging stations. At the time of installation, the subwatersheds in which the gaging stations were located ranged in size from 113 acres to 117 square miles for the entire watershed. Changes in watershed, channel, and operating conditions during the ensuing months necessitated the modification of the data collection program with the deletion of two gaging stations and the addition of two others. At the present time runoff and sediment data are collected from the entire watershed of 117 square miles which includes 11 complex subwatersheds ranging in size from 0.80 square miles to 50.20 square miles (Figure 1).

The standard instrumentation at each gaging site consists of a Stevens continuous water level recorder, type A-35, installed in a wooden shelter over a 24-inch corrugated iron pipe well. A wire-weight gage, attached to a permanent type structure and usually located near the water level recorder, is used to check and verify the water surface elevation indicated by the recorder gage.

Fifteen recording and 15 nonrecording rain gages were placed on the watershed between November 21 and December 26, 1956. The nonrecording gages did not give the desired information during this early period on the watershed. The records from the nonrecording gages were good for monthly and annual precipitation values; however, they were of little value in studying individual storms and intensities. By July 1, 1959 all nonrecording gages in the watershed were replaced with recording gages and two additional gages were added to complete the network of 32 recording gages (Figure 1).

DATA ACQUISITION

The primary objectives for the sediment yield studies are as follows:

1. To relate measured sediment yield to calculated gross erosion and watershed characteristics and conditions.

2. To establish methods and procedures for predicting the effect of conservation and flood control programs on sediment delivery and yields.

3. To make total sediment transport measurements and field determinations of the relationships between total sediment transport and the flow qualities, including slope, depth, temperature, size of transported bed particles, and corresponding resistance coefficients.

Since storm runoff is the vehicle for sediment transport and the resultant of many of the variables which correlate directly with sediment yield, it is considered the most important factor and should be measured with the greatest degree of accuracy possible. Streamflow gaging stations are located in defined channels at the lower end of each of the subwatersheds. Generally accepted methods and procedures are used to measure streamflow and to obtain sediment samples at each of the uncontrolled stream cross-sections. Standard Geological Survey procedures are used for velocity measurements, and the depth-integration method is used to collect samples of the water sediment mixture. Velocity measurements are made with standard current meters, and the DH-48, US D-49 and 200-pound P-63 samplers are used to collect sediment samples. Bed material samples are taken from the top 2 inches of the stream bed with the US BM-54 bed material sampler. Automatic pumping samplers are used to collect supplementary samples. In some instances it is necessary to design special type equipment and modify techniques in order to meet the demands of the particular problem at hand (3). In all cases, flow data are obtained in a manner to give representative concentrations of the total sediment in transport.

When the depth and velocity of a stream permit, velocity measurements and samples are collected by wading with hand equipment. At higher stages, heavier equipment is used and the work is done from cableways, footbridges, or highway bridges. Each sample is identified as to the exact position from which it is obtained together with stage, time of sampling, and temperature of water. A summary of the accumulative water discharge and sediment measurements made during the period of record is shown in Table 1.

TABLE 1.--Summary of accumulative water discharge and sediment measurements for Pigeon Roost Creek Experimental Watershed

Dates	Gaging Station-Subwatershed	Drainage Area (sq. mi.)	Accumulative Discharge Meas.	Accumulative Sediment Meas.
12-12-56/9-30-69	4	2.47	310	1146
12-12-56/9-30-69	5	1.76	389	1247
12-14-56/9-30-69	10	8.64	428	996
10-2-56/9-30-69	12	35.60	648	1383
10-2-56/9-30-69	17	50.20	930	1793
2-15-57/9-30-69	17-A	5.00	246	555
12-12-56/9-30-65	19 1/	0.38	136	464
12-12-56/9-30-69	24	0.80	270	636
1-4-57/9-30-69	28	1.69	147	448
12-12-56/9-30-69	32	31.30	544	1405
10-2-56/9-30-69	34	117.00	883	3037
12-12-56/9-30-69	35	11.80	386	1042
3-8-57/9-30-69	35-A	1.70	263	687

1/ Study discontinued 9-30-65.

All presently used sediment load equations (bed load, bed material load, or total load) were formulated for limited sets of conditions and as a general rule hold only for those conditions. As a result, when one of the equations is applied to conditions other than those for which it was derived, the calculated sediment load rarely corresponds very closely to the measured values. In recognizing that there was urgent need for extensive information on the factors affecting the amounts, occurrence, and movement of total sediment material in streams, the Sedimentation Laboratory initiated a comprehensive program of total-load study, in conjunction with other studies, in the Pigeon Roost Creek Watershed during the latter part of 1963. The field data necessary for this study include measurements of hydraulic gradients, channel geometry, water temperatures, velocities, concentrations in selected channel reaches, and concurrent stream discharge and sediment concentrations at total-load sections and normal sections. Frequent surveys of channel cross-sections throughout the watershed are made in order to document changes in channel geometry.

A land-use survey of the subwatersheds was begun in 1957 and has continued on an annual basis. Considerable efforts are made to evaluate the contribution of sediment from all sources and to differentiate between the major and minor source areas. Field data necessary for this study include an accurate determination of land use and cover conditions, the percent and length of slope, the area of active gully erosion, and the location of sediment-detention structures, gully plugs, and farm ponds. This information is mapped on aerial photographs in the field, and the area and annual erosion rates are computed separately for each delineated area and combined to give total watershed erosion.

DATA PROCESSING AND ANALYSES

In 1960 the processing of runoff and sediment data at the USDA Sedimentation Laboratory was reoriented toward the use of electronic equipment. This helped to reduce and, in many instances, eliminate the routine calculations that were previously necessary in computing the water and sediment discharge. The data output from the computer is arranged in a form that is more useful for further analysis with or without digital computers. Computer programs have been written to compute runoff and sediment discharge from large complex watersheds

and smaller unit source areas to include fractional-acre plots, and also for the reduction of precipitation data. Two programs have been written to do computations in connection with stream channel resistance coefficient and slope studies, and three programs are used to do computations for releases through Hydrologic Data publications.

All samples collected in the field are analysed in the laboratory for sediment concentration, and in many instances for particle size distribution. For reporting purposes and sediment computations, material greater than .062 mm in diameter is classed as sand. The data are then used to establish sediment rating (discharge-sediment concentration) curves for each gaging station. Similarly, stage-discharge relationships and flow duration curves are established from stream discharge measurements and water stage records. Periodic adjustments are often necessary as these relationships may change frequently in the unstable sand-bed channels of the study area. This requires a continuous gaging and sampling program so that adjustments and corrections can be made when they become necessary.

Water yield computations for the subwatersheds are based upon continuous water-stage hydrographs and current meter measurements which define the stage-discharge relationship of a shifting sand-bed stream (4). Sediment computations, on the other hand, are more difficult due primarily to sampling limitations in a natural sand bed stream.

In the computation of sediment yields, sediment rating curves are used to determine the applicable sediment discharge for those periods in which sediment samples are not available. The sediment rating curve establishes rates of sediment discharge for different flow rates or for appropriate periods of time. As shown in Figure 2, which is typical of sediment discharges, the points scatter widely but a reasonably good average curve can be defined. The 45-degree slope of the upper part of the curve indicates that the concentration of measured sediment becomes relatively indipendent of water discharge at high rates of flow.

Measured sediment yields are usually computed by plotting concentrations of the sediment samples on the water-stage hydrograph to the same time scale (abscissa) as the gage height curve (Figure 3). This is a base for the continuous

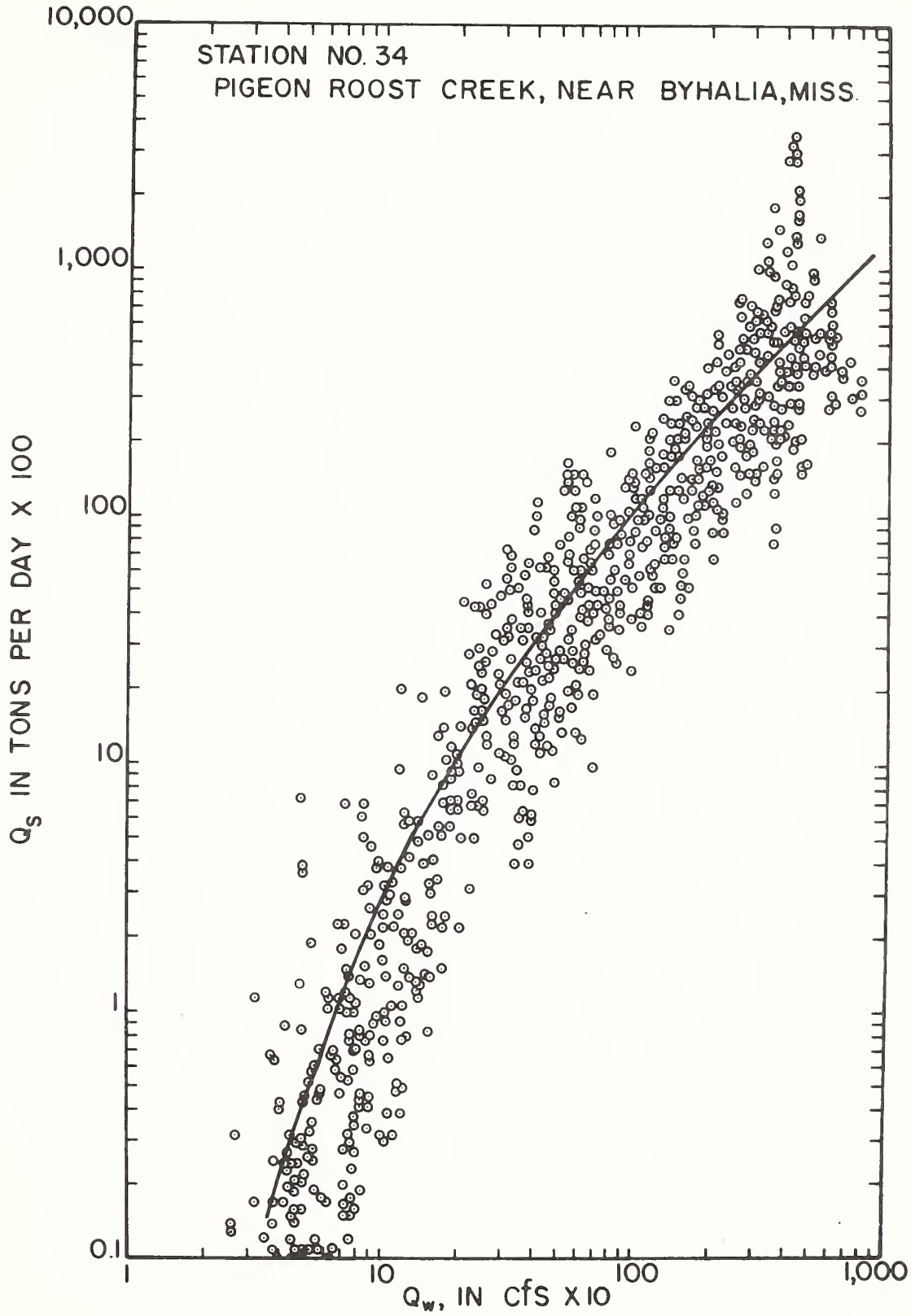

FIGURE 2.-- MEASURED SEDIMENT RATING CURVE

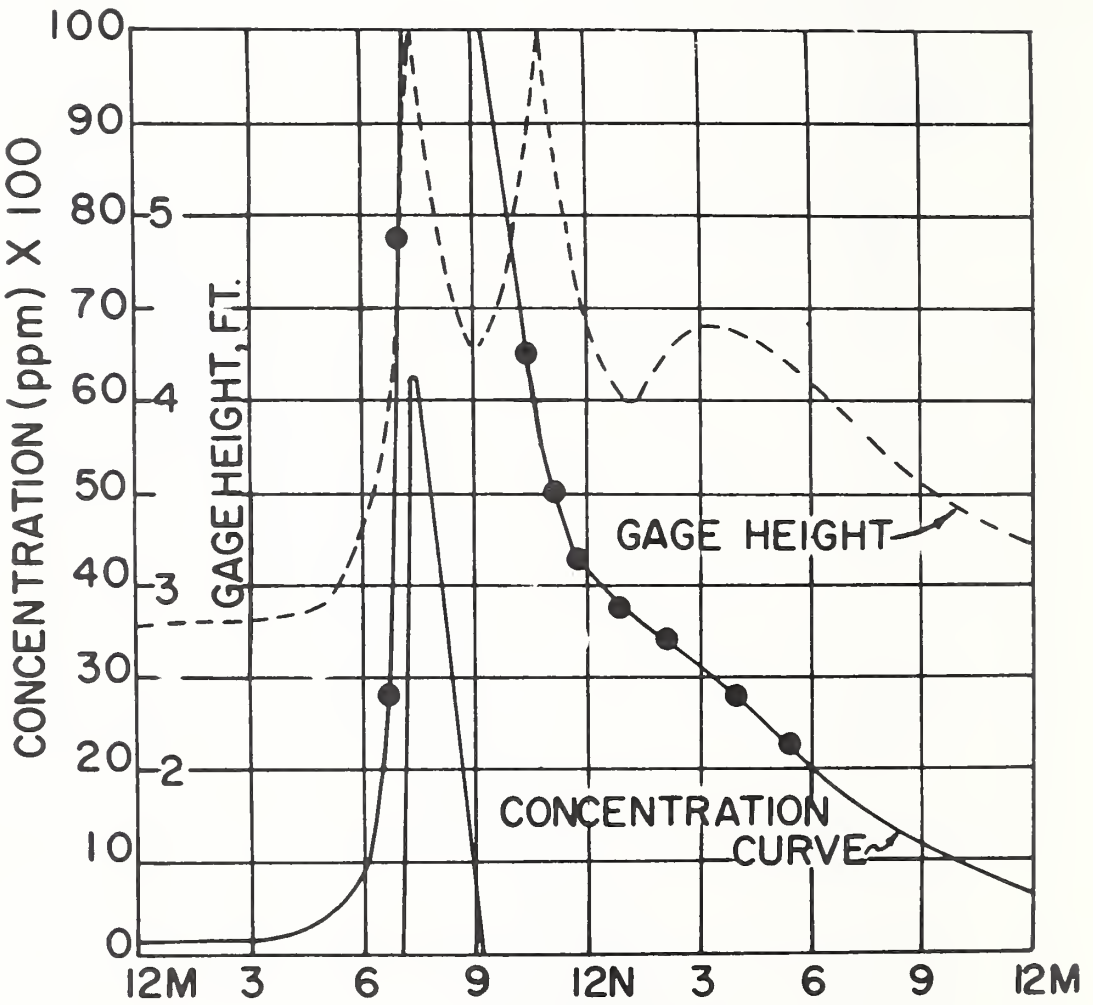

FIGURE 3.--SEDIMENT CONCENTRATION CURVE FOR STATION NO. 34, PIGEON ROOST CREEK

concentration curve from which measured sediment discharges are derived. The concentration ordinate is usually 1000 parts per million to the inch. For nonsample periods, or whenever the concentration curve is inadequately defined by samples, concentration is established on the basis of the trend of the gage height curve, the instantaneous water-sediment relationship (sediment rating curve), similar sampled rises, and precipitation records. Mean daily measured sediment discharge is computed directly from the records of streamflow and the continuous curve of concentrations.

Ordinary sampling equipment such as the DH-48, US D-49, and the P-63 samplers will not sample the entire depth of flow. As shown in Figure 4, a small zone between the sampler nozzle and the stream bed is not sampled under normal conditions. Sediment in this zone is called unmeasured sediment and it is computed by the Colby mean velocity method (5). Total sediment yields are obtained by adding the measured and unmeasured yields and are computed as storm, daily, and monthly values. Sand yields (sediment > .062 m.m.), both measured and unmeasured, are also computed on a monthly basis.

COMMENTS

The relationship of direct runoff to sediment yield on the Pigeon Roost Creek Watershed, whether on a storm or annual basis, is usually quite consistent. Differences in direct runoff between watersheds account for much of the variation in sediment yields. A large percent of the variation in annual direct runoff, after adjusting for variation in climatological factors, can be attributed to watershed slope, cover, variations in soil type, conservation practices, and drainage density. A portion of the remaining variation is suspected to be channel transmission losses. A comparison of the 12-year average (10-1-57/9-30-69) weighted precipitation, runoff and sediment yield for part of the Pigeon Roost Creek Watershed is shown in Table 2.

Other factors that should be taken into consideration when examining sediment yields in a watershed is the deposition of eroded material onto adjacent flood plains caused by overbank flow, and that part of the total sediment discharge influenced by stream channel degradation. As shown in Figure 5, the duration of flow for the lower Pigeon Roost Creek Station

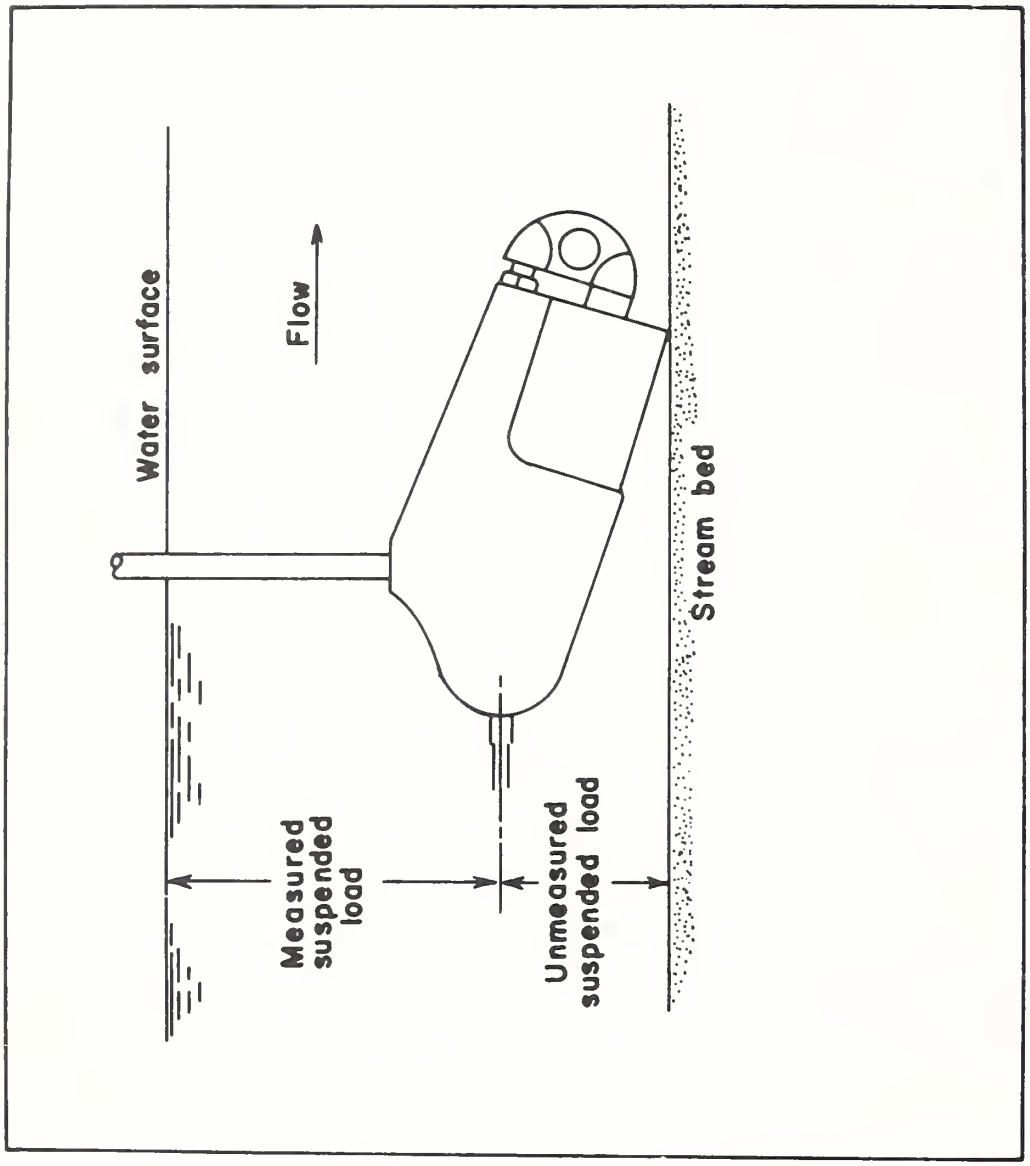

FIGURE 4.-- SAMPLING LIMITS - USDH - 48 DEPTH INTERGRATING HAND SAMPLER.

TABLE 2.--Average annual precipitation, runoff, and sediment yield for the Pigeon Roost Creek Watershed, 10-1-57 to 9-30-69

Watershed Number	Drainage Area (acres)	Precipitation 1/ (inches)	Runoff (inches)	Measured Sediment (tons/acre/yr.)	Total Sediment (tons/acre/yr.)
4	1,580	48.65	5.42	2.36	3.25
5	1,130	49.43	11.14	4.58	6.80
10	5,530	50.57	9.05	4.92	7.13
12	22,800	48.75	6.40	2.63	3.59
17	32,100	49.20	9.86	2.99	3.82
17A	3,200	48.07	8.20	3.24	4.52
32	20,000	49.63	10.54	6.74	8.59
34	75,000	49.30	13.59	3.62	4.47
35	7,550	49.39	10.77	6.27	7.94
35A	1,090	47.70	12.28	4.27	5.68

1/ Thiessen weighted.

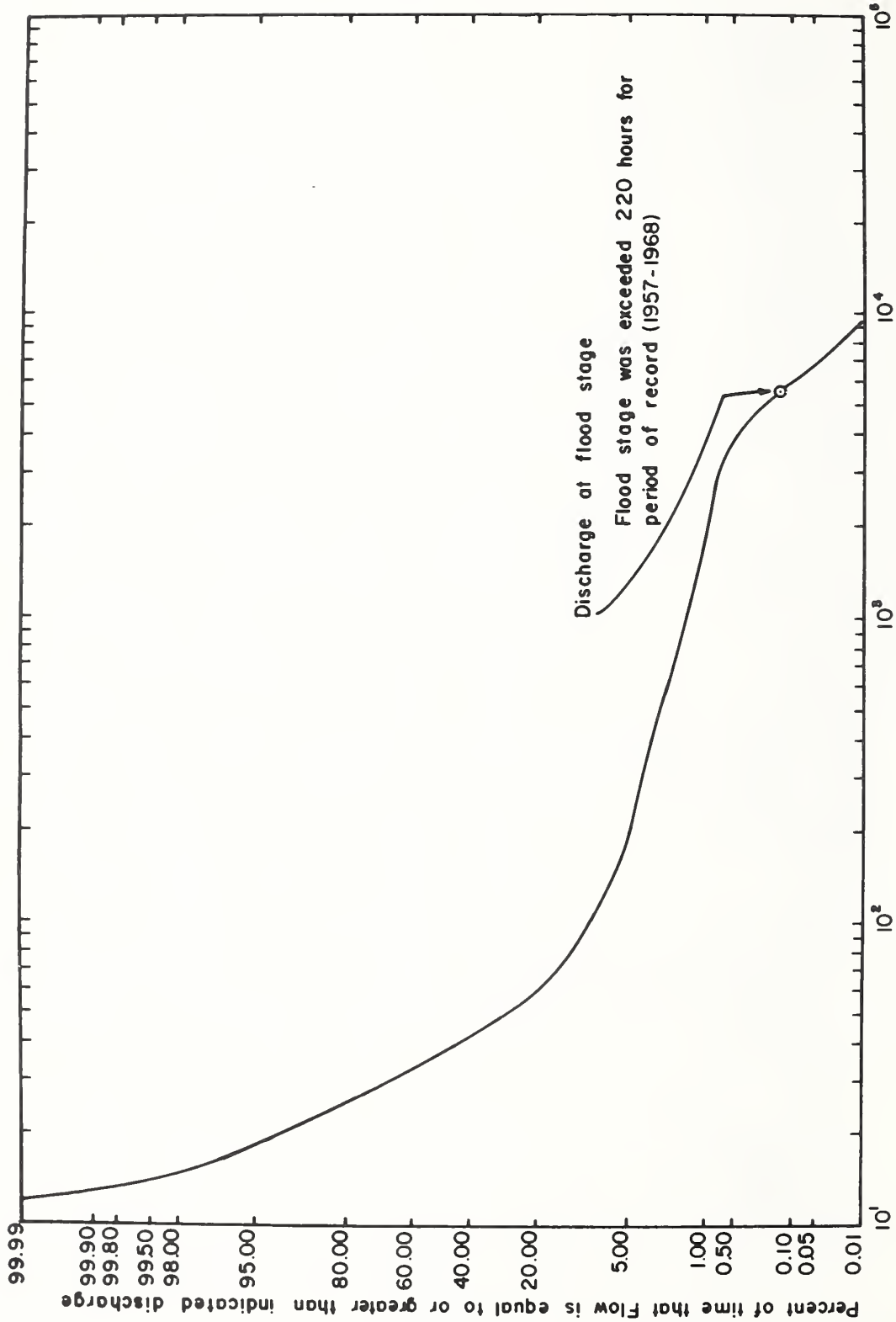

FIGURE 5.-- Flow duration curve for watershed No. 34 Pigeon Roost Creek.

indicates that flood stage has occurred approximately 220 hours for the period of record. Not only does this complicate computations of runoff and sediment discharge downstream, but in many instances detail surveys are required in order to estimate the amount of material deposited from the channel.

Resurveys on most of the major channels in the Pigeon Roost Creek Watershed, completed late in 1968, showed considerable channel and bank erosion in most of these streams. Some of the results of the survey are given in the following table:

Watershed Number	Channel Erosion, 1958-68 (Yds.^{3})	(Tons/ac./yr.) 1/
4	19,091	1.16
5	2,818	0.30
10	48,316	1.06
12	145,804	0.78

1/ Based on an estimated in situ unit weight of 90 lbs./ft.^{3} for the eroded material and total watershed area as shown in Table 2.

It should be noted that these values do not reflect total channel erosion in any of these watersheds. Many of the smaller tributary streams were not surveyed. It is also noteworthy that channel erosion amounts to a significant percentage of the average annual sediment yield from these watersheds, ranging from 4.7 percent for Watershed 5 to 36 percent for Watershed 4.

As stated earlier in this report, one of the objectives of the sediment yield investigations study is to relate measured sediment yield to calculated gross erosion and watershed characteristics and conditions. In conducting these studies, comparisons are made between total sediment measured at streamflow gaging stations and computed gross erosion in the subwatersheds. In order to get as many comparisons as possible, the Musgrave equation is used to compute gross erosion for the total contributing area, and both the Musgrave and Universal equations are used to compute gross erosion for the major sediment source area. The major sediment source area in the Pigeon Roost Creek Watershed is considered to be cultivated land 2-percent slope and above, and bare gullies only.

Recent studies have shown that when the major sediment source area of a watershed is considered alone there is a fairly good correlation between computed gross erosion and the sediment yield of the watershed as measured at the gaging station (2). The relationship between computed gross erosion and the 9-year (1957-1966) average annual measured sediment yield is shown in Table 3. Regardless of the method used, when compared with total measured sediment in a given watershed, the indications are that the erosion estimates from the two major sediment-source areas may be a reasonably good prediction of watershed sediment production.

Another objective of the sediment yield investigation study is to make total sediment transport measurements and field determinations of the relationships between total sediment transport and the flow qualities. In order to get a comparison of concentration with present day techniques of sampling, it is necessary to collect samples at a so-called normal section at the same time samples are collected at a total-load section. The total sediment discharge must be about the same at the two sections, and, also, the normal section must be located upstream a sufficient distance as required to eliminate influence from the total-load section.

An analysis of the samples collected gives the difference in concentrations at the two sections, and with a breakdown of the size distribution, the proportions and magnitudes of the several bed material sizes in transport can be determined. A breakdown of .062 mm is used to separate the fine material in transport from the sands. As shown in Figure 6, a comparison of fine material ($<$ .062 m.m.) measured at a total-load section and a normal cross-section indicates that there is very little difference in the concentration of fines between the two sections.

When a comparison of total measured concentration is made between the two sections, it is found that under most conditions the concentration at the total-load section is considerably higher than the normal section. Since the concentrations of fines are almost equal at the two sections, then this difference in total concentration (20 percent to 40+ percent) is sands, or particle sizes greater than .062 mm in size. Figure 7 shows a comparison of total measured concentration at a total-load section and normal cross-section.

TABLE 3.--Computed gross erosion and sediment yield

Watershed No.	Computed Gross Erosion			Total Measured Sediment 9-yr. Av. 1957-1966
	Total Contributing Area	Cultivated Land 2%-slope and Above, and Gullies		
	Musgrave (T/A/Y)	Musgrave (T/A/Y)	Universal (T/A/Y)	(T/A/Y)
4	6.7	3.0	4.2	3.2
5	9.0	5.3	8.4	6.4
10 1/	9.4	6.0	8.7	6.3
12	7.6	3.5	4.8	3.4
17	7.1	3.4	4.9	3.6
17A	6.4	3.4	4.2	4.4
19 1/	6.9	2.4	2.3	1.9
24 1/2/	6.6	4.0	4.0	3.9
28 1/	2.7	1.5	2.0	1.4
32	10.5	7.6	9.4	8.0
34	8.0	4.7	5.9	4.3
35	10.2	5.7	8.7	7.5
35A	8.7	5.1	5.8	4.9

1/ 8-year average (10-1-57 to 9-30-65).
2/ No cultivated land in this watershed.

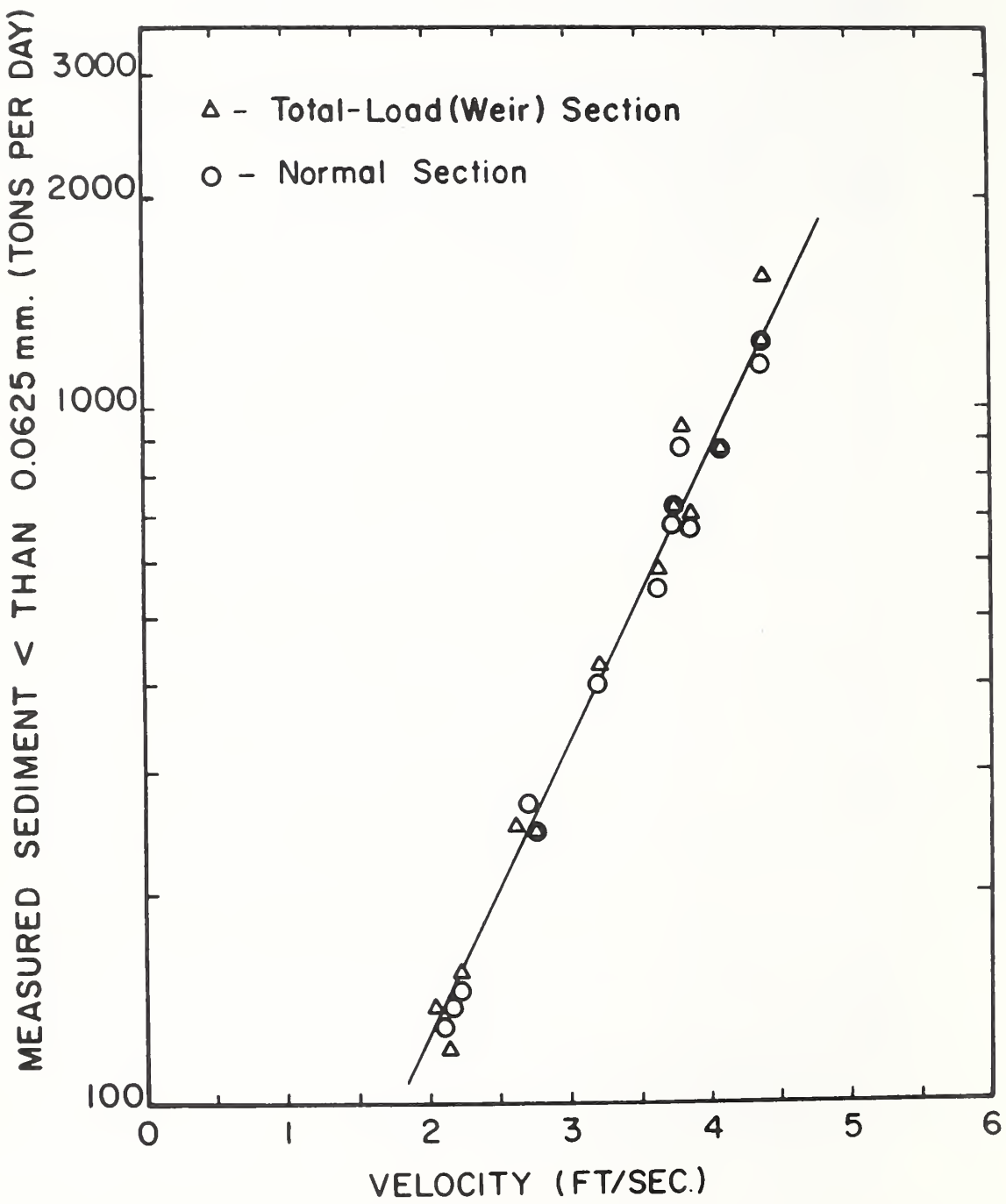

FIGURE 6.--Comparison of Fine Material Measured at a Total-Load (Weir) Section and at the Normal Cross-Section.

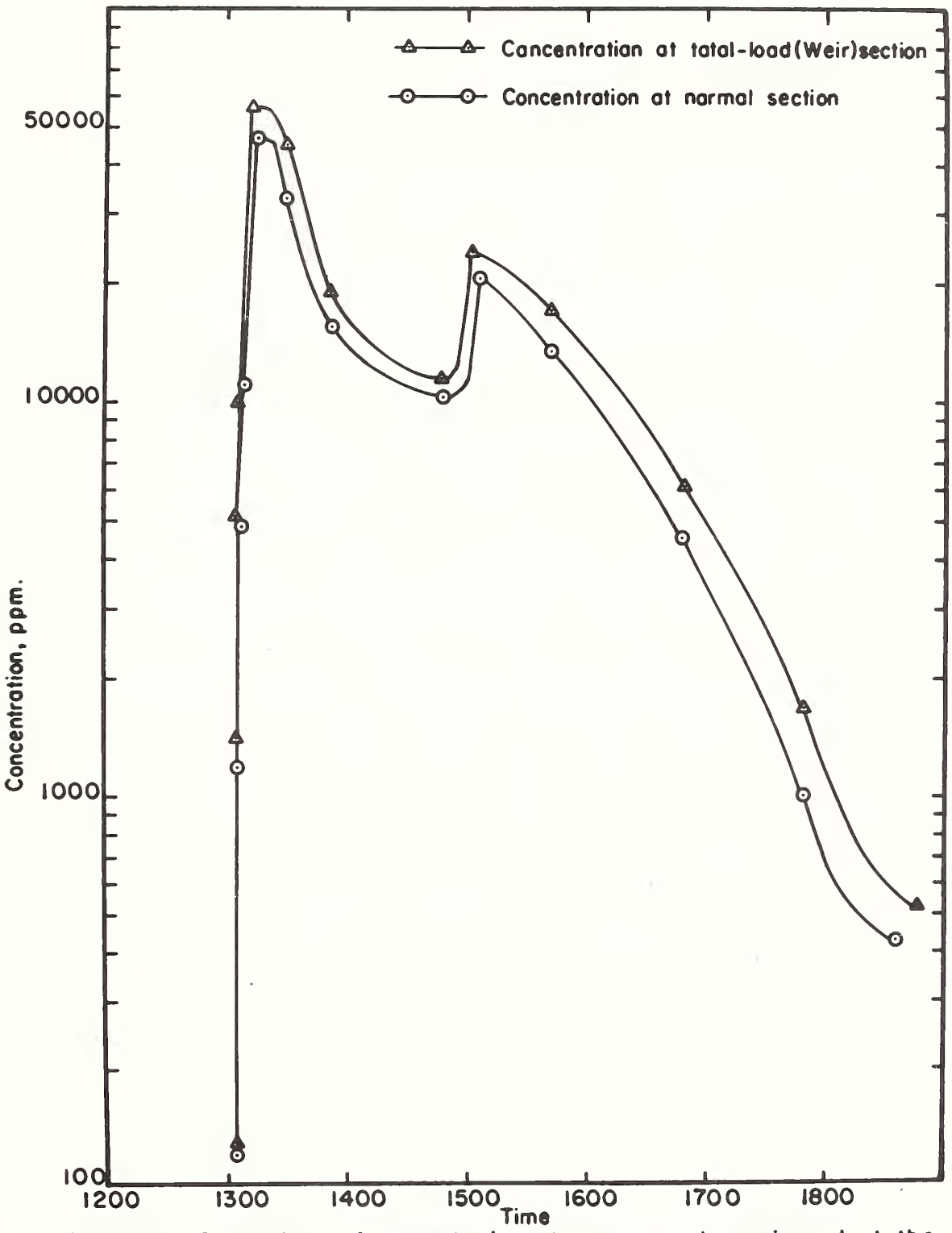

FIGURE 7.-- Comparison of concentration at a rectangular weir and at the normal cross-section for storm of April 9, 1969.

SUMMARY

The Soil and Water Division of the Agricultural Research Service selected a 117-square mile complex watershed located in the upper drainage area of the Pigeon Roost Creek Basin, North Mississippi, for extensive and detailed studies of sedimentation processes and the factors affecting stream channel equilibrium. The erosion and sedimentation problems in the Pigeon Roost Creek Watershed are considered representative of many of the conditions found in other areas of the Southeast. In general, the land is severely eroded with gullies prevalent throughout the watershed.

Runoff and sediment data are collected from the entire watershed of 117 square miles which includes 11 complex subwatersheds ranging in size from 0.80 square mile to 50.20 square miles. Generally accepted methods and procedures are used to measure streamflow and to obtain sediment samples at each of the gaging stations in the watershed. In all cases, flow data are obtained in a manner to give representative concentrations of the total sediment in transport. All samples collected in the field are analysed in the laboratory for sediment concentration, and in many instances for particle size distribution. Electronic data processing equipment is used to compute storm, daily, and monthly values of runoff and sediment yields.

Special studies are conducted in selected channel reaches on total sediment transport, flow qualities, and corresponding resistance coefficients. Frequent surveys are made on most of the major channels in the watershed in order to determine the effects of channel degradation, and in many cases deposition, on total sediment yields. Gross erosion is computed from field surveys and compared with the total sediment yield as determined from measurements made at streamflow gaging stations.

REFERENCES

(1) Bowie, Andrew J., et al.
1969. Unpublished Report, Runoff and Sediment Investigations on the Pigeon Roost Creek Watershed in Northern Mississippi.

(2) Spraberry, J. A., Bowie, Andrew J.
1969. Predicting Sediment Yields From Complex Watersheds. Trans. Amer. Soc. Agri. Eng. Vol. 12, No. 2, pp. 199-201.

(3) Bowie, Andrew J., et al.
1964-1967. Annual Reports, Studies to Improve Sediment Data Collection. USDA Sedimentation Laboratory, Oxford, Mississippi.

(4) Colby, Bruce R.
1960. Discontinuous Rating Curves for Pigeon Roost and Cuffawa Creeks in Northern Mississippi. USDA, ARS 41-36, 31 pp.

(5) Colby, B. R.
1957. Relationship of Unmeasured Sediment Discharge to Mean Velocity. Am. Geophysical Union, Trans., Vol. 38, pp. 708-717.

WATERSHED RESEARCH IN THE SOUTHERN PLAINS[1/]

W. O. Ree[2/]

Agricultural watershed research started in the Southern Plains Branch area in 1927 when nine small watersheds were established at Spur, Texas. Soon watersheds were established at other locations in Texas and in Oklahoma, New Mexico, and Kansas until in 1942 there were 82 watersheds under observation at 12 locations. World War II and the immediate postwar years saw a reduction in watershed research. By 1950, only 4 locations were still in operation and in 1954 the number of watersheds reached a low of 30. In 1960 a resurgence in watershed research activities began. The high point was reached in 1967 when 88 watersheds were in operation at 8 different locations. Today there are 82 watersheds plus six major river stations in operation at 7 locations in the Southern Plains.

Watersheds have been operated at 17 locations during the past 42 years. See figure 1. The locations for the code numbers given on the map are:

Code	Location
34	Cherokee, Oklahoma
35	Guthrie, Oklahoma
36	Muskogee, Oklahoma
37	Stillwater, Oklahoma
38	Garland, Texas
39	Spur, Texas
40	Tyler, Texas
41	Vega, Texas
42	Riesel, Texas
43	Hays, Kansas
47	Albuquerque, New Mexico
48	Mexican Springs, New Mexico

1/ Contribution from the Southern Plains Branch, Soil and Water Conservation Research Division, Agricultural Research Service, U. S. Department of Agriculture, Stillwater, Oklahoma, in cooperation with the Oklahoma Agricultural Experiment Station. For presentation at the ARS-SWC Workshop on Hydrologic Models, Tucson, Arizona, March 16-19, 1970.

2/ Hydraulic Engineer, U. S. Department of Agriculture, Stillwater, Oklahoma.

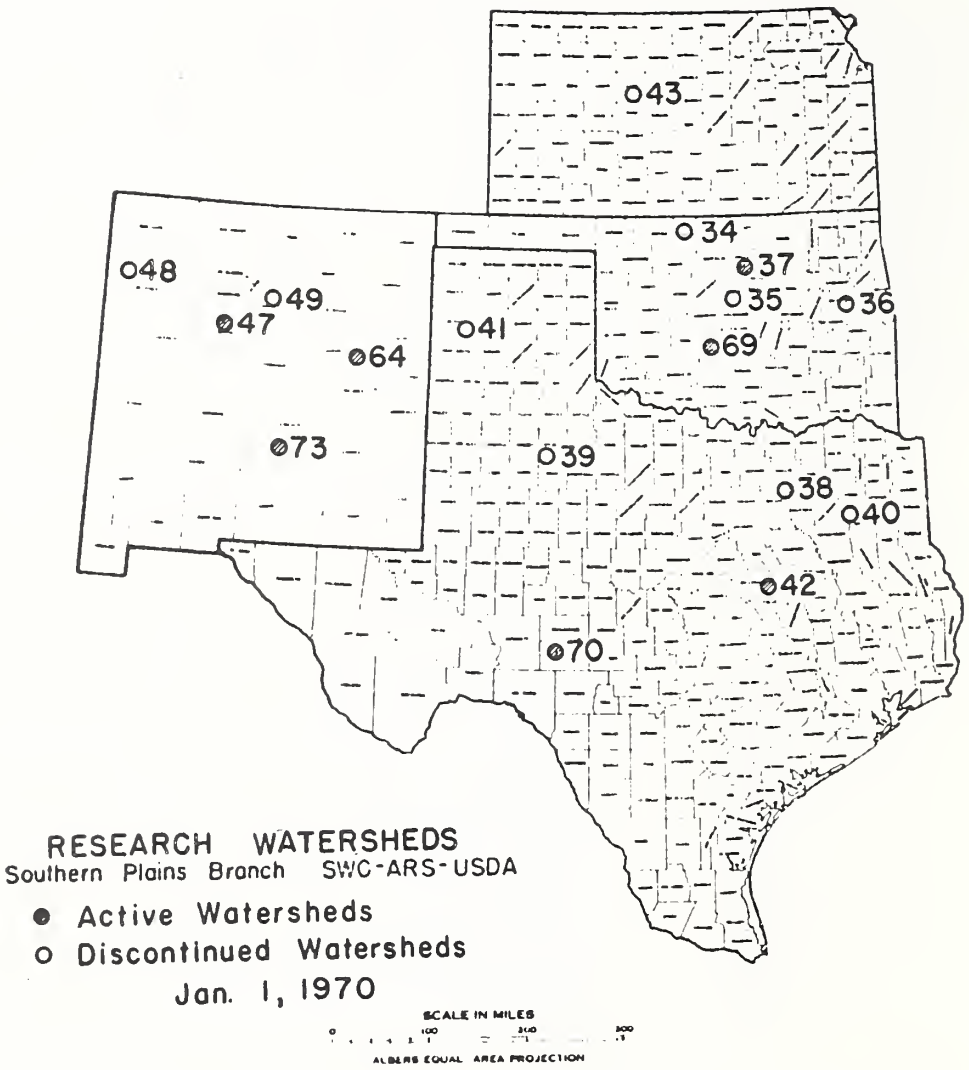

Figure 1 Watershed locations in the Southern Plains Branch, past and present.

Code	Location
49	Santa Fe, New Mexico
64	Santa Rosa, New Mexico
69	Chickasha, Oklahoma
70	Sonora, Texas
73	Ft. Stanton, New Mexico

The years during which watersheds were in operation at these locations are shown in table 1. The average life span of a watershed in the discontinued group was 11 years. The average life of watersheds at the active locations is 12 years at present. However, this average life will increase as the watersheds continue to be operated. Some now have been in operation for 33 years. Figure 2 shows the distribution of all watersheds, past and present, by life span.

The experimental watersheds have ranged in size from a quarter acre to 133 thousand acres. Distribution of all watersheds, past and present, by size category is shown in figure 3.

The size distribution for the 82 watersheds in operation during 1969 covers the same range. However, the number in the two categories ranging from 1 to 10 acres in size dropped from 52 to 7. The watersheds today are larger, but still half of them are less than 100 acres in size. These smaller watersheds, in general, are unit source areas.

The cover on the most of the present watersheds is grass or brush and grass. Table 2 lists watershed numbers by location and cover.

Table 2.--Number of watersheds by location and by treatment

	Cultivated	Grass	Mixed Land Use
Riesel, Texas	3	6	10
Albuquerque, New Mex.		3	
Stillwater, Okla.		3	
Santa Rosa, New Mex.		1	
Sonora, Texas		13	
Chickasha, Okla.	7	15	13
Ft. Stanton, New Mex.		2	
Total*	10	43	23

*Does not include the six river stations at Chickasha.

Table 1

NUMBER OF WATERSHEDS IN OPERATION IN SOUTHERN PLAINS BRANCH, BY LOCATION & YEAR

Code	Location	Year, 1927 through 1969																																									
		27	28	29	30	31	32	33	34	35	36	37	38	39	40	41	42	43	44	45	46	47	48	49	50	51	52	53	54	55	56	57	58	59	60	61	62	63	64	65	66	67	68	69
39	Spur, Texas	5	5	5	9	9	9	9	9	9	9	9	9	9	9	9	9	9	9	8																								
35	Guthrie, Okla.				1	4	5	5	5	5	5	5	5	5	5	5	10	10	10	10	10	10	9	9	9	9	7	7	1	1														
40	Tyler, Texas					1	3	3	3	3	3	3	3	3	3	3	3	1	1																									
43	Hays, Kansas						1	1	2	2	2	2	2	1	1	1	1	1	1	1	1	1																						
43	Riesel, Texas											4	18	29	29	29	29	29	14	14	14	14	14	14	14	14	14	14	14	14	14	15	15	15	19	19	19	19	19	19	19	19	19	19
48	Mexican Springs, N. M.											9	12	10	7	7	7																											
41	Vega, Texas												2	2	2	2	2	2																										
38	Garland, Texas												2	3	3	3	3	3	3	3	3	3																						
36	Muskogee, Okla.												1	3	3	3	3	3	3	3	2	2																						
47	Albuquerque, N. M.													3	3	3	3	3	3	3	3	3	3	3	3	3	3	3	3	3	3	3	3	3	3	3	3	3	3	3	3	3	3	3
49	Santa Fe, N. M.													3	3	3	3	3	3	3	3	3	3																					
34	Cherokee, Okla.															1	9	9	9	9	9	9	9	9	9	9	9	9	9	9	9	9	9	9	9	6	6	6	6	6	6	6		
37	Stillwater, Okla.																									3	3	3	3	3	3	3	3	3	3	3	3	3	3	3	3	3	3	3
64	Santa Rosa, N. M.																														1	1	1	1	1	1	1	1	1	1	1	1	1	1
70	Sonora, Texas																																			6	6	7	10	10	13	13	13	13
69	Chickasha, Okla.																																			6	15	20	21	30	35	41	41	41
73	Ft. Stanton, N. M.																																									2	2	2
	TOTAL	5	5	5	10	14	18	18	19	19	19	32	54	71	68	69	82	73	56	54	45	45	38	35	35	38	36	36	30	31	30	31	31	31	35	44	53	59	63	72	80	88	82	82

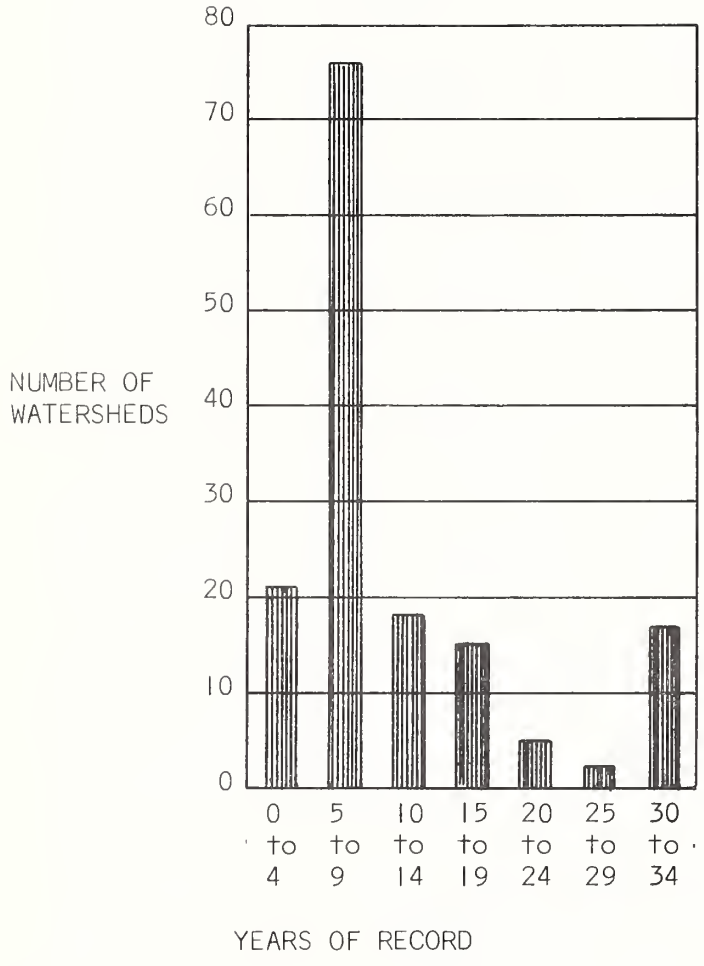

Figure 2 Distribution of all watersheds, in the Southern Plains Branch by number of years in operation.

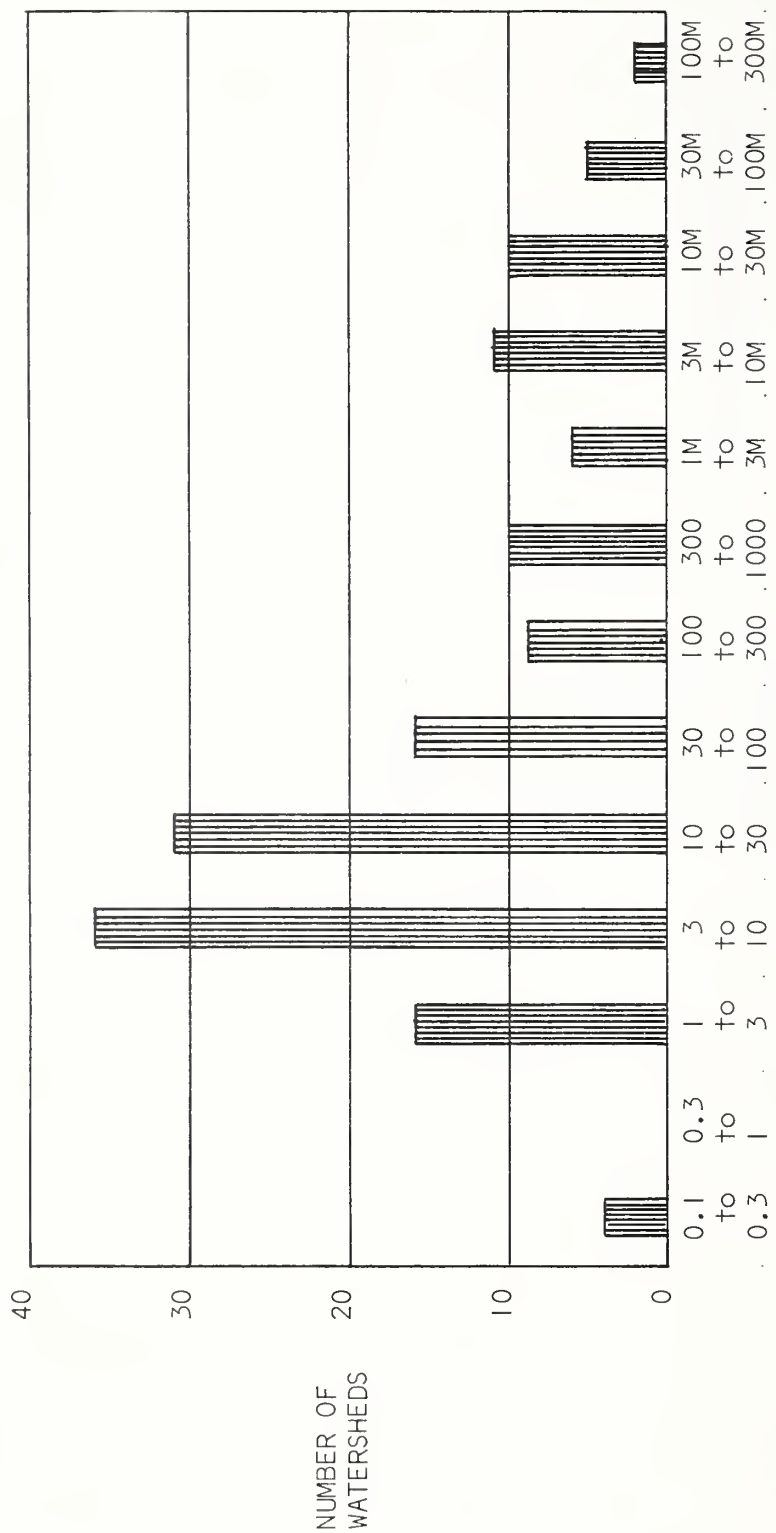

Figure 3 Distribution of all watersheds, past and present, in the Southern Plains Branch by size, acres.

How well has the watershed research program in the Southern Plains Branch met the need for runoff data by the Soil Conservation Service? A study of the detailed research needs statement of 1963 (the latest available) shows a number of land research areas with an A priority need for rainfall-runoff data correlation. These land resource areas are shown on figure 4. When this map is compared with the map on figure 1, it is found that 12 of the locations for which some runoff data are available fall in the area of need. The situation may have changed since 1963 because of data obtained since then. Still there is evidence that the research program has not yet filled the need for runoff data in the Southern Plains Branch.

Runoff Experiment Design

Since this is a meeting on watershed modeling, it will be appropriate to examine past and current watershed research to determine the model which governed the design of the experiment. The nature of the models for the earlier watersheds will be deduced from the design.

The earliest watersheds were at Spur, Texas, a conservation experiment station. Nine watersheds, ranging in size from 3.5 to 11.7 acres, were operated there for 15 or more years. It is evident that the objective was to determine the effect of different cultivation practices on runoff. The model was that runoff is a function of cultural practices. The experimental design was replication and comparison. Three watersheds were established for each of three selected cultural practices. Rainfall and runoff were measured. A praiseworthy feature of this study was the use of replication. Later studies at other locations seldom had this feature, and this is regrettable. The results of the Spur experiment are given in the following table:

Table 3.--Average runoff for the period of record for the Spur watersheds, grouped by cultural practice

Cultivated Straight Row	Cultivated Terraced	Cultivated Contour Row
(in.)	(in.)	(in.)
2.70	1.56	1.93
1.21	1.87	.39
1.35	2.00	.59
mean 1.75	1.81	0.97

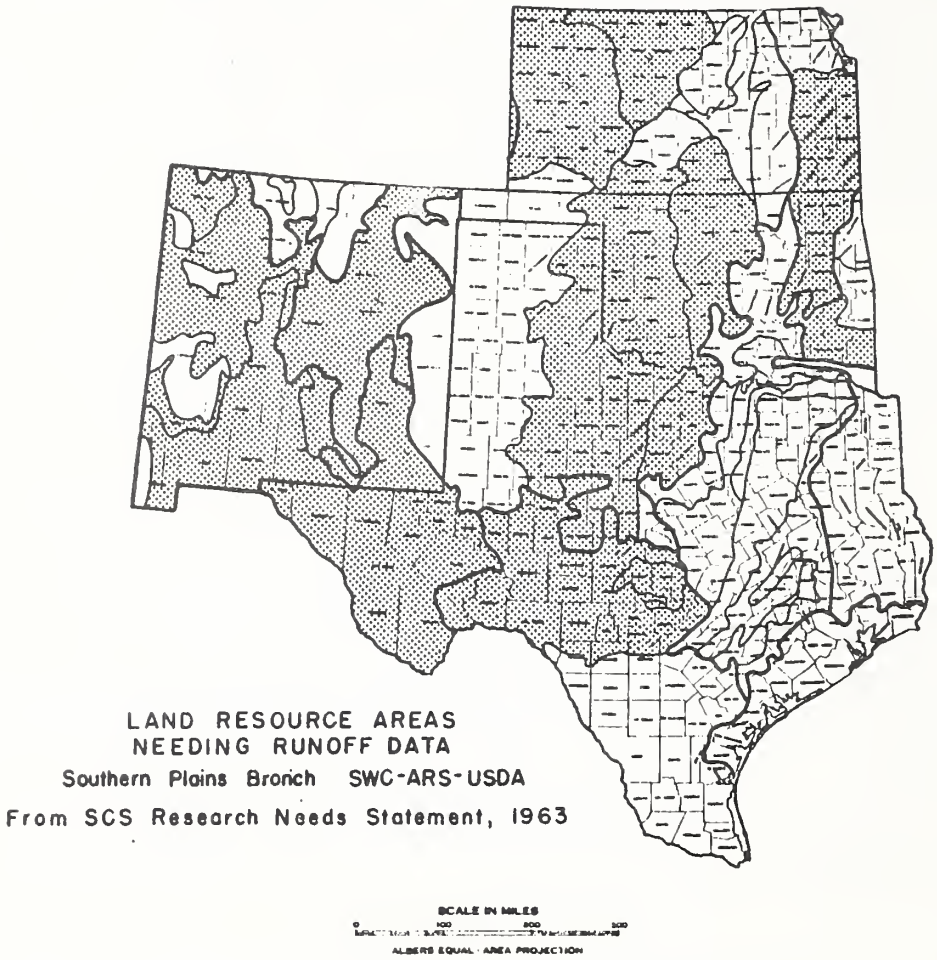

Figure 4 Land resource areas in the Southern Plains Branch designated A priority need for rainfall-runoff correlation, survey of 1963.

Evident immediately is the considerable variation in runoff amounts for a single cultural practice. The contour row watersheds had the lowest mean runoff yet included one watershed with a runoff amount exceeding the mean runoff from the other two groups. This indicates that watershed differences had as great an effect on runoff as treatment differences. This is not news, but it is well to mention it at this time for whatever bearing it might have on model design.

The first Guthrie, Oklahoma watersheds were established in 1930 and 1931. This was a comparison type experiment having five watersheds, each with a different treatment. The early model was simply that runoff is a percentage of rainfall. The objective appeared to be to determine the effect of various conservation treatments on runoff. Additional watersheds established in 1942 were replicated.

It wasn't until 1937 and the establishment of the watersheds at Mexican Springs, New Mexico and Riesel, Texas, that the idea of a complex model became evident. Each project had watersheds in tandem covering a range of sizes.

The Riesel project included unit source areas within the experimental watersheds. Apparently, data were to be obtained to test or to develop models for predicting runoff from composite watersheds and for flood routing. The Riesel model will be discussed in greater detail by Walter Knisel.

In 1938 and 1939, watersheds were established at Vega and Garland, Texas, Muskogee, Oklahoma, and Albuquerque and Santa Fe, New Mexico. The size range for these watersheds was from 10 to 790 acres. Detailed soil surveys were made and soil profiles determined. Close interval contour maps were made. Instrumentation was carefully engineered. These watersheds were to supply high quality, basic data for the testing of models to be developed. No replications were provided. Land use and size were variables for the Vega, Garland, and Muskogee watersheds. At Albuquerque and Santa Fe, cover was the same for all watersheds at each location and size was the variable.

The next watersheds to be established were the nine small ones at Cherokee, Oklahoma. The objective here was to determine influence of various wheat tillage practices on the rainfall-runoff relation. The model was simply that runoff is a percentage of rainfall. This was a replicated experiment with three watersheds in each of three treatments. The

treatments were rotated with the treatment changing each year for each watershed. This rotation scheme was adopted to cope with inherent watershed differences and annual rainfall differences. The experiment was continued for 10 years, so each watershed was subjected to three full rotations.

The results of the study were evaluated by comparing precipitation retentions, P-Q, for the three treatments. The results were:

Table 4.--Average annual precipitation retention for a 10-year period for nine Wheatland watersheds at Cherokee, Oklahoma

Treatment	Mean Annual Retention
	(inches)
Disc plowing	22.88
Stubble mulch tillage	21.96
Basin listing	22.87

The differences between means are not significant. The greatest difference between means was 0.92 inches, whereas it would require a difference of at least 2.20 inches to be significant at the 10 percent level.

The Stillwater, Oklahoma watersheds were established in 1951. Their purpose was to test the use of highway culverts for runoff measurement. There was no hydrologic model involved in the design of the experiment. However, the watersheds were carefully selected for uniformity of cover. All are in native grass, most of the grass is grazed, but some is cut for hay. One watershed, 206 acres in extent, includes 3 ponds which intercept the drainage from 40 acres. A computation scheme, or model if you prefer, has been developed to account for ponds interception of runoff. A recent addition to the small, 16.7 acre, watershed has been a sediment sampler. This is part of an experiment to determine the effect of grazing level on sediment production. Current thinking is that water runoff can be increased by heavy grazing. Can this effect be used to maximize both beef and water production? Sediment production and grass survival are the constraints on this scheme.

The watersheds at Santa Rosa, New Mexico, Sonora, Texas, Chickasha, Oklahoma, and Ft. Stanton, New Mexico have been established since 1955. These will be discussed by others.

Watershed research in the Southern Plains Branch in the future likely will be directed toward the study of the hydrology of grassland areas. Pollution control will also be given considerable attention and is expected to influence the watershed program. May new models come out of this meeting which will help in the design of these new experiments as well as provide better predictions of runoff.

PREDICTION OF SOIL MOISTURE FROM RAINFALL AND PAN EVAPORATION RECORDS[1/]

M. A. Hartman[2/]

In making estimates of flood runoff from ungaged watersheds the amount of soil moisture is a most significant factor, for it is an indicator of the amount of rainfall that can be retained on a watershed. The purpose of this paper is to describe an accounting procedure for estimating soil moisture which requires that only daily rainfall and daily evaporation as measured in an evaporation pan be available. The procedure is based on development of rates of soil moisture dissipation from research data at the Blacklands Experimental Watershed near Riesel, Texas.

Soil moisture dissipation, as used here, is the soil moisture used or lost from the upper three feet of soil by evaporation, transpiration, and deep percolation and as influenced by capillary movement of water from temporary perched water tables. Soil moisture dissipation differs from consumptive use (1), evapotranspiration (5,6,8) or potential evapotranspiration (9) because of the opportunity or availability of water for evapotranspiration, deep percolation and capillary movement.

The change in soil moisture dissipation can be expressed by a decay type curve, that is, a curve decreasing in a manner such that the incremental change is directly proportional to the amount of soil moisture. The amount of water dissipated progressively declines with decreases in opportunity for depletion as indicated by the available soil moisture (7). This type of curve can be expressed by the equation:

$$SM_t = SM_o K^t \qquad (1)$$

[1/] Contribution from the Southern Plains Branch, Soil and Water Conservation Research Division, Agricultural Research Service, U. S. Department of Agriculture, Chickasha, Oklahoma, in cooperation with the Oklahoma Agricultural Experiment Station. For presentation at the ARS-SWC Workshop on Hydrologic Models, Tucson, Arizona, March 16-19, 1970.

[2/] Hydraulic Engineer, U. S. Department of Agriculture, Chickasha, Oklahoma.

Where:

SM_t = soil moisture above 18 percent in top 3 feet of soil t days after the last observation. (inches)

t = number of days since last observation

SM_o = soil moisture above 18 percent in top 3 feet of soil at last observation. (inches)

K = the dissipation constant or ratio of the soil moisture on any day to the previous day's soil moisture

Using the parameters of rates of soil moisture dissipation, amount of soil moisture, and pan evaporation developed for the various periods between sampling dates, a number of relationships were tested by multiple regression methods. The most satisfactory were the seasonal relationships developed for these parameters. The equations for the relationships of native grass meadow at Riesel, Texas are:

$$K_s = 0.982 + 0.005\ SM_o - 0.289\ PE \qquad (2)$$

$$K_w = 0.9922 + 0.002\ SM_o - 0.145\ PE \qquad (3)$$

Where:

K_s = dissipation constant for March to October

K_w = dissipation constant for October to March

SM_o = as previously defined

PE = average daily pan evaporation for the period. (inches)

In these runoff studies, runoff is treated as a residual of rainfall; i.e., the amount of daily runoff is the difference between daily rainfall and the daily amount of abstractions or retentions. There is significant correlation between the amount of moisture in the soil before the rain and runoff.

The rainfall retention relationship with a third parameter, soil moisture, was found to be a hyperbolic function. One form of this relationship can be expressed

$$Q = P - \frac{P}{a + bP} \qquad (4)$$

Where:

Q = daily runoff in inches
P = daily rainfall in inches

a and b = constants determined from the following general equations:

$$b = \frac{1}{b_1 - a_1 SM} \tag{5}$$

$$a = 1 - bP_1 \tag{6}$$

Where:

P_1 = inches of daily rainfall that can be retained with no runoff.
SM = inches of soil moisture above 18 percent in top 3 feet of soil. (Also referred to as the Soil Moisture Index)
a_1 and b_1 = constants determined from recorded rainfall, runoff and soil moisture data for soil and land use complexes.

The parameter P_1 is also related to soil moisture

$$P_1 = a_2 + b_2 \, SM \tag{7}$$

Where:

a_2 and b_2 = constants determined from recorded data. (Soil Moisture Index vs Inches Rainfall for events when runoff was greater than zero but less than 0.03 inch.)

The value of b is determined from recorded data for various soil and land use complexes by solving equation (4) for b after substituting equation (6) for a.

$$b = \frac{\frac{P}{P-Q} - 1}{P-P_1} \tag{8}$$

This b value and its respective soil moisture index are related for the recorded events. This relationship is used to compute the a_1 and b_1 constants in equation (5).

For water budget computations, equation (1) was modified as follows:

$$SM = SM_o K^t + (P-Q) \qquad (9)$$

Sample computations are shown in table 1. Note here that the computations were begun on December 19, 1957, on which date the soil moisture was determined by sampling. Had this sample not been available, satisfactory results could have been obtained by starting the computations at an earlier date with an assumed level of soil moisture.

TABLE 1. COMPUTATION OF SOIL MOISTURE INDEX
Native Grass Meadow, Riesel, Texas

March to October
$K = 0.9821 + 0.005\ SM_o - 0.289\ PE$

October to March
$K = 0.9922 + 0.002\ SM_o - 0.145\ PE$

$SM_t = SM_o K^t$

SM_o = Soil moisture at beginning of period (inches).
SM_t = Soil moisture at end of period (inches).
t = Length of period (days).
K = Dissipation constant.
PE = Average daily pan evaporation (inches).

(1) Date	(2) Days *	(3) Soil moisture** (inches)	(4) Pan evaporation (in/day)	(5) K	(6) K^t	(7) Soil moisture*** (inches)	(8) Rainfall (inches)	(9) Computed runoff (inches)	(10) Rainfall minus runoff (inches)
1957									
Dec. 19		7.76****							
25	6	7.85	0.108	0.992	0.953	7.40	0.50	0.05	0.45
27	2	8.03	.095	.994	.988	7.76	.27	T	.27
1958									
Jan. 12	16	7.64	.130	.990	.852	6.84	.85	.05	.80
13	1	7.56	.150	.986	.986	7.53	.02		.02
19	6	7.91	.073	.997	.982	7.42	.57	.08	.49
20	1	8.19	.090	.995	.995	7.87	.40	.08	.32
22	2	8.14	.085	.996	.992	8.12	.02		.02

* - Number of days since preceding line.
** - Soil moisture at end of day.
*** - Soil moisture when rainfall began.
**** - From sampling data.

PROCEDURE: Columns (1) and (8) are taken from daily rainfall records. In column (2) are the number of days since the preceding date. Column (4) is the average pan evaporation for the period taken from daily evaporation data. The first item in column (3) was taken from soil moisture sampling data. It may be an estimate based on preceding rainfall and growing conditions. (If an estimate, a period for six months prior to the date of interest should be computed. This will allow for the compensation of the error in the original estimate). The dissipation constant (K) in column (5) is computed by the soil moisture from the preceding date, column (3) and the average pan evaporation for the period, column (4); these values are used in the appropriate seasonal formulas for K shown at the top of the page. The dissipation constant is raised to the power equal to the number of days in the period and shown in column (6). Column (7) is the product of column (6) and the soil moisture at the beginning of the period which is column (3) on the preceding line. The runoff in column (9) is estimated on Figure 1 by using rainfall column (8) and the antecedent soil moisture, column (7). Column (10) is rainfall, column (8), minus computed runoff, column (9). The soil moisture at the end of the day, column (3) is the antecedent soil moisture column (7) plus column (10).

REFERENCES

1. Blaney, Harry F., Climate as Index of Irrigation Needs. USDA Yearbook of Agriculture, pp. 341-345, 1958.

2. Bloodgood, Dean W., Patterson, R. E., and Smith, R. L., Jr., Water Evaporation Studies in Texas. Texas Agricultural Experiment Station Bulletin 787, 1954.

3. Court, Arnold, Selection of "Best" Snow Course Points. Proceedings of Western Snow Conference, 1958.

4. Linsley, Kohler, and Paulhus, Applied Hydrology. McGraw-Hill Company, 1st Edition, pp. 419-423.

5. Penman, H. L., Natural Evaporation from Water, Bare Soil, and Grass. Proceedings Royal Society, London, 193A: 120-145, 1948.

6. Skinner, T. C., Climatic Influences on Crop Requirements. Journal of Irrigation and Drainage Division, ASAE, Vol. 83, No. IB2, September 1957.

7. Slayter, R. O., Evaporation in Relation to Soil Moisture. Netherlands Journal of Agricultural Science, Vol. 1, pp. 73-76, 1956.

8. Thornthwaite, C. W. An Approach Toward a Rational Classification of Climate. Geographical Review, pp. 55-94, 1948.

9. Thornthwaite, C. W., and Mather, J. R. The Water Budget and Its Use in Irrigation. USDA Yearbook of Agriculture, 1955.

WATER CONSERVATION STRUCTURES LABORATORY, STILLWATER, OKLAHOMA WITH EMPHASIS ON HYDRAULIC SIMULATION AND TESTING OF WATERSHED MODEL COMPONENTS[1/]

D. K. McCool[2/]

The outdoor hydraulic laboratory was established in 1940 at Stillwater for the purpose of conducting research on the hydraulics and erosion resistance of grassed outlets. Over the years the mission of the laboratory has changed to meet changing needs for hydraulic research. Current active projects include those on rate measuring structures, trash racks for drop inlets, drop inlet transitions, spatially varied flow with increasing discharge, and specific hydraulic model studies for the Soil Conservation Service.

The facilities include three model basins supplied by siphons from Lake Carl Blackwell. These basins have been used for such studies as the Virginia V-notch weir studies, the Walnut Gulch flume studies, specific model studies, and trash rack models. A newer model building with a recirculating water system can be used year-round and will enable more efficient testing. During part of the year testing is impractical or impossible with the exposed siphon system. To date, the new model building has been used solely for specific model studies.

The siphons can furnish flow as large as 165 cfs for large-scale outdoor experiments. Among the active large-scale experimental setups is the pipe outlet pool where hooded inlet, drop inlet, air demand, and drop inlet trash rack studies have been conducted. Another active experimental setup is the spatially varied flow facility, where tests on steady and unsteady spatially varied flows, with steady and unsteady base

---

1/ Contribution from the Southern Plains Branch, Soil and Water Conservation Research Division, Agricultural Research Service, U. S. Department of Agriculture, Stillwater, Oklahoma, in cooperation with the Oklahoma Agricultural Experiment Station. For presentation at the ARS-SWC Workshop on Hydrologic Models, Tucson, Arizona, March 16-19, 1970.

2/ Agricultural Engineer, U. S. Department of Agriculture Stillwater, Oklahoma.

flows, are conducted. The facility has also been used to obtain resistance values and velocity distribution coefficient values for the bermudagrass lining, as well as to obtain wave celerity values. The experimental setup consists of a 400-foot long asymmetrical, V-shaped, bermudagrass-lined test channel with bottom slope of 0.1 percent and maximum depth of 2.7 feet. Free outfall occurs at the outlet end of the channel; however, a gate is provided to control water level elevation at the outlet. Total system capacity is about 40 cfs.

Another outdoor testing facility is the unit channel area. This consists of 8 side-by-side channels 3 feet wide separated by concrete cut-off walls on which vertical walls can be mounted. The channels are 96 feet long with 5 percent bottom slope. This facility has been used for testing the hydraulic properties and erosion protective abilities of newly-emergent annual vegetation as well as for overland flow experiments.

Other outdoor facilities include various channels used in grassed outlet and artificial channel liner research.

The first work on modeling of watershed components was conducted at the old Spartanburg Laboratory and was reported by W. O. Ree in 1939 in the paper "Some Experiments on Shallow Flows over a Grassed Slope." It related some experiments which involved flow down a bermudagrass-lined trapezoidal shaped channel on a 3-percent slope. Five flows were passed down the channel. In the first 4 tests the water depth was less than the thickness of the vegetal mat. The fifth test flow submerged about 30 percent of the cover.

The data were analyzed by applying Horton's overland flow equation:

$$q = K \delta_a^M$$

where

q = direct surface-runoff rate
δ_a = average depth of surface detention
K = coefficient depending on slope and characteristics of the surface
M = exponent depending on the degree of turbulence in the flow.

The flow was found to be nearly 100 percent turbulent, giving an M value of 5/3. The resulting overland flow equation was

$$q_a = 1420\ \delta_a^{5/3}$$

During the 40's and 50's no work was done strictly for watershed modeling, but a great deal of information on friction factors for vegetation-lined channels was gained. Included were many low flow tests in wide channels. This information is necessary in the hydraulic approach to watershed modeling.

In the early 60's a renewed interest developed in applying the laws of physics to the study of runoff. Specifically, this amounted to a simultaneous solution of a dynamic equation, such as a momentum derived equation, and the continuity equation.

One of the first experiments at the outdoor hydraulic laboratory to evaluate the new concepts was conducted in the unit channel experimental setup. These were a cooperative effort of the outdoor hydraulic laboratory and the Agricultural Engineering Department at Oklahoma State University. The experimental setup consisted of a sprinkler system set up over one experimental channel. A flat concrete channel with 3 sizes of pea gravel glued to the surface was tested under steady flow conditions. Three types of steady flows were conducted:

1. Uniform flows introduced at the upper end of the channel,
2. Simulated rainfall applied over the channel,
3. Combination uniform flow and simulated rainfall.

It was found that the equation for uniform flow in wide open channels

$$y = \frac{fu^2}{8gS_o}$$

where

y = depth of flow
f = Darcy-Weisbach resistance coefficient
u = velocity
g = local gravitational acceleration
S_o = channel slope

was satisfactory for the calculation of profiles of steady overland flow over steep, rough surfaces.

Later experiments were conducted on the same facility with artificial grass installed on the concrete surface. The testing included the unsteady state. The data analysis is not complete.

In 1962 the spatially varied flow experimental setup was constructed. The purpose of the experiment was to utilize the continuity and momentum equations to predict the flow profiles and outflow rates in terrace and diversion channels where channel storage, ignored in conventional design methods, can be of importance.

The original setup was best suited to steady flows because of the instrumentation and the method of introduction of inflow. The steady state testing was essentially completed in 1965. This phase of the project was terminated by McCool's thesis Spatially Varied Steady Flow in a Vegetated Channel. It was found that the momentum theory gave a good prediction of the water surface profiles obtained experimentally if the uniform flow resistance could be accurately predicted.

The spatially varied flow setup was altered considerably in 1966 to give more diversity. It is now possible to conduct tests with steady or unsteady spatially varied flow entering the channel when it is conveying a steady or unsteady base flow. Tests have been conducted on all of the different possible flow combinations but the data analysis is not complete.

Wave celerity experiments were conducted in the spatially varied flow experimental setup by using an outlet control to create a uniform flow condition and by increasing the inflow sharply at the flume where the base flow is sent down the channel. These experiments were conducted in the fall of 1969 and the data analysis is not yet complete.

Future work on watershed modeling at the outdoor hydraulic laboratory might include more work on the unit channel facility. A rainulator was obtained some time ago and could be set up over the site. The clean water facilities at the recirculating model basin could be used in research with simulated rainfall on sloping surfaces. The spatially varied flow experimental setup could be altered in vegetation and configuration.

RIESEL AND SONORA, TEXAS, WATERSHED MODELS[1/]

Walter G. Knisel, Jr. and Monroe A. Hartman[2/]

Hydrologic measurements are being made at Riesel and Sonora, Texas, to provide basic data for hydrologic models of two land resource areas. The studies at Riesel were established in 1936 on 841 acres of government owned land and 5,000 acres of adjacent privately owned land. The experimental area is representative of the Blackland Prairie of Texas. The Sonora study area was selected in 1961 as representative of the Edwards Plateau of Texas. Measurements are made on a 48-square-mile area, 70 percent of which is controlled by Soil Conservation Service flood detention reservoirs.

The Riesel Model

The layout of experimental watersheds at Riesel, Texas, was made on the basis of subdivided areas. The size of drainages ranged from 20 to 5,860 acres. The tandem arrangement of watersheds is shown in a schematic drawing, figure 1.

The tandem arrangement of watersheds provided a flood routing model which started with 20-acre areas and built up to 40's, 80's, 100's, 300's, etc., to the 5,860-acre watershed. In addition to offering flood routing capabilities, the tandem arrangement of watersheds provided a water yield model for computing the runoff as a percentage of rainfall for the small areas and building up to the large areas. These models provided data for analyses of peak rate and water yield. Measurements of sediment yield on some of the watersheds provided a sediment yield and routing model by building from the smaller to the larger areas.

[1/] Contribution from the Southern Plains Branch, Soil and Water Conservation Research Division, Agricultural Research Service, U. S. Department of Agriculture, Riesel, Texas, in cooperation with the Texas Agricultural Experiment Station. For presentation at the ARS-SWC Workshop on Hydrologic Models, Tucson, Arizona, March 16-19, 1970

[2/] Research Hydraulic Engineer, U. S. Department of Agriculture, Riesel, Texas, and Director, U. S. Department of Agriculture, Chickasha, Oklahoma.

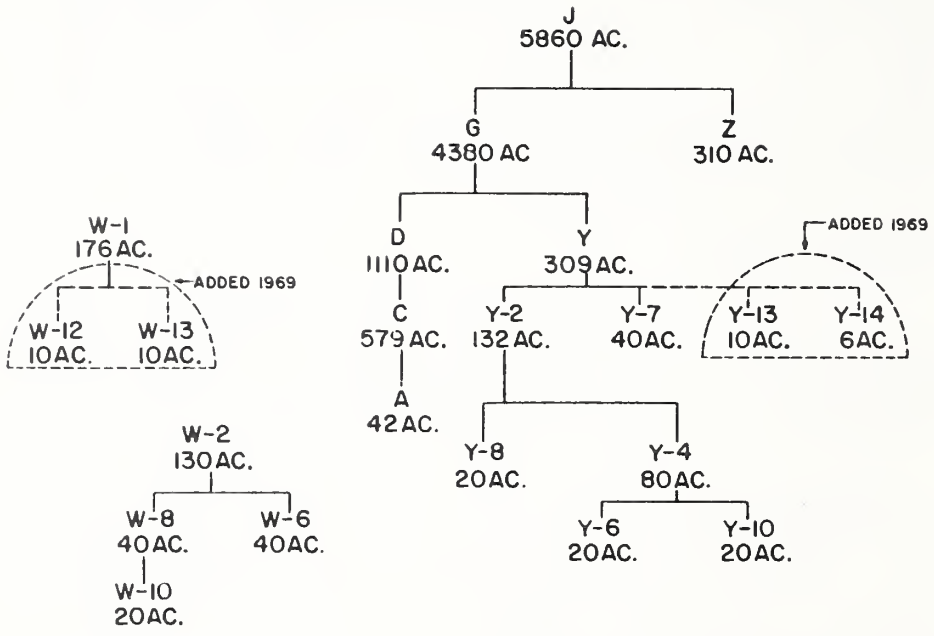

Schematic drawing of tandem arrangement or subdivisions of watersheds at the Blacklands Experimental Watershed, Riesel, Texas.

Figure 1

A paired watershed experiment was developed to test a simple model relating runoff rates and amounts and sediment yield to conservation treatment. In 1942, conservation treatments were applied on the Y drainage area. Y-2 was selected as the primary watershed to compare with the "base" watershed W-1 which was continued as a nonconservation watershed. The paired watershed experiment was also used in the analysis for USDA Tech. Bul. 1022 to determine the effect of conservation practices on peak rates of runoff and in Tech. Bul. 1406, which has just been published, to determine the effects of conservation practices on water yield.

In addition to the subdivided watersheds, four 1/4-acre plots and 14 watersheds, approximately 3 acres in size, were established within the W and Y areas. Data from these single crop watersheds were used in a model that computed ratios of Q/P and the results were applied to the larger mixed land use watersheds.

In 1955 it was realized that the previously mentioned models were not adequate for computations on mixed land use watersheds. At that time the 20-acre watersheds and two 3-acre watersheds were converted to unit source areas; i.e., a single crop each year for the major land uses in the Blacklands of Texas. Data from these watersheds were to be used in the development of a mathematical model for predicting daily runoff using daily climatic data as the input.

Hartman's model provided good estimates of daily runoff, but refinement was necessary. The Knisel-Hartman model expanded from the basic Hartman model by considering two soil water reservoirs with an opportunity for interchange of moisture and deep percolation. Additional climatic data were included in the model input. This model improved the accuracy of estimated water yield from mixed land use watersheds.

The Hartman and Knisel-Hartman models did not consider rates of runoff. A mathematical model was developed by Richardson, whereby rainfall data for increments less than 1 day were used with the infiltration approach. This model, as did Hartman's, considered a soil water reservoir and in the end provided estimates of runoff rates as well as volumes.

In 1969, four new watersheds were instrumented for a paired watershed model in erosion control and tillage effects. The four watersheds are shown on the schematic diagram. The model will test the hypothesis that graded furrow systems are

satisfactory in erosion control as compared with conventional terrace systems. The paired watershed model will also be used to test the hypothesis that deep tillage decreases the water yield over that from conventional tillage.

Graded furrow systems provide a watershed model in spatially varied flow. Each furrow carries its own runoff. Some studies have been made and more planned to determine furrow friction factors for different tillage types and field conditions. Reliable estimates of Manning's n value will provide a spatially varied flow model for graded furrow systems for the development design criteria.

A water quality model is being developed at Riesel. A hillside seep from perched ground water was instrumented for flow measurement. Water samples have been collected for plant nutrient and insecticide determination. These data will be used in the development of the model.

The Sonora Model

Studies began at Sonora, Texas, in 1961 on an SCS PL-566 project. Five reservoirs were instrumented to measure inflow, outflow, and losses from storage. A watershed model was developed to test the hypothesis that flood detention reservoirs significantly affected ground water recharge. A submodel was also developed to test the hypothesis that geologic strata, within the Edwards and associated limestones, have a significant effect on ground water recharge from reservoirs.

Seven unit source rangeland watersheds were instrumented for runoff measurement at Sonora. The seven areas provided a paired watershed model to test two hypotheses: (1) there is a significant difference in runoff from rangeland between good and poor treatment (light and heavy grazing); (2) there is a significant difference in runoff from rangeland between soil sites under the same grazing treatment. The unit source watershed data will be used to develop a runoff prediction model. These data and the runoff model will in turn be used to extrapolate from runoff production on source areas to water yield on the large watersheds above the flood detention reservoirs.

WATERSHED MODEL FOR THE WASHITA RIVER BASIN[1/]

Edward Seely[2/]

The research station at Chickasha, Oklahoma is beginning work on hydrologic simulation of the Washita River basin. The objectives of the research outline are the development of an understanding of hydrologic processes and the use of this knowledge in formulation of an analytic watershed model.

The Washita River model will be used to predict the effects of changes in basin parameters, such as land use and treatment on water use and movement within the basin. The model will also be used to explain the movement of water-borne pollutants within the basin and the relationship of hydrology to geomorphic change.

The model will be made up of analytic components capable of reproducing aspects of the hydrologic cycle. In addition to the distributing mechanisms, there will be generators of synthetic climatological data. The synthetic data will be used to show the effects of changes in basin parameters.

Procedure

Unit source watersheds and watersheds from small uniform hydrologic areas will be used to study mechanisms of surface runoff production by direct prediction from basic data and by use of infiltration and precipitation excess procedures. Data from an infiltrometer will be available for the latter study. The unit source watersheds will also be used to study the development of the flow hydrograph.

Flood routing methods will be investigated to find the best means of describing the development and transformation of the flow hydrograph in the channel and tributaries. The routing method will need to include sufficient detail to route pollutants and describe geomorphic change.

1/ Contribution from the Southern Plains Branch, Soil and Water Conservation Research Division, Agricultural Research Service, U. S. Department of Agriculture, Chickasha, Oklahoma, in cooperation with the Oklahoma Agricultural Experiment Station. For presentation at the ARS-SWC Workshop on Hydrologic Models, Tucson, Arizona, March 16-19, 1970.

2/ Hydraulic Engineering Technician, U. S. Department of Agriculture, Chickasha, Oklahoma.

Base flow studies will be made to insure adequate description of the extended flow portion of the hydrograph.

Climatological data will be examined using the techniques covered in the presentation on stochastic processes and a scheme for developing synthetic sequences of climatological data will be set up. This synthetic data will be used with the model to check the effect of variation in basin parameters on output of the watershed.

Work to Date

Much of the data which will be used has been and is being collected under other outlines. The only work to date on the analytic portions of the model has been preliminary study of two flood routing techniques. The first is an explicit method used by T.V.A. and described by Price, Garrison, and Granju in a paper published in the Hydraulics Journal of ASCE, Vol. 95, No. HY5, Sept. 1969; the second is an implicit method published in Streamflow Routing with Applications to North Carolina Rivers, Jan. 1969, by Michael Amein.

The first method showed little promise because of instability in establishing equilibrium flows and length of time to process routings of flows. In ranges of flow that are normal channel flow for the Washita (100-200 cfs), it was not possible to get equilibrium flow established. Estimates of channel conditions along the reach (elevation and velocity) were made and a constant flow fed into the reach. Oscillations in water level were set up which either increased without limit or converged so slowly as to make running to convergence prohibitive. In larger flows (1,000 cfs), convergence was reached; but because of the time factor on length of run, and the desire to use a method that would accept the range of flows that might be expected from low flow in a tributary to high flow in the main channel, the implicit method was set up and run, using the same data. The establishment of equilibrium flow was made and a trial routing completed. The method is easy to use and seems fairly stable. It will be examined to see if the way the channel geometry is represented can be improved and how critical the parameters such as routing interval and distance between intermediate stations are. Numerical criteria such as maximum difference in routed and actual flow, or average absolute or squared difference at intervals will be investigated along with the parameter studies to see if a more effective way of evaluating the changes in the parameters can be found than the more traditional plot of the routed against the actual flow.

NORTHERN PLAINS BRANCH RESEARCH PROGRAM

RESEARCH AT FORT COLLINS, COLORADO

by David A. Woolhiser

OBJECTIVES

The objective of the research program at Fort Collins is to develop stochastic and deterministic mathematical models of hydrologic systems and to develop simulation as a design technique in watershed engineering. Since 1967 research has been concentrated in the following three areas: (1) overland flow, (2) infiltration and (3) stochastic models of water and sediment yield. All work is cooperative with the Colorado State University Experiment Station.

OVERLAND FLOW

The kinematic wave equations have been used as a mathematical model describing flow over an impervious plane (Fig. 1) and a converging section (section of a cone)(Fig. 2). The plane and the converging section are common, idealized components of watersheds. The plane is also a common element of the kinematic cascade (Fig. 3) which can be used to represent complex slopes and shapes.

The equations describing overland flow on a plane are:

$$\frac{\partial h}{\partial t} + \frac{\partial uh}{\partial x} = q \qquad (1)$$

and

$$u = \alpha h^{N-1} \qquad (2)$$

where

h is local depth, u is the local velocity, x and t are space and time coordinates, q is the lateral inflow rate, α and N are parameters of the normal flow equation. If the Chézy formulation is used $\alpha = C\sqrt{S_o}$ and $N = 3/2$.

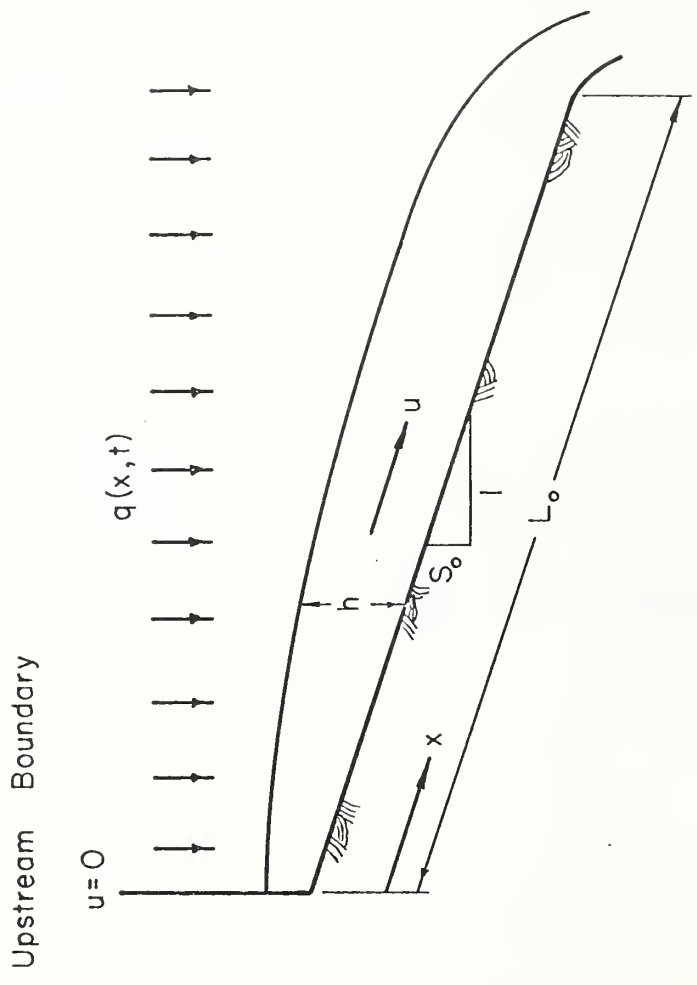

Figure 1. Definition sketch, overland flow.

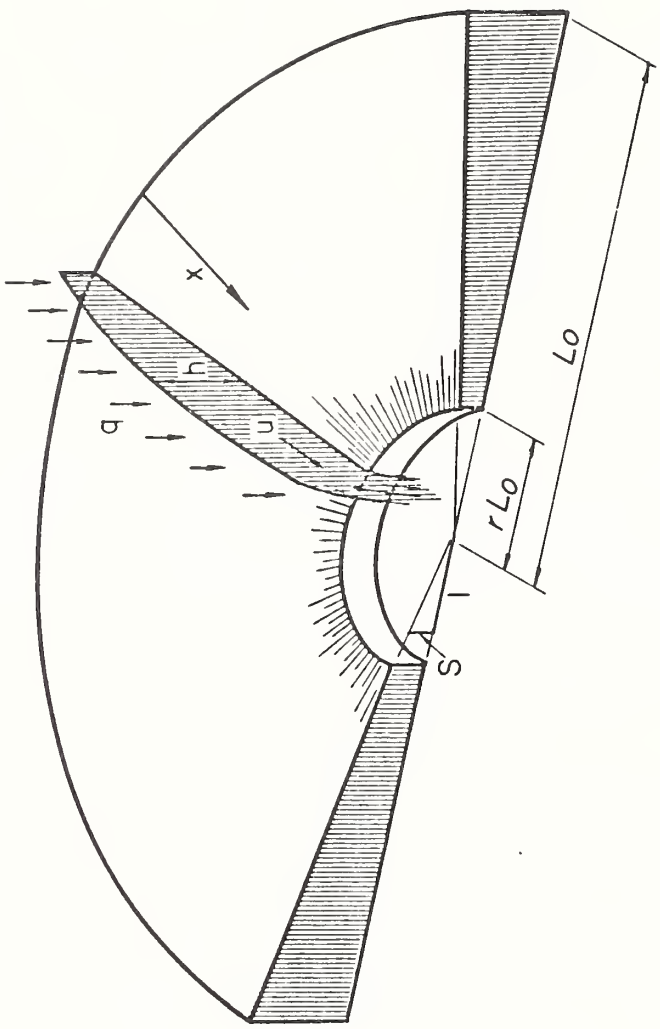

Figure 2. Geometry of Converging Section.

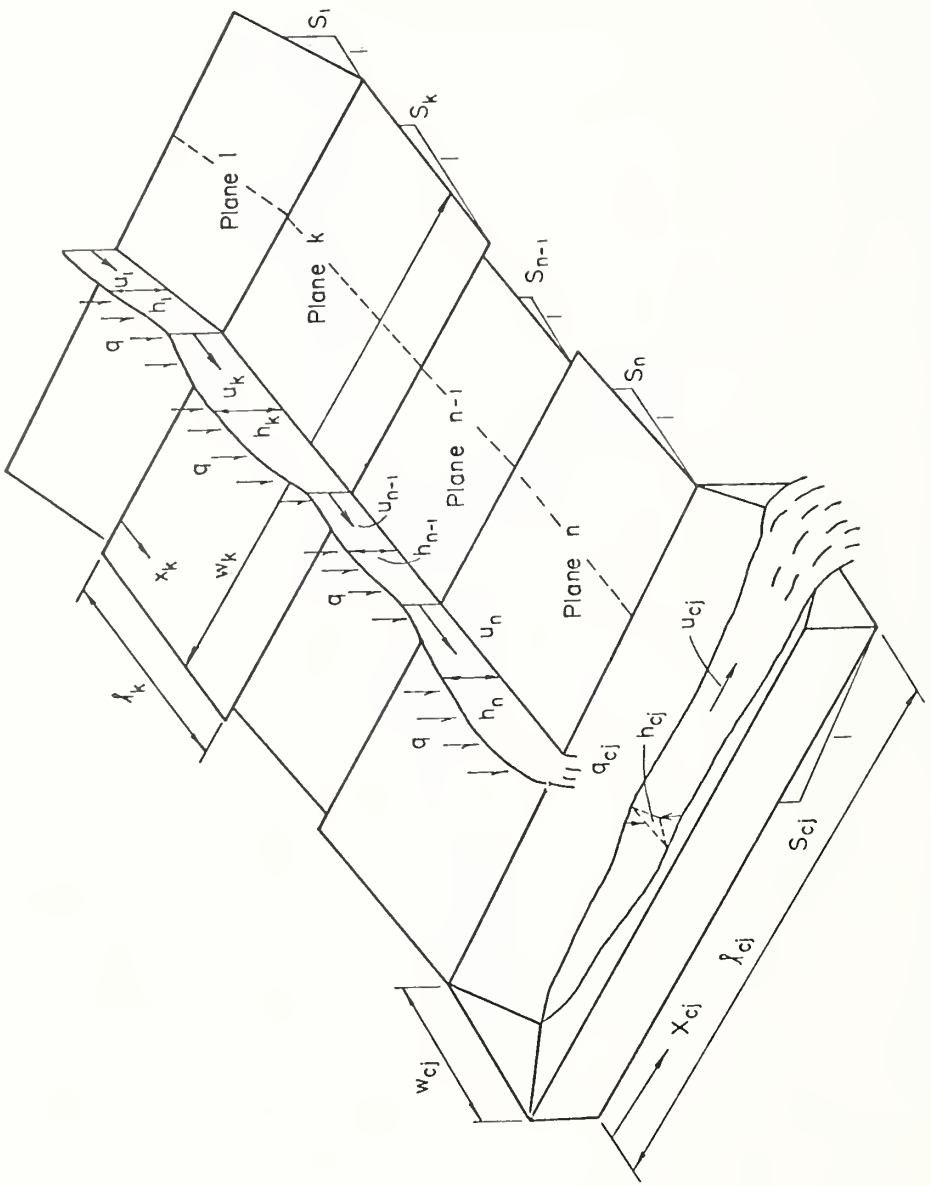

Figure 3. Cascade of n planes discharging into the $j^{\underline{th}}$ channel section.

For flow on a converging surface, the continuity equation becomes:

$$\frac{\partial h}{\partial t} + \frac{\partial uh}{\partial x} = q + \frac{uh}{(L_o - x)} \qquad (3)$$

$$0 \leq x \leq L_o(1-r)$$

where L_o and r are defined in Fig. 2.

The kinematic cascade utilizes equations (1) and (2). The upstream boundary condition for the uppermost plane is

$$h(0,t) = 0$$

but for subsequent planes the upstream boundary condition is specified by the discharge at the downstream boundary of the plane immediately above. This discharge is converted to normal depth for the plane under consideration. For example, if at time t the depth at the lower boundary of plane i is $h(t)_i$, the depth at the upstream boundary of plane $i + 1$ is

$$h(t)_{i+1} = \left(\frac{\alpha_i}{\alpha_{i+1}} \frac{w_i}{w_{i+1}} \right)^{1/N} h(t)_i \qquad (4)$$

where w_i is the width of the i^{th} plane.

The first objective of the research on overland flow was to study the mathematical properties of the equations and to develop accurate numerical techniques for solving them.

It has been shown that the converging section has response characteristics substantially different from that of the plane. When the lateral input is a uniform pulse with a duration shorter than the time to equilibrium, the plane response is a flat-topped hydrograph and the hydrograph from the converging section continues to rise (see Fig. 4). Because the upper reaches of many watersheds exhibit convergence, it may be that a converging component in an overland flow model will improve the agreement between computed and observed hydrographs.

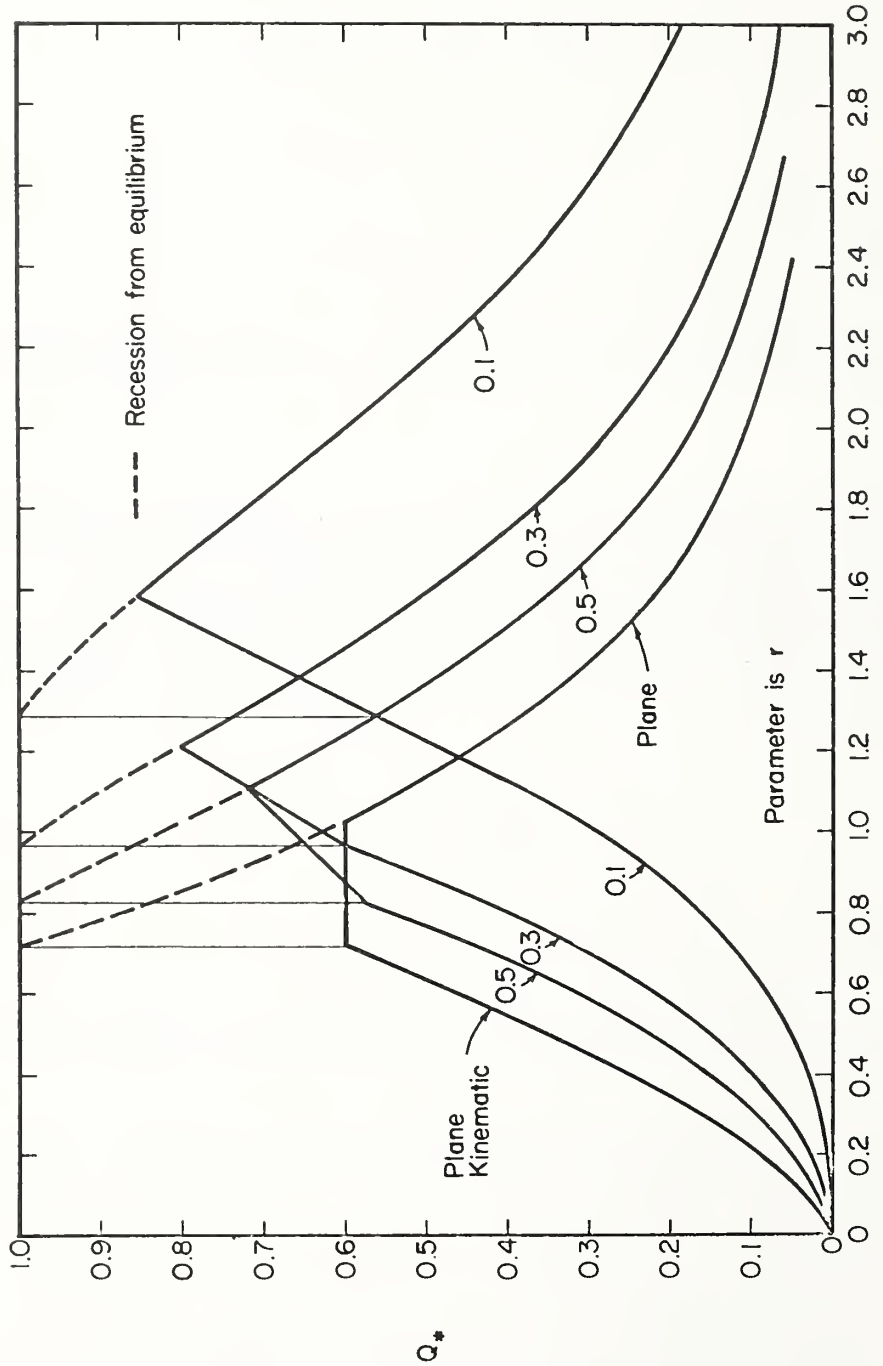

FIG. 4. RISE AND RECESSION FROM PARTIAL EQUILIBRIUM

It has also been discovered that the converging section can be approximated quite accurately with the kinematic cascade, see Fig. 5. These results suggest that the overland flow plane can be used as the basic element along with channels in a surface runoff model.

A second-order finite-difference scheme known as the single-step Lax-Wendroff method was found to be superior to other commonly used rectangular grid finite-difference methods.

The second objective of the overland flow research is to apply the kinematic model to real situations of increasing complexity. At each step the problem of parameter estimation would be considered. Also various geometric simplifications would be attempted to see if we can develop an objective technique for simplifying watershed geometry.

A series of experimental runs were performed during September and October, 1969 on the Colorado State University Experimental Rainfall-Runoff Facility. A sketch of this facility is shown in Fig. 6. Only the upper converging section was utilized during this study. The primary objective was to test the hypothesis that the kinematic wave equations are an adequate mathematical model for overland flow on a linearly converging surface. A secondary objective was to investigate the effect of spatially nonuniform roughness on the watershed response.

The surface of the watershed was made impervious by covering it with butyl rubber. Roughness was changed by spreading $1\frac{1}{2}$ inch diameter gravel on the butyl surface at a predetermined weight per unit area. Runs were also made with the gravel spread nonuniformly over the surface.

The data from these experiments have not been completely analyzed as yet. However, preliminary indications are that the kinematic model is adequate for converging sections with a 5% slope if we can estimate an appropriate roughness coefficient.

Solutions to the dimensionless form of equation (3) are shown in Figs. 7 and 8 along with a dimensionless plotting of experimental data. Discharge was normalized by dividing by the steady-state discharge. The normalizing time used was estimated from the recession hydrograph by a technique that was equivalent to the selection of an

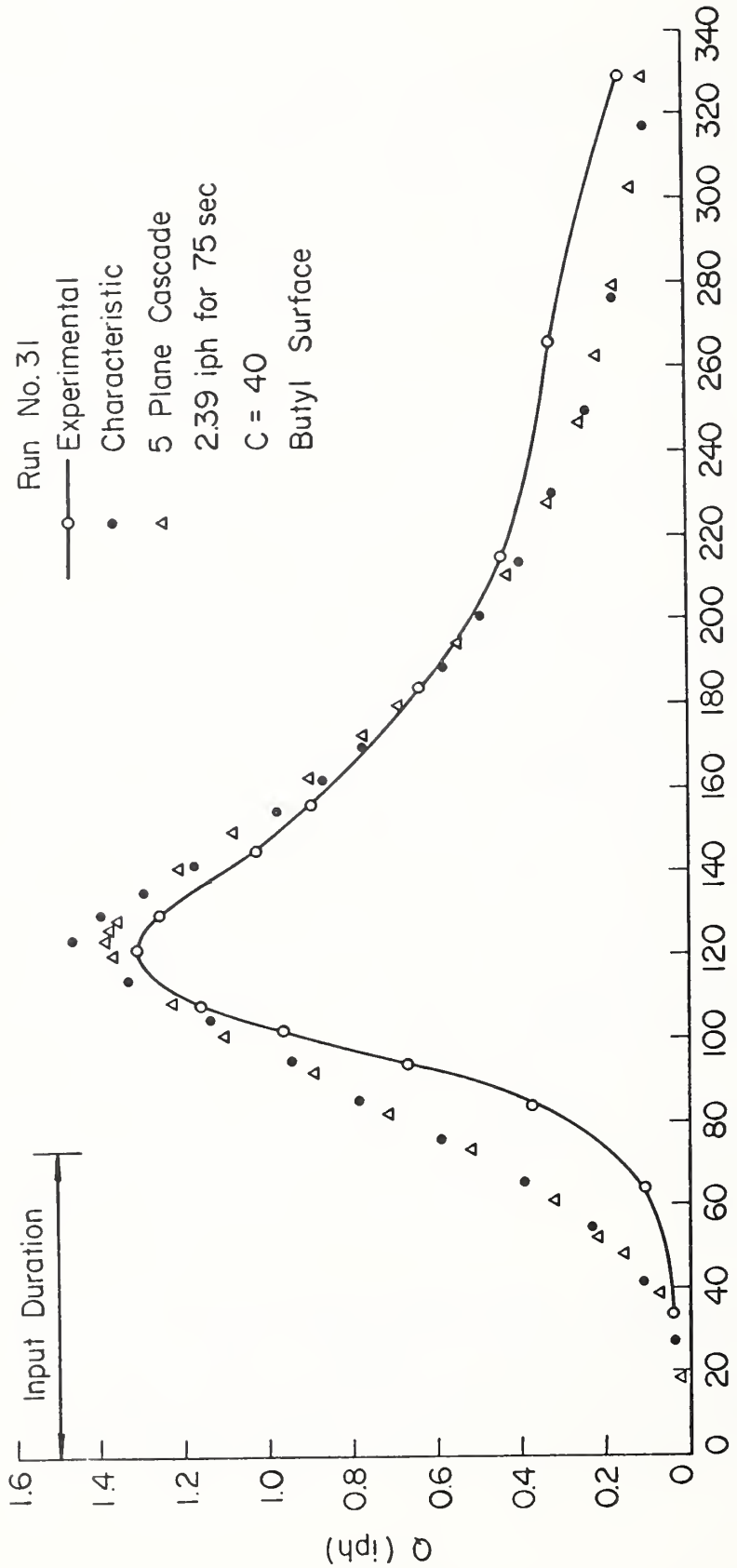

Figure 5. Comparison of kinematic cascade and converging section solutions with experimental data from Colorado State University Experimental Watershed.

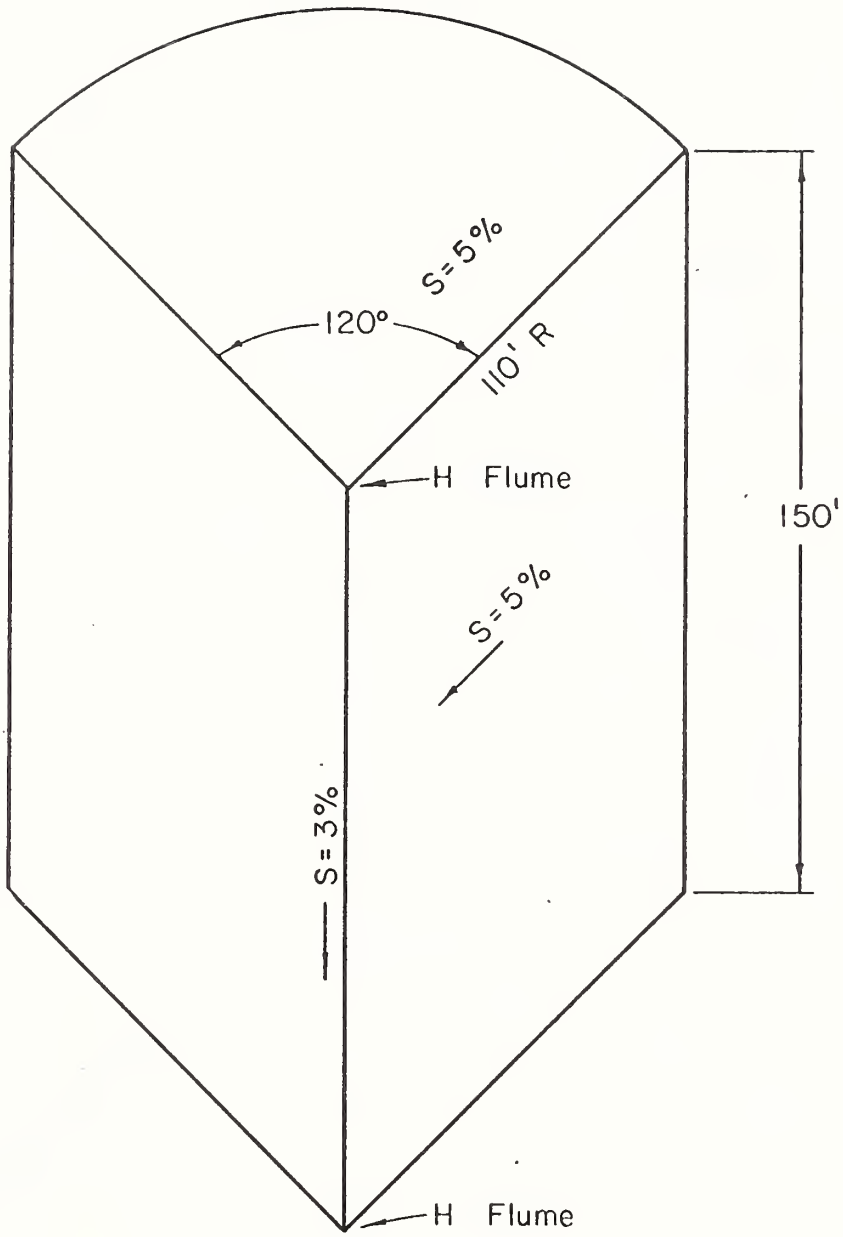

Figure 6. Colorado State University Rainfall-Runoff Facility.

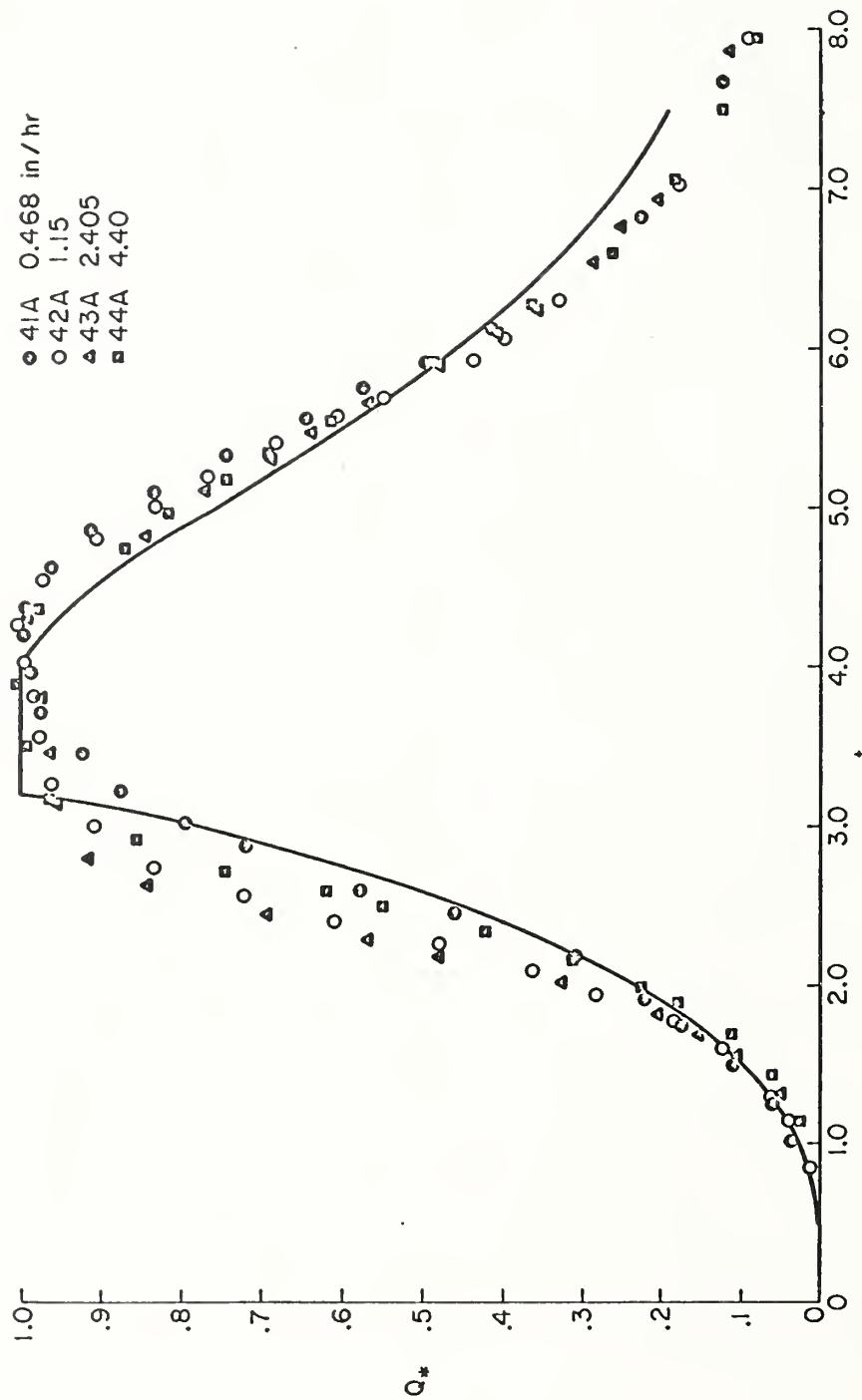

Figure 7. Theoretical and Observed Hydrographs for Graveled Surface

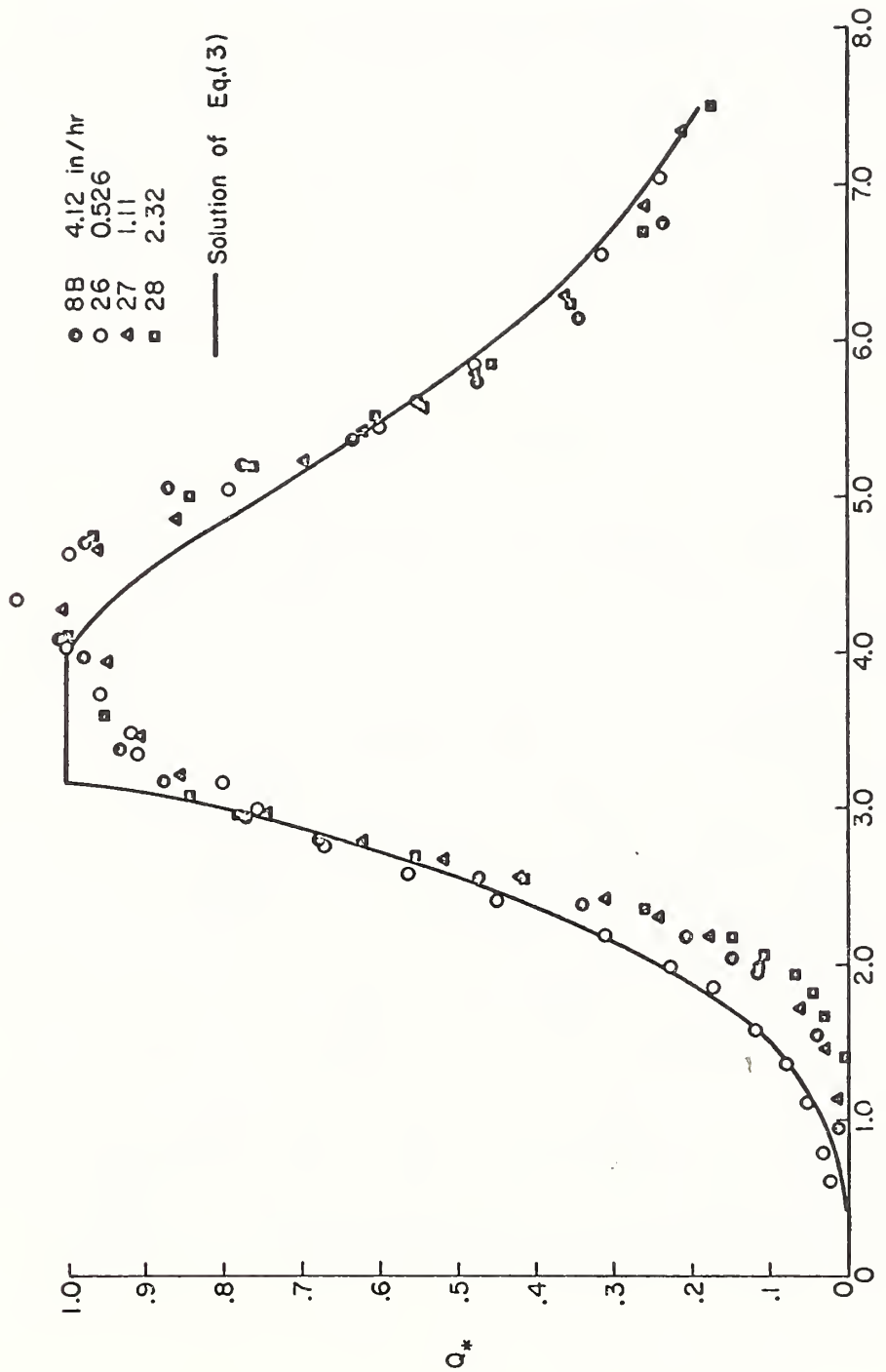

Figure 8. Theoretical and Observed Dimensionless Hydrographs for Butyl Surface

optimized Chézy parameter, C . Agreement between the hydrographs is quite good, however, the estimated Chézy parameter varied with the equilibrium flow rate for the smooth butyl surface.

We are presently analyzing some data from 12, 2-acre watersheds at Cottonwood, South Dakota using the kinematic overland flow model. We have selected a storm with a total duration of nearly eleven hours. We are attempting to simulate the response to a short burst of rainfall near the end of the storm period when infiltration rates are very low (0.10 in./hr.) and can be assumed constant with small errors. An optimized Chézy parameter will be obtained for each watershed. The objective is to get an estimate of the variability of C for relatively similar watersheds as well as to see if this parameter is affected by grazing intensity.

INFILTRATION STUDIES

An infiltration model is an essential element of a general surface runoff model. The work done on overland flow at this location has been concentrated on the special case of an impervious surface in an attempt to gain a thorough understanding of the free surface flow problem. The next logical step is to integrate an infiltration model with the overland flow model to study the interactions and to investigate possible simplifications. Roger E. Smith, Cooperative Graduate Research Assistant, Colorado State University, is responsible for the infiltration studies.

A numerical solution of the partial differential equations describing the flow of water in unsaturated porous media (Richards Equation) has been combined with the numerical solution of the kinematic cascade. A schematic representation of the linkage of these equations is shown in Fig. 9. A slope may be approximated by n planes. Each plane may have a specified number of Δx increments and a different number of vertical infiltration components. The soil may be layered and the layers may show a linear variation in thickness on each plane. Input to the computer program consists of geometrical properties of the planes, roughness coefficients, soil curves, initial conditions and rainfall intensity as a step function of time. Surface runoff begins whenever the surface element at an infiltration node becomes saturated.

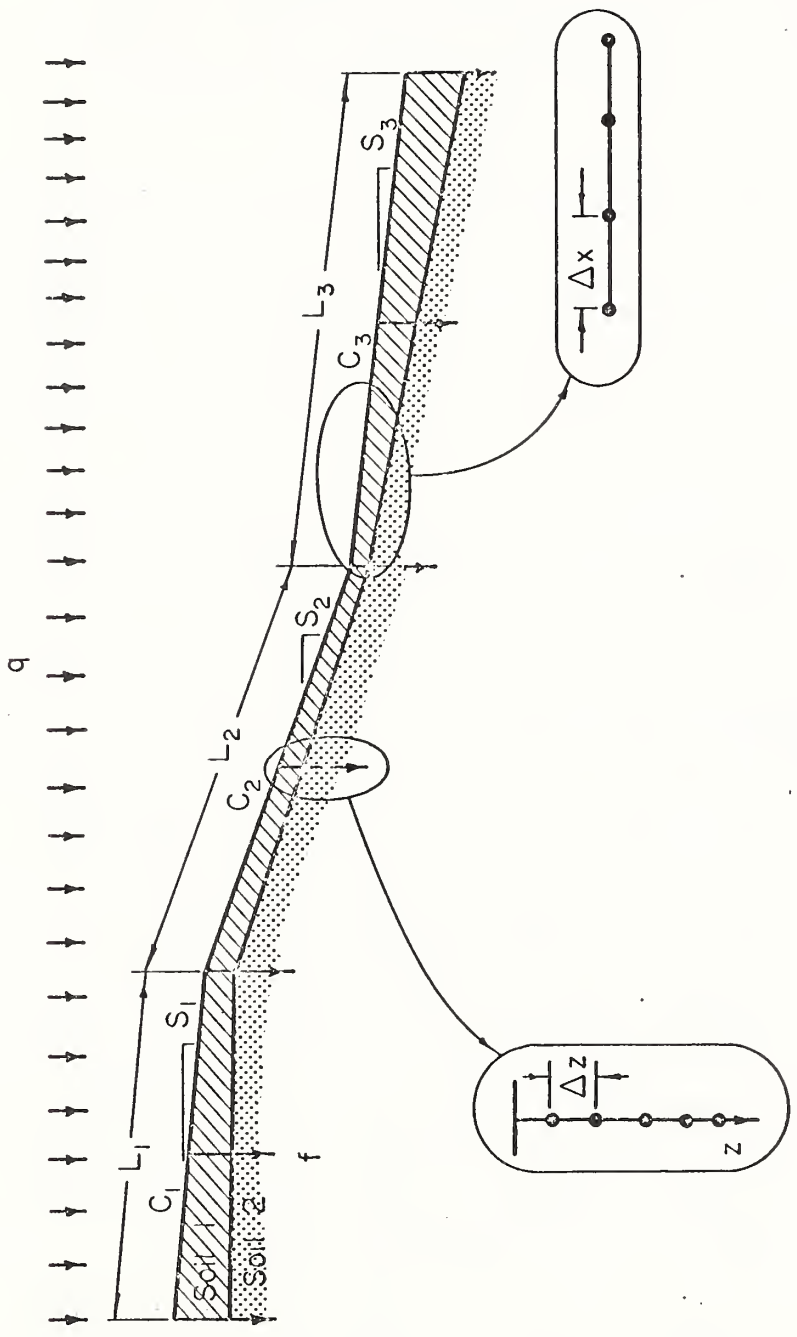

Figure 9. Kinematic cascade with infiltration.

The lateral inflow rate is thus the rainfall rate less the infiltration rate. The kinematic cascade program routes the rainfall excess and computes the hydrograph at the lower boundary. When rainfall stops, infiltration continues at every node as long as surface water is present.

Experimental data have been obtained from a soil flume 40 ft. long, 4 ft. deep and 2 in. wide with lateral inflow added at the surface. Surface runoff was measured at the downstream boundary and soil moisture measurements were obtained at a vertical section with gamma ray apparatus. The objective of these experiments was to test the hypothesis that the kinematic wave formulation and Richards equation are an adequate model for this simple, controlled situation.

Analysis of these data, numerical experiments with the infiltration--overland flow model and simulations of some small watershed runoff events will form the basis of Mr. Smith's Ph.D. dissertation.

STOCHASTIC MODELS OF WATER AND SEDIMENT YIELD

Some theoretical work has been done on the development of formal, stochastic models for runoff and sediment yield from ephemeral streams. Such models are desirable for two reasons. First, we need a model as a basis for analyzing a time series such as observations of annual sediment yield. Any analysis requires a model of some sort, but very often the assumptions and limitations are not made explicit. Secondly, if we have specified a stochastic process with parameters that may be related to climate, soil or to agricultural practices, it is possible to determine the relative importance of these parameters. With this information, land management practices can be designed that are the most effective in controlling water or sediment yield. Stochastic models should also provide valuable insight into the general process and should aid in the design of field and laboratory experiments.

The processes of rainfall, runoff and sediment transport are obviously related. Without rainfall there is no surface runoff, the primary mechanism of sediment transport (snowmelt situations excepted). Raindrop impact is also an important agent in the detachment of soil particles. Rainfall is a stochastic process so the runoff and sediment yield processes are also stochastic.

Consider continuous measurements of precipitation intensity over a watershed and runoff and sediment transport rates at the mouth. Let the instantaneous precipitation rate be ξ_t, the runoff rate be ζ_t and the associated sediment transport rate be η_t. One possible realization of these measurements is shown in Fig. 10. An event is defined as any continuous period of rainfall or surface runoff. In general, there will always be a sediment yield event if there is a surface runoff event, although it is possible to have a rainfall event without an associated runoff event. Because of storage on the watershed, it is possible to have more than one rainfall event associated with a single runoff event. Except for snowmelt runoff, it is not possible to have a surface runoff event without a rainfall event.

Associated with the $i^{\underline{th}}$ rainfall event is the time of ending, τ_i. The times of ending of the runoff events and the sediment transport events coincide and are denoted by T_i. In the time interval $(t - t_o)$ M rainfall events occur and N runoff and sediment transport events occur. In general $M \geq N$. $\{\xi_t ; t \geq t_o\}$, $\{\zeta_t ; t \geq t_o\}$ and $\{\eta_t ; t \geq t_o\}$ are stochastic processes with continuous parameter set and state space.

If observations begin at time t_o, the total amount of precipitation, runoff or sediment yield at time t is given by equations (5), (6), or (7), respectively.

$$\underline{X}_t = x_o + \int_{t_o}^{t} \xi_s \, ds \qquad (5)$$

$$Y_t = y_o + \int_{t_o}^{t} \zeta_s \, ds \qquad (6)$$

$$Z_t = z_o + \int_{t_o}^{t} \eta_s \, ds \qquad (7)$$

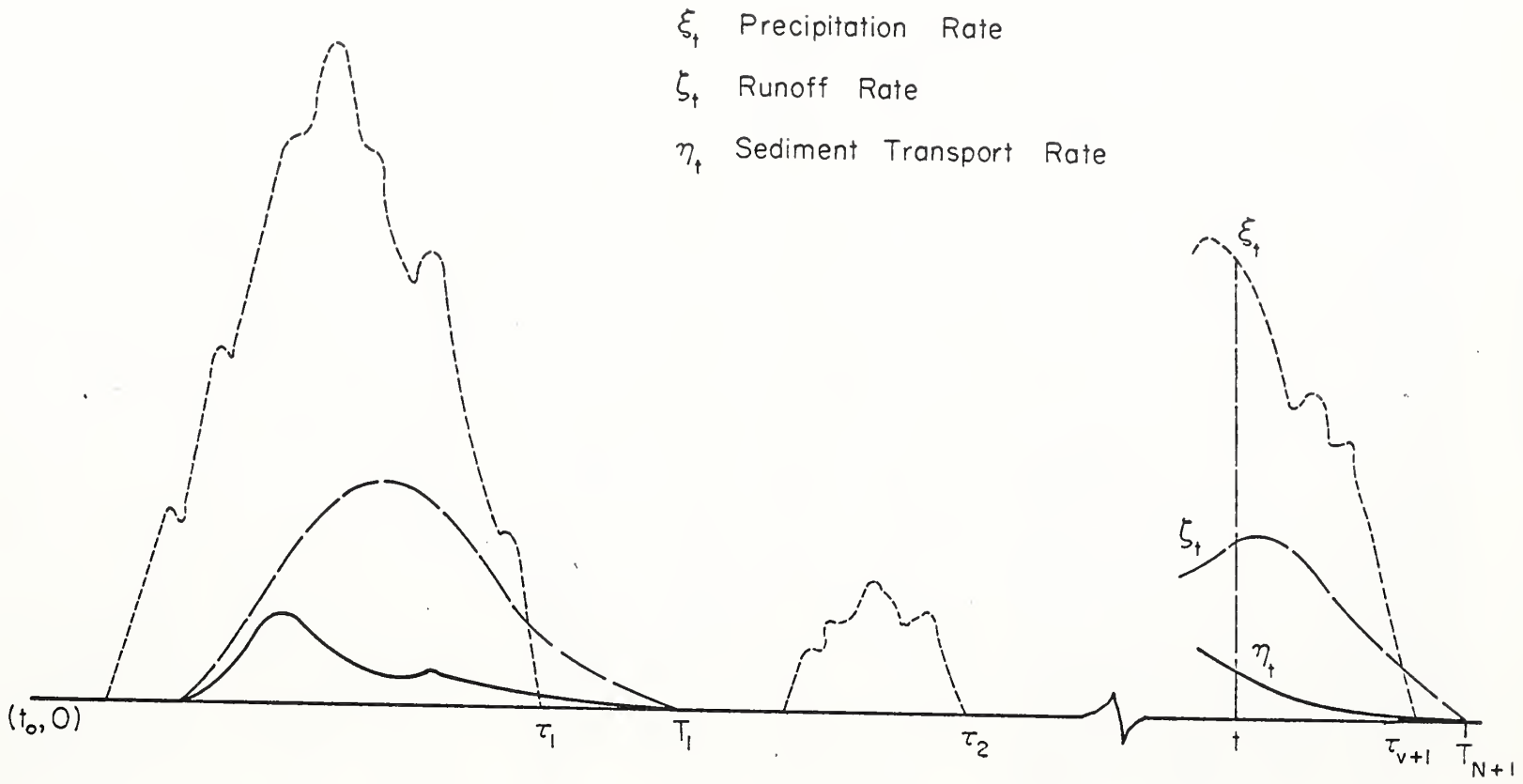

Figure 10. Sample functions of the stochastic processes ξ_t , ζ_t and η_t : $t > t_o$.

Sample functions of these three processes are shown in Fig. 11.

Todorovic* considered the following characteristics of the rainfall process:

M_t the number of precipitation events in (t_o, t)

$\tau_M - t_o$ the time elapsed up to the end of the $M^{\underline{th}}$ storm period

X_M the total amount of precipitation during exactly M storm periods.

P_M the total amount of precipitation during the $M^{\underline{th}}$ storm, and

X_t the total amount of precipitation during the time interval (t_o, t).

For a useful description of the runoff and sediment yield processes we can consider the following characteristics

N_t the counting process defining the number of runoff or sediment yield events in (t_o, t)

V_N the volume of runoff during the $N^{\underline{th}}$ runoff event

S_N the weight of sediment transported past the measuring point during the $N^{\underline{th}}$ event

Y_t the total water yield in the interval (t_o, t)

Z_t the total sediment yield during the interval (t_o, t).

Todorovic's most general expression for the probability mass function of the rainfall counting process M_t is given by the nonhomogeneous Poisson process

$$P\left[M_t - M_{t_o} = M\right] = \exp\left\{-\int_{t_o}^{t} \lambda_1(s)ds\right\} \frac{\left(\int_{t_o}^{t} \lambda_1(s)ds\right)^M}{M!} \qquad (8)$$

*Todorovic, Petar, A Mathematical Study of Precipitation Phenomena, Report No. CET67-68PT65, Engineering Research Center, CSU, Ft. Collins, March 1968.

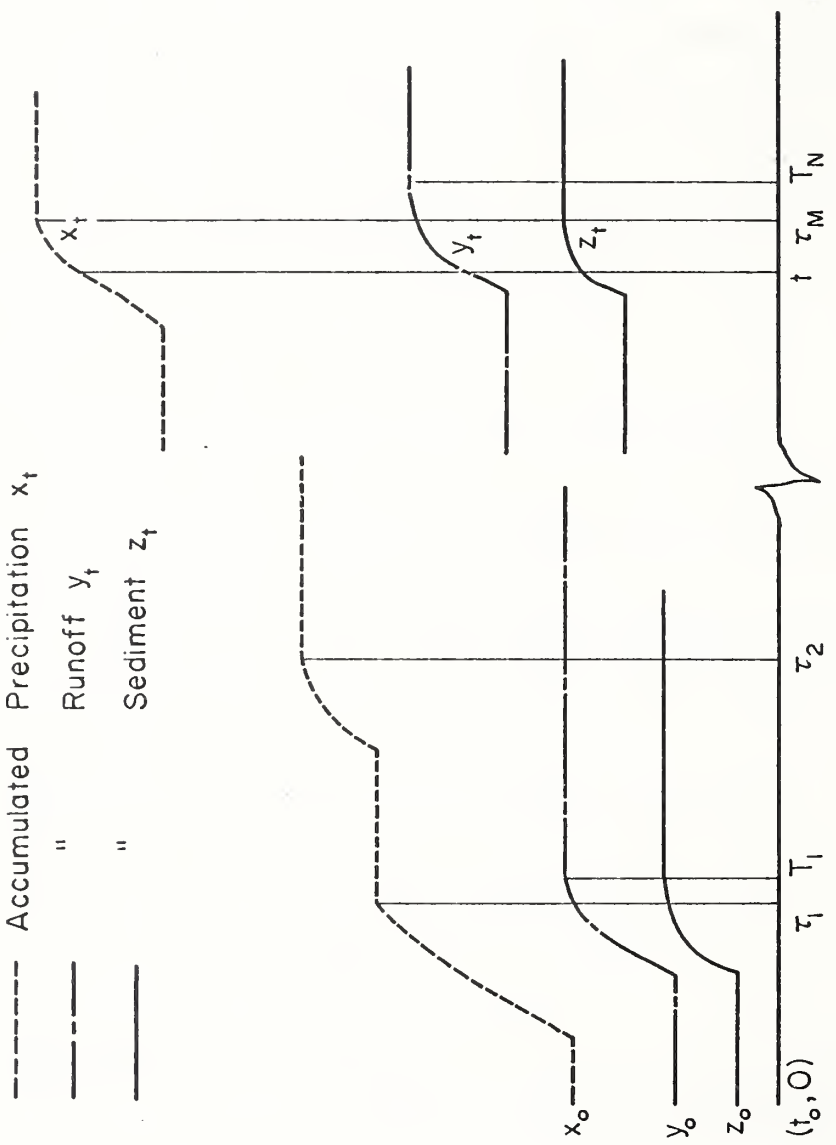

Figure 11. Sample functions of the stochastic processes X_t , Y_t , Z_t .

Where $\lambda_1(t)$ is the intensity function. The intensity function is the derivative of the mean value function m(t) where

$$m(t) = E(M_t)$$

If we assume that long term trends can be neglected $\lambda_1(t)$ will be a periodic function with periods of one year.

Because nonhomogeneous processes are difficult to deal with it is convenient and useful for many purposes to consider the number of events occurring in one year or discrete multiples thereof. The nonhomogeneous process specified by eq. (8) then becomes the homogeneous process

$$P[M_{T+t_o} - M_{t_o} = M] = \exp\{-\bar{\lambda}T\}\frac{(\bar{\lambda}T)^M}{M!} \qquad (9)$$

$$T = 1, 2, 3 \ldots$$

$$\bar{\lambda} = \frac{1}{T}\int_{t_o}^{t_o+T} \lambda_1(s)\, ds$$

$\bar{\lambda}$ can be interpreted as the mean number of events per year.

Work during the past year has been concentrated on finding a general expression for the annual runoff counting process N_T with parameters that are related to the rainfall counting process M_T. One approach that has some rational justification is as follows:

Given that m rainfall events have occurred in time T = 1, the number of runoff events is distributed by the binomial distribution with parameter p .

$$\Pi_n(N/M=m;\ p\ ;\ T=1) = \binom{m}{n} p^n (1-p)^{m-n} \qquad (10)$$

where p is also a random variable with density function f(p) and $0 \le p \le 1$.

The expression for the conditonal density function is

$$\Pi_n(N/M=m;\ T=1) = \binom{m}{n} \int_0^1 p^n (1-p)^{m-n} f(p)dp \qquad (11)$$

The joint mass density function $p(N,M;\ T=1)$ is:

$$p(N,M\ ;\ T=1) = \Pi_n(N/M=m\ ;\ T=1)\ p_m(M\ ;\ T=1) \qquad (12)$$

and the unconditional mass density function for number of runoff events per year is

$$p_n(N\ ;\ T=1) = \sum_{M=N}^{\infty} p(N,M\ ;\ T=1) \qquad (13)$$

If an appropriate runoff counting process can be defined, analytical expressions can be obtained for the mean and variance of annual water and sediment yields under the assumption that V_N and S_N are each independent identically distributed random variables with probability density functions of $f(V)$ and $g(S)$.

For annual yields one can assume with very little error that the water and sediment yields per event occur instantaneously, therefore equations (6) and (7) can be written

$$Y_t = \sum_{N=1}^{N(t)} V_N \qquad (14)$$

$$Z_t = \sum_{N=1}^{N(t)} S_N \qquad (15)$$

Therefore both water and sediment yields for the interval $t - t_o$ can be considered as the sum of a random number of random variables.

The density function of the annual water yield is

$$h(Y\ ;\ T=1) = \sum_{N=1}^{\infty} p_n(N,T=1)\ \{f(V)\}^{N*} \qquad (16)$$

where $\{f(V)\}^{N*}$ is the N^{th} convolution of $f(V)$ with itself.

The mean and variance of $h(Y\ ;\ T=1)$ are

$$E(Y;T=1) = E[N;T=1]\ E\ [V] \tag{17}$$

$$VAR[Y;T=1] = E[N;T=1]\ VAR[V] + VAR[N;T=1]\ E^2[V] \tag{18}$$

where $E\ [\cdot]$ denotes expected value. Analogous expressions can be written for sediment yield.

If we can approximate observed distributions of V and S and the counting process by mathematically tractable expressions, analytic expressions can be obtained for the density functions of annual water or sediment yield. If analytic expressions cannot be obtained, these density functions can be approximated by Monte Carlo techniques.

In many situations runoff records are much longer than sediment yield records. It has been observed that sediment yield per event S_N is correlated with certain flow parameters such as peak discharge Q_N or volume.

$$S_N = \phi(Q_N) + \varepsilon \tag{19}$$

where ε is an independent, identically distributed random variable. Under these circumstances, if we know the distribution of Q_N we can obtain $g(S)$ by making use of the theory of functions of random variables.

When we have obtained an estimate of $g(S)$ we can utilize the relationships of equations (17) and (18) to estimate the mean and variance of the accumulated sediment yield in T years. Such estimates should be useful in the design of sediment storage pools in reservoirs and detention structures.

SUMMARY

Research is underway at Fort Collins on (1) overland flow, (2) infiltration and (3) stochastic models of water and sediment yield. The overall objective of this work is to improve mathematical models of various components of a watershed model and to develop simulation as a design technique in watershed engineering. Research has not yet progressed to the point that the models under investigation can be easily utilized in operational studies.

PUBLICATIONS

1. Kibler, D. F. and D. A. Woolhiser, 1970. The kinematic cascade as a hydrologic model, Colorado State University Hydrology Paper No. 39, Fort Collins, Colorado.

2. Liggett, J. A. and D. A. Woolhiser, 1967. The use of the shallow-water equations in runoff computations. Proc. Third Annual Meeting, Amer. Water Resources Assoc., San Francisco, California, pp. 117-126.

3. Woolhiser, D. A. and J. A. Liggett, 1967. One-dimensional flow over a plane--the rising hydrograph. Water Resources Research, Vol. 3, No. 3, pp. 753-771.

4. Woolhiser, D. A., 1969. Overland flow on a converging surface. Trans. Amer. Soc. Agricultural Engineers, Vol. 12, No. 4, pp. 460-462.

ELN-1

NORTHERN PLAINS BRANCH RESEARCH PROGRAM

MONTANA FRAIL LAND STUDY

by

Earl L. Neff[1]

INTRODUCTION

Western United States rangelands include millions of acres of panspots and saline uplands. The best practices for managing this large resource area will not be known until basic information concerning hydrological, environmental, and vegetational characteristics is assembled. The Agricultural Research Service, U.S. Department of Agriculture, and the Bureau of Land Management, U.S. Department of the Interior, are cooperating to study range management practices on panspots and saline upland range sites in southeastern Montana. The area selected is representative of many similar range sites under both private ownership and BLM administration that are identified as "frail lands." In terms of reference for this study, "frail lands" are defined as rangelands comprised of (a) solodized Solonetz soils, (b) raw shale soils, and (c) Solonchak soils, all of which have developed under annual precipitation of 10 to 15 inches. These lands are low in productivity due not only to inherent soil deficiencies but also to overuse by wild and domestic livestock. The principal study objective is to evaluate contour furrowing effects on hydrologic characteristics, vegetation ecology, and soil physical and chemical properties.

LOCATION AND GENERAL DESCRIPTION

The study area is on public domain approximately 15 miles south of Ekalaka, Montana. Climatically the region is classified as either arid or semiarid depending upon the classification system used. Annual precipitation ranges

---

[1]Research Hydraulic Engineer, USDA, ARS, Sidney, Montana.

from 6 inches to over 22 inches, but averages less than 14 inches. About 80 percent of the annual precipitation results from convective storm activity during the warm season, April through September, with the months of May and June averaging about 2.5 inches each. It is also a land of extreme temperatures, with a maximum of 108° F. and a minimum of -43° F. being recorded at Ekalaka. The 130-day average growing season lies between the middle of May and the end of September.

Soils of the study area are derived from Pierre shale and are characterized by high clay content, high water-holding capacity, and low infiltration rates. In general, the vegetation consists of big sagebrush (*Artemisia tridentata*), western and thickspike wheatgrasses (*Agropyron smithii* and *Agropyron dasystachyum*), pricklypear cactus (*Opuntia polycantha*), and blue grama grass (*Bouteloua gracilis*) with alkali sacaton (*Sporobolus airoides*) among the dominant species on saline sites.

EXPERIMENTAL DESIGN

Several steps were followed in designing the experiment:

I. The stated experimental objective was to evaluate the effects of range management practices on the hydrology, vegetation, ecology, and soil physical and chemical properties of panspot and saline upland range sites. This objective specified the questions to be answered and defined the population for which inferences were to be drawn.

II. The possible sources of variation were identified as:

- A. Range management practices
  - 1. Mechanical practices
    - a. Contour furrowing
    - b. Pitting
    - c. Disking
    - d. Interseeding
  - 2. Grazing practices
    - a. "Normal" grazing
    - b. Complete deferment
    - c. Rest-rotation
    - d. Various degrees of grazing intensities
- B. Soils
- C. Land slope
- D. Aspect
- E. Replication or experimental error

It soon became apparent that the experiment could become unwieldy and exceed our financial and personnel limitations. For example, 288 watersheds would be required to investigate the effects of four practices on two soils with three degrees of slope and four aspects with the minimum requirement of three replications to determine experimental error. Since an investigation of this magnitude was impossible, we settled on the following:

A. Two practices
   1. No mechanical treatment
   2. Contour furrowing
B. Three sites where site conditions incorporated variations in soil, slope, and aspect
C. Three replications for experimental error

The two practices selected represent the extreme treatments that are in common use. Contour furrowing is a severe mechanical treatment in which furrows 6 to 10 inches deep and about 20 inches wide are machine dug on 5-foot centers. Check dams in the furrows provide incremental water storage and prevent complete surface drainage if some dams or ridges fail. Except for furrowing, the experimental areas are all treated alike.

This resulted in a split-plot design with a random whole-unit arrangement in which the replicates are nested within sites. The sources of variation are partitioned for analysis of variance as follows:

Source of Variation	Degrees of Freedom
3 Sites, S	$(s-1) = 2$
3 Reps: S, Error (a)	$s(r-1) = 6$
2 Treatments, T	$(t-1) = 1$
T × S Interaction	$(t-1)(s-1) = 2$
Error (b)	$s(r-1)(t-1) = 6$
Total	$(srt-1) = 17$

Error (a) is the experimental error which is a measure of the natural variation between experimental units treated alike, and error (b) is the random error and includes the treatment by replicate interaction within sites and the treatment by replicate interaction between sites.

This experimental design not only provides data for analysis of variance, analysis of covariance, and various techniques of multivariate analysis, but also makes information available to develop new and test existing theories of watershed modeling on rangeland.

PHYSICAL LAYOUT

Three sites were selected approximately 15 miles south of Ekalaka, Montana, on public domain administered by the Bureau of Land Management. Each site is characteristic of one main soil-vegetation complex found in saline upland and panspot ranges. Table 1 shows the variations in soil and vegetation characteristics; and figures 1, 2, and 3 show the instrument locations and physical layout of sites 1, 2, and 3, respectively.

Two-acre watersheds are constructed on each site. Site 1 has five watersheds, and sites 2 and 3 have six watersheds each. It was not possible to locate a sixth watershed on site 1 without going onto a different soil-cover complex, which would increase the within site variability and, consequently, the experimental error. Eight of the 17 watersheds are treated by contour furrowing, and all 17 were deferred from grazing in 1968 and 1969. After the two-year deferment there will be controlled grazing under a livestock management system that prevents overuse. It is standard BLM practice to interseed both native and adapted grass species during the furrowing operation. In this study, however, no seeding was done in order to evaluate natural vegetation response to mechanical treatment.

Precipitation is measured by a dense network of recording and nonrecording raingages at each site. At site 1 there are 6 recording and 11 nonrecording gages installed with the orifices approximately 40 inches above the ground surface. At each of sites 2 and 3 there are 7 recording and 12 nonrecording gages. Also, at each site there are recording pit gages installed with the orifices at ground level to measure the differences in catch due to wind influences.

Periodic measurements with a neutron scattering moisture meter determine soil water changes. Two samples are taken on each untreated watershed; two samples in the furrow and two samples on the ridges are taken on each treated watershed. Soil water determinations are made through the growing season and into the late fall.

Surface runoff from each watershed is measured by a 2.5 H-type flume with a maximum capacity of about 19 cfs. Careful prefabrication in the laboratory shop and field installation with individual calibration resulted in accuracies within 1 percent of standard throughout the full range of flows for each flume.

Table 1. Research site characteristics.

	Site 1 Saline-Upland	Site 2 Panspot	Site 3 Panspot
Soil Series[1]	Espey Clay	Jurica Clay Espey Clay	Alzada Clay Sykes Clay Catamount FS Loam
Soil Texture	Clay	Clay	Clay Loam
Soil Water - % by vol.			
Saturation	92-106	84-112	83-115
1/3 Bar	47-70	52-66	43-56
15 Bar	31-40	34-45	32-39
pH	6.1-6.6	7.6-8.0	7.5-8.0
Electrical Conductivity - mmhoes per cm @25° C.	12.4-18.2	1.5-10.8	5.9-12.0
Dominant Vegetation	Lichen Alkali Sacaton Nuttall Saltbush Western Wheatgrass Thickspike Wheatgrass Nuttall Alkali Grass	Sagebrush Lichen Buffalo Grass Blue Grama Grass Pricklypear Cactus Clubmoss Prairie Junegrass Western Wheatgrass Thickspike Wheatgrass	Clubmoss Sagebrush Lichen Blue Grama Grass Sandberg Bluegrass Pricklypear Cactus
Slope - %	2	5	1

[1]SCS proposed series, subject to approval and correlation.

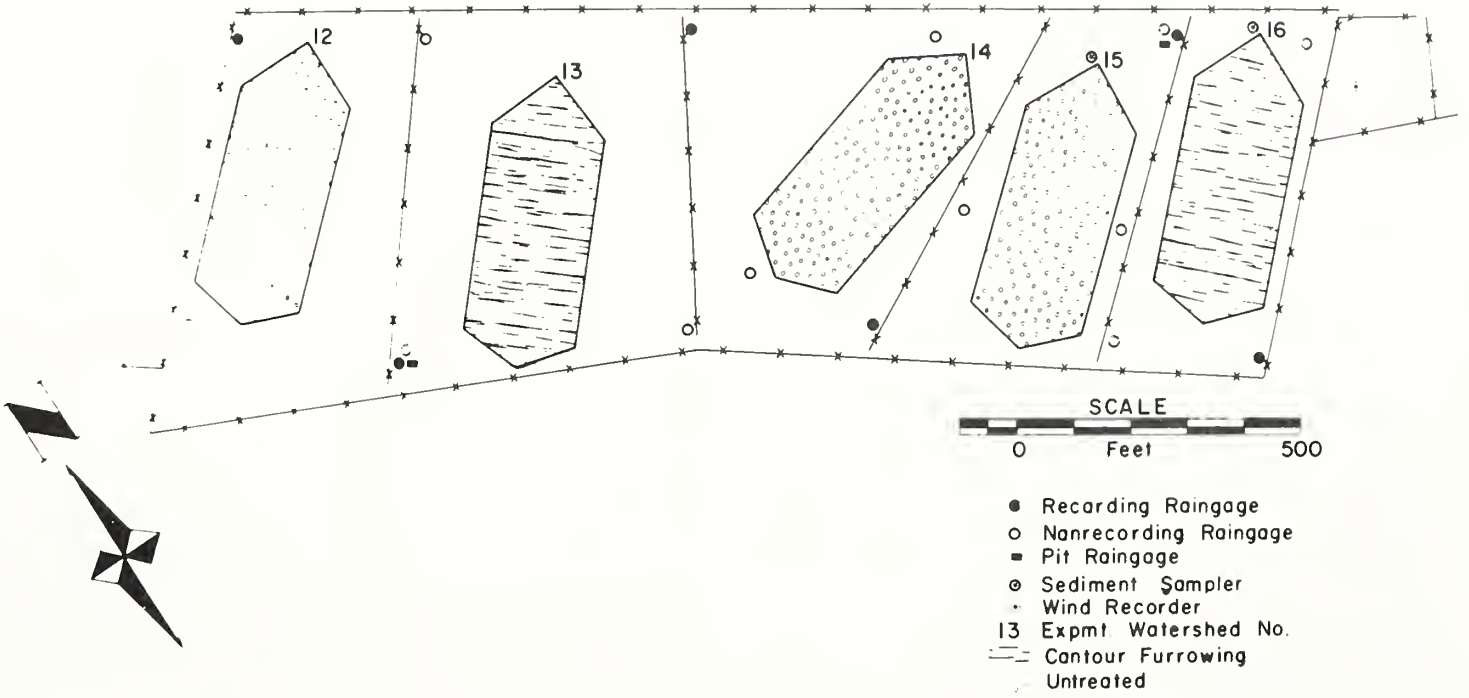

Figure 1. Plot layout, frail land study, site 1.

FRAIL LAND STUDY
Site No. 2

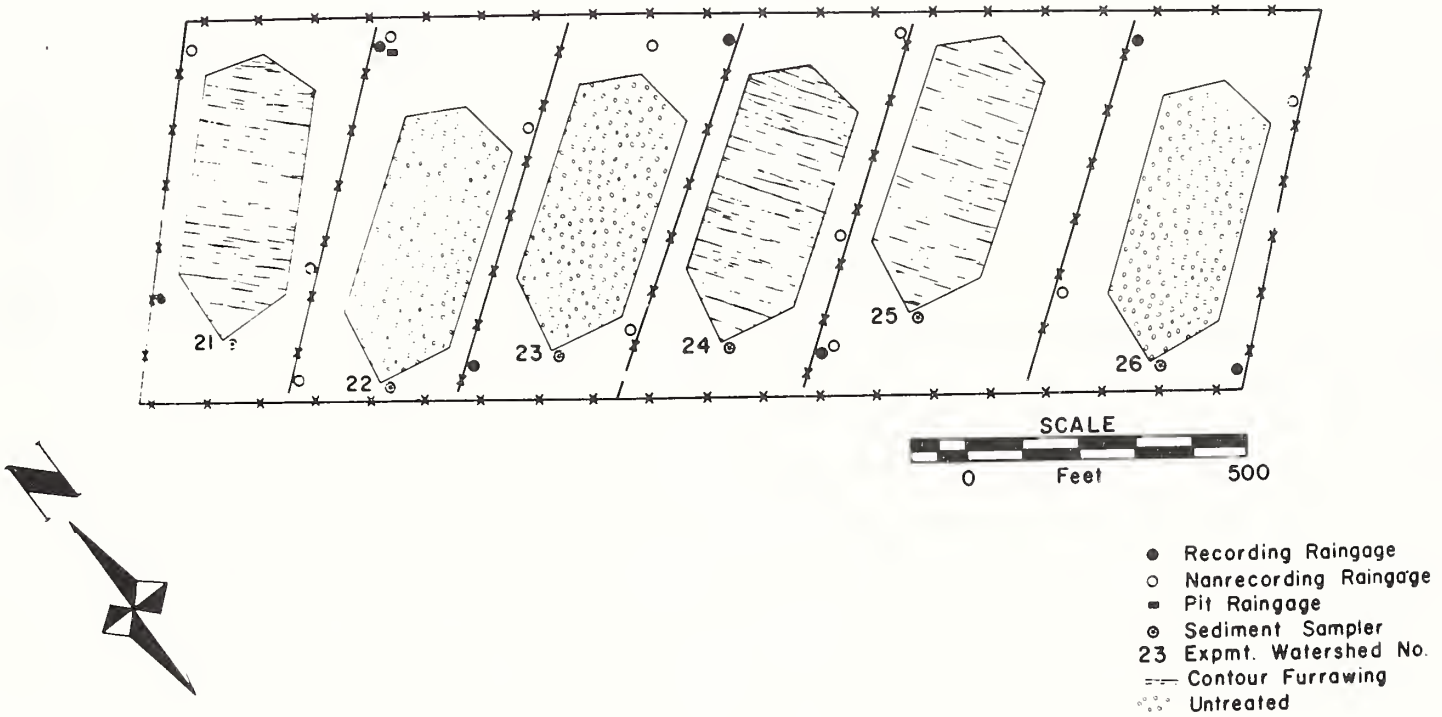

Figure 2. Plot layout, frail land study, site 2.

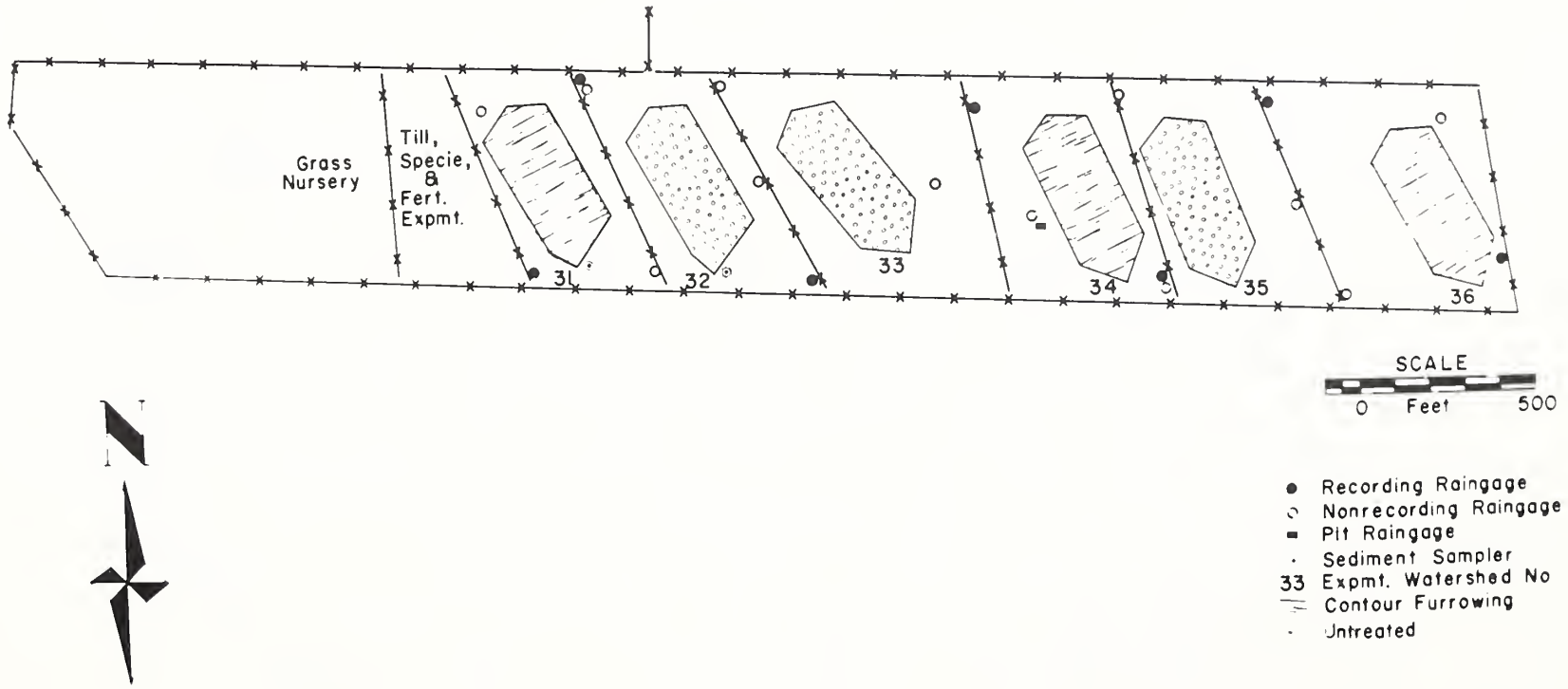

Figure 3. Plot layout, frail land study, site 3.

Punch-tape water stage recorders provide continuous discharge records. The flumes, the stilling wells, and the instrument shelters are heated electrically for winter operation.

Pumping type sediment samplers were installed at the six flumes on site 2 during the 1969 season. Two sediment samplers, one on a treated and one on an untreated watershed, will be installed at both site 1 and site 3 in 1970.

Additional data on wind speed and direction, soil temperature, air temperature, evaporation, and periodic short-term measurements of solar radiation are collected at a central weather station in order to relate plant response to environment.

Vegetation sampling transects are permanently located on each watershed, and initial sampling was completed before treatment application. Sample transects include both the pedestal and the depression areas in panspots and in furrows and between furrows on the treated areas. Vegetation yield in each watershed is estimated annually by clipping eight sampling plots each 50 by 200 cm. Basal, foliar, and litter cover is determined by point sampling. Species composition is determined from yield and percent basal cover. Permanent 1- by 10-meter belt transects are established for annual photographs. Protein and phosphorus contents of key species are determined annually.

Soil samples were taken by morphological horizons and by selected depth increments from each watershed at the beginning of the experiment for diagnostic and classification purposes. Panspot pedestal and depression areas were sampled separately, and the soil at each site was described and classified by U.S. Soil Conservation Service personnel. Each sample was analyzed for standard soil chemical and physical properties such as pH, electrical conductivity, cations and anions in saturated paste extract, cation exchange capacity, C:N ratio, available phosphorus, particle size distribution, water retention ability, hydraulic conductivity, and bulk density. During the experiment, annual samples from furrow and interfurrow areas of the treated watersheds will be analyzed for changes in pH, electrical conductivity, and soluble cations and anions. At termination, soil samples will be analyzed to determine long-term effects and changes due to contour furrowing.

INITIAL RESULTS

Because of the short period of record, no conclusive results are available. However, based on two incomplete year's data, some general statements can be made. Contour furrowing increases forage and decreases surface runoff. In the second year following treatment, forage had increased about threefold as compared to the untreated watersheds at each site.

No surface runoff has occurred from any treated watershed since the treatment was applied in the fall of 1967. However, the surface storage in the furrows has been decreasing as the banks and sides mellow and slough in and material is deposited in the furrow bottom. When the furrows were first dug, the storage was 3.5 to 4.0 inches. At the end of the 1969 season, it had decreased to about 3 inches; and there is evidence that the original channel system is reforming. As this continues, the effective storage will be reduced to an estimated 1 to 2 inches.

SUMMARY

The ARS and the BLM are cooperating to study the hydrology of small watersheds on saline upland and panspot range sites. Seventeen 2-acre watersheds, eight treated by contour furrowing and nine untreated, are located near Ekalaka, Montana. The experiment is designed to lend itself to statistical analysis of variance for the specific objective of evaluation of the effects of contour furrowing. Data will also be available to test existing watershed models as well as develop new modeling theories for these range conditions.

The experiment has not been in operation long enough to yield definitive results. In the first two seasons following treatment application, contour furrowing increased forage yield and eliminated surface runoff from both panspot and saline upland range sites. There is evidence, however, that the effectiveness of the furrows is decreasing and that the surface storage will be reduced to approximately one-third of what it was at the time of initial treatment.

Northern Plains Branch Research Program
Research at Cottonwood, South Dakota

by Clayton L. Hanson

Research projects on the Cottonwood Range Field Station are evapotranspiration and precipitation-runoff studies which lend themselves to model studies in the respective fields. The field station, a sub-station of the South Dakota Agricultural Experiment Station, is located at Cottonwood, South Dakota. Cottonwood is approximately 75 miles east of Rapid City.

The projects are located on Chestnut soils classified in the Opal-Samsil Association (Westin, Puhr, Buntley, 1967). In general, the soils are dark brown, moderately deep, slowly permeable heavy clays derived from the Pierre formation.

The pasture area containing these projects has been in a grazing intensity study since 1942. Previous to inception of the grazing study, this mixed prairie was dominated largely by mid grasses with an understory of short grasses and sedges. Under the three intensities of grazing initiated in 1942, the mid grasses have deteriorated on the moderately and heavily grazed pastures, leaving mostly short grasses and sedges. Japanese brome, Bromus japonicus, recently invaded the area, becoming most prevalent in the lightly grazed pastures.

The evapotranspiration study, initiated in 1969, is to develop a practical method for estimating evapotranspiration from native rangeland in the northern Great Plains. The evapotranspiration model developed from this study will be directly applicable to watershed models where an estimate of the soil water is needed.

The evapotranspiration equation will be based on the potential evapotranspiration rate for the northern Great Plains. The potential evapotranspiration will be computed by two methods, the first of which will be to use Class A pan evaporation as a potential value. The second method will base potential of evapotranspiration on equations that use incoming radiation and other meteorological data. The actual evapotranspiration rate will be a function of the potential.

Data from Cottonwood, South Dakota; Gillette, Wyoming; and Sidney, Montana will be used as the basic check of the

validity of the evapotranspiration equation. Data from other ARS locations and state universities will also be used.

The actual evapotranspiration rate at Gillette, Wyoming and Sidney, Montana is determined by daily lysimeter observations. At Cottonwood, South Dakota there is one plot, 12 feet square, on each of three differentially grazed pastures (figure 1). Weekly neutron probe readings are used to determine a weekly water balance on each plot. The plots were established on the different pastures so that the difference in the evapotranspiration rate due to the variation in vegetal cover could be determined. The basic meteorological data such as precipitation, temperature, wind speed, Class A pan evaporation, and solar radiation are also recorded. There are no results from this study to report as the first year's data is just being analyzed.

In 1962, a project was established to determine the relationship between precipitation and runoff as affected by intensity of grazing on rangelands of western South Dakota. To accomplish this objective, watersheds on each of three differentially grazed pastures were established (figure 1). The pastures have been grazed heavily, moderately and lightly since 1942. Within each eight-acre watershed site in each pasture, four contiguous watersheds approximately 2 acres in size were constructed. The slopes of the watersheds vary from 7.0 to 8.8 percent. Each watershed is equipped with a two-foot H-type flume with approach box and a FW-1 water stage recorder. Four weighing and recording rain and snow gages are located on each set of watersheds. Six soil moisture access tubes for neutron reading are located on each set of watersheds.

Table 1 lists the annual and seasonal (May 14-October 31) precipitation on the watershed from 1963 through 1969. The seven-year mean is 0.09 inch less than the 68-year mean of 15.13 inches recorded at the Field Station headquarters (Spuhler, Lytle, and Moe, 1968). The seasonal precipitation (May 14-October 31) is about two-thirds of the annual total.

Table 2 shows the annual and seasonal runoff from the heavily, moderately and lightly grazed watersheds. The period from May 14 through October 31 is separate because there was no snowmelt runoff during this period. For both the annual and seasonal runoff, these data indicate that the most runoff can be expected from the heavily grazed and the least from the lightly grazed watersheds. The annual runoff was 1.04, 0.79, and 0.64 inches for the heavily, moderately and lightly grazed watersheds, respectively. The seasonal

Figure 1. Location of evapotranspiration and watershed research projects on the Field Station at Cottonwood, South Dakota

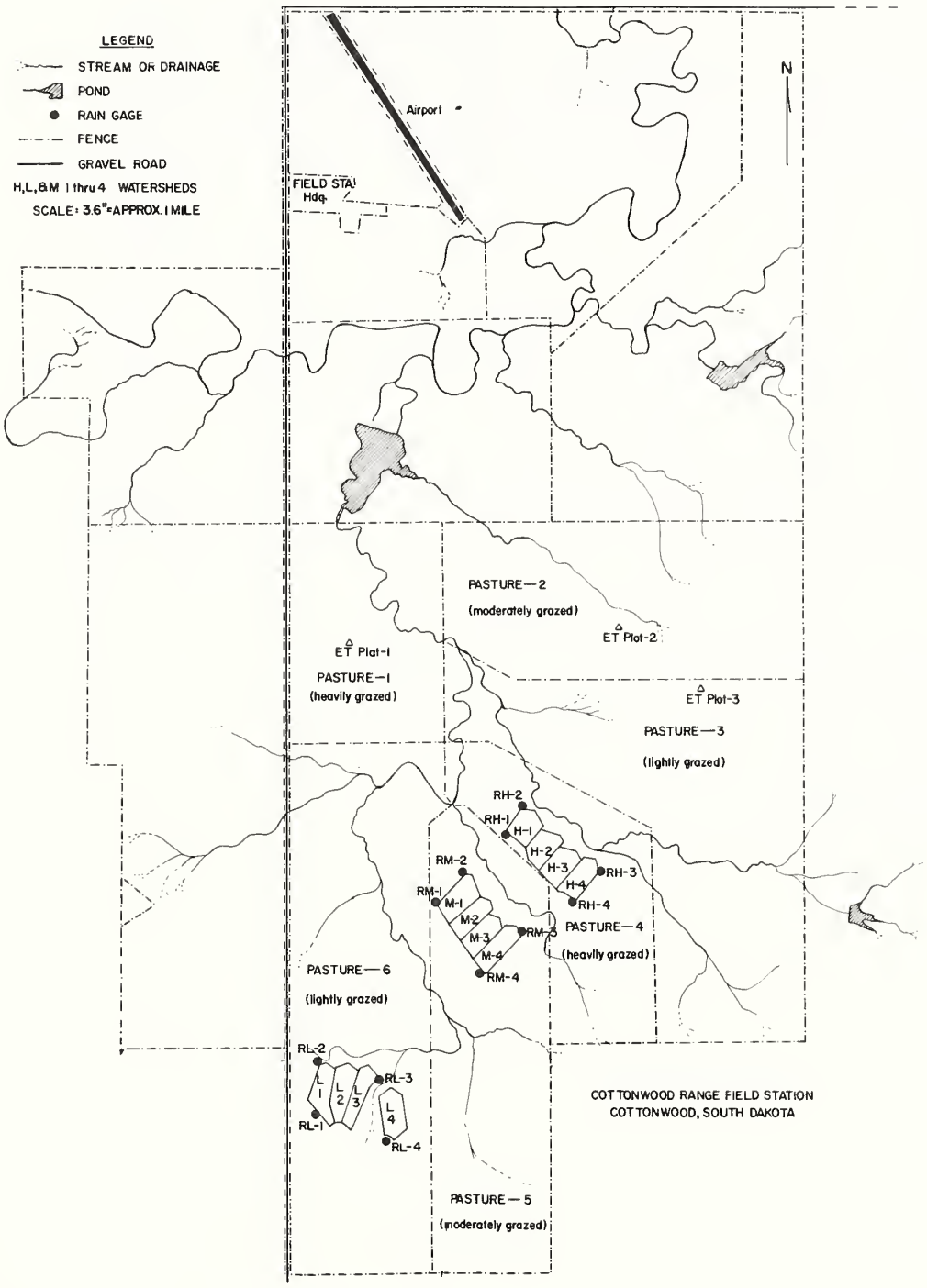

Table 1. Annual and seasonal (May 14-October 31) precipitation on the watershed areas, Cottonwood, South Dakota

Year	Precipitation	
	Annual	Seasonal
	Inches	
1963	15.34	12.26
1964	13.46	8.30
1965	15.34	10.92
1966	14.20	9.34
1967	16.66	11.02
1968	14.58	10.80
1969	15.68	12.06
Mean	15.04	10.67

Table 2. Annual and seasonal (May 14-October 31) runoff from differentially grazed watersheds, Cottonwood, South Dakota

Year	Runoff					
	Heavy[1/]		Moderate[1/]		Light[1/]	
	Annual	Seasonal	Annual	Seasonal	Annual	Seasonal
	Inches					
1963	1.79	1.79	1.57	1.57	1.39	1.39
1964	0.68	0.66	0.28	0.28	0.05	0.05
1965	0.13	0.13	0.14	0.14	0.12	0.12
1966	1.65	0.16	1.37	0.02	1.52	0.00
1967	1.41	1.21	0.81	0.79	0.62	0.54
1968	0.40	0.40	0.20	0.20	0.02	0.02
1969	1.22	0.32	1.16	0.07	0.75	0.03
Mean	1.04	0.67	0.79	0.44	0.64	0.31

1/ Average of four watersheds

runoff from the heavily and moderately grazed watersheds was a little over half of the annual total, whereas it was less than half from the lightly grazed watersheds. Snowmelt runoff occurred during four of the years but it was significant only in three.

Mean (1963-1967) oven-dry weights of live vegetation on the watersheds in July were 520, 560 and 937 pounds per acre from the heavily, moderately and lightly grazed watersheds, respectively. The corresponding mulch or litter weights were 1,232, 1,531, and 2,763 pounds per acre. These data show that the different rates of grazing have caused a difference in the cover composition between the watersheds.

The two years with the greatest runoff were 1963 and 1966. In 1963, the runoff was all due to rainfall when 2 three-inch rains produced most of the runoff. In 1966, however, there was little rainfall runoff but snowmelt caused about 1.5 inches of runoff. Seasonal runoff (May 14-October 31) varied from 1.79 inches from the heavily grazed watersheds in 1963 to none from the lightly grazed watersheds in 1966. For the seven-year period, there were 36, 24 and 17 rainfall-runoff events on the heavily, moderately and lightly grazed watersheds, respectively.

Preliminary regression analysis indicate that total precipitation and some measure of soil water are two of the primary factors that will have to be considered in a rainfall-runoff model of the individual watersheds. When all of the watersheds are considered together, the watershed cover is also very important. Snowmelt runoff will have to be considered in any annual runoff model as well as individual rainfall-runoff events.

References

1. Spuhler, Walter, W. F. Lytle, and Dennis Moe. 1968. Climatological Summary No. 14, Climatography of the U. S., No. 20-39, from U. S. Weather Bureau Records.

2. Westin, Fred C., Leo F. Puhr, and George J. Buntley. 1967. Soils of South Dakota. Soil Survey Series, No. 3. South Dakota Agricultural Experiment Station, Brookings, South Dakota, 32 pp.

Northern Plains Branch Research Program
Research at Newell, South Dakota

by A. R. Kuhlman

Introduction

Soil and water conservation hydrologic research from Newell, South Dakota comprises off-station observations on approximately 70 watersheds located within 135 miles radius from the Newell Field Station.

Isolation and relative evaluation of runoff producing potentials of range sites in western South Dakota

Objectives

1. To evaluate the relative runoff producing potentials of principal range sites in the Northern Smooth High Plains and Pierre Shales and Badlands resource areas.

2. To evaluate vegetative and soil factors that cause differences in runoff production between range sites.

3. To characterize and evaluate such range sites further with the aid of rainfall simulators.

Procedures

In 1962 one 43-acre mixed range site was subdivided to assess runoff from panspots and sandy range sites. Other sandy and panspots sites were chosen for study also. The study includes silty and shallow range sites in Wyoming.

Runoff data is charted at 3-H type flumes. Recording rain gages chart the precipitation data.

Vegetation is assessed annually for volumes of cover and for composition on all watersheds.

Results

Mulches and litter comprise 50 to 90 percent of the rangeland cover. The balance of cover is standing vegetation. Yields of total cover range from 1000 pounds to 3000 pounds per acre.

Runoff is discussed as that coming from the snow season, the rain season and the annual amount. Precipitation falling as snow produces much annual runoff. However, aspect, vegetal cover, soil and air temperatures, configuration of the watersheds, and wind movement are important factors influencing snowmelt amounts. Snow may blow into or out of a watershed, making a difficult true assessment of the precipitation which really fell. However, snowmelt is important to the rancher's water storage facilities during March and April. Snowmelt may be the only year's runoff from a sandy range site where the runoff has ranged from a trace to as high as 5.713 inches in 7 years.

Table 1 shows the high and low precipitation, the low and high snowmelt yield, the annual snowmelt for each watershed. Ironically, the high season of snow precipitation is not always the highest producer of snowmelt. High volumes of snow precipitation shown in table 1 were not the high runoff producers. Data show that a low snow precipitation season of half the amount may produce over 6 times as much snowmelt as does the high snow precipitation season. Predicting the snowmelt from a given snowfall is a very erratic situation subject to many factors influencing snowmelt volumes. Basically, when a rancher or other group is planning to collect and store snowmelt, they must be prepared on short notice to store a large volume quickly under certain conditions.

Table 2 shows the distribution of snowmelt by months in 1969. On some years, the storage facility or the stream channel must be ready to handle huge volumes of runoff in January or February and little in March or April. In the Northern Great Plains snows may occur in May, and even as late as June 13, as was the case in 1969.

Runoff from rainfall has been summarized (table 3) to include by groups all runoff from rain storms over 0.10 inch to storms as high as the 2.0 inch group. Other factors included in this summary are the 5-day and 10-day antecedent precipitation, the maximum 10-minute intensity, the storm intensity and the storm duration for each event.

During the 1963-1968 period, the sum total of 765 observations for the "n" value was used in the regression analysis for all panspots sites. The "n" value for the runoff producing group was 383. At the sandy site group, the "n" value of 53 for the runoff producing portion was taken from a total of 505 observations. During this period a combined Q/P ratio for the 5 panspot sites group would be 0.1437 as compared to 0.0074 for the 3 grouped sandy sites.

Table 1. The range of low and high snow precipitation (P)[1/], the low or high runoff (Q) and the total of P and Q for panspots and sandy range site watersheds Newell, South Dakota, 1963-1969

Precipitation Low	Precipitation High	Runoff Low	Runoff High	Total years P	Total years Q
			Inches		
			PS-2		
1.09	6.62	0.0	2.515	27.86	4.484
			PS-6		
1.06	5.06	0.0	1.051	25.33	3.931
			NC		
1.48	6.65	Tr	5.713	23.20	9.444
			SCA		
1.48	6.65	Tr	4.634	23.20	10.010
			SCB		
1.48	6.65	Tr	5.391	23.20	12.780
			SY-1		
1.09	6.62	0.0	2.429	27.80	5.283
			SY-3		
1.09	6.62	0.0	0.582	27.86	1.554
			SY-5		
1.06	5.06	Tr	2.309	25.33	5.616

1/ Snow season - November 1 through April 26

Table 2. Distribution of snow precipitation (P) and runoff (Q) by months for the Nov.-Apr. snow season[1/] Newell, South Dakota, 1969

	Jan.		Feb.		Mar.		Apr.		Runoff from snow
	P	Q	P	Q	P	Q	P	Q	
	Inches								Percent
PS-2	0.08	---	0.38	---	0.38	2.304	1.28	0.211	71.4
SY-1	0.08	---	0.38	---	0.38	1.619	1.28	---	99.8
SY-3	0.08	---	0.38	---	0.38	0.583	1.28	---	95.7
PS-6	0.10	---	0.18	---	0.26	0.950	1.40	0.101	72.9
SY-5	0.10	---	0.18	---	0.26	2.309	1.40	---	100.0
SCA	0.15	---	0.43	---	0.80	4.312	1.37	0.322	96.6
NC	0.15	---	0.43	---	0.80	5.551	1.37	0.162	83.2
SCB	0.15	---	0.43	---	0.80	2.373	1.37	0.535	75.2
Total		0		0		19.956		1.331	

1/ Range of additional (P) for all watersheds - November, 0.67 to 0.82, December, 0.63 to 0.66. Runoff - 0.0.

Table 3. Summary of inches precipitation (P) and runoff (Q) from rain events over 0.10 inch, Newell, South Dakota, 1963-1968

	PS-2	PS-6	SCB	NC	SCA	SY-1	SY-3	SY-5
P	84.98	64.29	71.22	71.22	71.22	84.98	84.98	64.29
Q	8.249	3.189	9.272	13.462	11.999	0.425	0.765	0.441

	Combined 5 panspots range sites, 3 sandy sites	
Ratio Q/P	0.1437	0.0074
Observations	765	505
Events, runoff producing	383	53
Events, nonrunoff producing	382	452

In table 4, precipitation and runoff are reflected as Q/P ratios for the snow season, the rain season, and the annual mean for each watershed.

In the panspot group, the ratio may reach 55 percent for snow runoff depending upon watershed configuration, azimuth, and other associated functions. In the rain season, the range of 4.96 percent to over 19.00 percent is shown after summarizing 765 observations from 1963-1968. The annual means were up to over one-fourth of the precipitation, depending upon factors influencing snowmelt.

At the sandy range sites, snowmelt may be up to one-fifth of the precipitation and actually comprise nearly 100 percent of the year's runoff. Small ratios under one percent were observed from rain. As a whole the ratios on the annual basis were under 5 percent.

Table 4. Precipitation and runoff, reflected as Q/P ratios for the seasons of snow, rain and the annual ratio, Newell, South Dakota, 1963-1969

	Snow season	Rain season	Annual mean
		Percent[1/]	
		Panspots range sites	
PS-2	16.09	9.70	10.61
PS-6	15.51	4.96	7.89
NC	40.70	19.44	27.72
SCA	43.14	16.84	22.47
SCB	55.08	13.09	21.63
Combined sites		14.37	17.15
		Sandy range sites	
SY-1	18.96	0.50	4.61
SY-3	5.57	0.90	1.91
SY-5	22.17	0.83	5.22
Combined sites		0.74	4.10

1/ Percent - ratio of Q/P x 100.0

Water yield and sediment accumulation from rangeland watersheds in Northern Great Plains

Objectives

1. To secure data on water yields and develop methods of estimating inch yields on rangeland watersheds in the D-4, D-10, and D-11 conservation problem areas[1/] as represented by stockpond sites on moderately coarse- and fine-textured soils in western South Dakota.

2. To secure data on and develop equations for estimating rates of sedimentation in stock ponds of the areas.

Procedure

Runoff and sedimentation observations were started in 1957 on 16 watersheds equipped with stage recorders located in stilling wells. The initial sedimentation surveys were started in September 1957. Since 1962 observations have been increased to include some 54 rangeland watersheds, most of which were located within 2 miles of the normal traveled roads in the area. Ponds of various ages were on these additional watersheds which were selected at random.

Water stage observations are taken by a Jacob's staff device at bi-weekly intervals or immediately after major storms. Rainfall data is secured at non-evaporative storage type gages on the watershed or from the nearest recording rain gage. The stage storage curves and tables have been revised after each sediment survey.

Sediment surveys have been repeated 2 to 3 times on all watersheds. The range end method in relation to permanent base lines was used. Sediment volumes were computed by several methods. Samples were taken from the boat with a spud and a sediment sampler.

Results

Table 5 lists the maximum and minimum precipitation and runoff, the mean annual values and the means for each watershed, shown by principal range site and the soil textural group. May and

1/ Also known as Northern Smooth High Plains and Pierre Shales and Badlands land resource areas.

Table 5. Maximum and minimum precipitation (P) and watershed runoff (Q), mean annual P and Q by major range sites and soil textures, Newell, South Dakota, 1958-1968

Watershed	Major range site	Maximum		Minimum		Mean annual	
		P	Q	P	Q	P	Q
		Inches					
Moderately coarse textured soils							
W-2	Silty	15.97	1.228	8.49	0.058	12.23	0.522
W-5	Sandy	22.03	1.371	8.27	0.025	15.27	0.693
W-7	Sandy	17.22	0.991	8.81	0.003	13.78	0.402
Mean		18.41	0.896	8.52	0.029	13.76	0.539
Fine textured soils							
W-12	Shallow	22.60	6.123	8.54	0.066	13.61	2.467
W-13	Clayey	16.52	2.509	8.21	0.003	12.46	0.970
W-14	Clayey	19.39	2.330	8.97	0.261	14.14	1.269
W-15	Clayey	20.67	2.525	10.20	0.261	14.34	1.146
Mean		19.80	3.372	8.98	0.148	13.89	1.463

June data show the highest precipitation and runoff. March was the leading month for snowmelt runoff. The highest mean runoff occurred on watersheds within the fine-textured group. The mean annual Q from the fine-textured soils was 2.71 times that on the moderately coarse-textured watersheds. In the highest P group, runoff was 3.76 times greater from the fine-textured soils as compared to the moderately coarse-textured group.

Table 6 shows the accumulation of sediment and the resulting loss of pond volume storage for the various ponds in the 2 soil texture groups. The rate of sediment accumulation in some of the ponds is very low on the moderately coarse-textured soils. The low average rate of 0.69 tons per acre was approximately a fourth of the erosion loss on the fine-textured soils. The loss in pond storage capacity was over 5 times greater on the fine-textured soils.

Table 6. Sediment erosion and pond volume loss at ponds on rangeland watersheds of two soil textural groups after surveys, 1958 through 1968, Newell, South Dakota

Pond	Watershed area	Years	Erosion	Pond volume loss
			Tons/ac./yr.	Ac. ft./sq. mi./yr.
		Moderately coarse textured soils		
W-1	790	5.83	0	0
W-2	115	7.83	0.18	0.07
W-3	90	7.00	0	0
W-4	105	8.08	0.19	0.06
W-5	43	6.83	0	0'
W-6	30	7.92	0	0
W-7	160	5.25	0	0
W-8	160	8.00	1.00	0.35
W-9	815	8.00	4.87	1.84
Average			0.69	0.26
		Fine textured soils		
W-10	280	7.92	1.21	0.55
W-11	160	7.83	3.84	2.45
W-12	90	6.92	6.51	3.18
W-13	160	7.75	0.12	0.05
W-14	45	8.75	3.88	1.62
W-15	115	8.67	0.31	0.13
Average			2.65	1.33

Collection and storage of rainfall runoff for domestic and stock water supply

Objectives

1. To determine physical means of providing and conserving domestic and livestock water supply.

2. To check the quality of water from range sites.

3. To study the economics of such water supplies for these uses.

Brief procedure

A large 20 acre watershed of largely panspots range site was subdivided into 3 smaller watersheds, each with a fenced pond capable of storing 90 to 100,000 gallons of runoff water.

The dugout type ponds with a surface area of about 25,000 square feet were approximately 11.5 feet deep. One pond was lined with butyl rubber. Another pond was treated with bentonite in the fall of 1963. The remaining pond served as a check. Instrumentation included 3 H-type flumes with waterstage recorders, and a 10-inch stilling well with waterstage recorders at each pond. Rainfall data were gathered at 2 recording rain and snow gages. A 4 foot Class A Weather Bureau evaporation pan was instrumented with a FW-1 recorder housed in an insulated shelter. Data is recorded on an enlarged scale. Water was added to the pan twice a week. Other instruments chart relative humidity, air temperature, pond water temperatures, and the current wind flow and direction.

Results

Range sites are a source of runoff water for the livestock supply storage. The storage of water merits the attention of the user so that the greatest value is obtained from the storage effort. Data from these 3 ponds illustrate the need for more storage containers and direct attention to the type of containers. Full data began on June 20, 1966.

Table 7 shows the runoff available for storage on each watershed, the portion stored annually and the dissipation.

At the butyl lined pond (SCB) only 11.58 percent of the water was stored during this 4-season period. The remainder was discharged over the metal spillway to down stream areas.

Table 7. Annual runoff from 3 contiguous watersheds, as watershed inches, the resultant storage and the dissipation by evaporation (SCB) and or seepage, and the end of year balances, Newell, South Dakota, 1966-1969

Year	Runoff		Storage Balance	Storage Inflow	Portion stored	Dissipation or loss	End Balance
	Inches	Total cubic feet	Cubic feet		Percent	Cubic feet	Cubic feet
			Butyl lined (SCB)				
1966	2.229		0	11,914		3,405	8,509
1967	6.249			15,907		6,811	8,226[1/]
1968	1.977			11,994		5,775	11,546[1/]
1969	3.877			3,736		6,732	8,550
Summary		362,095	0	43,551	11.58	22,723	20,828
			Check (SCA)				
1966	2,747		606	19,930		20,499	37
1967	6.926			27,787		27,649	175
1968	0.978			22,639		22,300	514
1969	4.797			25,837		26,055	296
Summary		360,009	606	96,193	26.88	96,503	296
			Bentonite (NC)				
1966	2.153		5,158	34,281		39,042	397
1967	9.758			50,352		48,382	2,367
1968	1.049			31,006		32,771	602
1969	6.830			35,451		35,838	215
Summary		520,823	5,158	151,090	29.00	156,033	215

1/ Liner leakage and pumping

This pond was full most of the year, resulting in considerable overflow. However, of the stored water balance, the ratio of dissipation to storage was 0.5217. This was considered as evaporation. In April of 1967 and 1968 liner repairs were made because of ice damage. The resulting leakage and pumping to a level below the damaged area was 20,828 cubic feet.

In comparison, at the check pond, the dissipation by seepage and evaporation lowered the pond level rapidly. It was possible to store larger amounts of the runoff water -- as much as 26.88 percent of the available runoff. However, at the end of each season the stored balance was nil.

Some effects of bentonite treatment were noted, particularly in 1963 and 1964 when the loss was reduced as much as 50 percent. Erosion rills on the 2 to 1 sloping perimeter during flash showers has shifted the bentonite to the pond bottom. The pond storage area was larger than either of the other ponds. Over 29 percent of the available runoff water was stored.

The April-October losses at all ponds usually exceeded the total storage in that period. This indicates that water users must depend on snowmelt also for their annual storage.

The mean daily dissipation of stored water per unit of surface area was 0.0878, 0.049 and 0.0116 feet in depth, respectively, for the check, the bentonite and the butyl ponds during the April-October period (210 days) from 1966 through 1969. The ratios of loss at the butyl pond to that of the check was 0.1321 as compared to 0.1504 for the bentonite pond during the evaporation period.

On an annual basis, the mean (365 days per year) daily depth per unit area dissipation (evaporation) at the butyl pond was 0.0076 feet or a 0.3052 ratio to the total stored water. The corresponding daily depth losses were 0.0745 and 0.0466, respectively, at the check and bentonite ponds. The ratios of the butyl pond loss to the other pond losses were 0.1020 and 0.1630, respectively.

It appears that the butyl lined pond lost 0.33 feet of water depth in the off season period from November 1 through March 31. In comparison, the bentonite pond lost 6.7 feet of depth and the check pond lost 8.8 feet of depth for this period. For all practical purposes, the storage for actual livestock consumption at the check pond was nil after October 31.

EVALUATING COMPONENTS OF A HYDRAULIC SIMULATION MODEL[1/]

By

W. R. Hamon, D. L. Schreiber,

G. R. Stephenson and L. M. Cox[2/]

INTRODUCTION

The development and management of a total watershed requires a rather complete understanding of the hydrologic regime and methods for predicting the response to inputs for a range of conditions.

The hydrologic cycle has been conceptually and qualitatively well defined. The principal components of the cycle are easy to identify and the interactions between the major components are well known. Procedures to quantitatively define the separate components and their linkages, however, are still in the development stage.

Hydrologic simulation models have gained wide acceptance as an approach to predicting the performance of complete hydrologic systems.

1/ Contribution from the Northwest Watershed Research Center, Soil and Water Conservation Research Division, Agricultural Research Service, USDA, Boise, Idaho; Idaho Agricultural Experiment Station cooperating.

2/ Research Hydraulic Engineers, Geologist, and Soil Scientist, Northwest Branch, Soil and Water Conservation Research Division, Agricultural Research Service, USDA, Boise, Idaho.

Figure 1 is a schematic diagram, similar to that of Freeze and Harlan (16), outlining the methods of hydrologic simulation. These methods are classified into the two broad categories of physical hydrology and hydrologic systems investigations.

Investigations in physical hydrology are concerned with physical models and physically-based mathematical methods for representing the mechanisms of the component processes within the hydrologic cycle. If each of the processes could be described by a well-established physical law with an exact mathematical representation, then it should be possible to model entire watersheds. This remains a long-term research goal.

Hydrologic systems investigations are classified into parametric and stochastic methods which incorporate measurements of observable variables in the hydrologic cycle and the development of explicit relationships between these parameters in the parametric models.

At the present stage of hydrologic simulation, the best attainable model will surely be a combination-simulation hydrologic response model with physically-based and parametric models of flow components and a stochastic model of inputs. Of major importance is the degree of representation given to the spatial and sequential variations in the input and output parameters. A lumped-system would treat the watershed as a "black box" whereas a distributed-system would treat the internal processes of the watershed.

A schematic drawing showing storage and flow components of a hydrologic simulation model is presented as Figure 2. Simulation models, similarly structured, have been developed into a digital model by Crawford and Linsley (11) and into an electric analogue model by Riley, et al. (42). Other models, such as the simplified, mathematical model of Lichty, et al. (33), have been recently proposed.

Most of the flow components or subsystems in the hydrologic cycle, Figure 2, are complex and interdependent and exhibit great variability in space and time. Possibly only precipitation needs to be treated purely on a statistical basis. For most of the other components, some form of a mathematical model is needed in terms of physical parameters so that outputs may be generated over a wide range of inputs and controls. Experimental data are a necessity for the creation of improved models or for the testing of existing models.

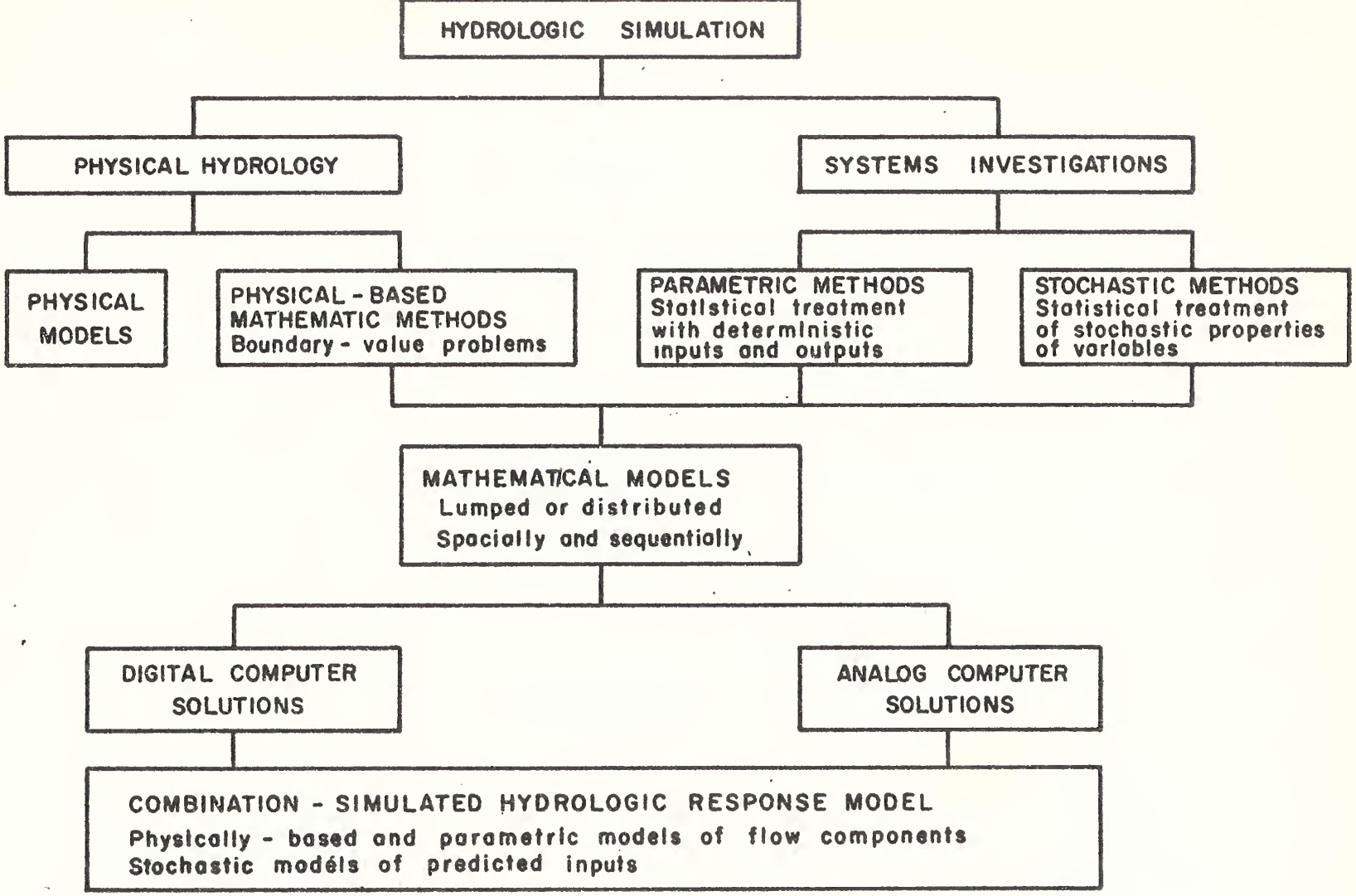

Figure 1. Flow chart of methods for hydrologic simulation.

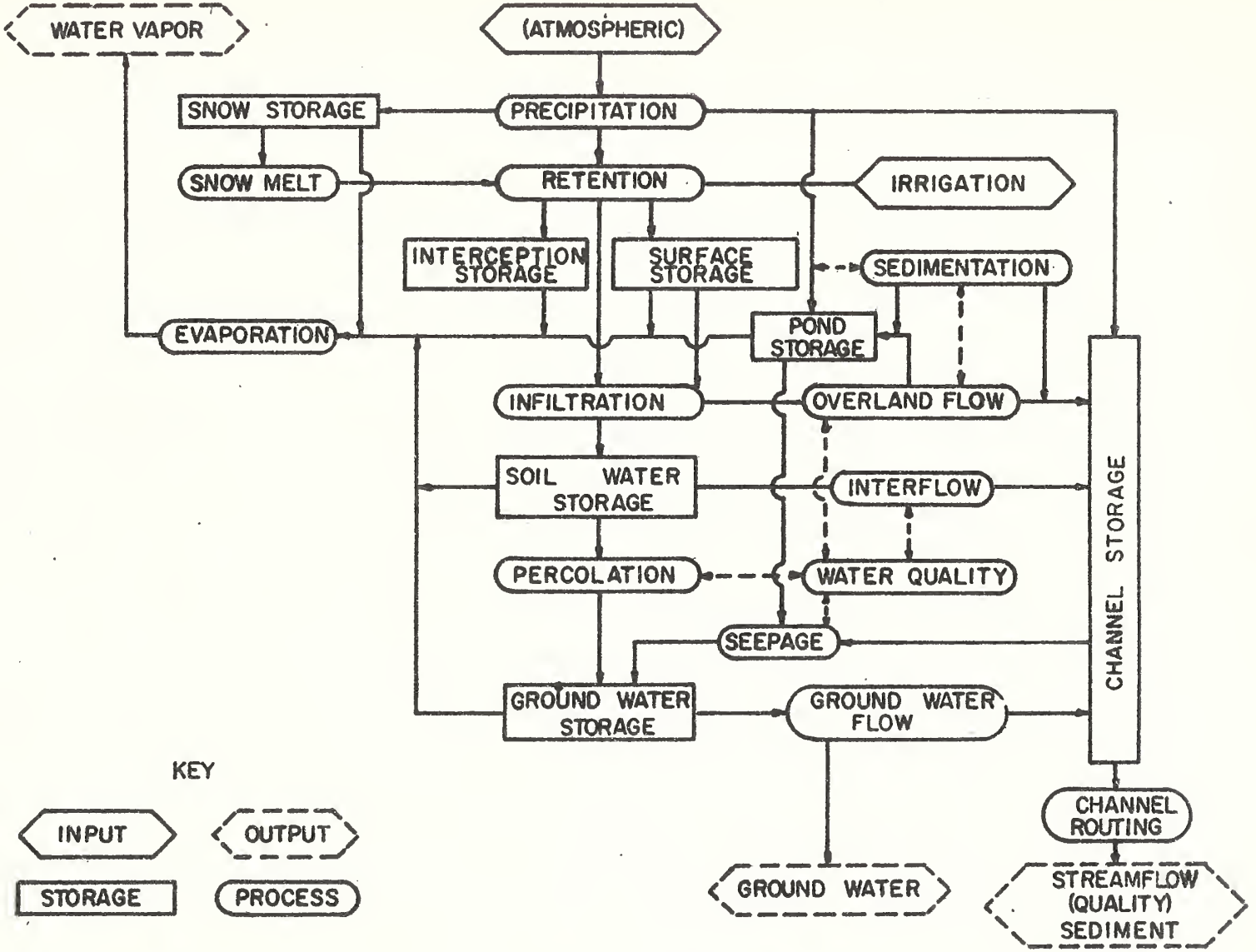

Figure 2. Flow chart of hydrologic model for land areas based on stepwise routing approach.

Field research at the Northwest Watershed Research Center, Boise, Idaho, is concentrated on the various subsystems of the hydrologic cycle, with the purpose of arriving at the physical and mathematical descriptions of the flow processes or empirical descriptions. Investigations are conducted in the 90-square-mile Reynolds Creek Experimental Watershed, Figure 3, southwestern Idaho.

Elevations in the watershed range from 3500 to 7200 feet, m.s.l., and the principal geologic materials are basalt and granite. Soils in the watershed have been classified into 30 soil series. Vegetation in the watershed is principally sagebrush and related woody species with an understory of annual or perennial grasses.

The watershed is used as a laboratory to develop empirical relationships for hydrologic components that cannot be handled on a physical basis, to develop a stochastic model of predicted inputs, and to determine values of parameters and coefficients for calibration of physically-based mathematical representations of component phenomena, Figure 2. Progress in the development and testing of models to represent the separate hydrologic flow components of precipitation and snowmelt, evaporation, infiltration and soil moisture, surface runoff, and ground water is presented in the remainder of the paper.

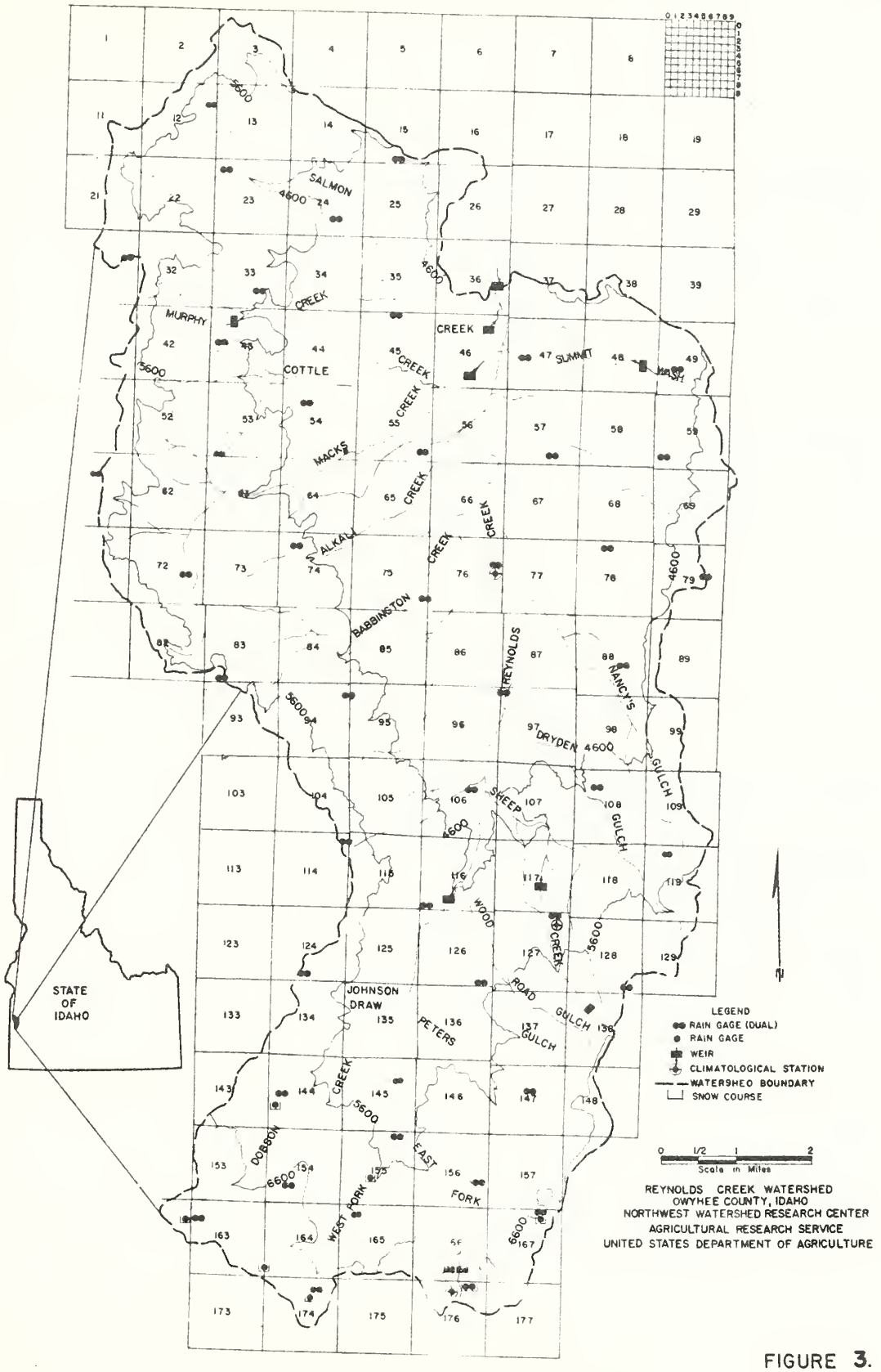
SALMON
MURPHY
CREEK
COTTLE
SUMMIT
MACKS
ALKALI
BABBINGTON
REYNOLDS
NANCY'S
DRYDEN
GULCH
SHEEP
WOOD
ROAD
JOHNSON
DRAW
PETERS
DOBSON
EAST
FORK
WEST FORK
STATE
OF
IDAHO
5600
4600
6600
LEGEND
RAIN GAGE (DUAL)
RAIN GAGE
WEIR
CLIMATOLOGICAL STATION
WATERSHED BOUNDARY
SNOW COURSE
Scale in Miles
REYNOLDS CREEK WATERSHED
OWYHEE COUNTY, IDAHO
NORTHWEST WATERSHED RESEARCH CENTER
AGRICULTURAL RESEARCH SERVICE
UNITED STATES DEPARTMENT OF AGRICULTURE

FIGURE 3.

PRECIPITATION AND SNOWMELT

Atmospheric Precipitation

The performance of any hydrologic simulation model is directly dependent upon the adequacy of the precipitation estimates as an input. The temporal and spatial estimates of precipitation reflect the errors in point estimates. These point or network measurements can be exceedingly large for snow, as will be demonstrated later. In the case of snow, it is redistributed over the terrain in relation to windspeed, topography, and vegetative cover.

Rainfall data obtained by the initial precipitation network (installed in 1960-61) of one gage per square mile in the Reynolds Creek Watershed was examined for spatial variability in precipitation. The simple correlation coefficient of catch between gages for 38 selected sites and 15 general rainstorms was related to the distance between gages by the regression equation

$$r = 1 - 0.027\ (d - 0.25) \qquad (1)$$

for all positive values of (d - 0.25) where, r is the correlation coefficient and d is the distance between gages in miles.

From the above relationship, it is seen that the average coefficient of determination approaches 1 for a distance of one-fourth mile between gages and reduces from 0.95 at a distance of 1.2 miles (gage density of 1 per square mile) to 0.92 at a distance of 1.7 miles (gage density of 1 per 2-square miles). In other words, the average coefficient of determination is reduced by only 3 percent by cutting the gage density in half; i.e., from 1 per square mile to 1 per 2-square miles. The optimum spacing of gages, as indicated by Equation 1, is in the order of one-fourth mile apart when the general rainstorm totals are considered.

The precipitation network in the Reynolds Creek Watershed was reduced from a density of 1 gage per square mile to 1 gage per 2-square miles in 1967-68 as shown in Figure 3. Each site was instrumented with an unshielded and shielded (rigid) gage with orifices at 10 feet. The requirement for the dual gages is explained ahead. The recording gages for use in inaccessible locations were modified to strip-chart recordings.

Attempts to establish definitive precipitation-elevation relationships for other than strictly rainfall data have been unsuccessful when using unshielded gage data. The weak correlations obtained are attributable to the inability of the unshielded gage to capture the falling precipitation, particularly snow, when exposed to even light winds. Usable data can be obtained by computing "actual" precipitation from measured catches by a shielded and an unshielded gage located at the same site. Such data have been obtained since installation of the dual gage network in 1967-68.

Procedures for computed "actual" precipitation were developed from the basic equations relating the ratios $\frac{U}{A}$ and $\frac{S}{A}$ to windspeed where U and S represent catches by unshielded and shielded gages, respectively, and A represents the vertical flux of precipitation. These basic equations take the form

$$\text{(1a)} \quad \frac{S}{A} = e^{-a\bar{W}} \quad ; \qquad \text{(1b)} \quad \frac{U}{A} = e^{-b\bar{W}} \qquad (2)$$

which may be combined to obtain

$$\frac{U}{S} = e^{-(b-a)\bar{W}} \qquad (3)$$

where a and b are constant and $\bar{W}$ is the windspeed. When wind is eliminated by simultaneous solution of equations 1b and 2, a calibration equation is obtained in the form

$$\ln \left(\frac{U}{A}\right) = B \ln \left(\frac{U}{S}\right) \qquad (4)$$

The calibration constant, B, has been evaluated as approximately 1.73 from profile measurements of unshielded precipitation gage catch and wind. Also, data from a snow pillow site along with catches by shielded and unshielded gages were used to substantiate the profile computations.

Computed precipitation values obtained by use of Equation 3 are essentially uninfluenced by wind or type of precipitation. The constants in Equations 2 and 3 are greatly different for rain and snow and the ratio of unshielded to shielded catch, or better the ratio of unshielded catch to computed "actual" precipitation, can be used to determine the occurrence of "rain" or "snow" at exposed, windy sites.

Data from the dual gage network have been used to compute "actual" precipitation by use of Equation 4. Some preliminary analyses have been made to examine the precipitation-elevation relationship using the computed values.

The ratios of monthly unshielded to shielded catch for a 12-month period from 10 dual gage sites are shown in Table 1. Since the ratio is about 0.90 for rainfall with a wind of 25 miles per hour. It can be assumed that the precipitation at a location is essentially snowfall for those months where the ratio is less than 0.90. Precipitation, therefore, occurs predominantly as snow at an elevation of about 4000 feet from December through April and at 7000 feet, the snow season extends from September into May. On this basis, the one year of computed precipitation indicates that about 45 percent of the precipitation occurs as snow at 4000 feet elevation and about 80 percent as snow at 7000 feet elevation. A better assessment must await the analyses of data on a storm basis since significant rainstorms do occur during the winter months.

Computed values of precipitation were obtained for a general storm, beginning on November 11, 1969, with a 24-hour duration. The air temperature at an elevation of 6800 feet was 30°F. during the storm. The precipitation-elevation relationship, using computed precipitation values, for the curve shown in Figure 4 is represented by the regression equation

$$Y = 0.2735X - 0.6865 \quad (r = 0.98) \qquad (5)$$

where Y is the computed precipitation in inches, X is the elevation in thousands of feet and r is the simple correlation coefficient. The ratios of unshielded catch to computed precipitation indicates that snow fell at elevations above 5300 feet. The ratio of unshielded catch to computed precipitation was only 0.23 at a ridge site (station 174X17 at 6760 feet elevation).

The precipitation-elevation curves obtained from monthly totals for unshielded and shielded gages, and computed precipitation accumulated over a period of one year are shown in Figure 5.

The regression equations are as follows with definitions the same as for Equation 5:

TABLE 1.--Ratio of monthly unshielded to shielded catch for period July 1968 through June 1969.

Station	Elev. (ft.)	July	Aug.	Sept.	Oct.	Nov.	Dec.	Jan.	Feb.	Mar.	Apr.	May	June
057X96	3885	--	0.97	1.00	0.95	0.91	0.87	0.93	0.81	0.83	0.82	1.00	0.95
075X89	3950	--	0.99	1.00	0.97	0.94	0.87	0.87	0.86	0.86	0.88	0.96	1.00
106X36	4270	1.00	0.98	1.00	0.94	0.93	0.85	0.92	0.63	0.84	0.80	1.00	0.98
043X41	4580	1.00	0.99	0.94	0.87	0.82	0.77	0.87	0.67	0.74	0.80	0.85	0.97
116X91	4770	1.00	0.97	0.90	0.91	0.90	0.83	0.88	0.67	0.82	0.77	0.96	0.95
145X37	5195	1.00	1.00	0.96	0.95	0.92	0.90	0.92	0.76	0.73	0.76	1.03	0.99
031X48	5880	1.00	0.96	0.90	0.92	0.80	0.63	0.60	0.60	0.47	0.64	0.92	0.95
144X62	5930	0.96	0.95	0.85	0.91	0.90	0.85	0.89	0.73	0.73	0.71	0.86	0.91
176X07	6800	--	0.98	0.89	0.87	0.87	0.77	0.78	0.59	0.63	0.67	0.95	0.95
163X20	7100	1.00	0.96	0.82	0.83	0.82	0.77	0.81	0.74	0.46	0.71	0.91	0.94

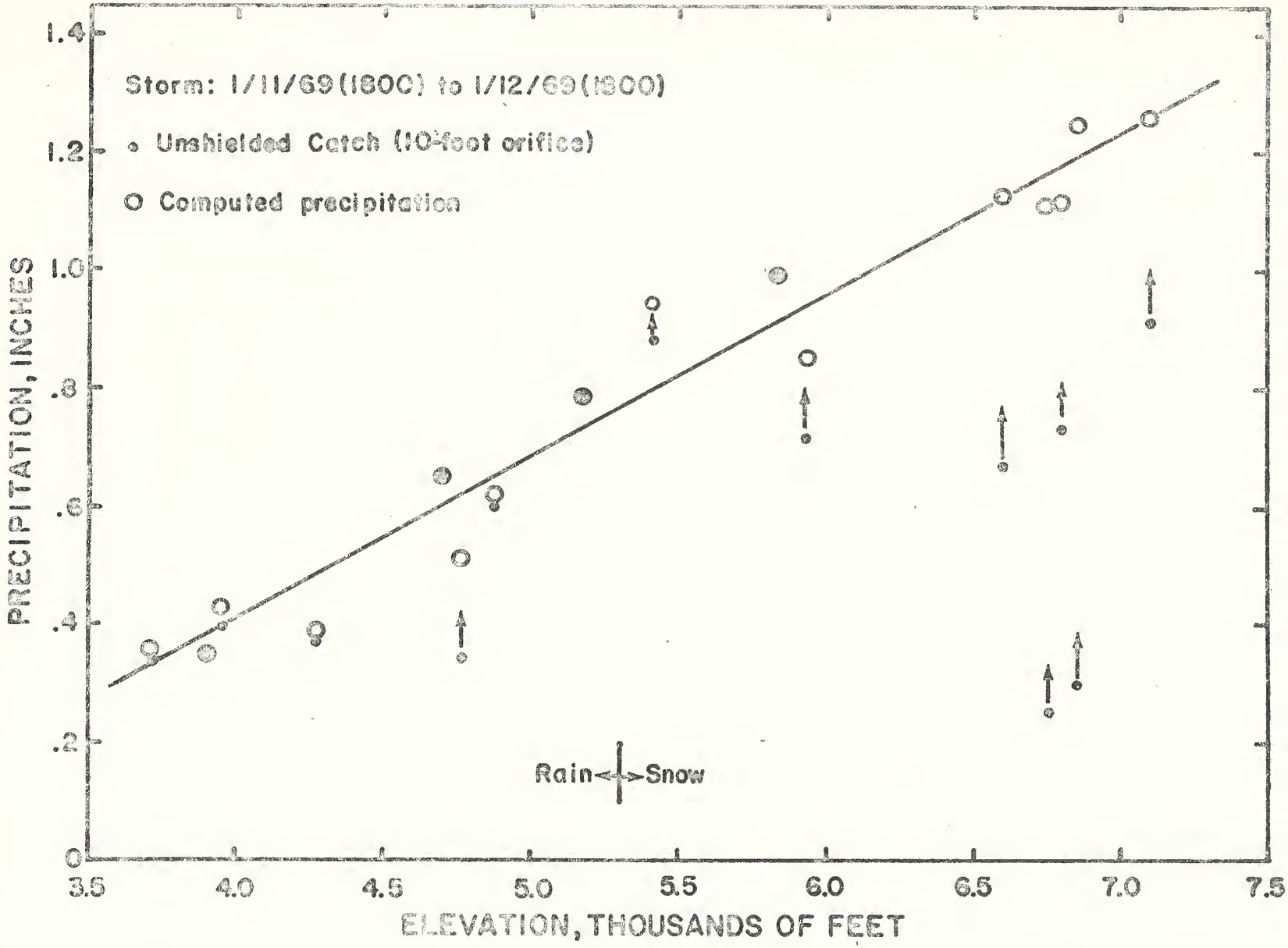

Figure 4. Precipitation-elevation relationship for computed storm totals.

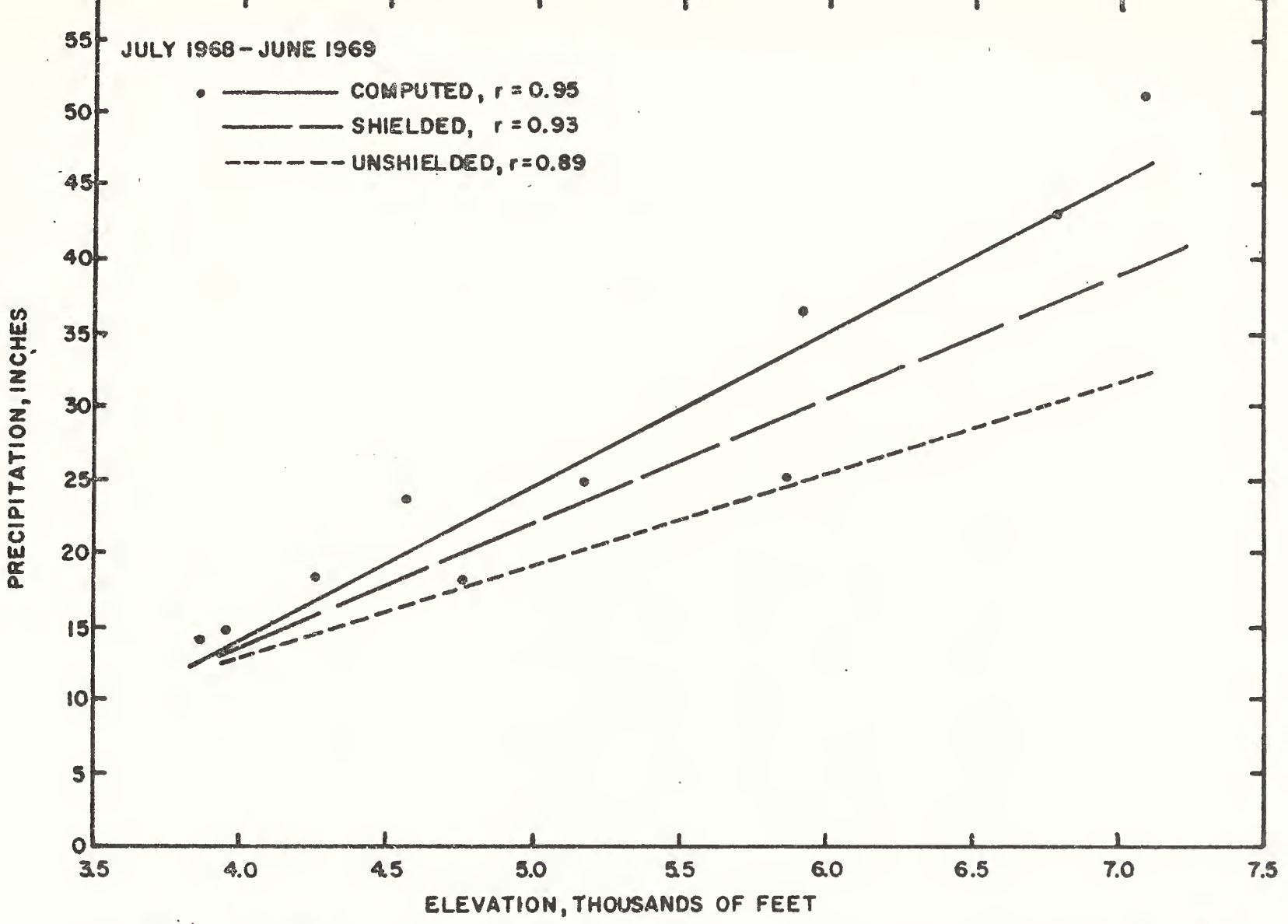

Figure 5. Precipitation – elevation curves from monthly totals for unshielded and shielded gages, and computed precipitation accumulated over a one-year period.

(Unshielded)

$$Y = 6.34X - 12.46 \quad (r = 0.89) \qquad (6)$$

(Shielded)

$$Y = 8.43X - 20.09 \quad (r = 0.93) \qquad (7)$$

and

(Computed)

$$Y = 10.45X - 27.60 \quad (r = 0.95) \qquad (8)$$

Use of monthly data rather than storm data in Equation 4 may introduce a slight bias since the calibration coefficient was obtained from storm data and because of the nonlinear relationship.

The highest correlation between precipitation and elevation is for the computed precipitation as might be expected. The increase in shielded catch over unshielded catch is about 23 percent and the computed values are increased by about 43 percent over the unshielded catch. The rigid shield, in effect, only corrects for slightly more than 50 percent of the wind effect on the unshielded gage catch.

The precipitation during the winter season occurs principally as a result of the moist southwestern air current which experiences lifting by mountainous terrain and by frontal systems. Air mass convective storms, however, are the principal sources of summertime precipitation. Comparisons of the precipitation-elevation relationship for these two seasons are shown in Figure 6. On the basis of one year of computed precipitation, the regression equation for the November-April period is

$$Y = 8.69X - 26.75 \quad (r = 0.94) \qquad (9)$$

and for the May-October period the regression equation for computed precipitation is

$$Y = 1.76X - 0.87 \quad (r = 0.92) \qquad (10)$$

and for unshielded catch, the regression equation is

$$Y = 1.38X + 0.52 \quad (r = 0.89) \qquad (11)$$

(As stated for Equation 5, Y is the precipitation in inches, X is the elevation in thousands of feet and r is the simple correlation coefficient.)

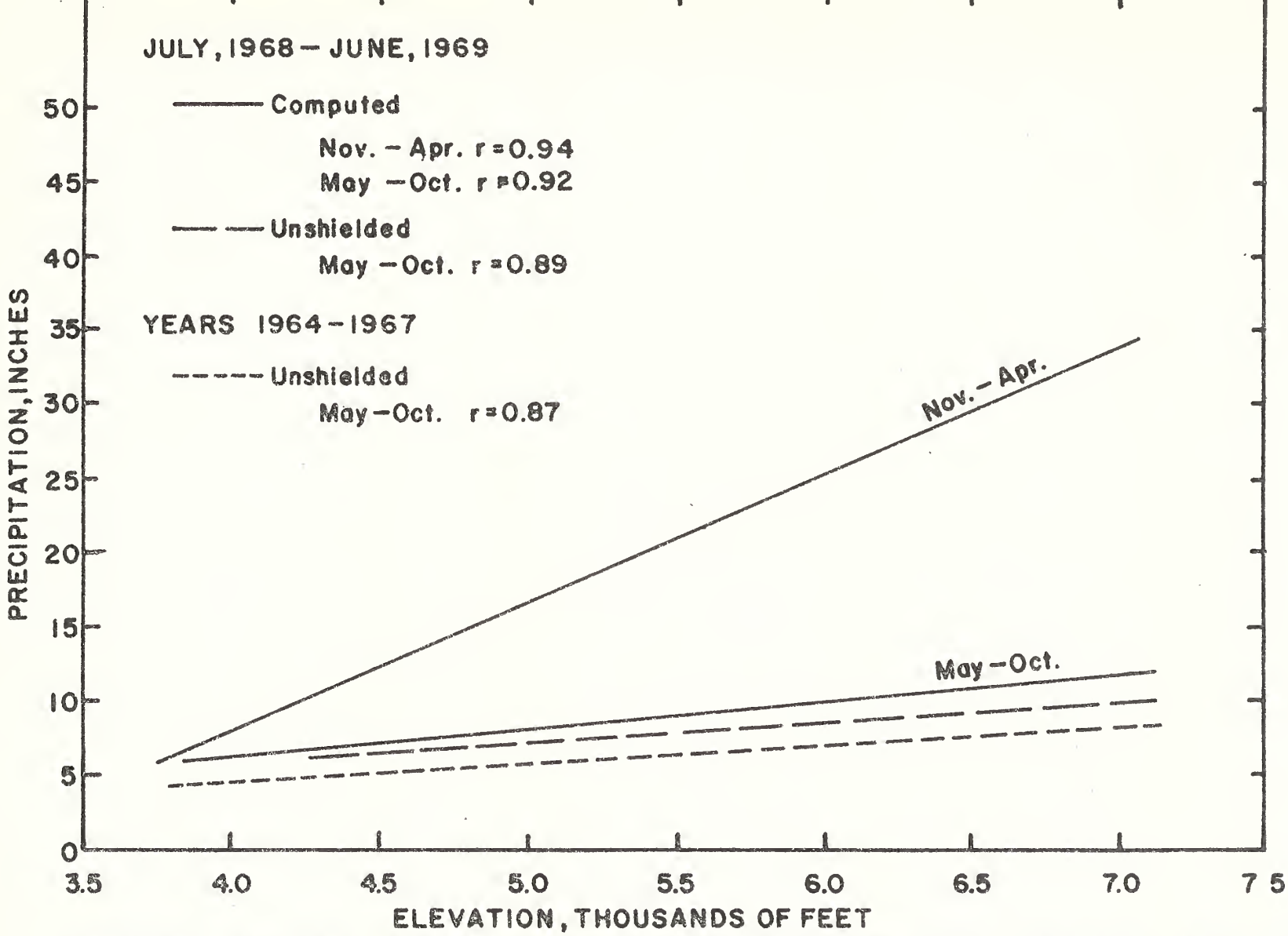

Figure 6. Seasonal precipitation – elevation relationship for computed precipitation and unshielded gage catch.

For comparison with a longer period, the precipitation-elevation relationship for unshielded gage catch over a four-year period for May-October is represented by the regression equation

$$Y = 1.38X - 1.09 \quad (r = 0.87) \qquad (12)$$

It is significant that the slope of the regression lines are identical for the one-year and four-year periods. Because of this fact the computed precipitation-elevation relationships for November-April (Equation 9) and for May-October (Equation 10) may be considered as representative, bearing in mind that the data used are from stations in the western, and southern portions of the watershed. During the November-April period, precipitation increased 8.69 inches (Equation 9) with each 1000-foot rise in elevation, while during the May-October period, this increase was only 1.76 inches (Equation 10).

The availability of accurate point precipitation data (computed) in the Reynolds Creek Experimental Watershed has made it possible to define precipitation-elevation relationships for a particular slope-aspect topography. The data reveal also that a normalization is needed to adjust the point values for their topographiic situation. The general precipitation elevation-topographic situation results will form the basic data for the determination of depth-duration-frequency and depth-area-duration relationships. The final step will be the structuring of a probabilistic precipitation model that incorporates the temporal and spatial variability of precipitation.

Ground Level Precipitation

The disposition of precipitation when occurring as snow is of major concern in assessing the snowmelt factor for actual inputs to a hydrologic model.

In the Reynolds Creek Watershed, seven snow courses are maintained at strategic locations. Photogrammetric surveys of a 100-acre watershed have been used to determine an accurate distribution of snow. As reported by Smith, et al. (46) in 1967, the standard error of the average snow depth obtained in the photogrammetric model was about 0.02 feet. These results indicate that inaccuracies in photogrammetric measurement of average snow depth over a large area can be expected to arise almost entirely from overall errors or bias in reading the model.

Data from snow courses, photogrammetric surveys, transects, and from a network of snow-sampling points will be used to develop a snow-cover-depth-water content relationship for a mountainous terrain. Such information is essential in the application of any snowmelt model.

Snowmelt

An intensity study of snowmelt on a watershed basis is extremely difficult because of the great variability in snow cover and site exposure. To overcome this difficulty, a special universal surface precipitation gage was designed by Cox and Hamon (10) to measure total precipitation reaching the ground site, snowmelt rates, and snow-water equivalent of the snow remaining in storage at the site. The instrument consists of a 5-foot-diameter platform made of light-weight concrete, supported by a liquid-filled 100-foot-coil of butyl tubing and a rigid border. An opening in the center of the platform allows for the collection of atmospheric melt, rain percolate and melt, or a combination of these, and rainfall.

Data from the universal surface precipitation gage will be used to test the snowpack energy balance equations as presented by Anderson (1) in 1968. This approach offers a more rational method of the snowmelt process than currently used temperature indexes or simple energy balance methods to determine the heat gained by the snowpack during periods of melt.

The energy balance of a snowpack for any increment of time can be expressed as

$$Q_\theta = Q_r + Q_h + Q_e + Q_l + Q_s + Q_n \qquad (13)$$

where Q_θ is the change in heat storage of the snowpack, Q_r is the net radiation heat transfer, Q_h is the sensible heat transfer. Q_e is the gain or loss of latent heat caused by evaporation, condensation, or sublimation, Q_l is the gain or loss of latent heat caused by freezing or melt, Q_s is the net transfer of heat by conduction at the snow-ground interface, and Q_n is the net heat transfer by a gain or loss of water.

In developing a usable snowmelt model for use in the hydrologic model, a number of assumptions and approximations will be made. Further, simplified empirical functions will be tested for representation of the critical components in the energy balance equation, (Equation 13).

EVAPORATION

The vapor loss from a watershed constitutes a major portion of the available water resulting from precipitation and ranged from near 70 percent in the humid East to over 90 percent in the arid West. An adequate procedure for estimating evaporation, therefore, is essential in the application of any simulation hydrologic model.

A variety of schemes based on pan-evaporation and potential evaporation procedures have been utilized to estimate watershed evaporation. It should be recognized that potential evaporation requires a 100 percent humidity at the evaporating surface. Estimates of actual evaporation by potential evaporation methods, therefore, can serve only as some reference index which must be modified to approximate actual evaporation.

Recent advancement in meteorological instrumentation has made it possible to measure evaporation in the field by the energy balance method where vertical gradient equations are used for sensible and latent heat transfer. This technique, perfected in 1965 by Fritschen (20), and referred to as the Bowen ratio method, may be represented as

$$E = (H-S) \; / \; (1 + \beta) \qquad (14)$$

with

$$\beta = \gamma \frac{T_1 - T_2}{e_1 - e_2} \qquad (15)$$

(with the transfer coefficients assumed equal) and where H is the net radiation flux, S is the soil heat flux, γ is the psychrometric constant, T is the air temperature and e is vapor pressure. The procedure requires no measurement of surface conditions or windspeed but extremely precise measurements of temperature and vapor pressure at two levels are needed. Under rather dry surface conditions, the equality of the transfer coefficients no longer holds and the vapor pressure gradient becomes particularly sensitive.

The combination of aerodynamic and energy balance approaches for measuring and predicting watershed evaporation appears to hold great promise. Penman, et al. (39), by assuming T_o and e_o as the virtual values of temperature and vapor pressure at the level where the virtual value of V (windspeed) is zero, have derived a general combination equation for evaporation in the form

$$E = \frac{\left[(\Delta/\gamma) \; H \right] + \left[1/h_o) \; E_a \right]}{(\Delta/\gamma) + (1/h_o)} \qquad (16)$$

where Δ is slope of the saturation vapor pressure curve, de/dT, at the mean air temperature, h_o is the virtual relative humidity, and E_a is an aerodynamic term involving windspeed, vapor pressure, and relative humidity at a height, and in addition, roughness and the virtual relative humidity. If the surface is saturated so that $h_o = 1.00$, then Equation 16 reduces to the ordinary Penman equation that is used to compute potential evaporation, E_p.

Another generalized combination method for determining evaporation from unsaturated surfaces has been presented by Tanner and Fuchs (51). Their equation is of the form

$$E = \left[(\gamma + \Delta) / \Delta\right] E_p - (\rho\, c_p / \Delta)\, h\, (e_o^* - e_z) \qquad (17)$$

where E_p is potential evaporation obtained from Equation 16 with $h_o = 1.0$ (a saturated surface), ρ is the density of dry air, c_p is the specific heat of air, h is the transfer coefficient, e_o^* is the saturated water vapor pressure corresponding to the surface temperature, T_s, and e_z is the water vapor pressure in the air at height z.

The measurement requirements are considerably less exacting in using Equation 17 than in the Bowen ratio method, Equation 14, when dealing with a well-defined surface. As pointed out by Fuchs et al. (21): "The advantages gained by introducing the surface temperature, T_s, measurement in the combination method is twofold. First, $(T_s - T_z)$ includes the layer of air close to the surface where the vertical temperature gradient is the largest. This alleviates the accuracy requirement of the temperature measurements and simplifies the instrumentation. Second, since T_s is taken at the level of zero wind velocity, the transfer coefficient, h, can be computed from a wind velocity measurement at a single height. When T_z and V_z (temperature and wind at height z) are measured close to the soil surface (e.g., 25 to 50 cm.), the adiabatic corrections are small and the fetch requirement is minimized."

The relation of actual evaporation to potential evaporation, as represented by Equation 17, demonstrates how the increase of the surface temperature depresses the evaporation below the potential rate. Fuchs et al. (21) state: "In practice this combination equation is limited to surfaces such as bare soils where the sensible heat is exchanged with the atmosphere from a well-defined surface. The

extension of the method to vegetation is improbable because sensible heat and latent heat exchanges between the surface and the air occur within the canopy as well as with the free atmosphere, and the surface temperature is not well defined."

Somewhat contradictory to the above statement is the use of a wind profile for determining h where the virtual value of V is zero. Further, the adiabatic wind profile is adjusted for the Richardson number which is expressed as a function of T_z, T_s, Z, V_z, D, and Z_o. It appears possible, therefore, as an engineering approach to consider, instead of the surface temperature, T_s, to determine e^*, the virtual value of temperature, T_o, or the temperature where the virtual value of V is zero. Equation 17 would remain unchanged except for the definition of e^*_o. The determination of h would remain as stated by Fuchs et al. (21) in the form

$$h = K^2 V_z \left[\Psi + \ln (Z + D) / Z_o \right]^{-2} \qquad (18)$$

with Ψ, the adiabatic curvature, as a function of the Richardson number, (Ri), in the form

$$Ri = (9/T) \left[(T_z - T_o) / V_z^2 \right] \left[\ln (Z + D) / Z_o \right] Z \qquad (19)$$

where K is the vonKarman constant, T is $(T_o + T_z)/2$ and D is the height displacement or the sum of the height above the soil where the wind velocity is zero and of the roughness length.

A field evaluation of procedures for measurement and prediction of watershed evaporation has been undertaken as a cooperative effort with the University of Idaho. Dr. George Belt of the College of Forestry has made complete energy budget and profile measurement at three sites in the Reynolds Creek Experimental Watershed. These data are for two dry sagebrush range sites and for an irrigated field. The energy balance determinations, using the Bowen ratio method, for a sagebrush site with moisture in the top foot at 20 percent by volume is shown in Figure 7. For this case, the ratio of sensible heat flux to latent heat flux is about 2.0 with only 28 percent of the net radiation used in evaporation.

The data obtained will be utilized in examining the procedure as outlined above. It seems reasonable to expect that the use of Equations 17, 18 and 19 with the surface temperature, T_s replaced by the virtual temperature, T_o, or the temperature where the virtual value of V is zero will offer an enlightening approach to watershed evaporation. Indeed, such an approach seems far superior to empirical correlations of E/E_p to soil water.

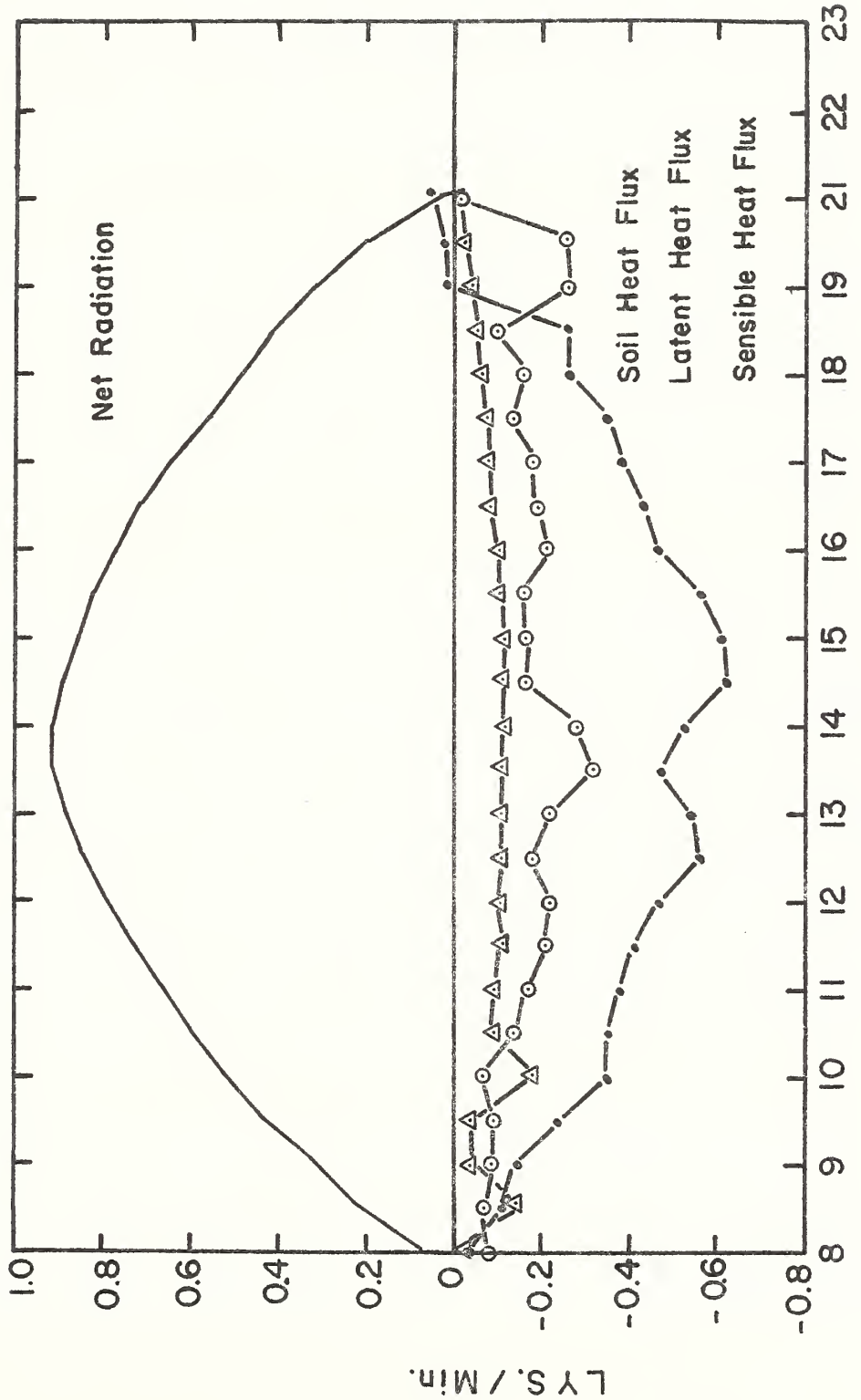

Figure 7. Energy balance at Sheep Creek Site, June 4, 1969.

INFILTRATION AND SOIL MOISTURE

Mathematical Models

Infiltration is an important link in the hydrologic cycle. The occurrence and magnitude of overland flow, quantities of interflow and base flow, and recharge to ground-water storage are determined by the rate of infiltration in relation to rainfall intensity or snow melt rate. Infiltration characteristics of soils within a basin must be well understood if an effective, physically-based mathematical hydrologic response model is to be developed.

Ground-water hydrologists and soil physicists have studied the physics of flow through porous media in much detail. Darcy's Law and the law of conservation of mass can be used to derive the general equation of flow, which is Equation 24 reported in the ground-water section of this report. One, two, or three-dimensional formulations of either steady or transient flow through saturated or unsaturated media can be developed from the general equation. Furthermore, the fluid can be compressible or incompressible, and the medium can be heterogeneous and anisotropic.

Initial research in unsaturated porous media flow involved the reduction of the general equation to the one-dimensional vertical flow case and the subsequent solution for a variety of boundary conditions. The finite difference approach was first used by Klute (31) in 1952. Philip (40) in 1957 made significant contributions in his outstanding seven-part infiltration paper. Numerical solution of the vertical moisture flow equation for layered soils was reported in 1962 by Hanks and Bowers (23). The constant rainfall case was considered by Rubin and Steinhardt (44) in 1963, and two years later Whisler and Klute (58) investigated the problem of hysteresis. Other significant findings were reported by Staple (48) and Rubin (43), who were concerned with the redistribution problem. Freeze (14) reported in 1967 of studying the continuity of flow between the saturated and unsaturated zones. He investigated one-dimensional, vertical, unsteady infiltration or evaporation above a recharging or discharging ground-water flow system.

Following Freeze's study, a research and development planning survey on theoretical and experimental aspects of watershed infiltration in terms of basic soil properties was conducted by Nelson and Jeppson (38). They presented an equation of flow similar to Equation 24, mentioned previously, except that it was formulated in terms of three soil properties: (1) moisture saturation, s, (2) intrinsic moisture conductivity, K, and (3) the capillary pressure, p_c. Their equation was the following:

$$\frac{\partial^2\phi}{\partial x^2} + \frac{\partial^2\phi}{\partial y^2} + \frac{\partial^2\phi}{\partial z^2} + \left(\frac{\rho g}{k}\right)\left(\frac{dk}{dpc}\right)\left(\frac{dpc}{dp}\right)\left[\left(\frac{\partial\phi}{\partial x}\right)^2+\left(\frac{\partial\phi}{\partial y}\right)^2+\left(\frac{\partial\phi}{\partial z}\right)^2\right.$$

$$\left. + \sin\alpha\,\frac{\partial\phi}{\partial x} - \cos\alpha\,\frac{\partial\phi}{\partial z}\right]\frac{\partial p}{\partial\phi} = \frac{uP}{k}\left(\frac{dS}{dpc}\right)\left(\frac{dpc}{dp}\right)\left(\frac{\partial p}{\partial\phi}\right)\frac{\partial\phi}{\partial t} \qquad (20)$$

Other variables in the above equation are defined as follows:

ϕ (x, y, z, t)	is the potential energy per unit weight of water
p (x, y, z, t)	is the pressure of the water
ρ	is the constant mass density of the water
g	is the gravitational constant
α	is the angle of inclination of the x axis with the horizontal
x, y, z and t	are respectively the Cartesian coordinates and time
u	is the dynamic viscosity of water and
P	is the porosity of the soil.

Nelson and Jeppson suggested two feasible approaches for measuring soil properties in the field. In either one the saturation and capillary pressure must be measured for a range of conditions on the same soil mass. Conductivity is to be obtained directly from the saturation-capillary pressure relationship in the first approach, where the second approach requires an analytic or numerical solution for the flow system. They recommended the first approach, and suggested testing the approximate equation of Brutsaert (6, 7) for the saturation-capillary pressure relationship

$$S_e = \frac{1}{\left(\frac{p_c}{p_b}\right)^{\lambda} + A} \qquad (21)$$

The above relationship can then be used to provide a relationship for the intrinsic conductivity,

$$k = \frac{P\sigma^2 S_e^2}{5} \int_{S_N}^{S} \frac{dS}{p_c^2} \qquad (22)$$

An equation of this form is termed a modified Burdine integral, which is developed and discussed by Brooks and Corey (5) and Laliberte et al. (32). The variables in Equations 21 and 22 are defined as follows:

S_e is the effective saturation

p_c is the capillary pressure

p_b is the bubbling pressure

λ and A are soil parameters to be determined

k is the intrinsic moisture conductivity

P is the soil porosity

σ is the fluid surface tension and

S is the saturation.

Freeze's work (14) differed from that of Nelson and Jeppson (38) in that the former had to consider both saturated and unsaturated flow in the same model. This was not the case in the latter study, since capillary pressure was used as the linking variable rather than saturation.

Application at Reynolds Creek

Guidelines were suggested by Nelson and Jeppson (38) for studying the problem of watershed infiltration. This program is currently being undertaken by the Northwest Watershed Research Center and its cooperators, Dr. Roland W. Jeppson at Utah State University and Dr. Royal H. Brooks at Oregon State University.

Study I - A Laboratory and Field Evaluation for in-place Measurement of Saturation and Capillary Pressure--is being conducted by Dr. Brooks and has an overall objective of providing the instruments and techniques for realistic in-place measurement of saturation and capillary pressure in the field.

Dr. Jeppson is developing the mathematical models for Study II - Evaluation of the Accuracy Needed in Capillary Conductivity - Capillary Pressure Results Based upon Steady Flow Solutions. The Northwest Watershed Research Center is primarily responsible for the experimental portions of the study. In June 1969 Jeppson (29) reported a theoretical model for the two-dimensional, steady-state flow system resulting from watershed infiltration. Output from the model is illustrated in Figure 8, which was obtained for a hypothetical watershed profile having a homogeneous soil and with approximately the upper third of the profile covered with a snowpack. Collection of field data for verification of the mathematical model is presently underway at Reynolds Creek. A watershed slope, which produces water during the snowmelt season, was selected on the Upper Sheep Creek study basin (57). Data from this profile will include water-table depths at several sites, vertical capillary pressure distribution at the sites, and capillary pressure in the soil beneath the snowpack. Moisture contents at these sites will also be measured during the snowmelt season.

One other steady-state investigation is currently being conducted by a Ph.D. candidate at Utah State University under the direction of Dr. Jeppson. The objectives of this investigation are: (1) to develop a mathematical model for steady-state axisymmetric infiltration through partially saturated soils, (2) to evaluate influences of the soil parameters used in the capillary-conductivity relationship, Equation 22, (3) to determine the importance of the steady-state "spreading effect" of moisture movement from a circular application area, and (4) to combine the steady-state results with existing one-dimensional unsteady vertical solutions to estimate transient intake rates.

The importance of the steady-state "spreading effect" of moisture movement from a circular plot is indicated in Figure 9. The rate of infiltration flux as determined by the numerical solution from the 20-foot diameter plot is $Q/K = 468.9$ square feet, whereas the rate of infiltration flux from an identical plot based on a one-dimensional solution (no spreading allowed) is $Q/K = 301.2$ square feet (Q is the flux with units of cubic feet/second and K is the saturated permeability with units of foot/second). Consequently, the boundary influence for the particular soil and geometry used in the solution cause the steady-state infiltration rate to equal 1.56 times that which would occur over an infinite area. The solution also shows that at the water table only 39 percent of the flux occurs within the original 20-foot diameter.

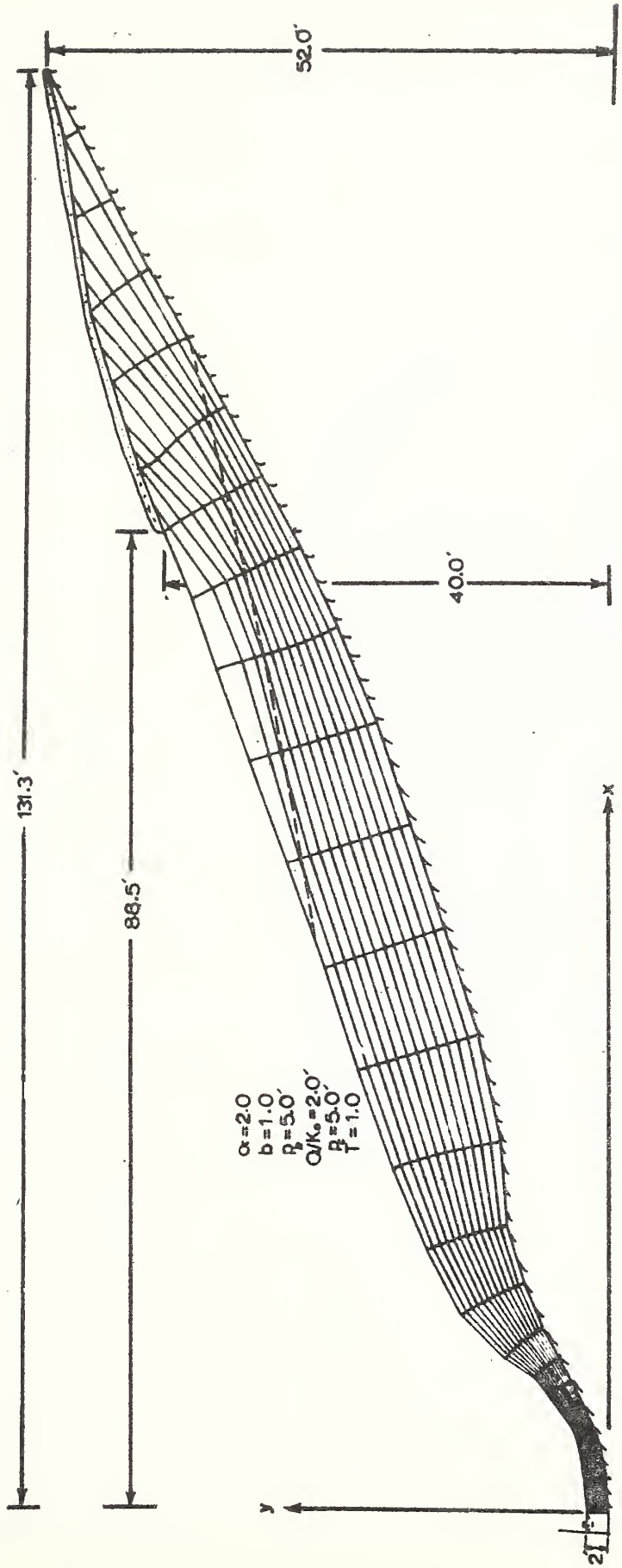

Figure 8. Flow net due to snowmelt on a hypothetical watershed profile having a homogeneous soil.

Model: $K_r = \dfrac{1.0}{\left(\dfrac{p_c}{p_b}\right)^{\eta} + b}$, $\eta = 2.5$ $b = 1.0$

$\dfrac{p_b}{\gamma} = 3.5$ $\dfrac{p_c}{\gamma} = 1.0$

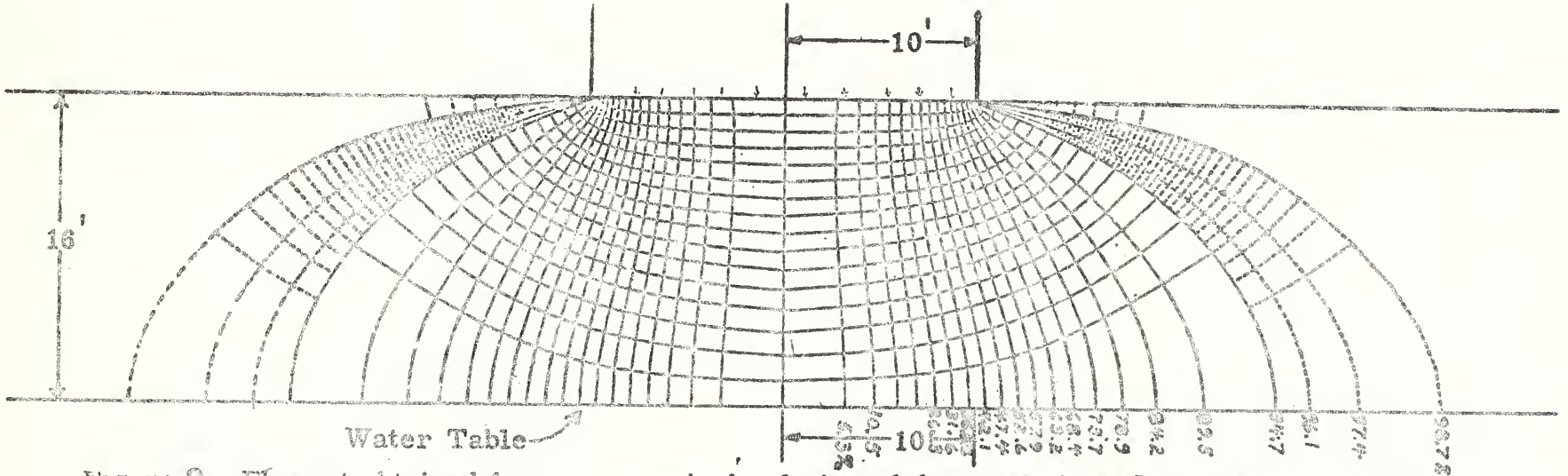

Figure 9 Flownet obtained from a numerical solution of the partially saturated flow resulting from surface application of water over a circular area. The dashed lines are streamlines (and corresponding potential lines) through which one-quarter as much flux passes as through the solid lines.

In order to verify the above mathematical axisymmetric infiltration models a portable gamma-probe, rainfall simulator infiltrometer was designed under a cooperative project for the Northwest Watershed Research Center by the University of Idaho Engineering Experiment Station (56). This device will be used to control surface applications of water for determining hydraulic properties of field soils in situ. The most important hydraulic properties are the pressure-permeability and saturation-permeability curves of soils under dynamic flow conditions. A gamma-ray probe is used to measure the water content of the soil during and after surface applications of water. A multiple-cell tensiometer, which is being developed at Oregon State University under a cooperative agreement with the Northwest Watershed Research Center, will be installed under the rainfall simulator and adjacent to the gamma-ray probe to provide data on capillary pressure during infiltration and redistribution of water.

The first operational version of the gamma probe-rainfall simulator infiltrometer was field tested on the Thompson Watershed near Moscow, Idaho, on August 15-16, 1969. For the tests, five tensiometers were installed near the gamma-density probe access tubes to measure soil-water suction at the ground surface and at 10, 20, 30 and 40 centimeters below the surface.

Soil samples were obtained about 10 hours after ending of the rainfall-simulation run. The soils data are listed in Table 2.

The wet densities were used with density standards to obtain a density-calibration curve of the form

$$X = 4.91 - 2.77 \log (Y \times 10^{-3}) \qquad (23)$$

where X is the field density in gm./cm.^{3} and Y is the number of counts over a 1-minute period. The percent moisture by dry weight was considered far more accurate than bulk density determination; therefore, the bulk density values of the soil samples were adjusted by use of these moisture values and the calibration curve.

These adjusted densities are tabulated in Table 2. Percent moisture by volume was computed for selected field test data by use of the calibration equation and the adjusted bulk densities.

No useful field data were obtained by the tensiometer units. At the beginning of the test, the tensiometers worked well, but as the test progressed air leaked into the water lines causing the tensiometers to become insensitive.

TABLE 2.--Soil sample data and adjusted bulk densities for gamma-probe infiltrometer test at Thompson Watershed near Moscow, Idaho, August 16-17, 1969 1/

Depth 2/ In.	Moisture % Dry Wt.	Bulk Density gm./cm.^{3}	Comment	Depth In.	Adjusted Bulk Density gm./cm.^{3}
0-1	32.90	1.048	Silt Loam	0.5	1.41
1-2	23.50	1.509	Silt Loam		
2-3	22.70	1.433	Silt Loam	2.0	1.61
3-4	22.63	1.513	Silt Loam		
4-5	17.30	1.613	Sandy-Silt Loam	4.5	1.67
5-6	17.98	1.565	Sandy Loam		
6-7	13.62	1.758	Sandy Loam	6.0	1.49
7-8	19.95	1.365	Silt-Sandy Loam		
8-9	24.14	1.278	Silt Loam	8.5	1.17
9-10	18.34	1.296	Silt Loam		
10-11	15.54	0.987	Silt Loam	10.0	1.13
11-12	10.58	--	--	12.5	1.13
13-15	10.79	1.045	Silt Loam	14.0	1.14
15-17	11.75	1.022	Silt Loam	16.5	1.06
19-21	11.80	--	--		
23-25	11.49	--	--		

1/ Wheat-stubble site about 20-feet from drainageway on a north-facing slope of 2 to 3 percent.

2/ Sample taken at 11:30 a.m. with 2 5/8-inch diameter sampler between south probe and gamma source.

3/ Wetting front clearly visible to 9.5 inches.

Initially, the field testing of the gamma-probe infiltrometer and of tensiometer system was not intended to collect usable data. As the test progressed, it became apparent that useful data could be obtained by running the system well into the night to obtain density values as the wetting front moved into the soil profile.

The data showed great variations during the late afternoon and early evening due to temperature effects on the gamma-density probe. The preamplifier for the probe is mounted in a special switch box and was exposed to ambient air temperature and direct sunshine. The system became stable about 9:00 p.m. Readings obtained the next morning, at the time soil samples were taken, were adjusted according to comparable readings at the 16.5- and 20-inch depths obtained during the evening run.

Simulated rainfall began at 4:30 p.m. on August 16 at a rate of 0.5 inch per hour and ended at 1:40 a.m. the next morning. There was slight runoff by 7:30 p.m.; ponding over one-half of the 6- by 6-foot plot occurred by midnight; and runoff was collected from 12:45 a.m. until the end.

The runoff rate for the period 12:45 a.m. to 1:30 a.m. was 0.03 inch per hour. Considering this rate as approximate for the whole period of runoff, the total runoff observed was only 0.1 inch or a little over 2 gallons.

The runoff water collected, however, was only a portion of the total runoff since the border frame was only superficially in place. Surface runoff was not the objective of this particular test.

Soil moisture profiles for four different times are shown in Figure 10. (No rainfall occurred at the site during the previous 8 weeks.)

At the 0.5-inch depth the soil was water-logged at 9:30 p.m. and the detectable wetting front extended to about 6 inches. By 1:20 a.m. the detectable wetting front had advanced to about 10 inches. The visual wetting front was at 9.5 inches at 11:30 a.m. the following day, but the detectable wetting front (density changes) extended downward to nearly 12 inches.

During the period 9:20 p.m. to 1:20 a.m. water was added by the rainfall simulator at a rate of 0.5 inch per hour. The increase in soil water, however, was only 0.33 inch for the period 9:20 p.m. to 11:20 p.m. and only 0.26 inch for the period 11:20 p.m. to 1:20 a.m. Ponding of

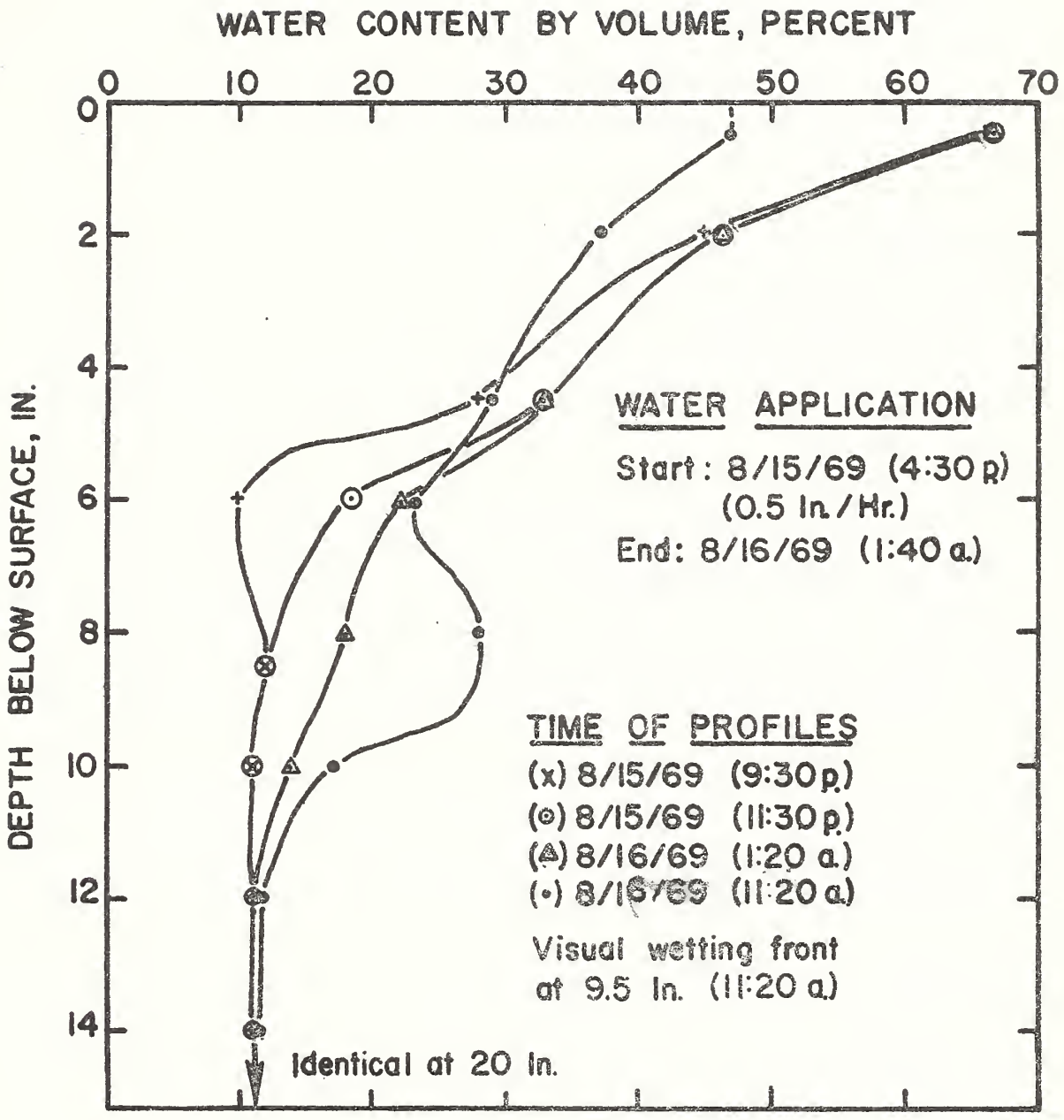

Figure 10. Moisture content profile obtained by gamma probe–rainfall simulator infiltrometer.

water on the plot with increasing runoff was apparent during these time periods.

The curve for August 16, 1969, at 11:20 a.m., Figure 10, shows the redistribution of soil water that occurred following the ending of simulated rainfall at 1:40 a.m. In the upper profile, 5.5 inches depth, the profile lost 0.47 inch of water and the lower profile gained 0.37 inch of water. Some downslope interflow possibly occurred in the saturated upper inch or two of soil.

The field test clearly demonstrated that the portable gamma probe-rainfall simulator infiltrometer can be used in the field for controlled application of simulated rainfall with concurrent measurement of soil-water changes. Such data can be used with an infiltrometer-flow system analysis to analyze infiltration or with a functional tensiometer system to determine in situ soil physical properties for use in mathematical infiltration models.

The multiple-cell tensiometer for measuring capillary pressure performs satisfactorily provided the soil moisture content is not too low. If the saturated tensiometer units are installed in dry soil, it is difficult to keep the capillary pressure in the cell below the critical pressure needed to remain saturated. If they are installed at many depths in the soil profile, a great deal of time occurs before the wetting front reaches the deeper cells, thus creating a difficulty in maintaining complete saturation.

It is very possible that the first 6 inches of any soil profile will largely affect the infiltration, subsequent runoff and seepage. Therefore, it may be necessary only to measure these hydraulic properties in the surface layer of the profile, thus simplifying field procedures and techniques.

A rapid response gamma-ray probe appears necessary for transient measurement of water content with capillary pressure. A simpler technique might be to start the rainfall simulator at a high intensity to quickly saturate the surface layer and bring it to a quasi-steady-state condition. By reducing the rainfall-simulator rate in small increments allowing for steady-state conditions to occur for each rate, the water content could be determined by slow-counting gamma-ray counters.

Rapid response-pressure transducers are readily available and a necessary part of measuring capillary pressure even under steady-state conditions.

Study III - Determination of the Approximations to be Used for Infiltration Problems - is proposed to determine the simplest, most usable approximations that are accurate enough to represent the soil characteristics (saturation, capillary pressure, and capillary conductivity) for the infiltration problem. This study will overlap Studies II, IV, V and VI.

The fourth study has essentially the same objectives as the second study but is extended to help evaluate the sensitivity of the time varying infiltration rate to the conductivity distribution, based upon a one-dimensional transient flow analysis, and it should consider the sensitivity of the infiltration rate to the saturation characteristics.

Study V - Evaluation of the Modified Burdine Integrals Used to Obtain Capillary Conductivity Characteristics - was included to determine the basic accuracy of the integrals. Nelson and Jeppson (38) performed the analytical integrations for the drainage case, thus these very accurate results and several approximate representations of saturation distributions can be used to compare to experimental measurements of conductivity for both draining and imbibing conditions. Sufficient experimental drainage data appears to be available, but far less imbibition data is available, thus Study VI was proposed.

Study VI - Laboratory Study of Soil Characteristics Under Imbibition Conditions. The objective of this investigation is to provide a complete set of experimental data for several soils under imbibition conditions. Several uses of the data were proposed, the most important was to develop a phenomenological description of saturation-capillary pressure characteristics for imbibition. Such a description would allow further evaluation of the modified Burdine equations as recommended in Study IV with The several approximate relationships can also be analyzed further these data. The magnitude of hysteresis effects can be studied on selected samples under draining conditions. It was recommended that 12 to 15 soil samples from the Reynolds Creek Watershed be selected for study.

The final study - Develop or Obtain Transient Two-Dimensional Solution Methods - was proposed to obtain stable numerical solution methods for partially saturated boundary value problems. Two-dimensional flow down a slope, when rain is falling or snow is melting and imbibition conditions exist, is of special concern. Nelson and Jeppson proposed an appropriate boundary value problem. Solution of this problem would provide a standard for evaluating the simpler approximate infiltration equations, such as Brutsaert's (6). Explanations

and insight into commonly observed field occurrences would also be provided by these mathematical solutions. Dr. Jeppson is currently formulating a model for this study. He proposes to follow this study by formulating a three-dimensional axi-symmetric transient solution.

In summary, the above studies were proposed in order to study in depth the underlying physical principles governing water inflow and movement through soils. The appropriate boundary value models specify that the interrelationship of water saturation, capillary pressure, and water conductivity must be measured in the field. Physically-based mathematical models such as these should provide a method of analyzing the interflow component of surface runoff, besides providing a necessary linking mechanism with the ground-water flow systems.

SURFACE RUNOFF

Mathematical Models

Surface runoff is the portion of total runoff which flows over the land surface and through the surface channel system. The two components of surface runoff are overland flow and stream channel flow. A hydrodynamic analysis of either overland flow or stream channel flow yields two partial differential equations, which describe spatially varied, unsteady, open channel flow. The equations are derived from the Laws of Conservation of Mass and Momentum.

Keulegan (30) in 1944, appears to have been the first to make a completely theoretical investigation of overland flow. His analysis accounted for variation in depth and velocity with time and space, frictional effects, and the momentum of entering flow. Izzard (27) followed closely in 1944 with an experimental analysis that has proven to be somewhat satisfactory for practical hydrologic analysis. Other early investigations of overland flow were conducted and reported by Gilcrest (22), Richey (41), Behlke (2), Liggett (34, 35), Chow (9), Chen (8), Woo and Brater (61) and Yu and McKnown (64). In 1953 Stoker (50) presented the hydrodynamic equations as applied to flood prediction and river regulation problems, and Isaacson et al. (26) solved the equations by using finite difference methods.

Both overland and channel flow can be described by the following one-dimensional hydrodynamic equations of continuity and motion:

$$y \frac{\partial v}{\partial x} + v \frac{\partial y}{\partial x} + \frac{\partial y}{\partial t} = q - i , \qquad (26)$$

$$\frac{\partial v}{\partial t} + v \frac{\partial v}{\partial x} + g \frac{\partial y}{\partial x} = g (S_o - S_f) - \frac{v}{y} (q - i), \qquad (27)$$

where:

- y is the water depth measured from the channel bottom
- x is the distance along the channel bottom
- v is the average velocity of flow through a channel cross section
- t is time
- q is lateral inflow or rainfall rate
- i is the rate of lateral outflow (infiltration)
- g is the gravitational constant
- S_o is the channel bed slope and
- S_f is the friction slope (slope of the energy line).

Total surface runoff models have been attempted by several authors. Wooding (62) combined overland flow and channel flow by solving the kinematic wave formulation of the complete Equations 26 and 27. In the kinematic formulation equation 27 is reduced to:

$$S_o = S_f \,, \tag{28}$$

which is essentially the uniform open channel flow equation. Harbaugh and Chow (24) used Equations 26 and 27 as a basis for a numerical mathematical model, in which overland flow is analyzed first with rainfall as the spatially-varied inflow; channel flow is then analyzed using the previously computed overland flow as the spatially-varied lateral inflow. Another model was proposed by Machmeier and Larson (36), who used the complete hydrodynamic equations to route unsteady flow through an idealized channel system.

Woolhiser and Liggett (63) concluded that for most practical overland flow problems the kinematic wave formulation is quite accurate. They also introduced a dimensionless parameter,

$$K_N = \frac{S_o \quad L_o}{H_o \quad F_o^2} \,, \tag{29}$$

known as the kinematic flow number, to determine when satisfactory overland flow solutions can be obtained from the kinematic wave formulation.

New parameters introduced in Equation 29 are defined as:

K_N is the kinematic flow number

L_o is the length of overland flow plane

H_o is the normal depth of flow at the downstream end for equilibrium discharge

F_o is the Froude number for normal flow at the downstream end for equilibrium discharge.

They demonstrated that if K_N is less than 10, the kinematic wave is a poor approximation; this usually occurs for short smooth planes with small slopes and high input. For most naturally occurring overland flow situations K_N rarely falls below 10. Brakensiek

and Onstad (4) stated that the kinematic formulation could be applied to upland areas having ground and channel slopes greater than 0.5 percent.

The use of a proper friction slope (S_f) relationship in either Equation 27 or Equation 28 is deemed very important by Schreiber (45). Attempts to simulate laminar or hydraulically smooth flow hydrographs by using a turbulent flow friction slope relationship, such as Manning's Equation or Chezy's Equation, were unsatisfactory. Likewise, hydraulically rough or turbulent flow hydrographs were not adequately simulated by using a laminar flow friction slope relationship. A laboratory study utilizing a rainfall simulator and a physical model catchment was conducted by Schreiber in cooperation with the Agricultural Research Service Erosion Laboratory at Pullman, Washington. The laboratory study was used to verify the mathematical model, which was based upon the kinematic wave formulation and parameter optimization.

Schreiber proposed that the Darcy-Weisbach friction factor (f) be used to express the friction slope (S_f) in Equation 28. The friction factor can be formulated for either laminar or turbulent flow, and it provides a roughness relationship that varies with depth of flow. For laminar flow the friction factor is given by

$$f = \frac{K}{R_N}, \qquad (30)$$

where K is a parameter that can vary from approximately 14 to 60 for laboratory flumes and R_N is the Reynolds Number. Since splashing raindrops have an effect of added resistance, the parameter K was allowed to vary throughout a hydrograph. Optimization procedures were used to zero in on a K-value for each section of the hydrograph. In general, K was highest at the beginning of a storm, and as depth increased, K subsided somewhat until rainfall ceased. After rainfall stopped, K dropped sharply and retained essentially a constant value during the recession phase of the hydrograph. A descriptive variation of the parameter K for two tests is illustrated in Table 3.

The corresponding hydrographs for these two tests are shown in Figures 11 and 12. The Q2 hydrograph (solid line) is the best fit sectionally optimized hydrograph for which Table 3 is appropriate. Hydrograph Q1 (++) is the best-fit hydrograph using a single value of K for the entire hydrograph. Also indicated in Figures 11 and 12 are the fitting statistics USTA1 and USTA2. These U-statistics are computed for every trial hydrograph as the sum of the squares of the deviations between the ordinates of the predicted and the laboratory hydrographs. The best-

TABLE 3.--Time variation of laminar friction parameter K for sectionally optimized hydrographs obtained from a concrete plane surface.

Test No., Bed Slope, Precipitation Rate, and Duration			
No. 19 S_o = 0.0465 Ft./Ft. P = 3.23 In./Hr. D = 1.0 Min.		No. 33 S_o = 0.0806 Ft./Ft. P = 1.20 In./Hr. D = 4.0 Min.	
Time, Min.	K	Time, Min.	K
0.2	78	0.2	11
0.4	77	0.4	30
0.6	51	0.6	30
0.8	39	0.8	25
1.0	36 1/	1.0	25
1.2	16	1.2	26
1.4	11	1.4	25
1.6	10	1.6	25
1.8	10	1.8	25
2.0	9	2.0	26
2.2	8	2.2	27
2.4	8	2.4	27
2.6	8	2.6	26
2.8	8	2.8	26
3.0	7	3.0	25
3.2		3.2	25
3.4		3.4	24
3.6		3.6	23
3.8		3.8	23
4.0		4.0	23 1/
Time, Min.	K	Time, Min.	K
4.2	14	4.2	5.2
4.4	11	4.4	5.4
4.6	9	4.6	5.6
4.8	8	4.8	5.8
5.0	8	5.0	6.0
5.2	7	2/	6
5.4	7		
5.6	6		
5.8	5		
6.0	5		
2/	5		

1/ Precipitation ceased at this time.

2/ The remainder of the hydrograph beyond duration plus two minutes was taken as a single section.

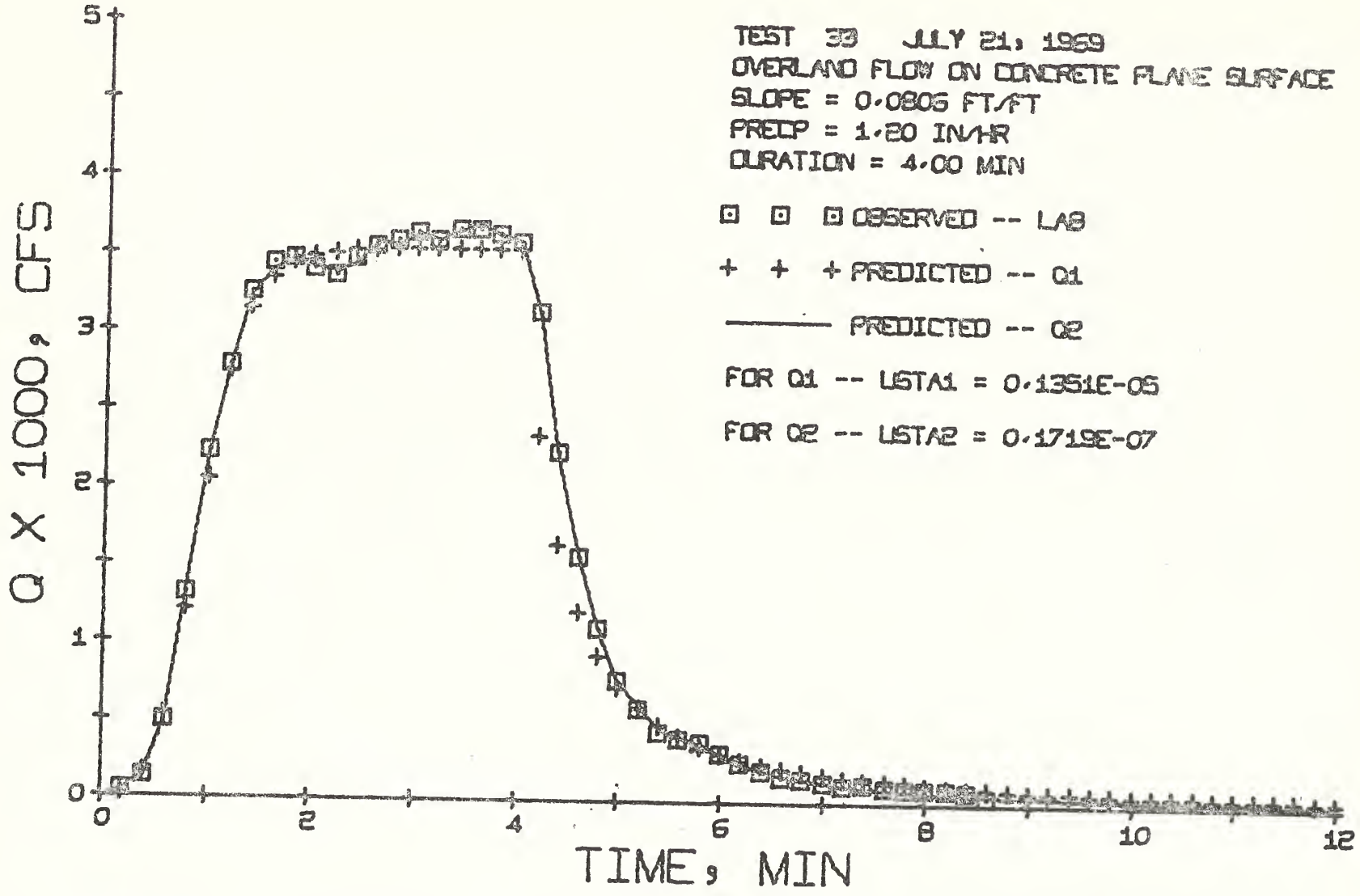

Figure 11. Comparison of predicted to observed equilibrium hydrographs.

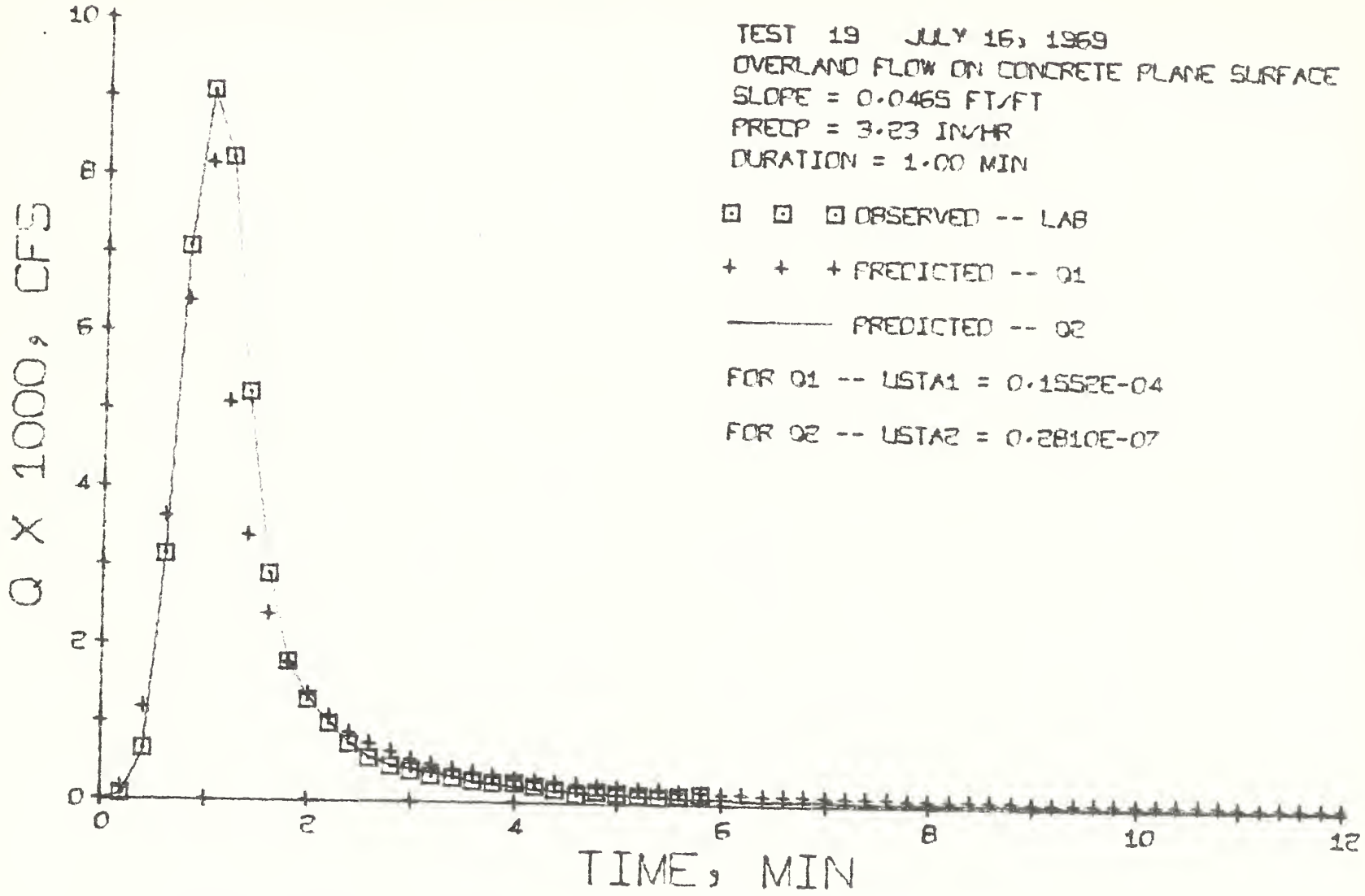

Figure 12. Comparison of predicted to observed nonequilibrium hydrographs.

fit hydrograph is the one for which the U-statistic is minimum. As indicated in both figures, the best-fit sectionally optimized hydrograph (Q2) is a better representation of the laboratory data than is the best-fit single parameter hydrograph (Q1).

Application at Reynolds Creek

Field testing of Schreiber's overland flow model by using test plots is anticipated. Plots will be chosen in order to analyze the effects of different slopes, slope lengths, soil types, and vegetative cover. Since the Reynolds Creek Watershed is located in a semiarid region, a rainfall simulator (sprinkler system) will be used to produce artificial storms on the plots.

In conjunction with field testing the overland flow model, a mathematical model having provisions for stream channels and topography will be developed. Laboratory data have been obtained for a catchment including various combinations of stream channels and topography, as well as overland flow planes. These data will be used to verify the mathematical model before field evaluation is attempted. Data from microwatersheds approximately two acres in area will be used before any attempt is made to simulate surface runoff hydrographs from larger watersheds.

It is believed that system decomposition may be used in a mathematical surface runoff model to subdivide the catchment system into homogeneous subsystems; i.e., overland flow planes and stream channels of various orders. The composite system hydrograph may then be reconstructed by combining the optimized subsystem hydrographs. Overland flow hydrographs would be used as input (lateral inflow) to channels having a Strahler-Horton Order of 1. Likewise, hydrographs for channels of succeeding orders could be obtained.

Since the surface runoff process is so extremely complex, using the hydrodynamic approach, even with the simpler kinematic formulation, may prove to be prohibitive. However, insight into the physical process is gained from solving the unsteady flow equations, and such insight should aid in evaluating less complex models. Therefore, our desire for a physically-based surface runoff model may need to be tempered with practical considerations which point toward parametric analysis of some of the components.

GROUND-WATER FLOW

Mathematical Models

Any mathematical model of a total watershed must not ignore the important component of ground-water flow. It would be questionable, indeed, to devise a hydrologic water balance model that did not include a ground-water component. Furthermore, an understanding of the basin-wide ground-water flow regime is necessary before many projects, such as waste disposal sites, large surface water reservoirs, and water supply systems, can be designed.

The physical laws governing steady-state ground-water flow were first presented in the correct mathematical structure in 1940 by M. King Hubbert (25). Transient (unsteady) ground-water movements were being studied at the same time by other hydrologists and applied mathematicians. As indicated by Freeze (15) researchers studying unsteady ground-water movement during the period 1935-1960 used the individual well as a unit of study, whereas Hubbert analyzed large-scale regional effects. The ground-water basin was finally established as an acceptable study unit in the 1960s. Tóth (52, 53, 54) expanded Hubbert's work in 1962 and 1963 by establishing that exact ground-water flow patterns could be derived as solutions to boundary value problems. Tóth's method was reasonably general, but the solutions were applicable only to homogeneous media and to the special cases considered.

Freeze's thesis study (15) was motivated by the desire to extend the available solutions to more general cases. His objectives were to obtain with a mathematical model the flow patterns for a general three-dimensional, nonhomogeneous ground-water basin having any water-table configuration and to investigate the effects of the water-table configuration and geologic boundaries on the flow system. This thesis was condensed into three papers published in 1966, 1967, and 1968 by Freeze and Witherspoon (17, 18, 19).

Finite difference solutions to the partial differential equation of ground-water flow,

$$\frac{\partial}{\partial x}\left[\rho K\,(x,\ y,\ z)\ \frac{\partial \phi}{\partial x}\right] + \frac{\partial}{\partial y}\left[\rho K\,(x,\ y,\ z)\ \frac{\partial \phi}{\partial y}\right] + \frac{\partial}{\partial z}\left[\rho K\,(x,\ y,\ z)\ \frac{\partial \phi}{\partial z}\right] = \rho\ \frac{\partial \theta}{\partial t} + \theta \frac{\partial \rho}{\partial t}, \qquad (24)$$

with the right-hand side equal to zero (steady state) comprised Freeze's mathematical model. The parameters in Equation 14 are defined as follows:

ρ	is the mass density of the fluid
K	is the permeability of the aquifer
x, y	are the horizontal coordinate directions
z	is the vertical coordinate direction or elevation head
ϕ	is the hydraulic potential energy per unit weight
θ	is the volumetric saturated moisture content or the porosity of the medium and
t	is time.

For boundary conditions Freeze assumed that the ground-water basin was bounded on the bottom by a horizontal impermeable layer, on the top by the water table, and on all sides by vertical impermeable boundaries (ground-water divides).

Recent unpublished research at Washington State University by J. Mellott and J. Crosby (37) has been directed toward revising Freeze's model to make it more universally applicable.

Another outgrowth of Freeze's work is being conducted at the University of Wisconsin by J. A. Spooner (47). This work is being directed towards a nonhomogeneous, simplified anisotropic case, simplified in the sense that the flow-field is horizontally isotropic. Spooner has written computer programs to calculate the potential distribution of the field and flow quantities across any specified boundaries. Program descriptions and data input procedures are very well defined.

Freeze and Harlan (16) indicate that an average water-table position should be an adequate steady-state boundary condition to simulate the ground-water component of a hydrologic response model, providing that the zone of fluctuation is small and the relative configuration of the water table remains constant. An unsteady state or transient mathematical model will be necessary if these two conditions are not satisfied. Finite difference solution models for the two-dimensional horizontal unsteady case have been developed by Tyson and Weber (55) and Pittenger, et al.(3).

Three-dimensional transient models for basin-wide ground-water flow have not yet been developed, but Davis and DeWiest (12) have derived the partial differential equation

$$K\rho \left(\frac{\partial^2 \phi}{\partial x^2} + \frac{\partial^2 \phi}{\partial y^2} + \frac{\partial^2 \phi}{\partial z^2}\right) + 2K\beta\rho^2 g \left[\left(\frac{\partial \phi}{\partial x}\right)^2 + \left(\frac{\partial \phi}{\partial y}\right)^2 + \left(\frac{\partial \phi}{\partial z}\right)^2 - \frac{\partial \phi}{\partial z}\right] = \rho^2 g \left[(1 - \beta)\alpha + \beta\rho\right] \frac{\partial \phi}{\partial t}, \qquad (25)$$

where the parameters are defined as in Equation 24. In addition:

β is the compressibility of the fluid

g is the gravitational constant and

α is the vertical compressibility of the granular skeleton of the medium (reciprocal of bulk modulus of elasticity).

A new powerful numerical approach for solving transient fluid flow problems in complex systems is reported by Javendel and Witherspoon (28) and Witherspoon et al. (60). This approach is called the finite element method and is adaptable to digital computers. The partial differential equation and the initial and boundary conditions are replaced by a corresponding calculus of variations problem. A finite number of subregions replaces the continuum, and the variational principle is expressed as a summation of functionals. The solution to the original boundary value problem is obtained by minimizing the resulting functional with direct methods of the calculus of variations. This method was verified by comparing results to published analytical solutions, but no field applications were given. Ground-water researchers at the University of Idaho, R. Williams and D. Allman (59). are currently striving to apply the finite element method to field situations.

Application at Reynolds Creek

The Northwest Watershed Research Center is presently involved in testing the workability of several of the above mathematical models with field data taken from the Reynolds Creek Experimental Watershed. Spooner's model (47) for steady-state, nonhomogeneous, anisotropic regional ground-water flow will be the first model tested, since it appears to be one most easily made operable. Excellent instructions are available

concerning how to use the computer programs and how to include necessary boundary conditions derived from field data. On the other hand, the programs given by Freeze (15) are difficult to make operable without modification, as indicated by Mellott and Crosby (37), and larger amounts of computer storage are required than for Spooner's model. But Mellott and Crosby do have their model operable on Washington State University's large IBM 360 digital computing system. Contact has been made with Mellott and Crosby, and they can run the Reynolds Creek data through their model under a cooperative project already in effect at Washington State University. This route may be followed if Spooner's model proves to be inoperable.

Steady-state models may not be appropriate to the natural conditions found at Reynolds Creek. If this proves to be the case, then testing of a finite-element transient model would logically follow. Williams and Allman (59) at the University of Idaho have indicated much interest in testing their finite-element transient model with data from Reynolds Creek as a part of a current cooperative study.

Data that are needed for input in either steady-state or transient models consist of water-table measurements, physical boundaries (geologic cross sections), and permeability ratios between successive geologic layers. These data are available for several subwatersheds at Reynolds Creek, including the two Reynolds Mountain study basins and the Cummings Field irrigated area. Representative geologic cross sections have been obtained from well logs and geologic mapping. Data from seismic refraction studies conducted by Stephenson and Zuzel (49) can also be used where absolute information is not available. Water-table measurements are available throughout most of the Reynolds Creek Watershed from a large network of wells. Likewise, permeability ratios have been obtained at strategic locations from pumping and injection tests.

Output desired from a ground-water model is the amount of water flowing through an aquifer and locations of discharge and recharge areas. This output is usually obtained as a second step after the potential distribution has been delineated. The ground-water models mentioned above give potential distribution over the prescribed area, and they do provide an estimate of the quantity of flow across a given section.

While several ground-water models are being tested with Reynolds Creek data, this does not preclude the possibility that none of these models will be applicable without considerable modification. This may necessitate the development of a separate model which would be more flexible in its application. Once a ground-water model has proven operable for a specific subwatershed at Reynolds Creek, then research can be directed towards combining the ground-water model with models for the other hydrologic cycle subsystems to arrive at a complete physically-based hydrologic response model.

REFERENCES

1. Anderson, E. A. 1968. Development and testing of snow pack energy balance equations. Water Resources Research, 4(1), February.

2. Behlke, C. E. 1957. The mechanics of overland flow, Ph.D. Thesis, Stanford University, Stanford, Calif.

3. Bittinger, M. W., H. R. Duke, and R. A. Longenbaugh 1967. Mathematical simulations for better aquifer management, Internatl. Assoc. Sci. Hydrol., Symposium of Haifa, Publ. No. 72, pp. 509-519.

4. Brakensiek, D. L. and C. A. Onstad 1968. The synthesis of distributed inputs for hydrograph predictions, Water Resources Research, 4(1): 79-85. (Feb.)

5. Brooks, R. H. and A. T. Corey 1964. Hydraulic properties of porous media, Hydrol. Paper No. 3, Colo. State Univ., Fort Collins, Colo., March.

6. Brutsaert, W. 1968. The adaptability of an exact solution to horizontal infiltration, Water Resources Research, 4(4):785-789.

7. Brutsaert, W. 1968. The permeability of a porous medium determined from certain probability laws for pore-size distribution, Water Resources Research, 4(2):425-434.

8. Chen, C. L. 1962. An analysis of overland flow, Ph.D. Thesis, Mich. State Univ., East Lansing, Mich.

9. Chow, V. T. 1959. Open Channel Hydraulics, McGraw-Hill Book Co., New York.

10. Cox, L. M. and W. R. Hamon 1968. A universal surface precipitation gage. Proc. West. Snow Conf., Lake Tahoe, Nev., April 16-18.

11. Crawford, N. H. and Linsley, R. K. 1966. Digital simulation in Hydrology: Stanford Watershed Model IV. Tech. Report No. 39, Dept. of Civil Engin., Stanford Univ., Stanford, Calif., 210 pp.

12. Davis, S. N. and R. J. M. DeWiest 1966. Hydrogeology, John Wiley & Sons, New York, pp. 175-183.

13. Dawdy, D. R. and O'Donnell, T. 1965. Mathematical models of catchment behavior, Jour. of the Hydraulics Div. of A.S.C.E., 91(HY4):123-137.

14. Freeze, R. A. 1968. The continuity between ground-water flow systems and flow in the unsaturated zone, Natl. Res. Council Canada, Proc. Hydrol. Symp. 6: Soil Moisture, Nov. 1967, Saskatoon, Saskatchewan, pp. 205-232.

15. Freeze, R. A. 1966. Theoretical analysis of regional groundwater flow, Ph.D. Thesis, Univ. of Calif., Berkeley.

16. Freeze, R. A. and R. L. Harlan 1969. Blueprint for a physically-based, digitally-simulated hydrologic response model, Jour. of Hydrology, 9(3):237-258.

17. Freeze, R. A. and P. A. Witherspoon 1966. Theoretical analysis of regional ground-water flow: 1. Analytical and Numerical Solutions to the mathematical model, Water Resources Research, 2(4):641-656.

18. Freeze, R. A. and P. A. Witherspoon 1967. Theoretical analysis of regional groundwater flow: 2. Effect of water-table configuration and sub-surface permeability variation, Water Resources Research, 3(2):623-634.

19. Freeze, R. A. and P. A. Witherspoon 1968. Theoretical analysis of regional groundwater flow: 3. Quantitative interpretations, Water Resources Research, 4(3):581-590.

20. Fritschen, L. J. 1965. Accuracy of evapotranspiration determinations by the Bowen ratio method, Bul. of the I.A.S.H. X^{e} Année, No. 2, pp. 38-48.

21. Fuchs, M., C. B. Tanner, G. W. Thurtell, and T. A. Black 1969. Evaporation from drying surfaces by the combination method, Agron. Jour., 61:22-26 (Feb.)

22. Gilcrest, B. R. 1950. Flood routing, Chapter 10, Engineering Hydraulics, Edited by H. Rouse, John Wiley and Sons, New York, pp. 635-710.

23. Hanks, R. J. and S. A. Bowers 1962. Numerical solution of the moisture flow equation for infiltration into layered soils. Soil Sci. Soc. Am. Proc., 26:530-534.

24. Harbaugh, T. E., and V. T. Chow 1967. A study of the roughness of conceptual river systems or watersheds, Paper No. A2, XIIth Congress, Int. Assoc. for Hydraulic Research, Fort Collins, Colo.

25. Hubbert, M.K. 1945. The theory of ground-water motion, Jour. of Geology, 48(8)(Pt. I):785-944.

26. Isaacson, E., J. J. Stoker, and A. Troesch, Numerical solution of flood prediction and river regulation problems, Reports II and III, New York Univ., 1954 (Jan.) and 1956 (Oct.).

27. Izzard, C. F. 1944. The surface-profile of overland flow, Trans. of the AGU, 25:959-968.

28. Javendel, I. and P. A. Witherspoon 1968. Analysis of transient fluid flow in multi-layered systems, Univ. of Calif., Berkeley, Water Resources Center Contribution No. 124, 119 pp.

29. Jeppson, R. W. 1969. Numerical solution of the steady-state two-dimensional flow system resulting from infiltration on a watershed, Project Report PRWG-59c-1, Utah Water Res. Lab., Utah State Univ., Logan, Utah, June.

30. Keulegan, G. H. 1944. Spatially variable discharge over a sloping plane. Trans. of the AGU, 25:956-958.

31. Klute, A. 1952. A numerical method for solving the flow equation for water in unsaturated materials, Soil Science, 73:105-116.

32. Laliberte, G. E., R. H. Brooks, and A. T. Corey 1968. Permeability calculations from desaturated data, Jour. of the Irrig. and Drainage Div. of ASCE, 94(IR1):57-71, Mar.

33. Lichty, R. W., D. R. Dawdy, and J. M. Bergmann 1968. Rainfall-runoff model for small basin flood hydrograph simulation. Symposium: The use of analog and digital computers in hydrology. Internatl. Assoc. of Sci. Hydrol., Public. No. 81:Vol. II, pp. 356-367.

34. Liggett, J. A. 1961. General solution for open channel profiles, Jour. of the Hydraulics Div. of ASCE, 87(HY6) November.

35. Liggett, J. A. 1959. Unsteady open channel flow with lateral inflow, Ph.D. Thesis, Stanford Univ., Stanford, Calif.

36. Machmeier, R. E. and C. L. Larson 1967. A mathematical watershed routing model, Proc. Internatl. Hydrol. Symp., Fort Collins, Colo., 1:64-72.

37. Melott, J. and J. Crosby 1969. Personal communication, Jan.

38. Nelson, R. W. and R. W. Jeppson 1968. Theoretical and experimental aspects of watershed infiltration in terms of basic soil properties--A research and development planning survey, Computer Sciences Corp., Richland, Wash., Oct.

39. Penman, H. L., D. E. Angus, and C. H. M. Van Bavel 1967. Microclimatic factors affecting evaporation and transpiration, In irrigation of agricultural lands, Amer. Soc. of Agron., Madison, Wis., pp. 483-505.

40. Philip, J. R. 1957. The theory of infiltration: I. The infiltration equation and its solution, Soil Science, 83:345-357.

41. Richey, E. P. 1954. The fundamental hydraulics of overland flow, Ph.D. Thesis, Stanford University, Stanford, Calif.

42. Riley, J. P., D. G. Chadwick, and E. K. Israelsen 1967. Application of an electric analog computer for the simulation of hydrologic events on a southwest watershed. Progress report PR WG 38-1. Utah Water Res. Lab., Utah State Univ., Logan, Utah, 53 pp.

43. Rubin, J. 1967. Numerical method for analyzing hysteresis-affected, post-infiltration redistribution of soil moisture, Soil Sci. Soc. Amer. Proc., 31:13-20.

44. Rubin, J. and R. Steinhardt 1963. Soil water relations during rain infiltration: I Theory, Soil Sci. Soc. Amer. Proc., 27:246-251.

45. Schreiber, D. L. 1970. Overland flow simulation by a nonlinear distributed parameter model, Ph.D. Thesis, Wash. State Univ., Pullman, Wash., June.

46. Smith, F. M., C. F. Cooper, and E. G. Chapman 1967. Measuring snow depths by aerial photogrammetry: evaluation and recommendations, Proc. Western Snow Conf., Boise, Idaho, April 12-18.

47. Spooner, J. A., 1970. Personal communications, Jan.

48. Staple, W. J. 1966. Infiltration and redistribution of water in vertical columns of loam soil, Soil Sci. Soc. Amer. Proc., 30:553-558.

49. Stephenson, G. R. and J. F. Zuzel 1967. Seismic refraction studies in watershed hydrology, paper pres. at 5th Annual Symposium on Engin. Geol. and Soils Engin., Pocatello, Idaho, April.

50. Stoker, J. J. 1953. Numerical solution of flood prediction and river regulation problems, Report I, New York Univ., Oct.

51. Tanner, C. B. and M. Fuchs 1968. Evaporation from unsaturated surfaces: a generalized combination method, Jour. of Geophy. Res., 73(4):1299-1304 (Feb.)

52. Tóth, J. 1963. A theoretical analysis of groundwater flow in small drainage basins, Jour. of Geophy. Res., 68(16):4795-4812.

53. Tóth, J. 1963. A theoretical analysis of groundwater flow in small drainage basins, Nat. Res. Council of Canada, Proc. of Hydrol. Sympos. No. 3, pp. 75-96.

54. Toth, J. 1962. A theory of groundwater motion in small drainage basins in Central Alberta, Canada, Jour. of Geophy. Res., 67(11):4375-4387. (Oct.)

55. Tyson, H. N., Jr. and E. M. Weber 1964. Computer simulations of groundwater basins, Jour. of the Hydraulics Div. of ASCE, 90(HY4):59-77.

56. U.S.D.A. Agricultural Research Service, N.W. Watershed Res. Center, Boise, Idaho, 1969 unpublished annual report, pp. 7-1 to 7-9.

57. U.S.D.A. Agricultural Research Service, N.W. Watershed Res. Center, Boise, Idaho, 1969 unpublished annual report, pp. 9-1 to 9-5.

58. Whisler, F. D. and A. Klute 1965. The numerical analysis of infiltration, considering hysteresis, into a vertical soil column at equilibrium under gravity, Soil Sci. Soc. Amer. Proc., 29:489-494.

59. Williams, R. and D. Allman 1969. Private communication, Oct.

60. Witherspoon, P. A., I. Javendel, and S. P. Neuman 1968. Use of the finite element method in solving transient flow problems in aquifer systems, Internatl. Assoc. Sci. Hydrol., Symposium on the use of analog and digital computers in hydrol., Publ. 81, 2:687-698.

61. Woo, D. C. and E. F. Brater 1962. Spatially varied flow from controlled rainfall, Jour. of the Hydraulics Div. of ASCE, 88(HY6):33-56 (Nov.)

62. Wooding, R. A. 1965 A hydraulic model for the catchment-stream problem, Part I-Kinematic wave theory, Jour. of Hydrol., 3:254-267.

63. Woolhiser, D. A. and J. H. Liggett 1967. Unsteady, one-dimensional flow over a plane--the rising hydrograph, Water Res. Res., 3(3):753-776.

64. Yu, Y. S. and J. S. McKnown 1963. Runoff from impervious surfaces, U.S. Dept. of Army, Corps of Engineers, Waterways Experiment Station, Feb.

KGR-1

AN ANALOG COMPUTER MODEL OF RUNOFF FROM A SEMIARID WATERSHED [1/]

K. G. Renard [2/]

INTRODUCTION

A cooperative effort between the staff of the Southwest Watershed Research Center and the Utah Water Research Laboratory at Utah State University has produced an analog computer model of the surface runoff process which seems to describe the hydrologic conditions of a semiarid watershed very well.

The model includes provisions for the spatial variation of hydrologic elements such as rainfall, slope, channel size, soil, and vegetation within the watershed. The surface runoff process involves both overland flow and channel flow with the equations of unsteady flow (continuity and momentum) adapted to route the excess rainfall over pervious surfaces and thereby allow infiltration to continue as long as water is available in detention storage.

[1/] Contribution of the Southwest Watershed Research Center, USDA, Agricultural Research Service, Soil and Water Conservation Research Division, in cooperation with the Utah Water Research Laboratory, Utah State University, Logan, Utah.

[2/] Director and Research Hydraulic Engineer, Southwest Watershed Research Center, Agricultural Research Service, USDA, SWC, 442 E. Seventh Street, Tucson, Arizona 85705.

Conceptual Model Description

This paper is a portion of a more detailed report by Amisial, et al. [3]. The runoff process considered in the model is that portion of the hydrologic cycle shown inside the dotted lines in Figure 1. Contrary to a general model, the runoff model described here is restricted to the following situations:

1. Short-duration storm events during which interflow and groundwater flow play no part.

2. Watersheds in which infiltration water does not reappear as surface flow within the watershed.

Only a portion of the rainfall occurring over a watershed appears as runoff in the channel at the watershed outlet. Most of the rainfall is accounted for by losses in the watershed. Some of the precipitation in the early portion of a storm is intercepted by vegetation, and some is stored in depressions on the land surface. This water subsequently evaporates or infiltrates to the soil profile. The remaining portion of the precipitation (precipitation excess) is the effective precipitation which produces overland and channel flow and is depleted by infiltration and channel seepage. Thus, the model being described has three phases in the surface runoff process:

1. The phase in which an effective precipitation is produced

2. The overland flow phase during which water flows over the land surface toward an established channel

3. The channel flow phase in which water collected from phase 2 flows in a channel system and ultimately produces an outflow hydrograph at the watershed outlet.

---

[3] Amisial, R. A., Riley, J. P., Renard, K. G., and Israelsen, E. K. Analog computer solution of the unsteady flow equations and its use in modeling the surface runoff process. Utah State University Technical Report No. , 1970.

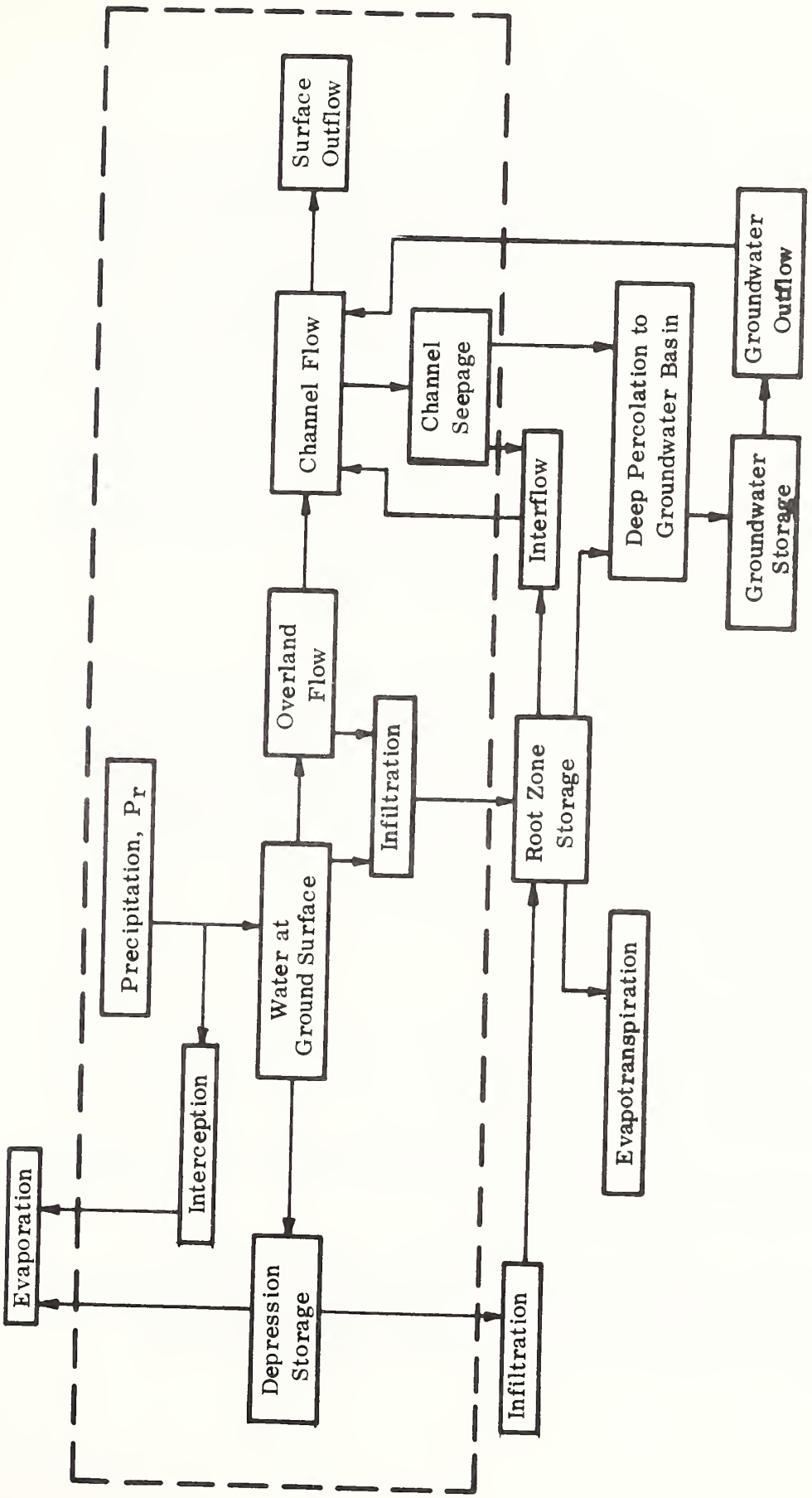

Figure 1.--Schematic diagram of the runoff cycle.

The watershed to be modeled was divided into Z subzones on the basis of the physiography. Each subzone, which is in fact a small drainage basin, is replaced by an equivalent basin having the same surface area as the subzone and composed of two identical rectangular sloping planes transected by a main channel (Fig. 2), (Wooding, 1965)[4]. The rectangular planes over which the overland flow occurs, have a width equal to the length of the main stream channel within the subzone, and a slope which is an average between the land slope and the slopes of smaller tributaries of the subzone. The portion of channel in the equivalent subzone is assumed to be a straight channel having the same characteristics (width, length, and average slope) as the corresponding segment of the prototype channel. The channel is fed on both sides by outflow from the planes and from upstream by runoff from the preceding subzone.

Effective Precipitation

A flow chart for the surface runoff model is shown in Figure 3. Point rainfall values from recording rain gages in the watershed are used to input a weighted subzone precipitation using a digital computer program capable of integrating the point measurements in time and space[5]. The program uses interpolation techniques to determine isohyetal lines for given time intervals (Δt). Elemental rainfall volumes are then computed as:

$$V_i = a_i \frac{P_i + P_{i+1}}{2} \qquad (1)$$

where: a_i is the elemental area

P_i and P_{i+1} are depths of rainfall on adjacent isohyetal lines.

---

[4] Wooding, R. A. A hydraulic model for the catchment-stream problem. J. Hydrol. 3:254-267, North Holland Publishing Co., Amsterdam, 1965.

[5] Kwan, J. Y., Riley, J. P., and Amisial, R. A. A digital computer program to plot isohyetal maps and calculate volumes of precipitation. Symposium: The Use of Analog and Digital Computers in Hydrology, IASH 1(80):240-248, 1968.

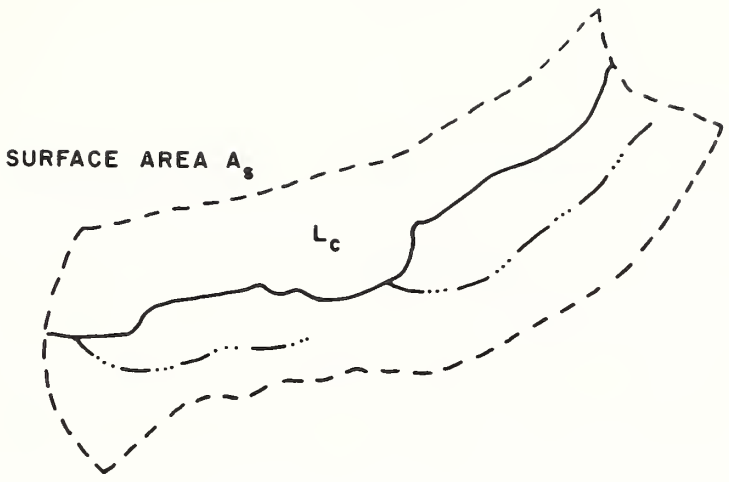

a. NATURAL SUBZONE

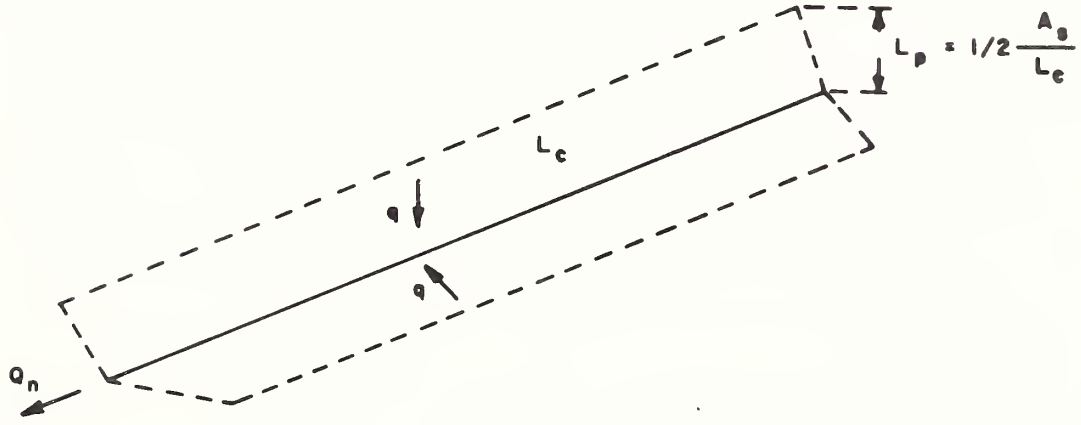

b. EQUIVALENT SUBZONE

FIGURE 2. SKETCHES SHOWING NATURAL SUBZONE 3 AND ITS EQUIVALENT SUBZONE.

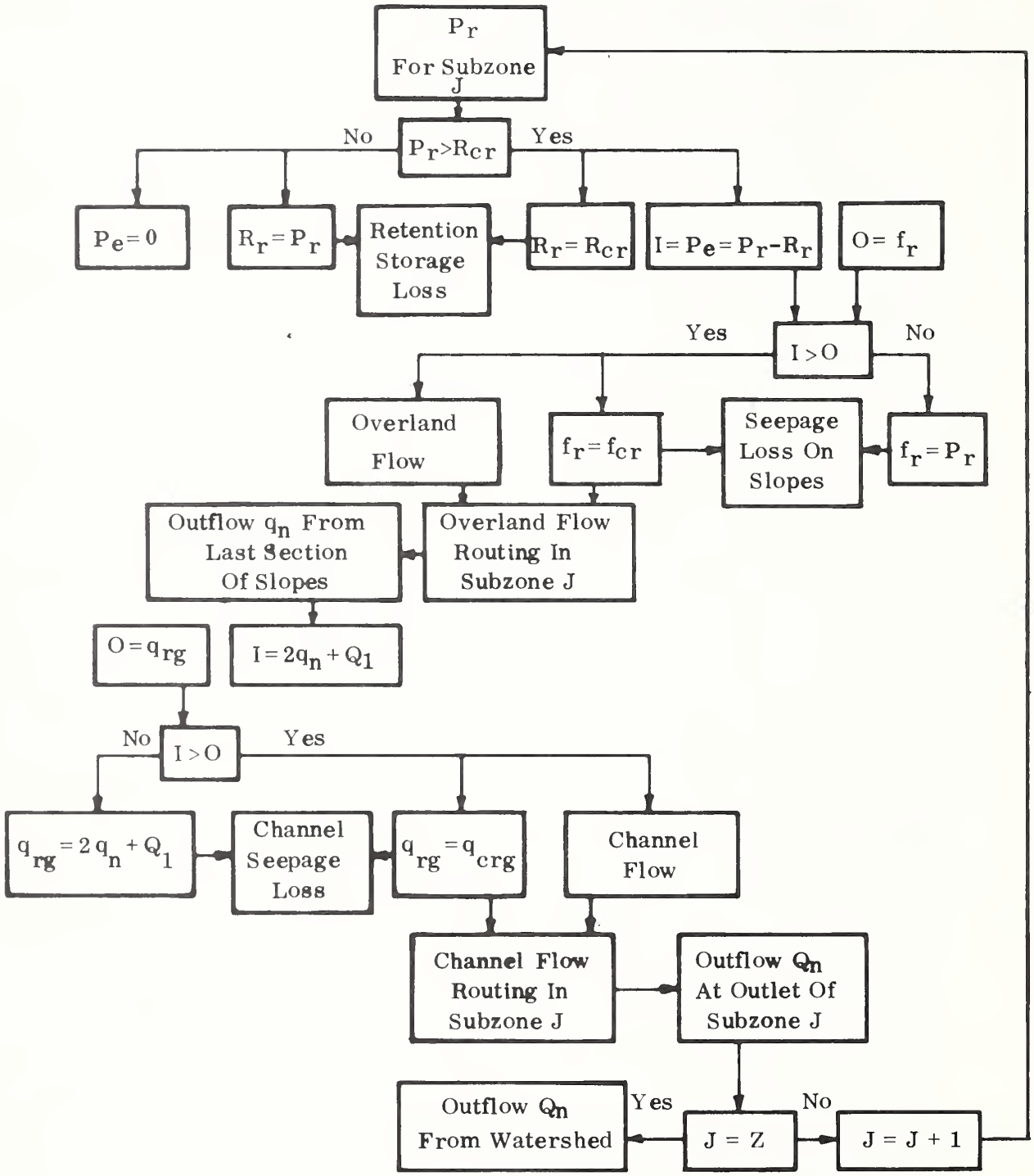

Figure 3.--Flow chart for the surface runoff model.

If the elemental area is bounded by one isohyetal line and a portion of the subzone boundary, rainfall values are determined by interpolation at several points along the portion of the boundary. The rainfall depth over the area is then computed as the average between the value on the isohyetal line and the average of the values at the chosen points along the boundary.

The rainfall rate over the subzone during the time period, Δt, is computed by summing the volumes over all elemental areas comprised in the subzone and dividing by the subzone area and time.

$$P_r = \frac{\Sigma_i V_i}{\Delta t \Sigma_i a_i} \qquad (2)$$

Losses due to the combined effects of depression storage and vegetation interception are termed retention. Once the vegetative cover becomes thoroughly wetted and the surface depressions are filled, additional retention losses become very small. In general, the retention losses can be expected to be relatively high at the beginning of the storm event, becoming negligible as the event progresses. An exception is the case of an initially wet watershed where the retention losses can be assumed to be equal to zero. It is assumed that the maximum rate at which rainfall is lost to retention storage, R_{cr}, is given by the following expression:

$$R_{cr}(t) = k_r(R_{cs} - R_s(t)) \qquad (3)$$

in which

R_{cs} is the retention storage capacity of vegetation and land surface,

k_r is a constant less than unity,

and

R_s = amount of rainfall in retention storage and is given as

$$R_s(t) = \int_o^t R_r dt \qquad (4)$$

The actual retention rate, R_r, is given by the following equations:

$$R = O \quad , \text{ if } P_r = O$$

$$R_r = P_r \quad , \text{ if } O < P_r < R_{cr}$$

$$R_r = R_{cr} \quad , \text{ if } P_r \geq R_{cr}$$

The effective rainfall rate for each subzone of the model is then obtained as

$$P_e = P_r - R_r \tag{5}$$

Obviously, there will be no water available for surface runoff and infiltration until the rainfall rate exceeds the retention capacity rate.

Overland Flow

The rectangular sloping planes of the equivalent subzones of the model (Fig 2-b) are treated as wide, open channels, and the discharge per unit width (q_n) at the downstream edge is computed from the unsteady flow equations. They are:

$$\frac{\partial A}{\partial t} + \frac{\partial Q}{\partial x} + O - I = O \tag{6}$$

and

$$\frac{\partial V}{\partial t} + \frac{1}{2}\frac{\partial V^2}{\partial x} + \frac{g}{B}\frac{\partial A}{\partial x} = g(S_o - S_f + G) \tag{7}$$

where

V = average velocity
x = distance
g = acceleration of gravity
S_f = friction slope
S_o = bed slope

$$B = \frac{\partial A}{\partial y}$$

$$G = \frac{1}{B}\left(\frac{\partial A}{\partial a}\right)\left(\frac{\partial a}{\partial x}\right)$$

O = unit rate of loss due to seepage
I = Unit rate of lateral inflow

The O term is the infiltration term in the overland flow computation and the (q_{crg}) seepage capacity rate in channel flow, while the I term is effective precipitation in the overland flow and the (q_n) or discharge per unit flow portion of the channel flow model.

In using these equations, the following assumptions are made:

1. The fluid is incompressible.
2. Acceleration is in the x-direction, being negligible in the other directions
3. Pressure distribution is assumed to be hydrostatic because the curvature of streamlines is small and the vertical velocity component is negligible. Thus, the pressure-distribution coefficient is equal to unity.
4. Shear stress (τ_o) is uniform over the perimeter of channel for an incremental distance, Δx
5. Lateral inflow and outflow rates are uniform for a particular incremental channel distance.
6. The momentum flux of the lateral inflow or outflow are ignored
7. The energy and momentum coefficients (α and β) are assumed to be equal to unity
8. The angle between bed and horizontal surface (θ) is small so that

   $$\sin \theta \approx S_o \equiv \text{slope of the bed}$$

9. The effects of resistance to flow in unsteady conditions are the same as for steady flow.

An implicit differential-difference system (Fig. 4) was used to solve the equations on the analog computer. In operational form, the equations programmed were:

$$\frac{dA_j}{dt} = I - O - \frac{Q_{j+1}}{2\Delta x} + \frac{Q_{j-1}}{2\Delta x} \qquad (8)$$

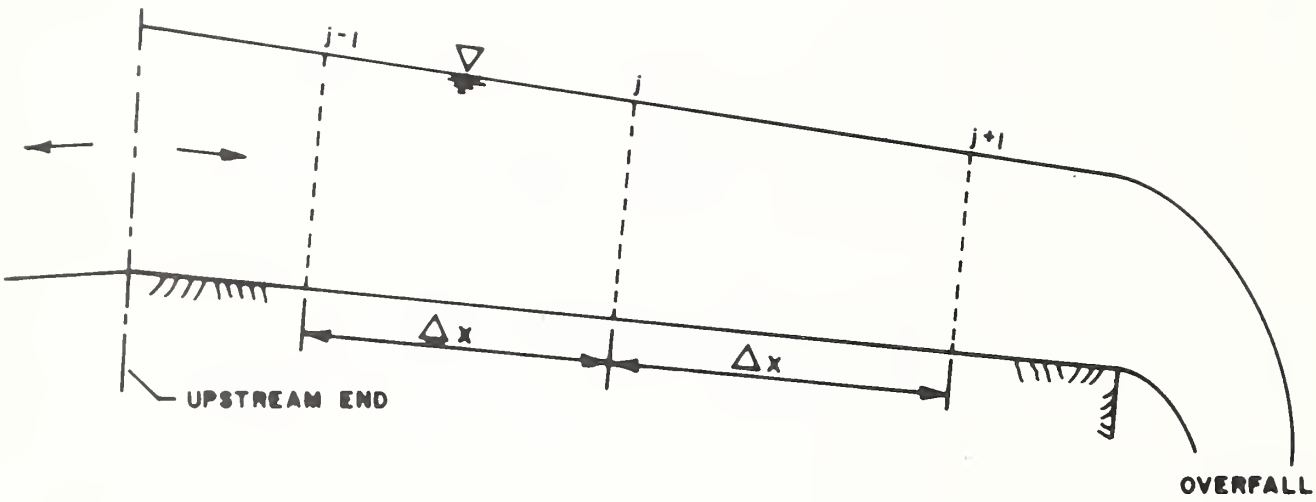

FIGURE 4. THE FLOW PROFILE FINITE INCREMENT PROCEDURE ADOPTED FOR THE MODEL.

$$\frac{dV_j}{dt} = gS_o + gG - gKV_j^2 - \frac{g}{2B\Delta x}\left(A_{j+1} - A_{j-1}\right) - \frac{1}{4\Delta x}\left(V_{j+1}^2 - V_{j-1}^2\right) \qquad (9)$$

$$Q_j = A_j V_j \qquad (10)$$

The slope of the energy line was taken as KV^2 instead of $K|V|V$, because the flow velocity is always positive.

The Horton form of the infiltration curve represented by the following equation was used:

$$f_{cr} = f_m + (f_o - f_m)\, e^{-k_f t} \qquad (11)$$

where f_{cr} = infiltration capacity rate

f_m = minimum value of infiltration rate

f_o = maximum value of infiltration rate

k_f = constant less than 1

t = real time

e = natural logarithim.

Because the infiltration rate on the planes is dependent on the effective rainfall rate and its relation to the infiltration capacity rate, boundary conditions had to be established. If t_o denotes the time at which the rainfall starts, t_e the time at which the effective rainfall rate P_e exceeds the infiltration capacity rate f_{cr}, and t_s the time at which the overland flow stops, then the actual infiltration rate per unit area can be defined by the by the expressions:

$$t_o < t < t_e \quad , \quad f_r = P_e$$

$$t_e < t < t_s \quad , \quad f_r = f_{cr}$$

where f_r is the actual infiltration rate.

Note: Readers are referred to the original, more detailed report for discussions of initial and boundary conditions as well as discussions of the mechanics of the analog computer.

Channel Flow

In the case of overland flow, the depth of flow was very small so that its influence on the infiltration rate was assumed to be negligible. The infiltration capacity curve of Horton can be looked upon as the seepage capacity rate curve under conditions of insignificant depth, but with increasing depth as is the case for channel flow, the seepage may be described by Darcy's Law. The seepage capacity rate, F_{cr}, was therefore assumed to be a function of Darcy's Law and an exponential decay in the form of the Horton infiltration curve:

$$F_{cr} = f_{cr} + cy \qquad (12)$$

in which

f_{cr} is given by Equation 11, with parameter adjustments for channel alluvium

y is the depth of channel flow

c is the constant which depends on the soil permeability and the distance of the water table from the ground surface.

The seepage capacity rate per unit length of channel is given by:

$$q_{crg} = BF_{cr} \qquad (13)$$

in which B represents the average width of channel.

If t_o represents the starting time of the storm, t_a the time at which the channel inflow $2q_n$ (flow from either side of equivalent planes) exceeds the seepage capacity rate q_{crg}, and t_s the time at which channel runoff ceases, then the actual seepage rate q_{rg} per unit length of channel can be obtained as

$t_o < t < t_a \qquad q_{rg} = 2q_n$

$t_a < t < t_s \qquad q_{rg} = q_{crg}$

Again, attention should be called to the fact that seepage will continue at capacity rate until water is no longer available in the channel.

(The reader is again referred to the Amisial report for a more detailed discussion of the initial and boundary conditions as well as conditions at a stream junction.)

MODEL REGULATION AND VERIFICATION

Subwatershed 11 of the Walnut Gulch Experimental Watershed was selected to test and verify the surface runoff model developed. This subbasin, with a drainage area of 2,035 acres, is situated in the northeastern portion of Walnut Gulch (Fig. 5). The predominant soil complex in the area is the Bernardino-Hathaway association with small areas of the Camoro soil in the alluvial swales [6/]. Vegetation of this watershed is dominated by black grama and curly mesquite with only limited amounts of brush, primarily along the channel banks.

The channels of this subwatershed contain three main branches (Fig. 6). The middle channel, which traverses the entire length of the watershed, is 4.4 miles long with an average slope of about 2%. This channel contains a stock pond (instrumented with a water-level recorder to provide information about its contribution to the watershed runoff). It contributes runoff to the area downstream only during times when the pond is full. The north channel, with a length of about 2 miles, also has a slope of about 2% and enters the middle channel about 3,000 feet above the supercritical-depth flume. The south channel, which enters the center channel about 1,000 feet above the outlet flume, has a slope of slightly over 2% and is 3.6 miles long.

[6/] Renard, K. G. The hydrology of semiarid rangeland watersheds. U. S. Dept. Agr. Pub. ARS-41-162, 1970.

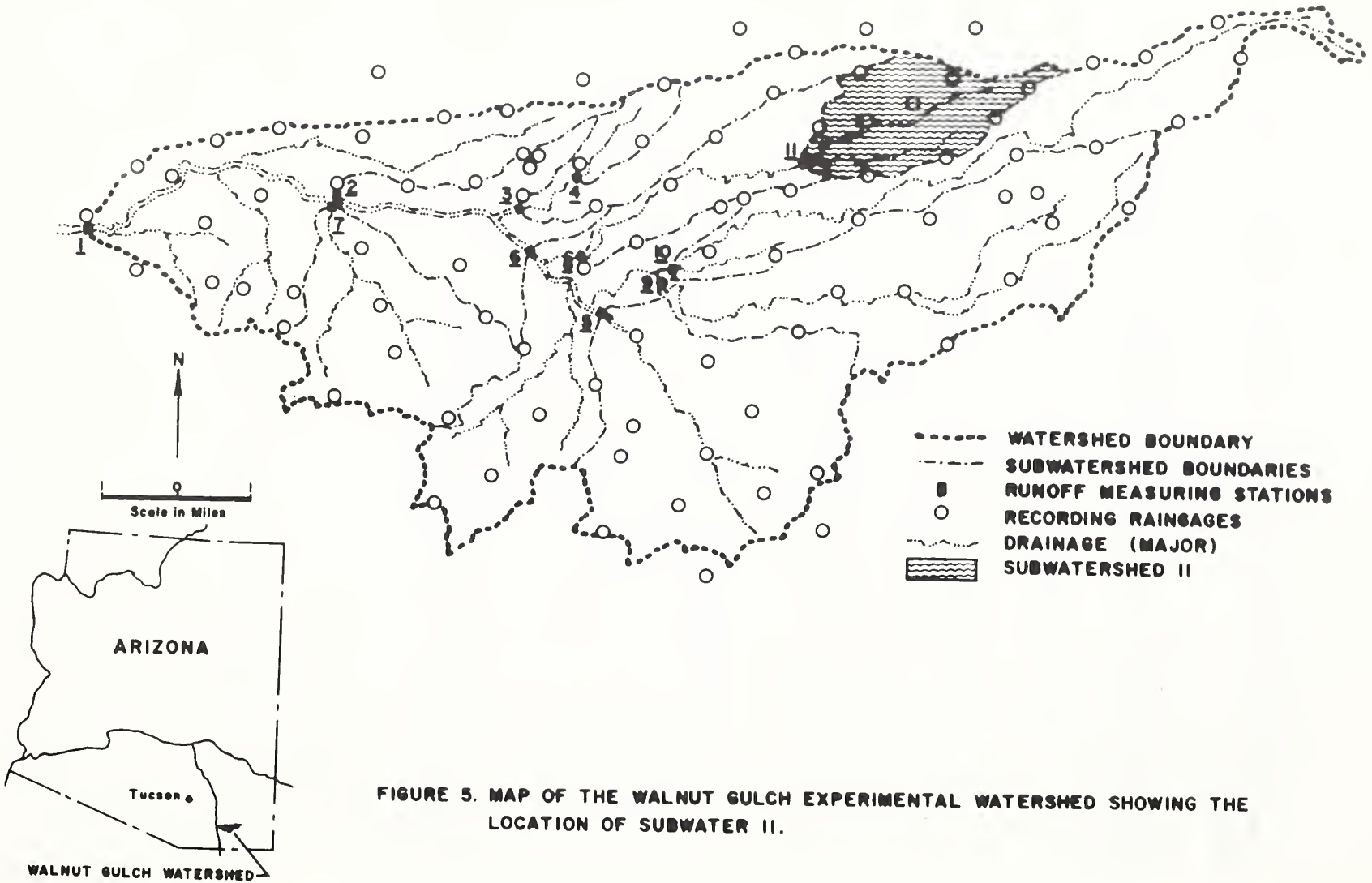

FIGURE 5. MAP OF THE WALNUT GULCH EXPERIMENTAL WATERSHED SHOWING THE LOCATION OF SUBWATER II.

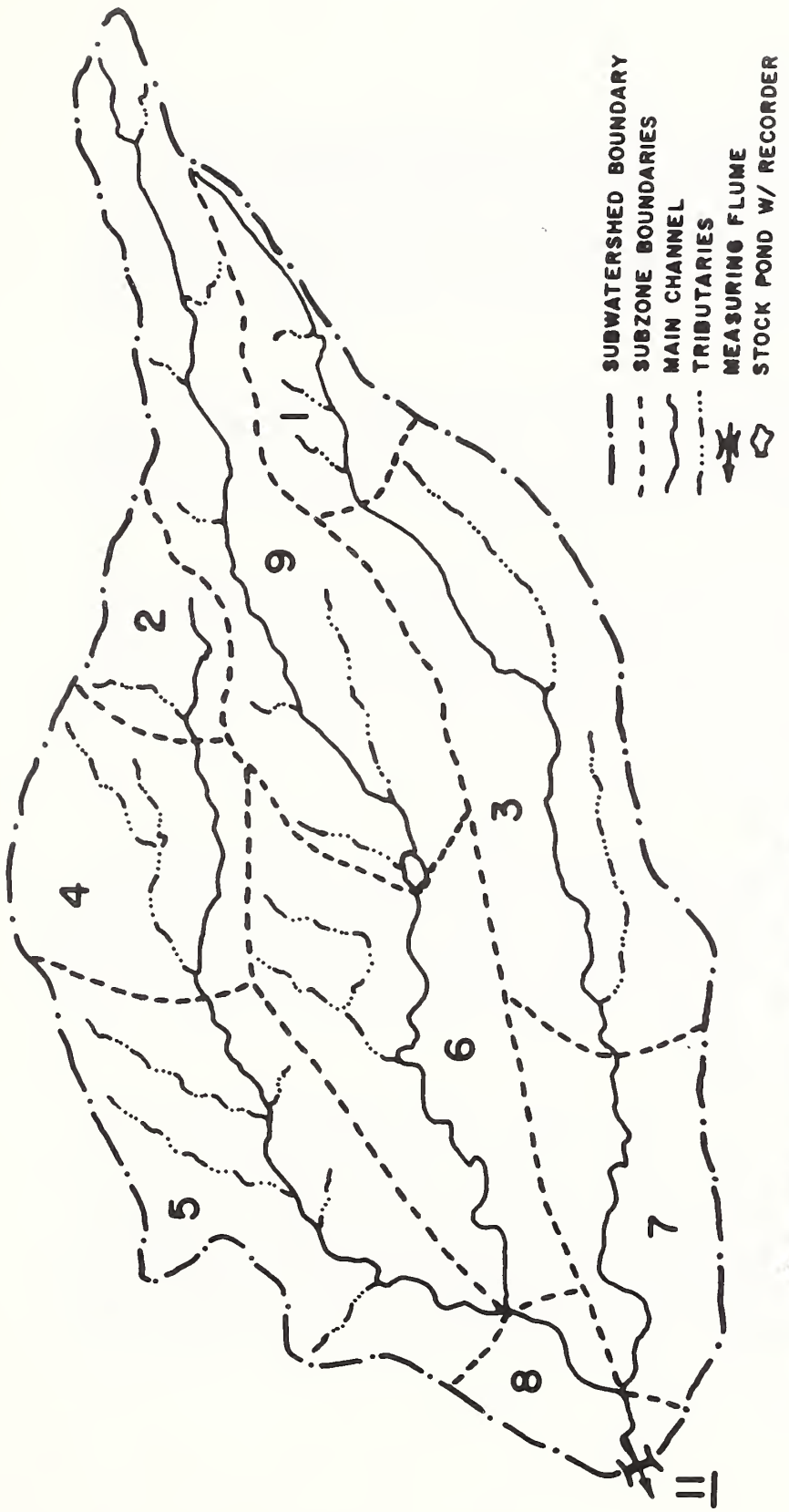

FIGURE 6. SUBWATERSHED 11 OF WALNUT GULCH EXPERIMENTAL WATERSHED, AS DIVIDED IN 9 SUBZONES.

The channel bed material is composed of coarse material which can be described by a log-normal size distribution. The geometric mean particle size in most segments of the channel is greater than 2 mm., with a geometric standard deviation of about 3.5 mm. The channels have the potential to absorb large quantities of the runoff because of high porosity and because they are dry prior to most flow events.

Precipitation in this subwatershed is measured by seventeen recording gages in and adjacent to the watershed. The subwatershed, which was divided into 9 subzones, thus had approximately 1 recording gage per subzone with eight additional gages defining the precipitation pattern around the subwatershed boundary.

The runoff model described involves the use of a number of parameters which must be fitted to a particular watershed by determining numerical values for the parameters. The parameters can be divided into two types, namely, the function parameters and the condition parameters.

Function parameters

The function parameters are those watershed characteristics which are constant with respect to time, such as length, width, and slope of the planes and channels. The function parameters pertaining to the plane are the width, length, and slope of the plane. The channel dimensions and slope are also considered as function parameters.

Condition parameters

The condition parameters are those parameters which vary with time within a given watershed and usually cannot be obtained by direct measurement. They are generally dependent upon surface and moisture conditions of the watershed. The retention rate accounts for losses due to interception and depression storage. The retention rate for the watershed model is determined when the constants R_{cs} and k_r, the rainfall rate and the watershed moisture conditions, are known.

The model distinguishes an infiltration value for the plane and another for the channel within the subzone. This distinction allows for the great difference in permeability between the channel bed material and that of the land surfaces. The constants required in the model are the maximum infiltration capacity rate, f_o, the minimum infiltration capacity rate, f_m, the time constant, k_f, and the constant c applied in the computation of channel seepage loss.

Within the analog computer program a different roughness coefficient may be used for each plane and channel section depending upon the condition of the soil surface and the meandering and irregularities of the channels.

Model verification was accomplished by fitting and regulating the parameters to coincide with the measured outputs for measured inputs. The model was regulated by a method of data adjustment involving the fitting of the condition parameters to a set of data under a particular set of criteria. The runoff events selected for study in this initial endeavor were those of July 20 and 29, 1966. Computed and measured outputs for these two storms are shown in Figures 7 and 8.

Adjustment or fitting of the condition parameter values is performed with a trial and error procedure. The approximations of individual parameters are refined after each computation until a close fit is obtained between the computed and observed hydrographs. Efforts were made to match the principal characteristics of the computed and measured hydrographs in the following priority:

1. Hydrograph peak discharge
2. Time to peak
3. Volume of runoff

The fitted value of the condition parameters for the overland flow and channel flow portions of the runoff model are shown in Table 1. Because of the uniformity of the vegetal cover, soil type, and channel alluvium within this subwatershed, one set of condition parameters was assumed to be indicative of the overland flow and another set for

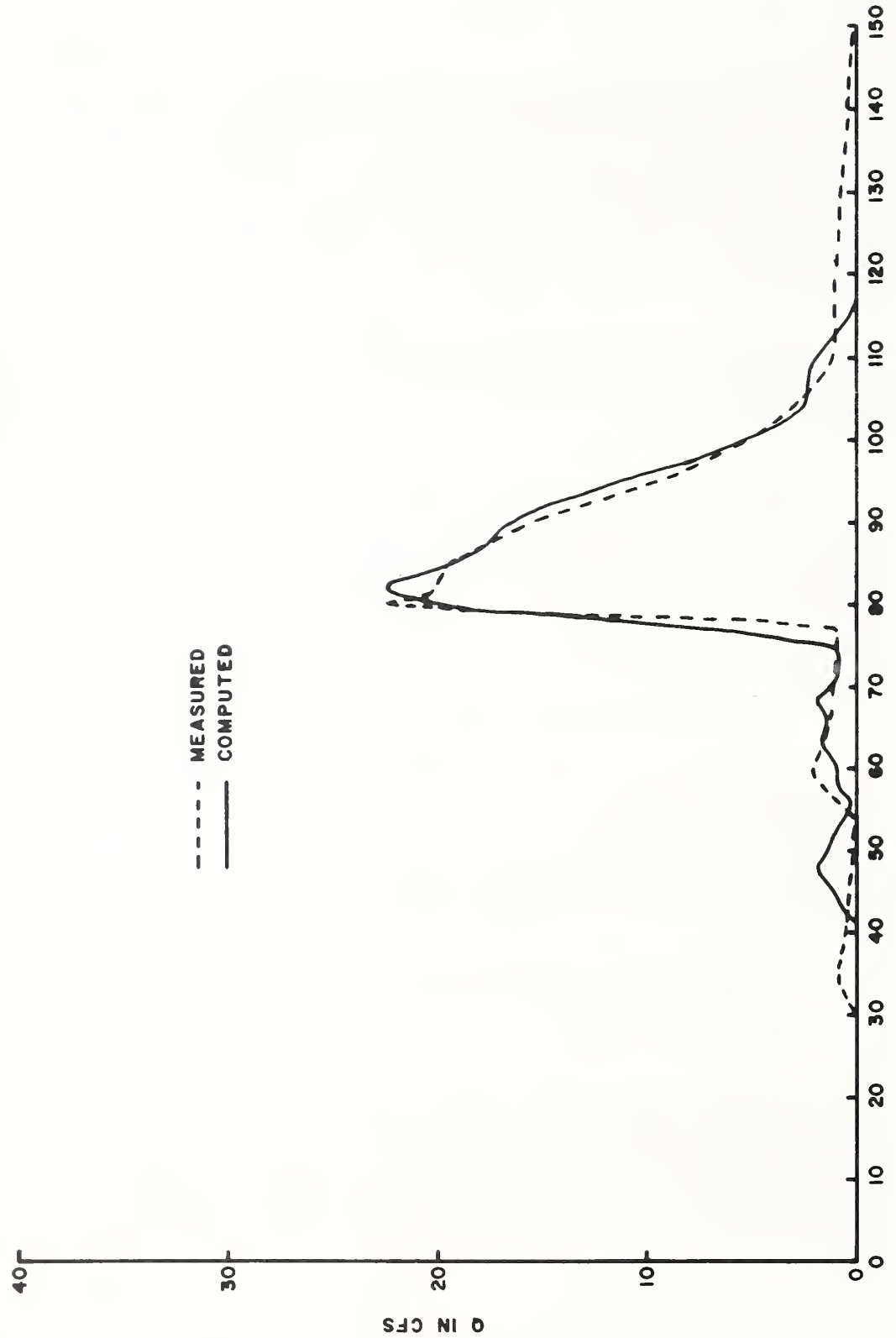

FIGURE 7. OUTFLOW FROM SUBWATERSHED 11 FOR THE EVENT OF JULY 20,1966.

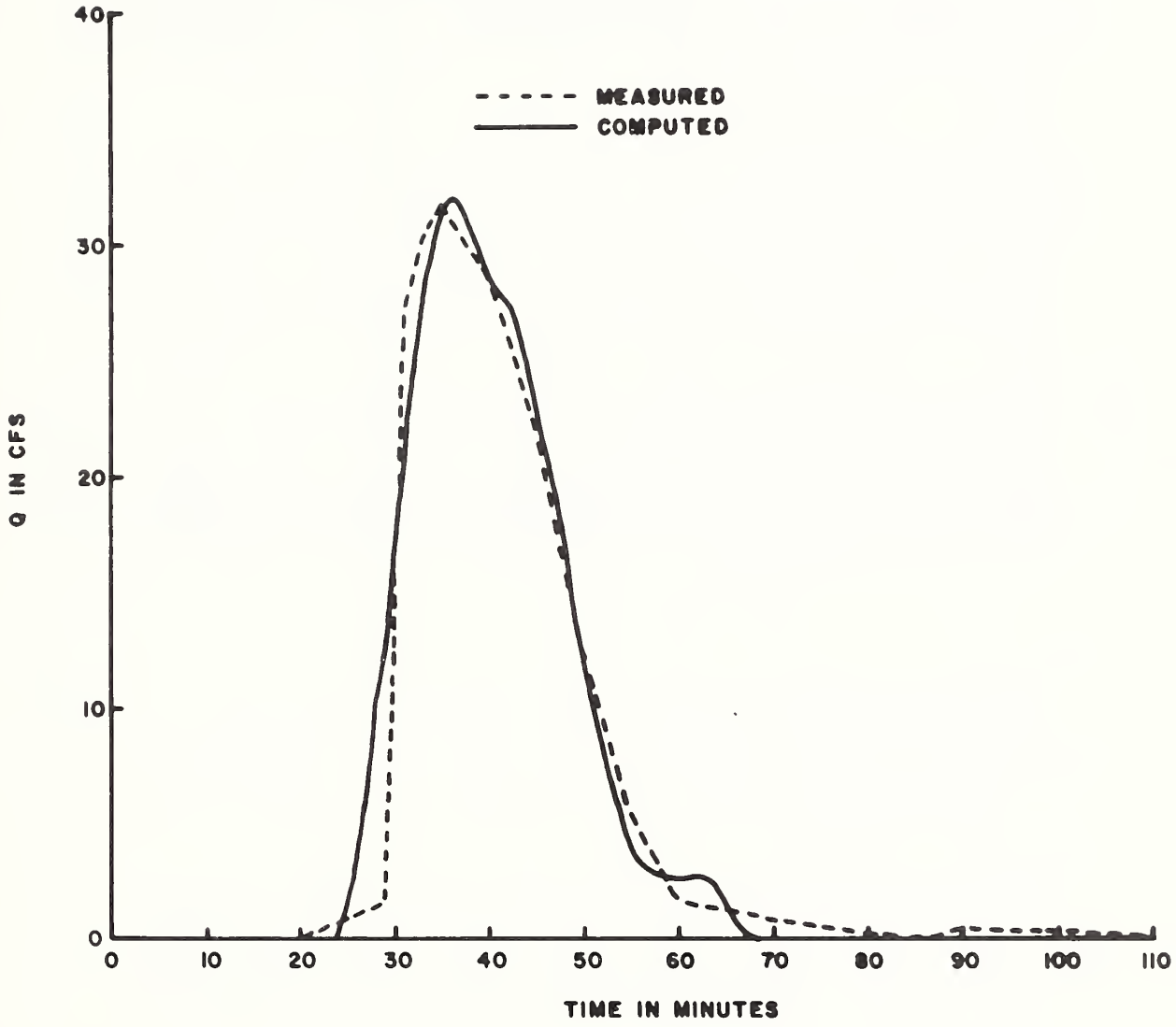

FIGURE 8. OUTFLOW FROM SUBWATERSHED II FOR THE EVENT OF JULY 29,1966.

TABLE 1.--Fitted values of constants in the runoff model

Constants	Units	Fitted values	
		Overland flow	Channel flow
R_{cs}	inches	0.15	---
k_r	---	1.0	---
f_m	inches/hr.	0.18	1.8
f_o	inches/hr.	1.8	4.2
k_f	---	0.60	0.04
c	$Sec.^{-1}$	---	.10
K	$Sec.^2/ft.^2$	0.093	.03

the channel flow. The infiltration values for the channel alluvium were assumed to be high because of the loose, coarse material. A higher roughness coefficient was assumed for the planes because the grass clumps and the erosion pavement relief are great in relation to the flow depths. These values were determined by solving the mathematical model for the July 20 storm. The fitted values were then used to predict the storm of July 29. The agreement between the computed and measured hydrograph appears to be very satisfactory.

The analog model was capable of producing graphs of precipitation, retention, and infiltration, as well as the hydrograph (Fig. 9). From these graphs, actual water lost to infiltration and retention, as well as the input and output water, can be computed. With a water budget for each subzone, the principle of conservation of mass for the subwatershed can be readily checked. For the areas checked, the error was found to be less than 1%.

The results of computations showing the distribution of the water to various portions of the model are shown in Table 2 for the storms of July 20 and July 29, 1966. Storm losses for July 20 are considerably larger than for the storm of July 29 because of lower antecedent moisture conditions on the earlier storm.

MODEL SENSITIVITY

The analog equipment used to solve the runoff equations was designed so that an outflow hydrograph could be obtained at three interior points in the model: at the downstream end of a unit width plane; at the end of a subzone; and at the outlet of the watershed.

To provide an idea of the magnitude of change in the computed overland flow and channel flow hydrographs caused by changes in the condition parameters, each parameter was systematically varied (the other parameters were kept constant), and the corresponding hydrograph was recorded with an automatic plotter. The responses of the overland flow model and the subzone channel flow to parameter variation were determined for subzone 2 (see sample in Figure 10).

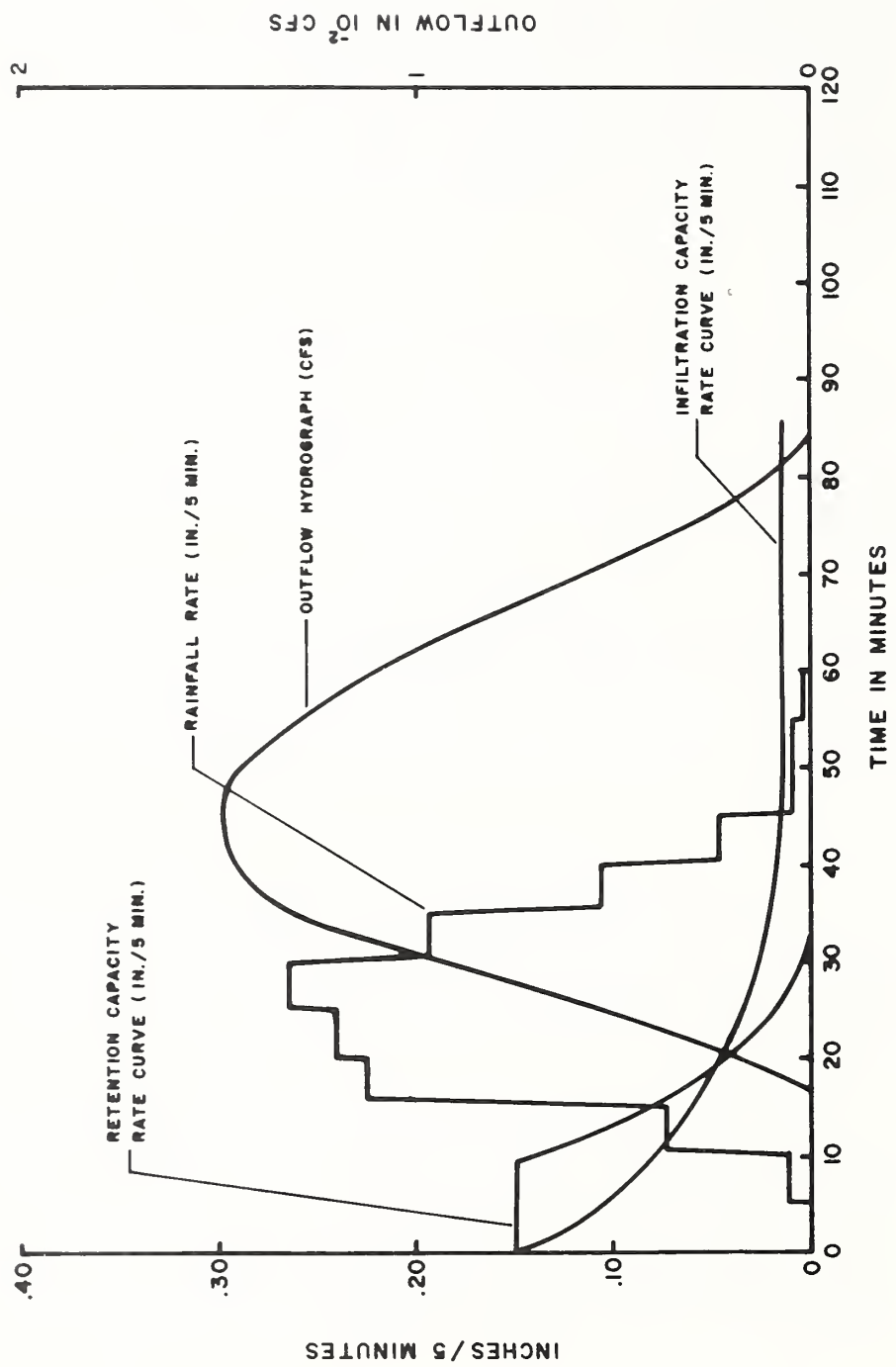

FIGURE 9. INPUT AND OUTPUT DATA FOR THE PLANE OF SUBZONE 2 USED IN THE CHECK ON THE CONSERVATION OF MASS PRINCIPLE, JULY 20, 1966.

TABLE 2.--Distribution of watershed losse sfor the runoff events of July 20 and 29, 1966 as computed from the model inputs and outputs

	Losses to infiltration and retention storage on land surface		Losses to channel seepage		Losses to blind drainage (rainfall - subzone 9
Date of runoff event	Total vol.	Vol. per sq. mi. of land	Total vol.	Vol. per mi. of channel	Total vol.
	(acre-ft.)	(acre-ft/mi^2)	(acre-ft.)	(acre-ft/mi)	(acre-ft.)
7/20/66	114.18	42.80	36.14	4.84	40.47
7/29/66	37.06	13.90	9.86	1.32	12.9

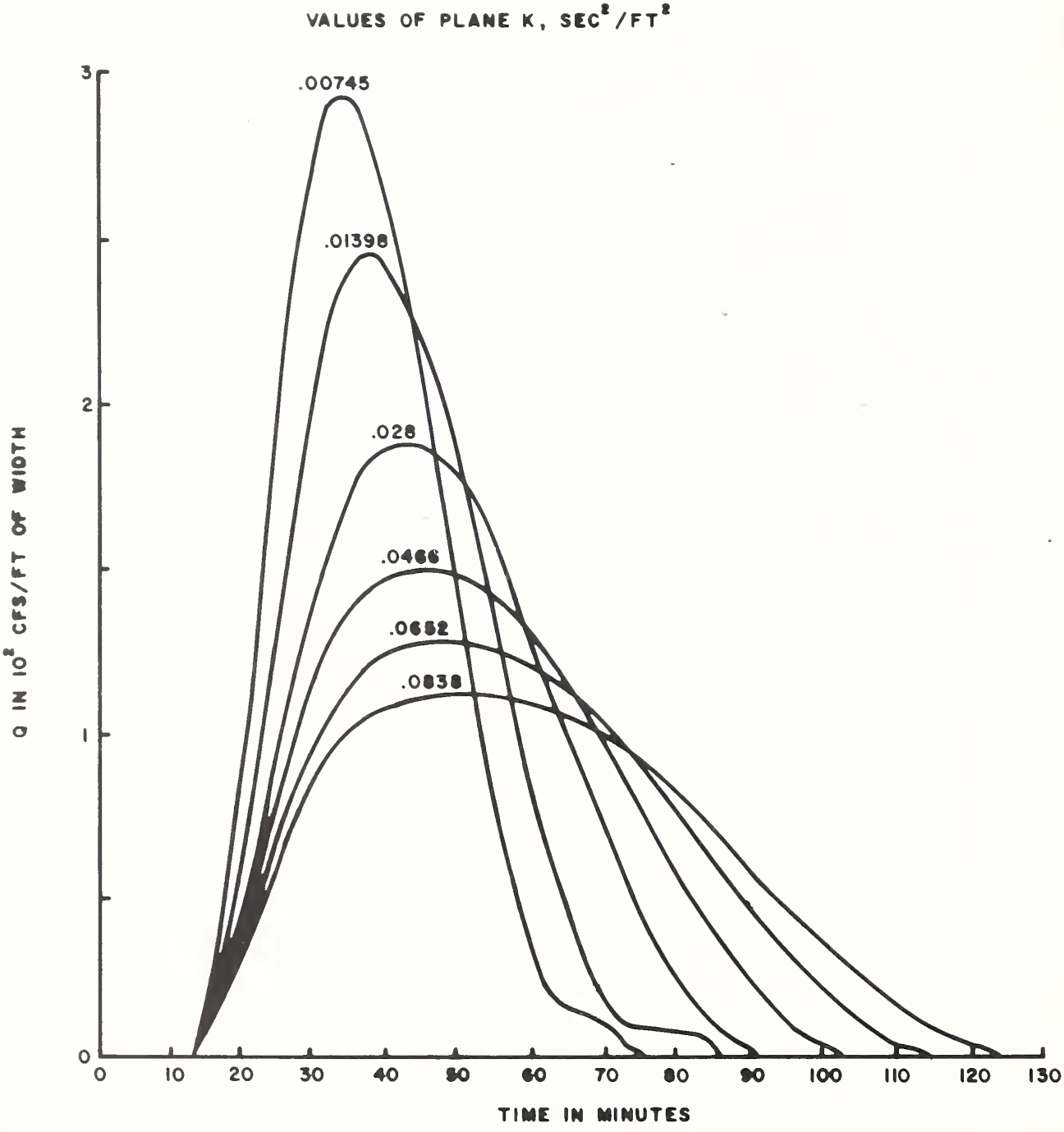

FIGURE 10. OVERLAND FLOW HYDROGRAPH FOR SUBZONE 2 AS AFFECTED BY CHANGES IN THE PLANE ROUGHNESS COEFFICIENT, K, JULY 20, 1966.

The hydrographs were subsequently integrated to obtain the flow volume. Figures 11 and 12 show the value of the runoff volume, peak discharge, and the time of rise (time from beginning of rainfall to peak discharge) as affected by variation in the condition parameter values.

As would be expected, the runoff volume from the plane decreased as the retention-storage capacity, R_{cs}, increased (Fig. 11). The time of rise changed very little, and the peak discharge decreased as the value of R_{cs} increased. For the same retention storage capacity, the amount of water lost to retention storage increases with decreasing k_r values. The effect of the plane roughness coefficient (K) on the flow hydrograph was quite dramatic and changed the hydrograph characteristics more than the other parameters. Although variations in the value of this term had essentially no effects on the runoff volume, the hydrograph peak, as well as the time of rise and flow duration, changed appreciably.

With the value of k_f held constant at 0.60, the characteristics of the hydrograph are significantly affected by changes in the minimum infiltration rate (f_m), while they experience little alteration when the initial infiltration rate (f_o) is modified. This is not the case for low values of k_f, and whether or not variation of f_m affects the hydrograph more than variation in f_o, depends on the value of k_f. An increased amount of infiltration loss with decreasing values of k_f was observed, which suggests that the maximum infiltration capacity rate plays an important role when the time constant k_f is small, while the minimum infiltration capacity rate is predominant for large values of k_f.

The channel flow hydrograph can be altered by changes in all the condition parameters of the model. Summaries of the changes in the hydrograph characteristics created by varying the plane condition parameters are shown in Figure 12. Figure 13 shows hydrograph characteristic changes caused by varying the channel condition parameters.

The effects of the retention terms (R_{cs} and k_r) were quite large on the runoff volume and peak discharge, but time of rise seemed somewhat independent of these terms. An interesting

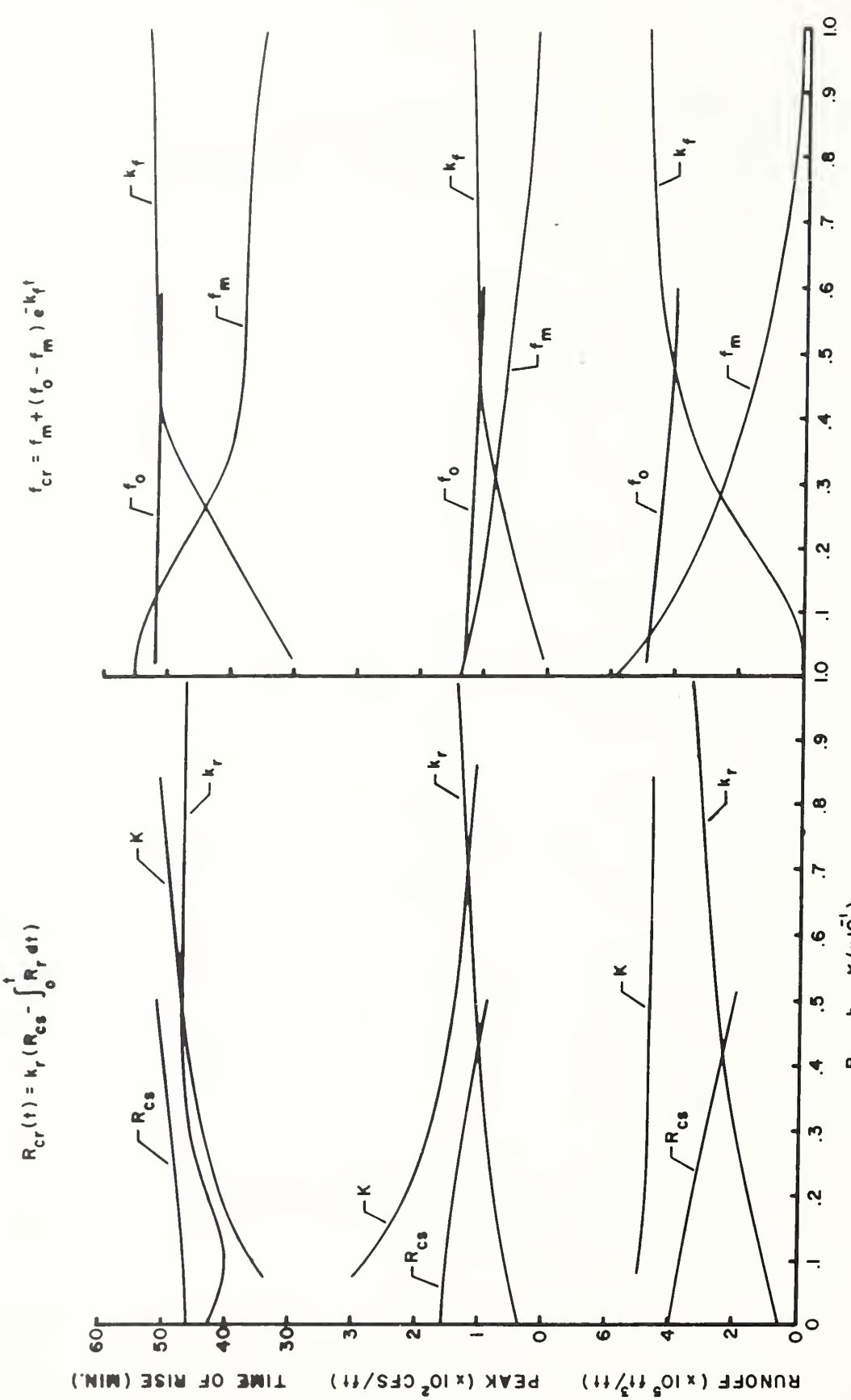

FIGURE 11. OVERLAND FLOW HYDROGRAPH CHARACTERISTICS AS AFFECTED BY CHANGES IN VALUE OF PLANE VARIABLES.

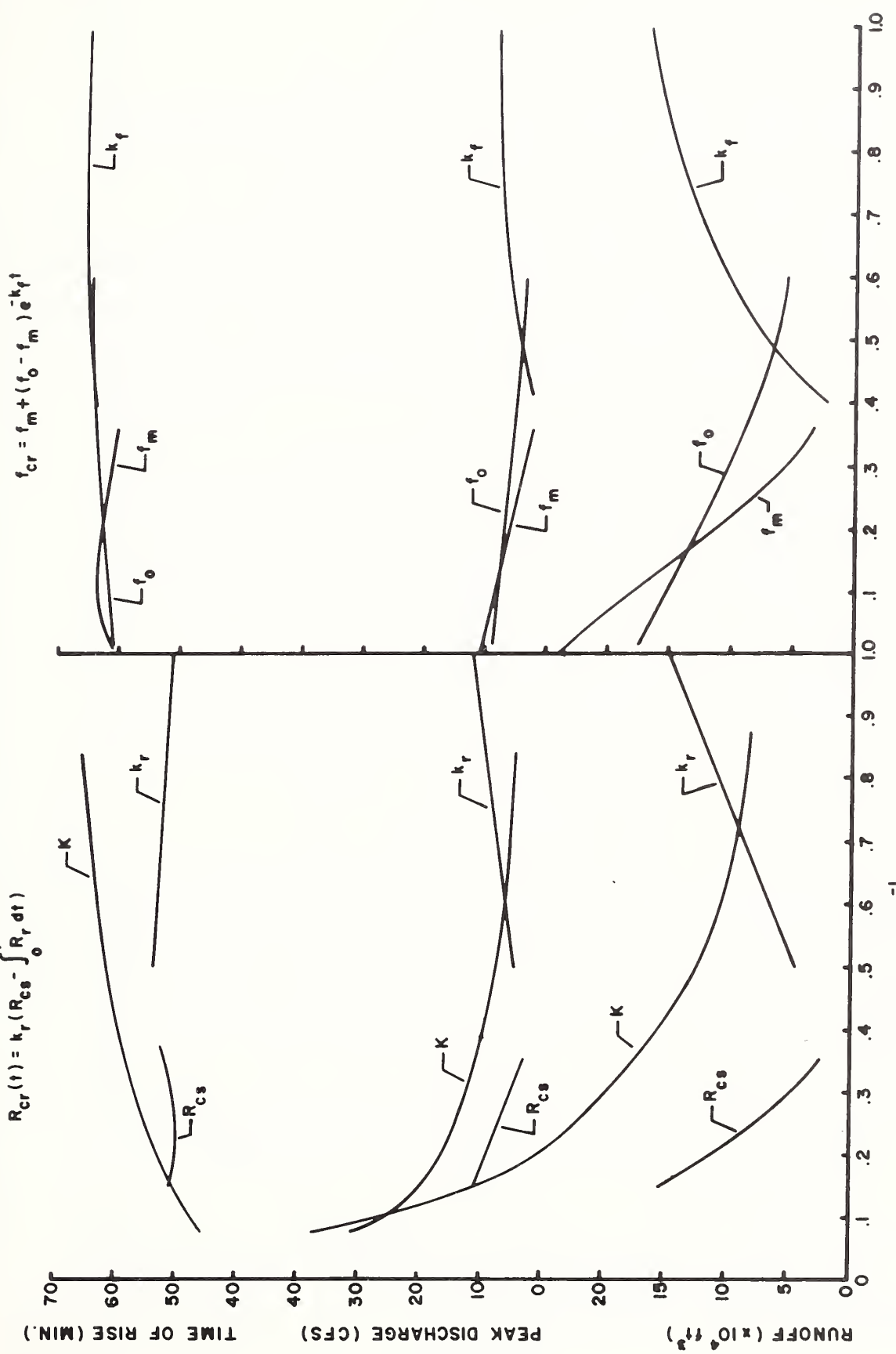

FIGURE 12. CHANNEL FLOW HYDROGRAPH CHARACTERISTICS AS AFFECTED BY CHANGES IN VALUE OF PLANE VARIABLES.

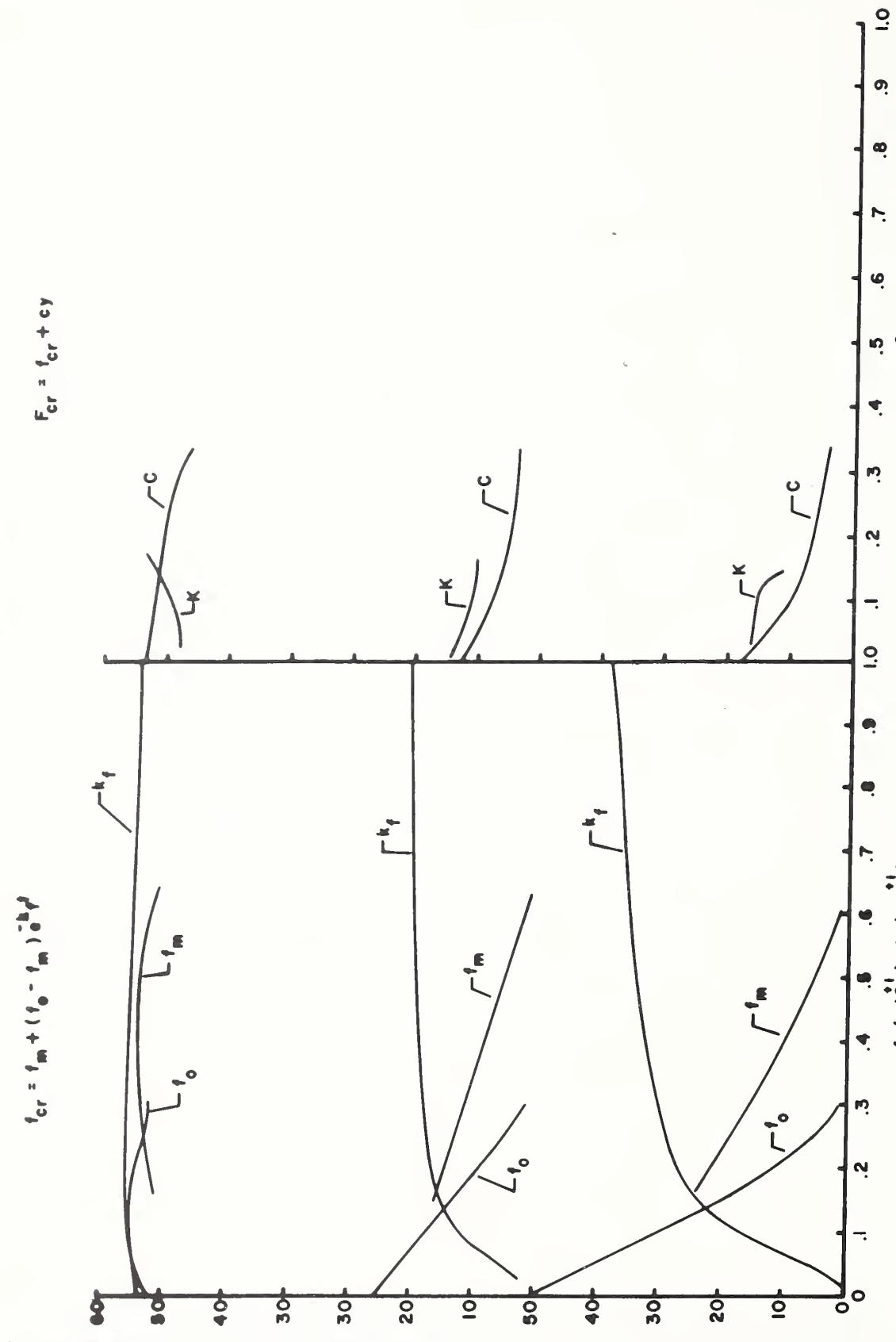

FIGURE 13. CHANNEL FLOW HYDROGRAPH CHARACTERISTICS AS AFFECTED BY CHANGES IN VALUE OF CHANNEL VARIABLES.

observation was that the time at which flow ceased for changes in R_{cs} was almost invariant for the overland flow while for the channel flow, increasing R_{cs} shortened the time at which the flow ceased.

The manner in which the channel flow model responds to changes in the plane and channel roughness coefficient is quite different. The chief difference between these two coefficients on the hydrograph characteristics for the range of values tested was in the hydrograph time of rise. The channel K has little effect on the hydrograph time of rise, whereas the plane K affects it significantly. Likewise, the plane K affected the runoff volume and peak discharge more than did the channel K.

The importance of the value of k_f in determining the relative weight of the initial and final infiltration values was again demonstrated. The hydrographs showed a greater sensitivity to changes in the plane f_m than to changes in the channel f_m. The hydrographs were also more sensitive to variation of channel f_o than to variation of the plane f_o.

The depth coefficient in the channel seepage term changed the hydrograph by decreasing the volume and peak discharges for increases in the value of c. The time of rise of the channel hydrograph appears to decrease only slightly with increasing values of c.

SUMMARY

1. The runoff model developed seems to describe the runoff process and provides a realistic outflow hydrograph after appropriate juggling of the condition parameters. The mathematical model of the surface runoff is flexible, and can be adapted to different flow conditions found on a watershed. It also presents the advantage of yielding directly such hydrograph characteristics as the time of rise without resorting to empirical formulas for this time delay.

2. Consideration of both overland and channel flow in the model allows computation of the water loss by retention and storage on the land surfaces and the channel seepage losses (transmission losses).

3. Subdivision of the watershed into subzones helps to describe the spatial precipitation distribution as well as the spatial distribution of both the function and condition parameters. Subdivision of the watershed also provides additional model calculation comparison points when the hydrograph is available at the outlet of subzones.

4. The results of sensitivity analysis or responses of the hydrograph to changes in parameter values agrees well with what might be experiences from field observations. The resistance term (K) of the overland and channel flow terms appears to have the largest effect on the computed hydrograph peak.

5. Additional checks on the runoff hydrograph from subzones or from the overland flow planes would be most desirable. All the condition parameters are now adjusted simultaneously to provide a computed hydrograph to match the observed hydrograph. Data for comparing the overland flow portion would provide an independent adjustment of first the overland flow and finally the channel flow.

APPENDIX A

List of Symbols

Symbol	Description	Unit
a_i	Elemental subarea in precipitation determination	$feet^2$
A	Cross-sectional area of the flow	$feet^2$
A_s	Watershed surface area	$feet^2$
B	Top width of cross-sectional area of flow	feet
c	Constant applied in channel seepage	Sec^{-1}
F_{cr}	Channel seepage capacity rate at any time	$in/hr/ft^2$
f_{cr}	Infiltration capacity rate at any time	in/hr
f_m	Minimum value of f_{cr}	in/hr
f_o	Maximum value of f_{cr}	in/hr
g	Acceleration due to gravity	ft/sec^2
I	Unit rate of lateral inflow into channel	ft^2/sec
j	Subscript indicating section number	
J	Subzone number	
K	Channel or plane roughness coefficient	sec^2/ft^2
k	Constant less than unity in Horton equation	

Symbol	Description	Unit
k_r	Constant ≤ 1 in retention capacity rate equation depending upon surface characteristics	
O	Unit rate of outflow loss due to seepage	ft^2/sec
P_e	Effective precipitation rate	in/hr
P_r	Actual precipitation rate	in/hr
Q	Total rate of flow at any section of channel	ft^3/sec
q	Rate of flow per unit width	$ft^3/sec/ft$
q_n	Rate of outflow at end of equivalent overland flow plane	$ft^3/sec/ft$
q_{crg}	Capacity rate of seepage loss per unit length of channel	in/hr/ft
q_{rg}	Actual rate of seepage loss from channel	in/hr
R_{cr}	Retention capacity rate	in/hr
R_{cs}	Retention storage capacity of vegetation and land surface	in/hr
R_r	Actual rate at which precipitation is entering retention storage	in/hr
R_s	Amount of precipitation in retention storage	inches
S_f	Energy grade line	ft/ft
S_o	Bed or land surface slope	ft/ft

Symbol	Description	Unit
t	Time	minutes or hours
V	Average velocity of flow	ft/sec
v_i	Volume of precipitation in elemental area between adjacent isohyetal	$in\text{-}ft^2$
x	Distance along plane or along channel	ft.
y	Flow depth	ft.
Z	Number of subzones	
γ_o	Bed shear	lb/ft^2
θ	Angle between channel bottom and horizontal	
$\alpha+\beta$	Energy and momentum coefficients	

SCHEMATIC REPRESENTATION OF THUNDERSTORM RAINFALL[1/]

H. B. Osborn[2/]

INTRODUCTION

Hydrologic research is being conducted by the Southwest Watershed Research Center of the Agricultural Research Service on the 58-square-mile Walnut Gulch watershed in southeastern Arizona (Fig. 1). Rainfall and runoff data have been collected on the watershed since 1953, with the precipitation network now totaling about 95 weighing-type recording rain gages (Fig. 2). Runoff results almost entirely from summer thunderstorm rainfall. Therefore, mathematical descriptions, or models, of thunderstorm rainfall are important to researchers and others involved in hydrologic investigations in the Southwest.

Arnold Court (1961) reviewed depth-area rainfall formulas proposed by half a dozen investigators. He compared all the methods that he reviewed by plotting a 2-inch maximum depth for each method (Fig. 3). Of particular interest to persons in the Southwest were his comments on a depth-area model suggested by Woolhiser and Schwalen (1959), and the Woolhiser-Schwalen paper itself. The Woolhiser-Schwalen model was the "slimmest" of the bell-shaped figures, which indicated the dominance of the purely convective thunderstorms in the region. Court concluded that "any realistic representation of the variation of rainfall amount with distance from the storm center should

---

[1/] Contribution of the Southwest Watershed Research Center, USDA, Agricultural Research Service, Soil and Water Conservation Research Div., in cooperation with the Arizona Agricultural Experiment Station, Tucson.

[2/] Research Hydraulic Engineer, Southwest Watershed Research Center, Agricultural Research Service, USDA, SWC, 442 East Seventh Street, Tucson, Arizona 85705.

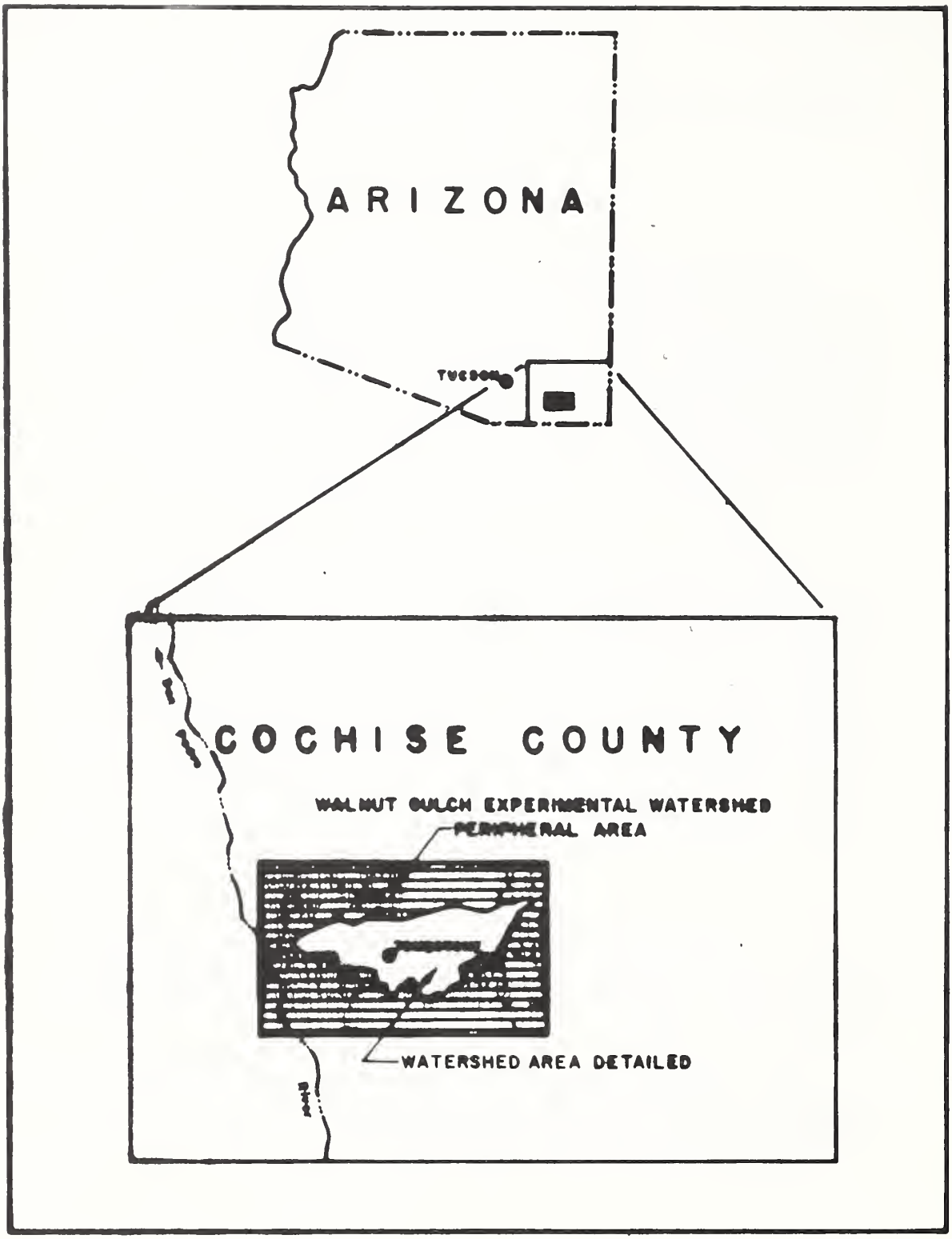
ARIZONA
TUCSON
COCHISE COUNTY
WALNUT GULCH EXPERIMENTAL WATERSHED
PERIPHERAL AREA
WATERSHED AREA DETAILED

FIGURE 1

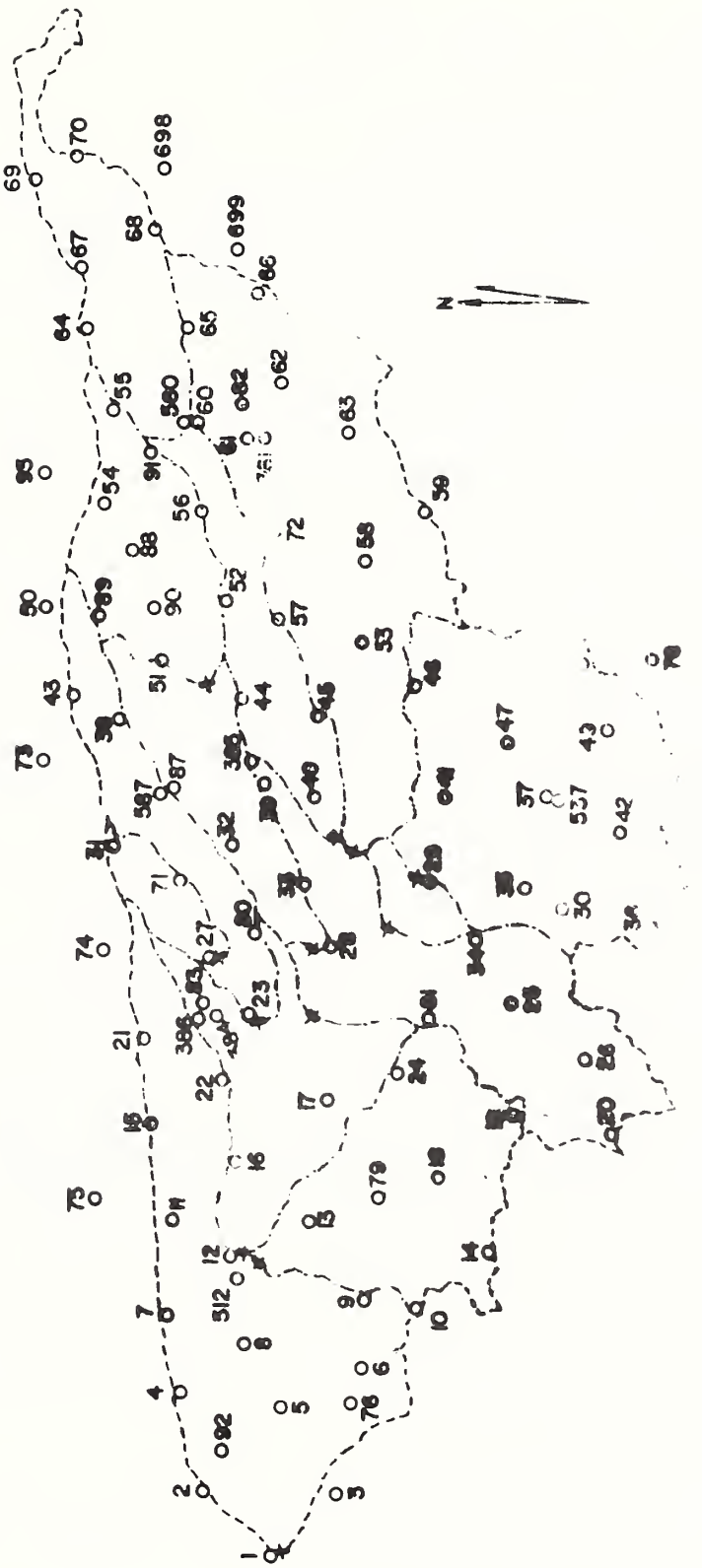

WALNUT GULCH WATERSHED

[illegible] NETWORK 1969

FIGURE 2

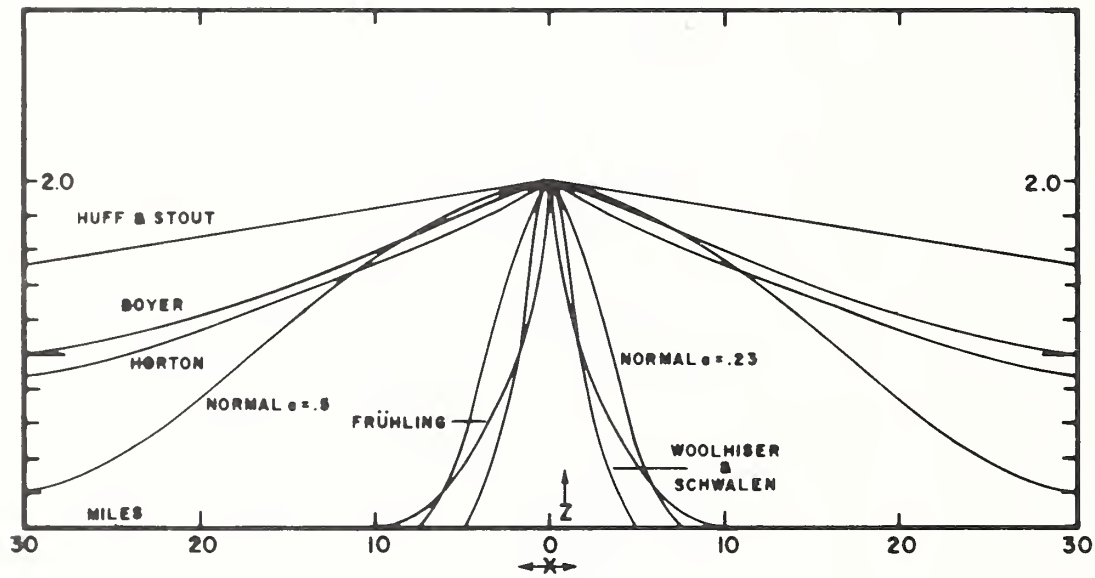

FIGURE 3. VARIATION OF ISOHYETAL VALUE Z (INCHES) WITH DISTANCE X (MILES) FROM STORM CENTER, ASSUMING CENTRAL PRECIPITATION TO BE M=2 INCHES, ACCORDING TO VARIOUS FORMULAS.

be smooth at the center." In other words, he felt that a dome-shaped figure was essential. Three of the models included in this review, including that by Woolhiser and Schwalen, and those based on a Gaussian distribution, met this condition.

Court also felt that "at the other extreme, an asymptotic approach to zero rainfall with increasing distance seems desirable." The Gaussian models met this condition, but the Woolhiser-Schwalen model did not.

Woolhiser and Schwalen based their model on data from the 18-square-mile Atterbury watershed near Tucson, Arizona. Although there are apparently significant climatological and topographical differences between the Walnut Gulch and Tucson areas, considerable similarity would be expected in the areal extents and magnitudes of thunderstorm rainfall at both locations. The 58-square-mile watershed should provide a better basis for either verifying or establishing a rainfall model because of the greater areal coverage of the rain gage network.

WALNUT GULCH RAINFALL

Storms on Walnut Gulch were analyzed for the period 1961 through 1968. Good isohyetal rainfall maps were available for this period. There were about 50 storms in which over 1" of rainfall was recorded at at least one storm center on the watershed.

From the 50 storms, about 45 storm centers were defined sufficiently to include in the analysis. None of the storms with centers of more than 1.2" could be completely defined to as low as the 0.6" isohyet. In other words, all storms with a maximum point rainfall of 1.2" or more were spread out over the watershed boundary and outside the rain gage network, and the isohyets could not be "closed." Rainfall below 0.6" was so poorly defined that no effort was made to include lower isohyets in the analysis.

In general, the storms on Walnut Gulch had one steep edge as represented by relatively closely spaced isohyets and one gently sloped edge as represented by relatively widely spaced isohyets. The

steep or tightly spaced isohyets are referred to in this paper as the "short axis" of the storm; the widely spaced isohyets are referred to as the "long axis." Although the long and short axis of the rainfall were not generally at right angles, the storms appeared to be more elliptical than any other simple shape.

In a significant number of storms, at least one edge of the storm was defined down to zero rainfall. Court's second premise was that an asymptotic approach to zero rainfall was necessary for a reasonable rainfall model. It appears that thunderstorm rainfall is definitely limited in areal extent and that the Woolhiser-Schwalen model, which does go to zero, is satisfactory, at least in this respect.

The distances from the storm center to each succeeding, and decreasing, isohyet were measured along the long and short axis. These values for the four largest storms during the period were plotted to give a schematic representation of thunderstorm rainfall (Fig. 4). By far the greatest rainfall both in maximum recorded depth and volume was recorded on the afternoon of September 10, 1967. Three and one-half inches of rain were recorded at the storm center. Maximum recorded point rainfalls for the next three largest storms were 2.65", 2.62", and 2.53". The September 10, 1967 storm was compared to averages of individual storms in the ranges from 2.21" to 2.40", 2.01" to 2.20", and 1.81" to 2.00" (Fig. 5), and to averages of individual storms in the ranges from 1.41" to 1.60", 1.21" to 1.40", and 1.01" to 1.20" (Fig. 6).

Several observations were made from these figures. In Figure 4 the September 10, 1967 storm does not cover significantly more area at the 0.6" isohyet than do the next three largest storms. The isohyets, particularly on the short axis, are extremely closely spaced for the largest storm. Above the 1.0" isohyets, the 1967 storm covered more area than any of the next three largest events because of the greater extent of the long axis of the storm. In Figures 5 and 6, the areal extent at each increasing depth was clearly greater for the 1967 storm. At the 0.6" isohyet, the larger storm was more extensive than the median-sized and smaller storms, again primarily because of the greater extent of the long axis.

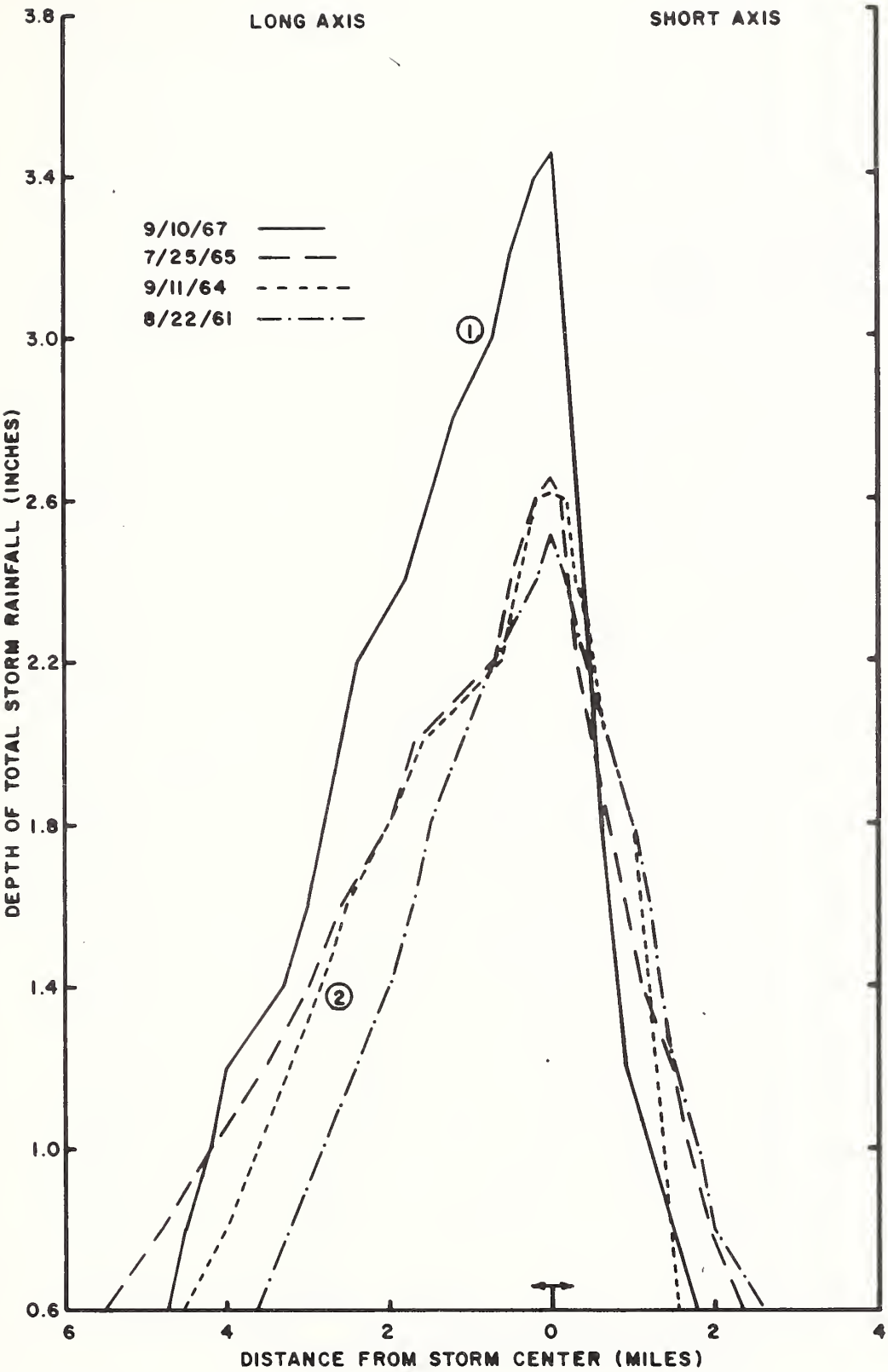

FIGURE 4. SCHEMATIC REPRESENTATION OF EXTREME STORMS BASED ON DISTANCE FROM STORM CENTER TO GIVEN ISOHYETS FOR 4 LARGEST EVENTS ON WALNUT GULCH, 1961—1968

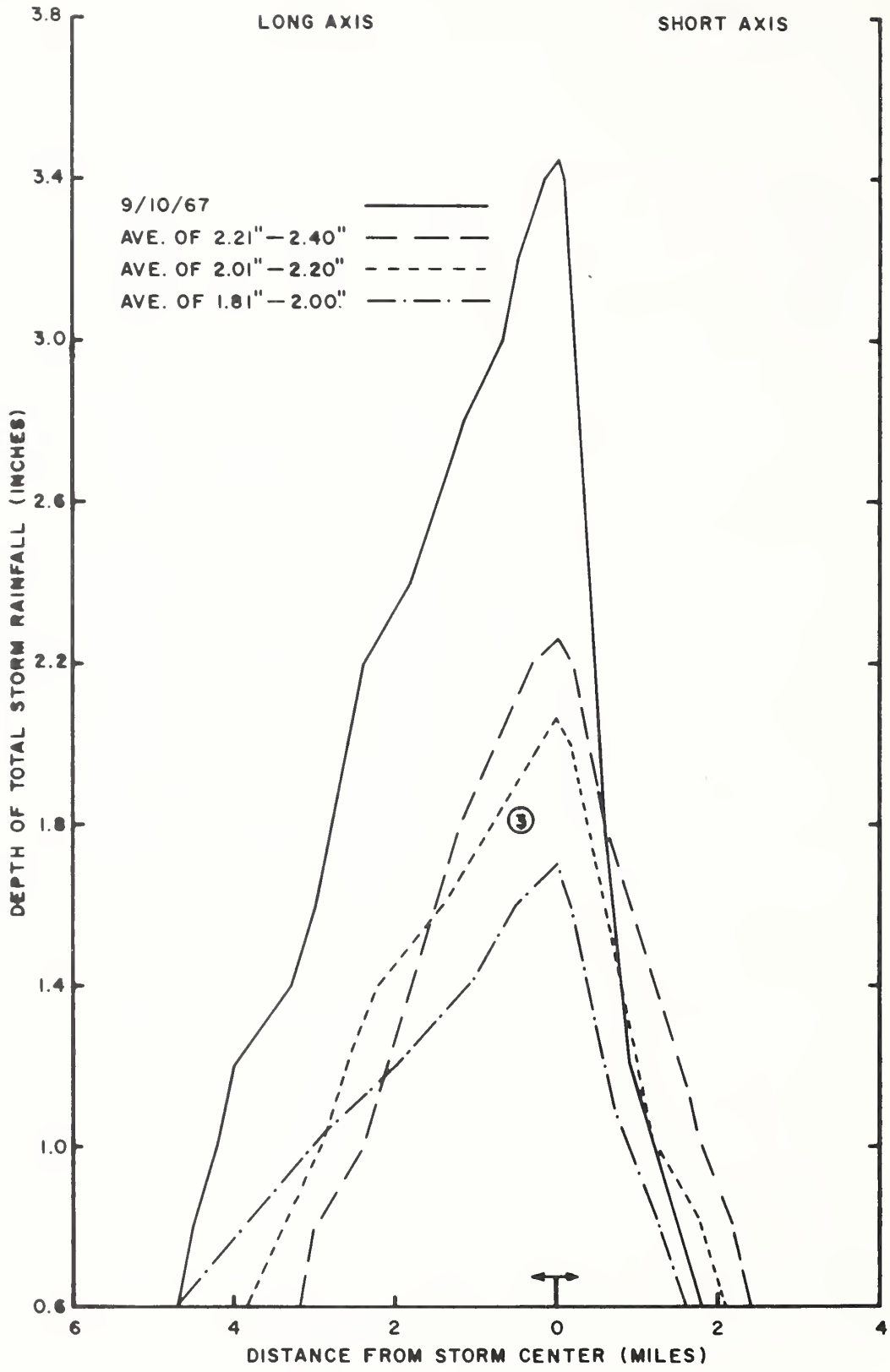

FIGURE 5. SCHEMATIC REPRESENTATION OF THE MAXIMUM STORM EVENT AND 3 AVERAGED EVENTS BASED ON DISTANCE FROM STORM CENTER TO GIVEN ISOHYETS FOR WALNUT GULCH, 1961-1968.

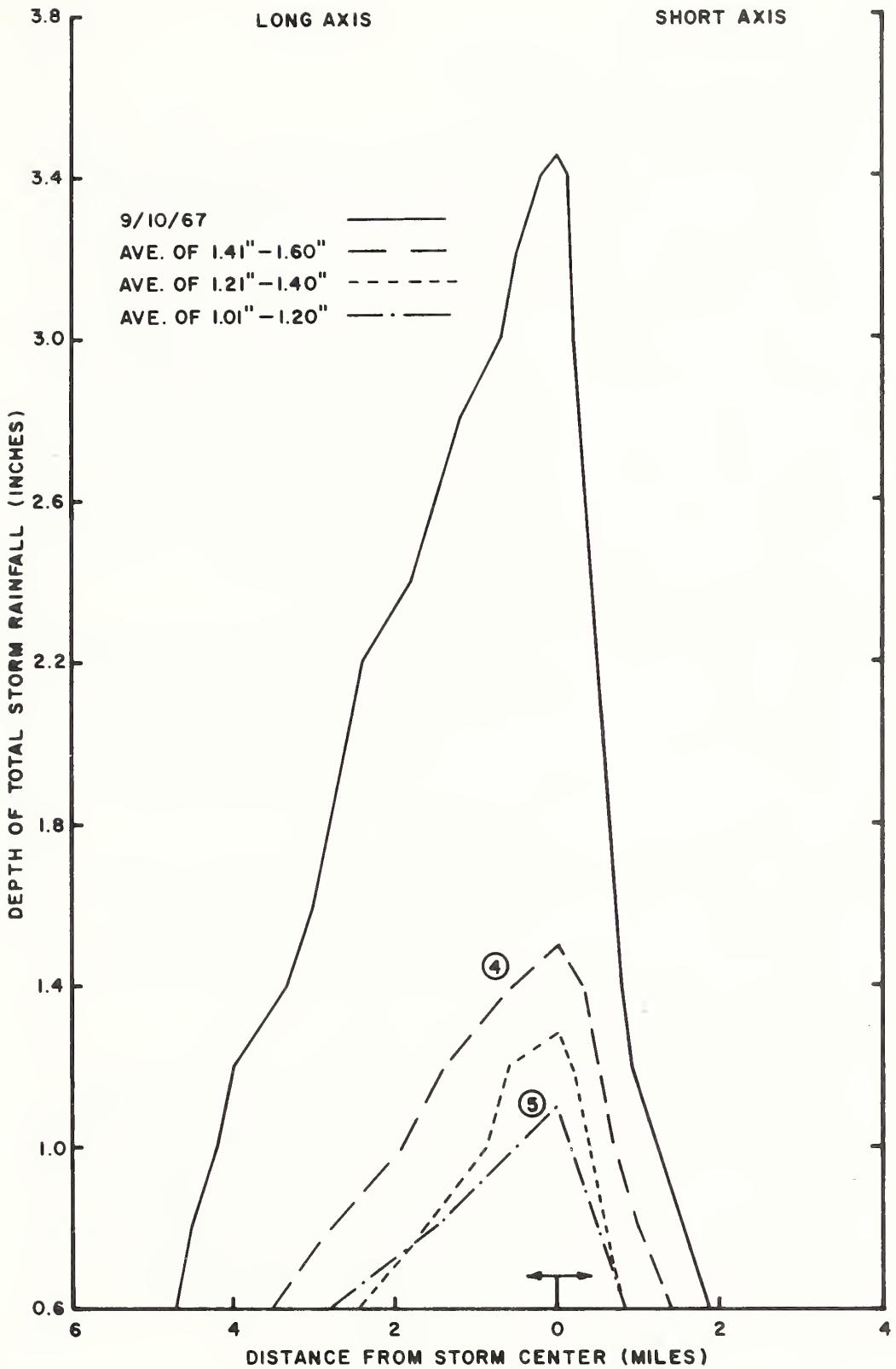

FIGURE 6. SCHEMATIC REPRESENTATION OF THE MAXIMUM STORM EVENT AND 3 AVERAGED EVENTS BASED ON DISTANCE FROM STORM CENTER TO GIVEN ISOHYETS FOR WALNUT GULCH, 1961-1968

Composite storms were developed from the schematic representations in Figures 4, 5, and 6. These composite storms were developed for maximum center rain depths of 3.5", 2.6", 2.0", 1.5", and 1.2" (Fig. 7). The largest composite storm was based on the 1967 storm; the second largest was based on the next three largest events; the three smaller composite storms were based on 13 or 14 storms each in their respective ranges of center depths. The final composite representations for all but the largest storm probably could be approximately by triangles. The schematic composites developed here have "lost" the bell-shaped dome that was evident in plotting true cross sections of thunderstorms as represented by isohyetal maps. The "dome" should probably be added for a rainfall model as indicated by Court and Woolhiser and Schwalen. For most purposes, the figures could be extended linearly to zero for a complete model.

The Woolhiser-Schwalen model and the Walnut Gulch schematic composite were compared in Figure 8, using a 2" storm for the basis of comparison. Both figures were in a sense bell-shaped, but the "dome" on the Walnut Gulch composite was "lost" in the averaging. The Woolhiser-Schwalen model implied a circular pattern of isohyets which appeared to be about the average between the long and short axis for the Walnut Gulch figure.

The volume of rainfall for the model and composite would be about the same if the composite were assumed to be an elliptical model. This indicated that both the Woolhiser-Schwalen model and the Walnut Gulch composite were in the right order of magnitude in representing thunderstorm rainfall.

Woolhiser and Schwalen based their model on a plot of "area enclosed by isohyet vs. depth at storm center minus depth of isohyet " (Fig. 9). A similar approach was attempted using Walnut Gulch storms. In Figure 10 the three largest events were compared using the distance along the long and short axis vs. the incremental depth, which was similar to the system used by Woolhiser and Schwalen except that distances replaced areal extent. In Figure 11 the composite storms were compared by using the axial distances vs. the incremental depth.

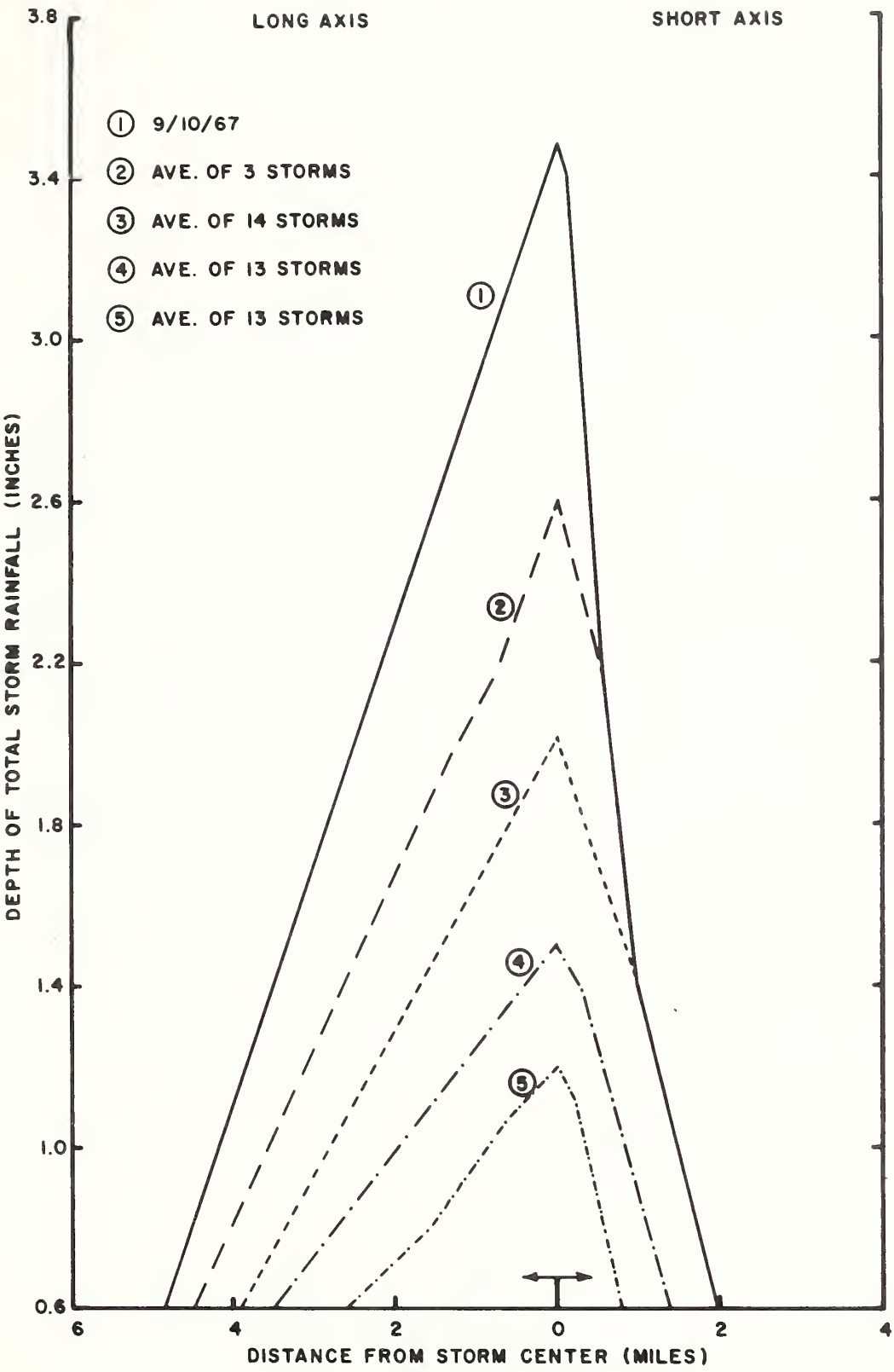

FIGURE 7. COMPOSITE STORMS BASED ON DISTANCE FROM STORM CENTER TO GIVEN ISOHYETS FOR WALNUT GULCH, 1961–1968.

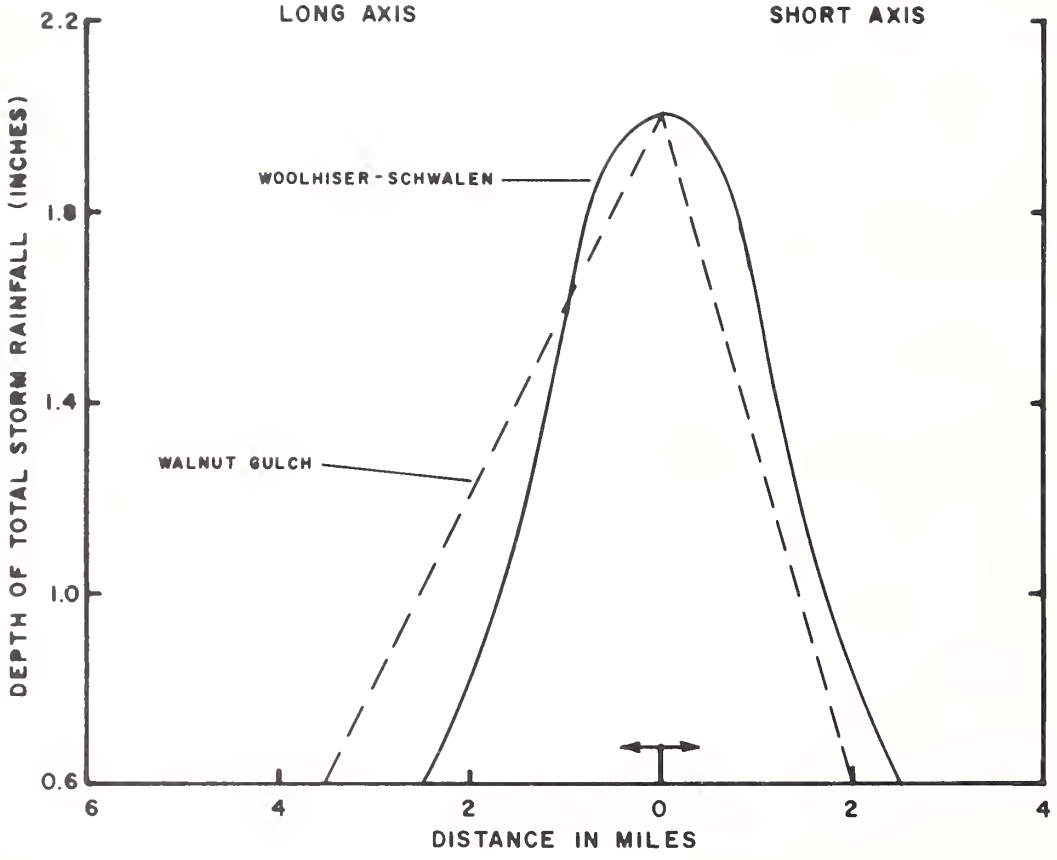

FIGURE 8. COMPARISON OF COMPOSITE SCHEMATIC WALNUT GULCH 2-INCH RAIN WITH WOOLHISER-SCHWALEN 2-INCH RAIN.

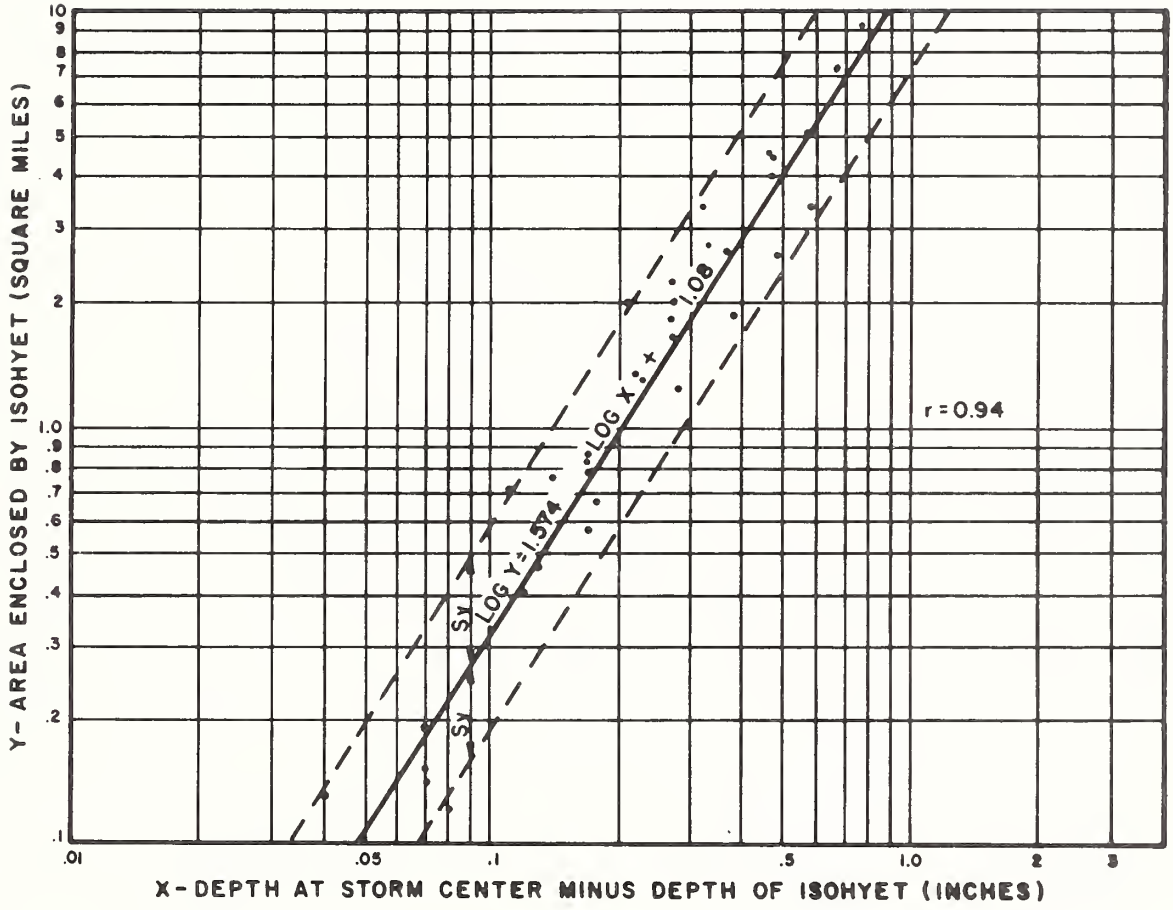

FIGURE 9. STORM CENTER AREA — DEPTH RELATIONS.

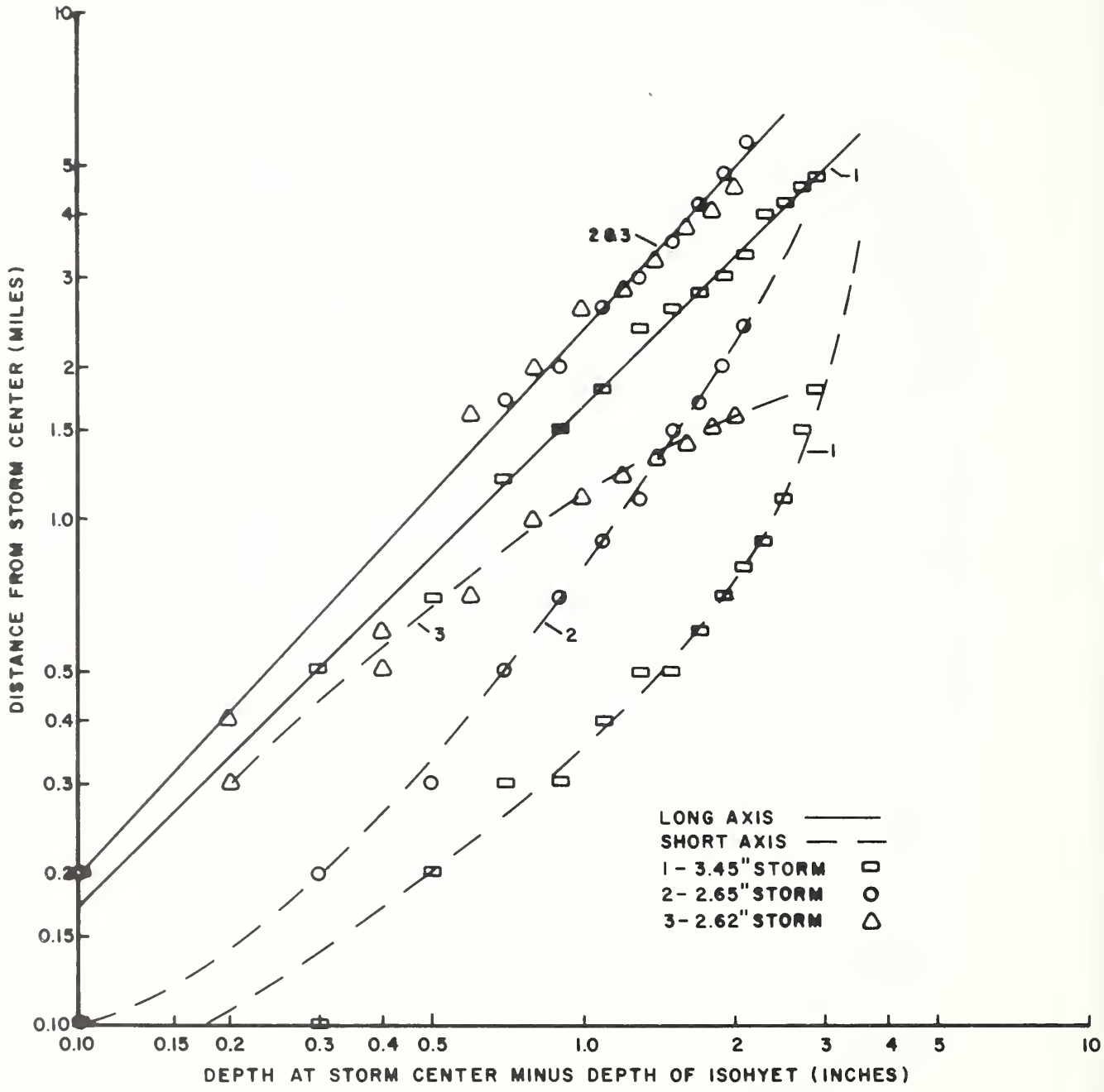

FIGURE 10. DISTANCE FROM STORM CENTER VERSUS INCREMENTAL DEPTH OF RAINFALL, FOR THE THREE LARGEST STORMS ON WALNUT GULCH, 1961-1968.

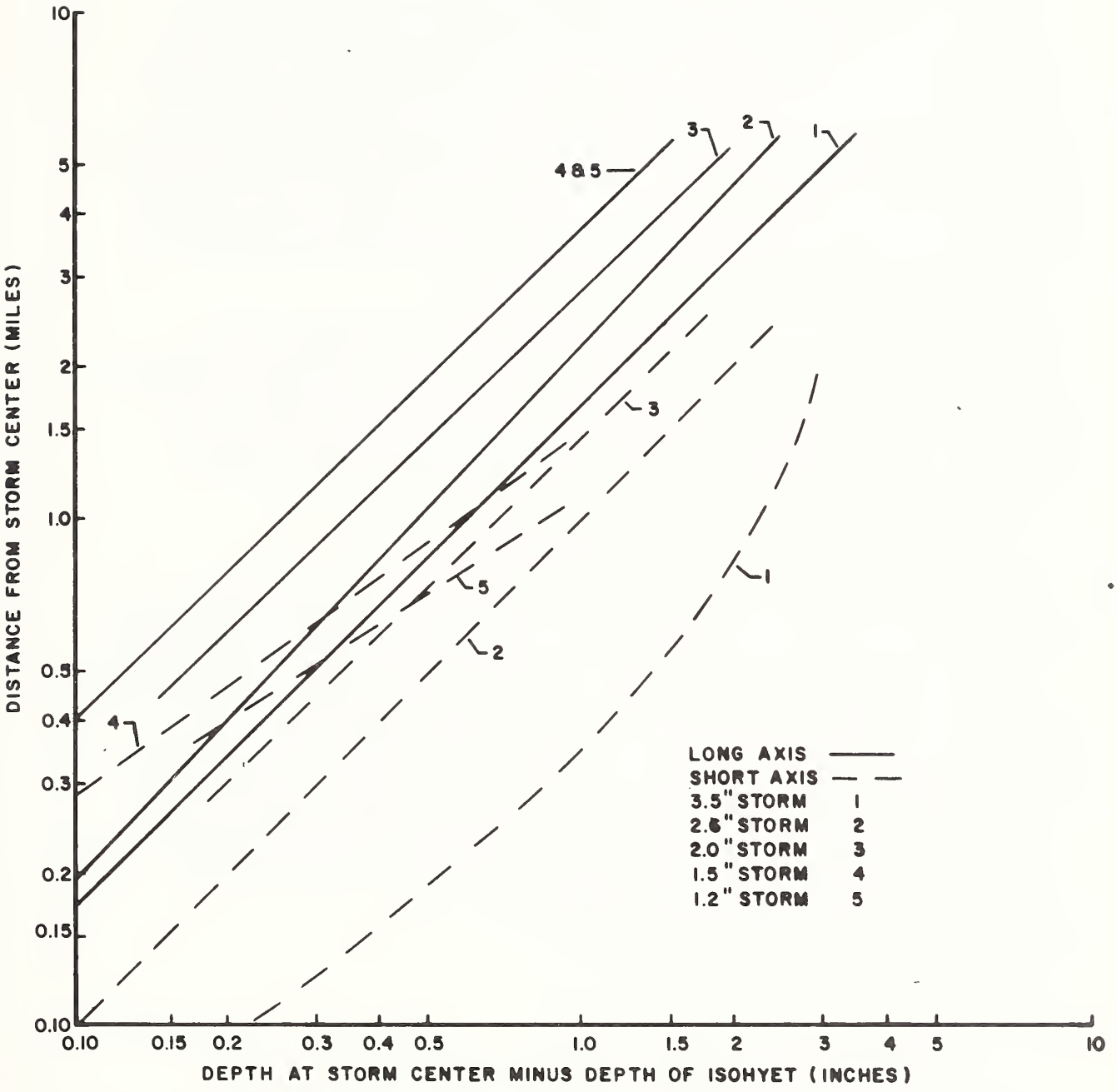

FIGURE II. DISTANCE FROM STORM CENTER VERSUS INCREMENTAL DEPTH OF RAINFALL, FOR THE COMPOSITE STORMS ON WALNUT GULCH, 1961–1968.

It is apparent that the Walnut Gulch storms do not, for every depth, fit into the same pattern as the Woolhiser-Schwalen storms. Woolhiser and Schwalen came up with one formula, $\log y = 1.574 \log x + 1.08$. For the Walnut Gulch storms, there would be a series of parallel formulas for the long axis, depending on the maximum depth of the storm center. The plots for the short axis of the 3 largest storms were clearly curved. Curvilinear lines on log-log paper are difficult to explain. When the composite storms were plotted, the lines on the short axis, except for the September 10, 1967 storm, tended to plot as straight lines as well as for the long axis.

The equation for the long axis for line 1 on Figure 10 was $\log y = \log x + 0.22$, or $y = 1.65 x$. Lines 2 and 3 could be represented by a similarly-sloped log-log equation. Possibly a family of log-log equations based on maximum storm depth could be developed, but further investigation is needed to determine the use and validity of such equations.

CONCLUSIONS

To this date the Woolhiser-Schwalen model and the Walnut Gulch schematic composites appear to be reasonable developments in thunderstorm rainfall analysis. Further analysis in this vein may answer some of the many questions concerning thunderstorm rainfall. They include the following: (1) In general, can thunderstorms be considered elliptical?, circular?; (2) If not, for specific studies, such as rainfall-runoff correlation, can thunderstorms be considered elliptical?, circular?; (3) If the thunderstorms cannot be considered elliptical or circular, can they be described in some other way?; and (4) Should thunderstorms be broken into shorter increments, say 10-minute periods, to develop rainfall models?

REFERENCES

Woolhiser, D. A., and H. C. Schwalen. Area-depth-frequency relations for thunderstorm rainfall in southern Arizona. Tech Paper 527, Agr. Engr. Dept., Arizona Agr. Expt. Sta., University of Arizona, 1959.

Court, Arnold. Area-depth rainfall formulas, Jour. Geophys. Res. Vol. 66, No. 6, 1961.

A STOCHASTIC MODEL FOR RUNOFF EVENTS FOR A SEMIARID WATERSHED IN SOUTHEASTERN ARIZONA [1/]

M. H. Diskin and L. J. Lane [2/]

INTRODUCTION

Stochastic hydrologic models are models used for the generation of synthetic hydrologic data in such a way that the statistical properties of the original data observed in the watershed are preserved in the synthetic data generated by the model. The parameters describing the various distributions associated with the original data serve as input to the stochastic models. The output of the models is in the form of sequences of hydrologic data that may be used for design purposes. Goodness of fit of the model is judged in terms of the agreement between the values of statistical parameters derived from the synthetic data and the corresponding parameters of the input data, including some parameters that were not used as input.

Systems represented by stochastic models are usually assumed to be stationary. If this is not the case, any nonstationarity, such as a trend or a cyclical variation, is removed from the original data. It is again superimposed on the output of the model. Stochastic models are usually employed for generation of either rainfall data or runoff data. There are only very few cases where stochastic models were used to represent the rainfall-runoff relationship.

1/ Contribution of the Southwest Watershed Research Center, USDA, Agricultural Research Service, Soil and Water Conservation Research Div., in cooperation with the Arizona Agricultural Experiment Station, Tucson.

2/ Research Hydraulic Engineer (visiting scientist on leave from Technion-Israel Institute of Technology, Haifa, Israel), and Hydrologist, respectively, Southwest Watershed Research Center, Agricultural Research Service, USDA, SWC, 442 E. Seventh Street, Tucson, Arizona 85705.

The purpose of the present paper is to describe a stochastic model that has been developed for runoff events on a subwatershed of the Walnut Gulch watershed in southeastern Arizona. The subwatershed considered is that contributing to Flume No. 6 (W-6). It is a brush- and grass-covered watershed with a well developed stream network. The area of the watershed is 36.7 square miles (Fig. 1). Flow in the tributary streams and in the main channel out of the watershed is intermittent with relatively long periods of no flow and short periods of runoff following local thunderstorm rainfall.

Discharge from the watershed is measured with a large supercritical-depth flume (Gwinn, 1964), and the measurements are considered to be of good quality. Runoff records for the watershed are available for the period 1962 through 1968. The great majority of runoff events occur in the summer season from the beginning of July to the end of September with occasional events in other times of the year. The model developed herein is based on data pertaining to the summer events only, and its purpose is to generate sequences of such summer runoff events that may be used in subsequent studies of the hydrologic behavior of the watershed considered.

STATISTICAL PROPERTIES OF RUNOFF DATA

The characteristics of runoff data from the watershed considered are shown in Figure 2, giving the time distribution of runoff volumes for the 7 years of available data. Examination of the runoff records of the watershed indicated that the runoff season can be described in terms of the starting date of the season, the number of runoff events that occur per season, and the mean time interval between runoff events. The seven years of records for Watershed 6 indicated that there is some negative correlation between the starting date and the number of events per season (Fig. 3). No correlation was found between the mean time interval between runoff events and either of the other two variables mentioned above.

The starting date of the runoff season for the 7 years of record was between July 2 and July 28 with a mean value of July 15 and a standard deviation of 8.7 days. The range of number of events per

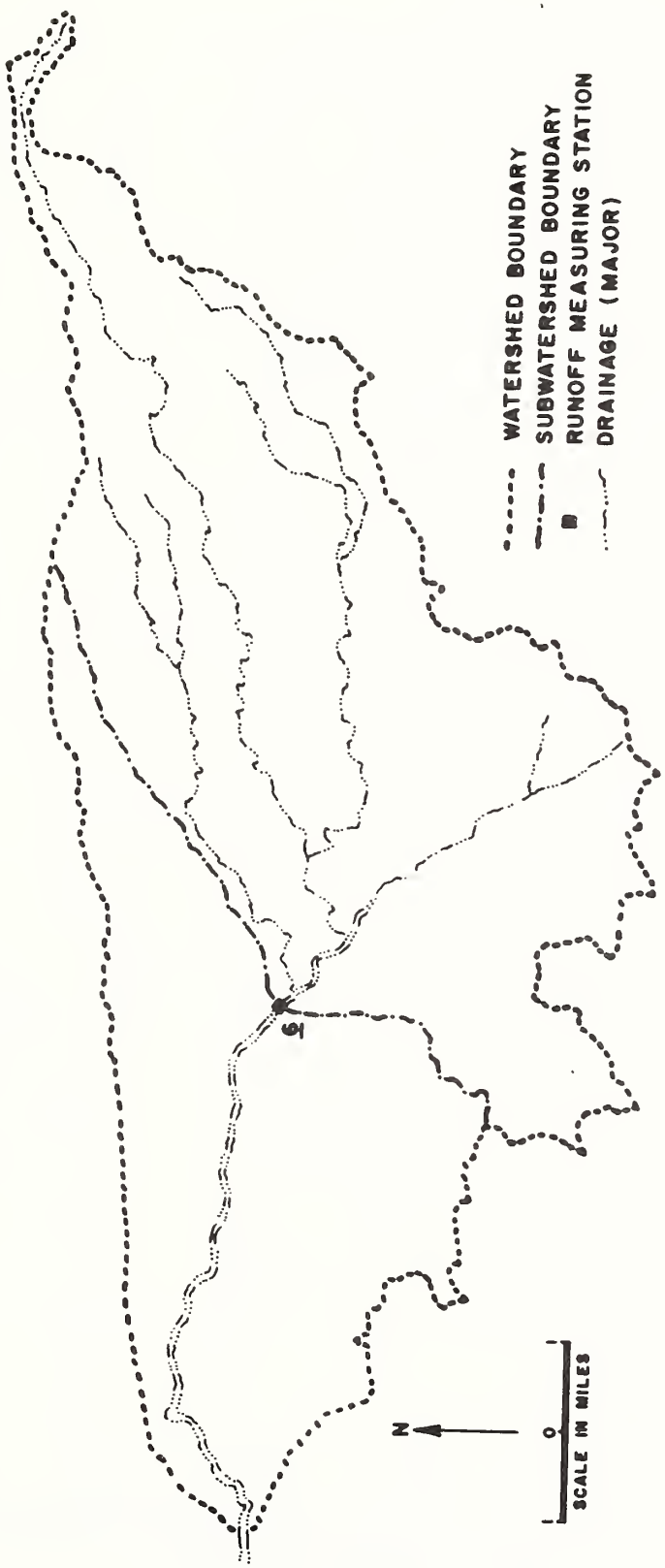

FIGURE 1. WALNUT GULCH EXPERIMENTAL WATERSHED

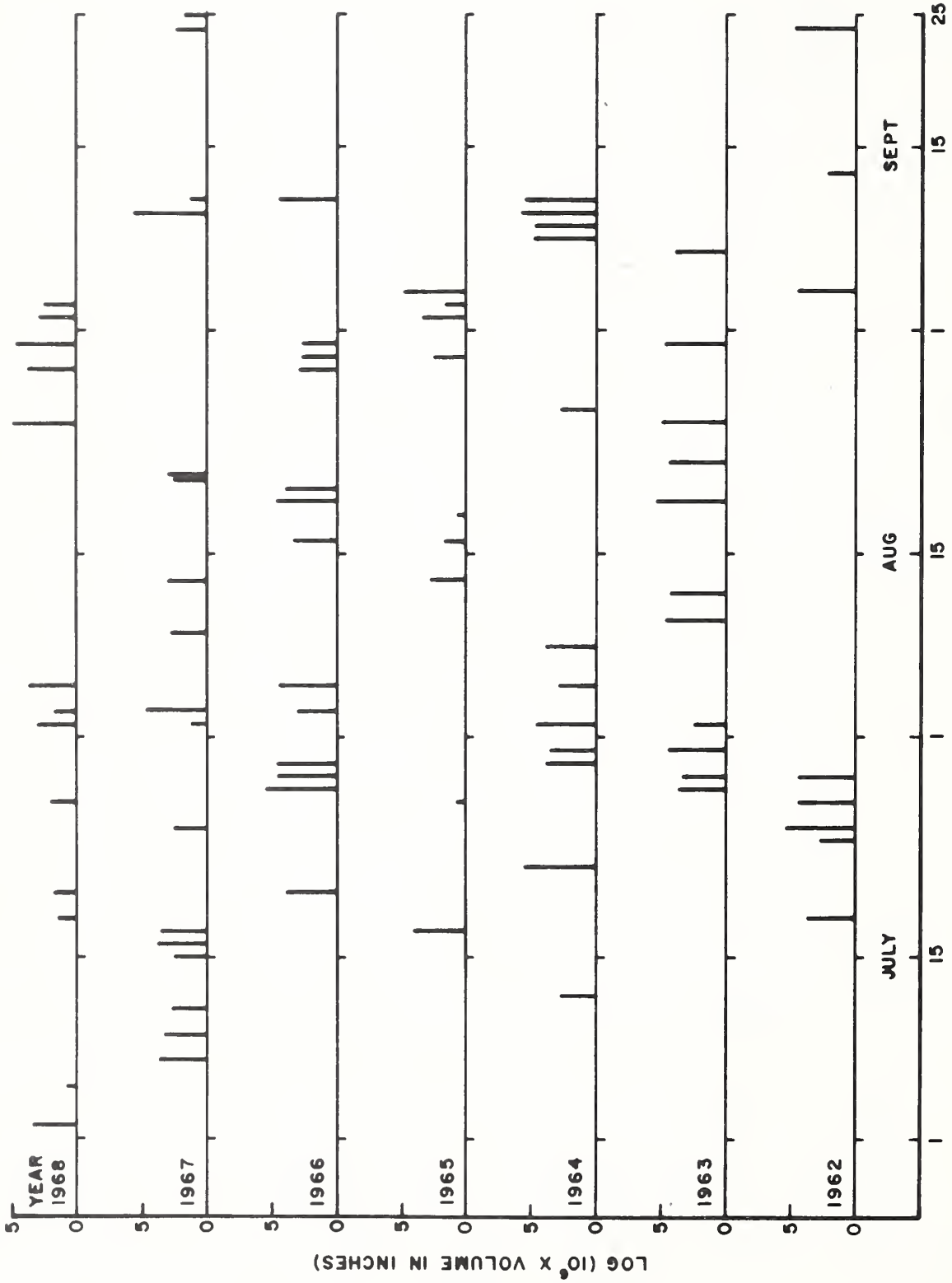

FIGURE 2. TIME DISTRIBUTION OF RUNOFF VOLUMES, OBSERVED DATA FOR WATERSHED 6.

FIGURE 3. LINEAR RELATION BETWEEN NUMBER OF EVENTS PER SEASON AND START OF SEASON.

season was 8 to 17 with a mean value of 12.0 and a standard deviation of 3.1. The seven years of record were insufficient to establish accurately the shape of the distribution curves for the starting date and for the number of events per season. Observations from an ARS experimental watershed in Safford, Arizona, where 30 years of records were available, indicated that the assumption of normal (Gaussian) distributions for these two variables is acceptable. The agreement between the measured values of starting date and number of events per season and the assumed normal distributions is shown in Figures 4 and 5.

The distribution of the time interval between runoff events was based on 77 values of this interval obtained by combining the number of intervals for all 7 years of record. The mean time interval was 5.38 days, and the standard deviation was 6.10 days. The negative exponential distribution was found to give a fairly good approximation of the actual distribution of the intervals. The agreement between the observed data and the negative exponential distribution adopted to describe the data is shown in Figure 6. Data from the Safford watershed mentioned above also supported the choice of the negative exponential distribution for the interval between runoff events.

Runoff events on Watershed 6, as well as on other watersheds in the Walnut Gulch area, tend to occur, because of local meteorological conditions, in late afternoon. Analysis of time of start of the 84 runoff events observed in Watershed 6 indicated that it may be assumed to be normally distributed with a mean value of 18.0 (6:00 p.m.) and a standard deviation of 3.53 hours (Fig. 7).

The above variables describe adequately the time of occurrence of the runoff events. To complete the description of the runoff data, more elements were considered. These were the volume of runoff and the peak discharge during the runoff event. The two variables were found to be highly correlated ($r = 0.98$), and their distribution curves were similar. As expected, the distributions of the volumes and the peaks were skewed with small values occurring more frequently than the high values. The mean volume of runoff was 49.0 acre-feet, and the mean peak discharge was 562 cfs. The standard deviations of the two variables were 98.4 acre-feet and 1165 cfs, respectively.

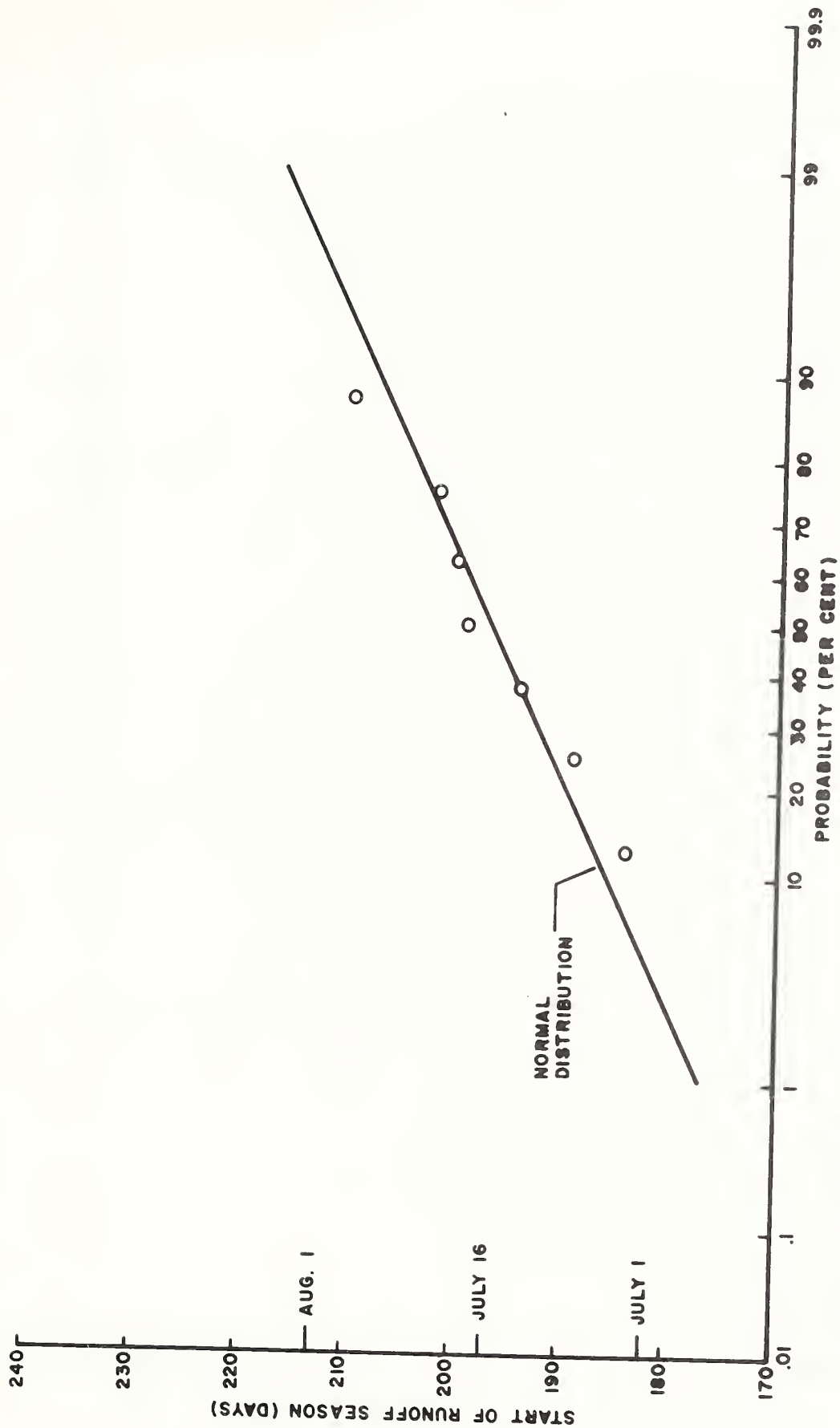

FIGURE 4. WATERSHED 6 DISTRIBUTION OF DATE OF FIRST RUNOFF EVENT OF SEASON.

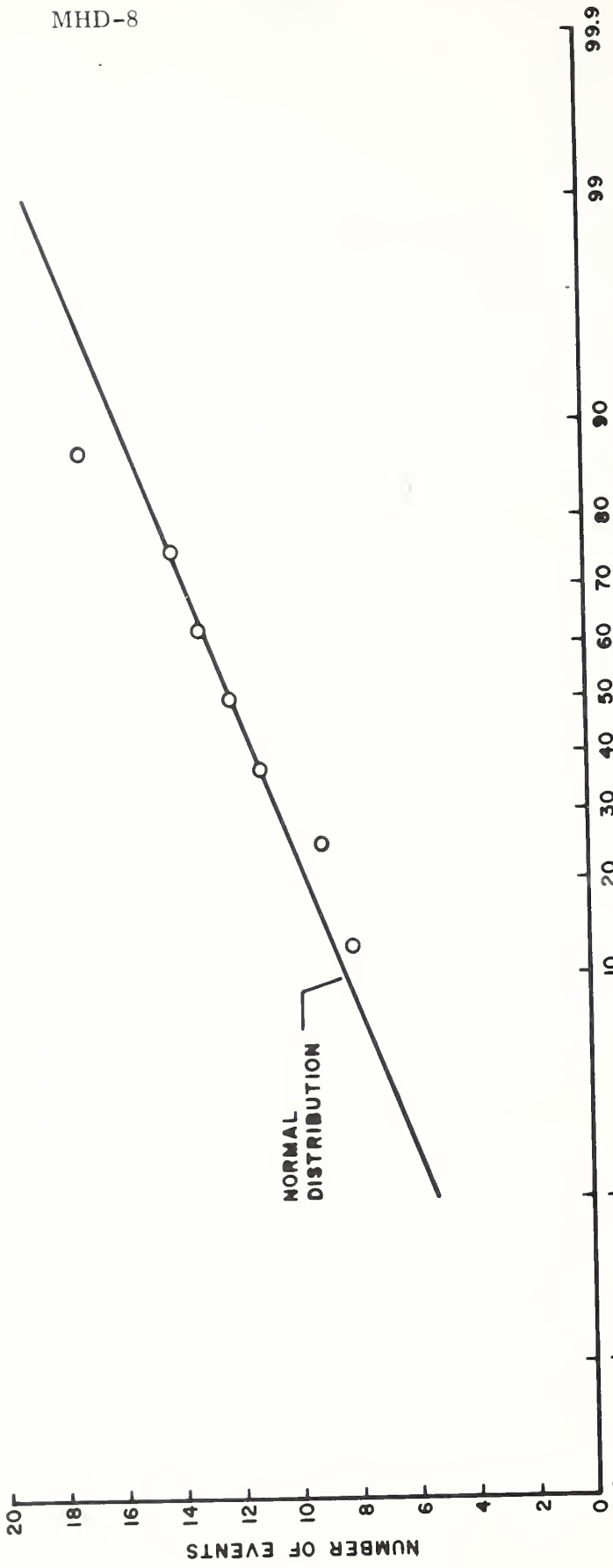

FIGURE 5. WATERSHED 6 DISTRIBUTION OF NUMBER OF EVENTS PER SEASON.

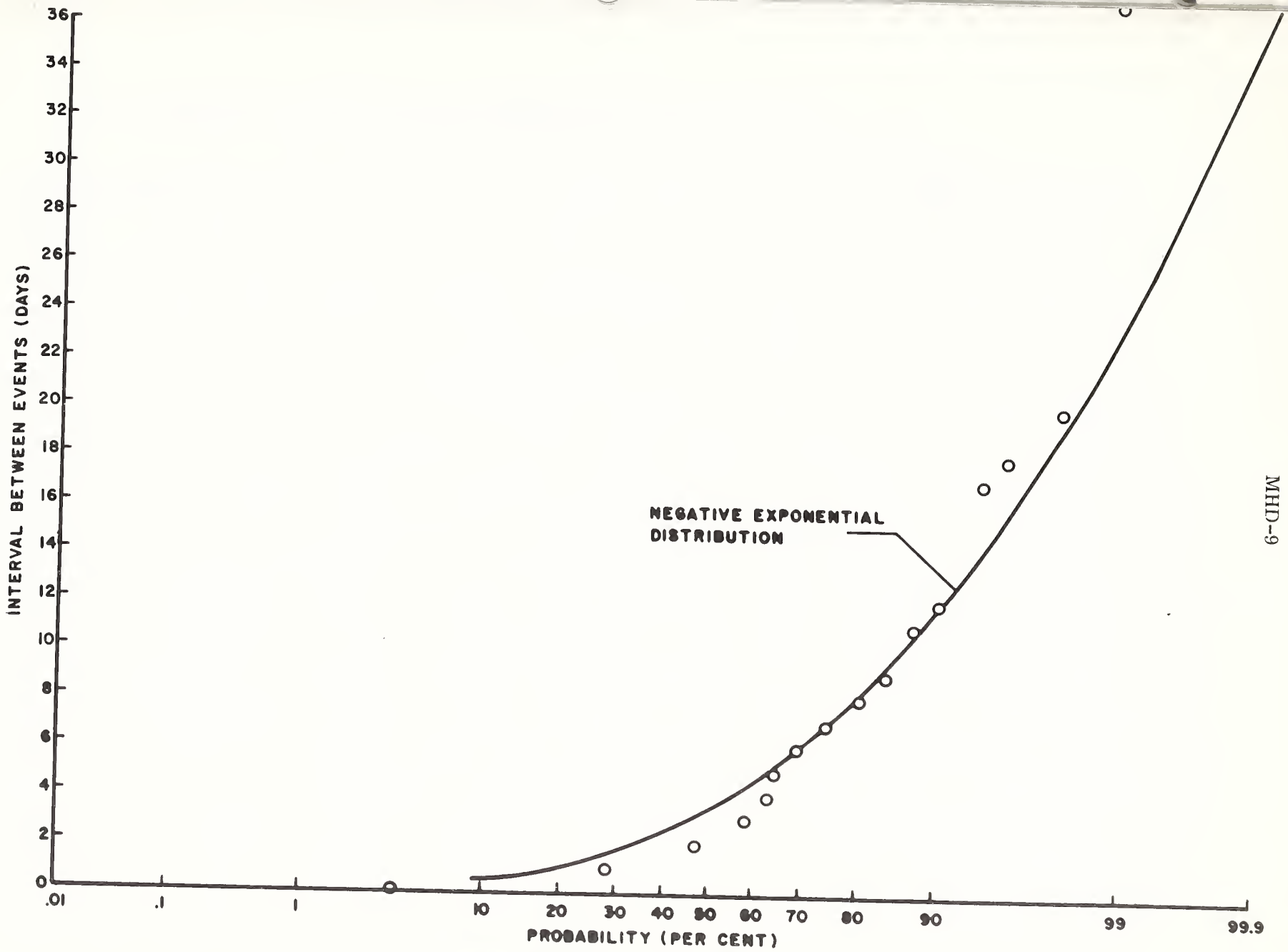

FIGURE 6. WATERSHED 6 DISTRIBUTION OF INTERVAL BETWEEN EVENTS.

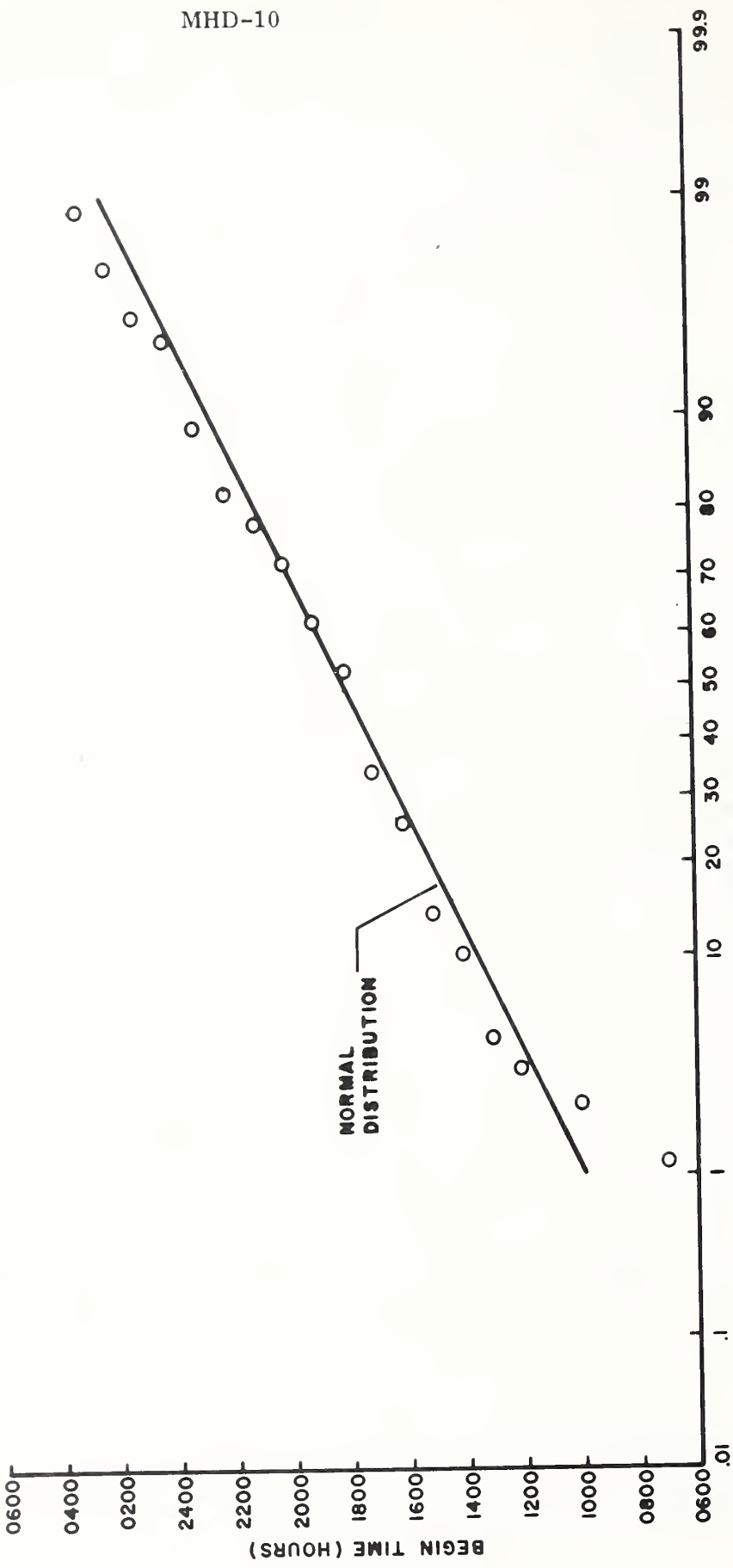

FIGURE 7. WATERSHED 6 DISTRIBUTION OF BEGIN TIME OF RUNOFF.

Adopting a logarithmic transformation for the volumes of runoff, it was found that the logarithms of the volume (expressed in 10^{-6}-inch units) were approximately normally distributed (Fig. 8), with a mean value of 3.30 and a standard deviation of 1.27. A better approximation could be obtained if a two-peaked distribution composed of two separate normal distributions is assumed.

The above description of runoff events in terms of the times of occurrence of the events, their volumes and peak discharges, is summarized in Table 1 which gives the mean and standard deviation for each variable.

DESCRIPTION OF THE STOCHASTIC MODEL

The stochastic model developed for generation of synthetic runoff data produces, as its output, sets of runoff events for the watershed considered. The runoff events are described in terms of the variables discussed above. The input to the model consists of the set of means and standard deviations, essentially as given in Table 1, as well as the parameters of the regression equations for the two variables that were found to be dependent on other variables.

A flow chart showing the structure of the model and the sequence of computations is given in Figure 9. A detailed description of the various steps involved is given below with reference to the operations enumerated in the flow chart.

The first step consists of reading in the values of the parameters used for generation of the synthetic data, reading the number of years for which data are required, and setting to "one" the sequential number of the year for which data are generated.

Using a subroutine for the generation of a reduced normal variate Z (with zero mean and unit standard deviation), the model first generates the starting date of the season. This is done by converting the reduced variate to the variable concerned

$$S = Z \cdot \sigma_S + \bar{S} \qquad (1)$$

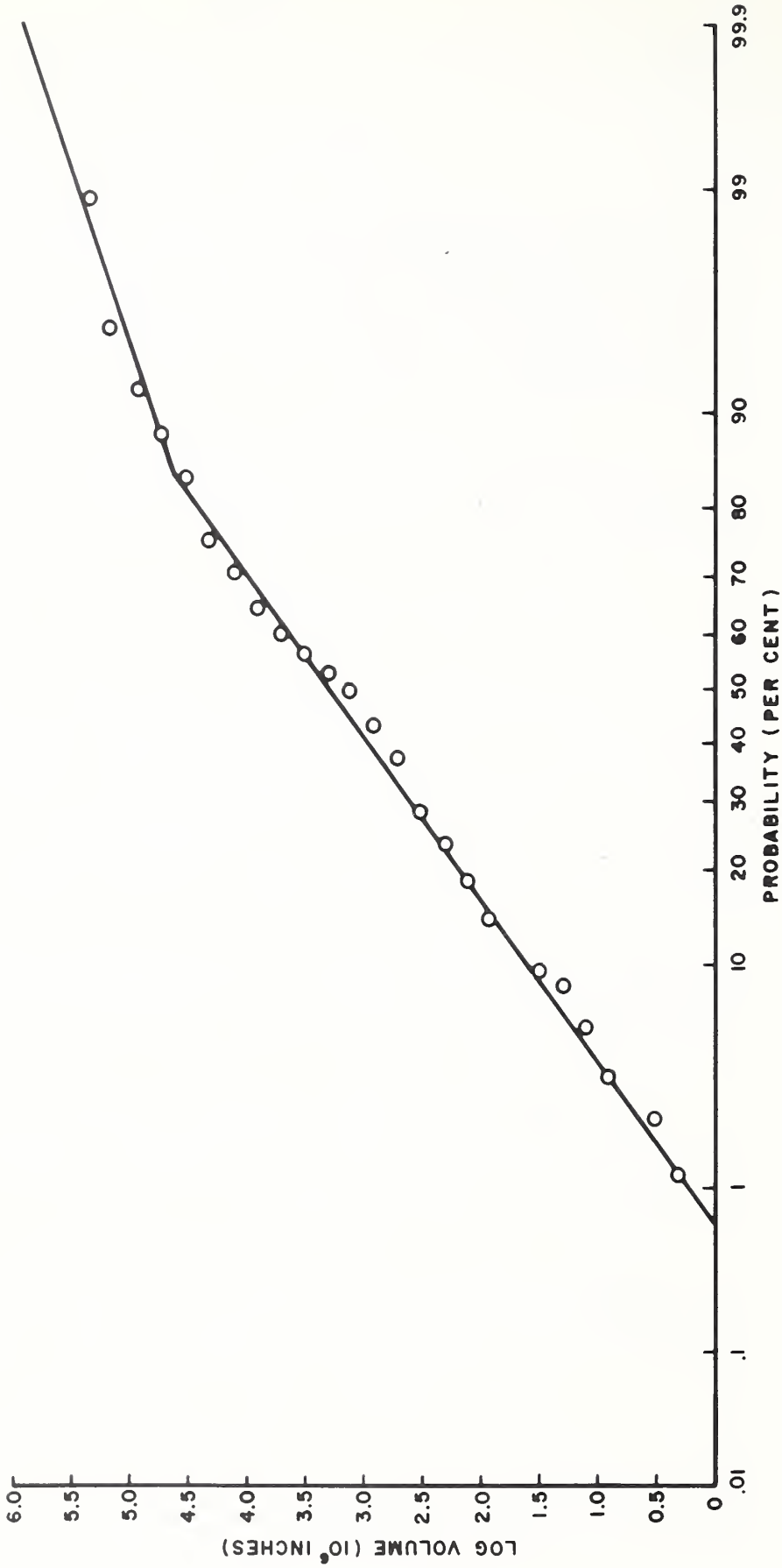

FIGURE 8. WATERSHED 6 DISTRIBUTION OF LOG (10^6 X VOLUME OF RUNOFF).

TABLE 1.--Mean and standard deviations for variables used in model

Variable	Property	Mean value	Standard deviation
S	Day of year of first runoff event (date)	196.0	8.70
N	Number of runoff events per season	12.0	3.06
T	Time of start of runoff event (hour)	18.0	3.53
V	Volume of runoff in acre-feet	49.0	98.4
L	Log_{10} of volume of runoff in 10^{-6} inches	3.30	1.27
P	Peak discharge in runoff event (cfs)	562	1165
D	Number of days between runoff events	5.38	6.10

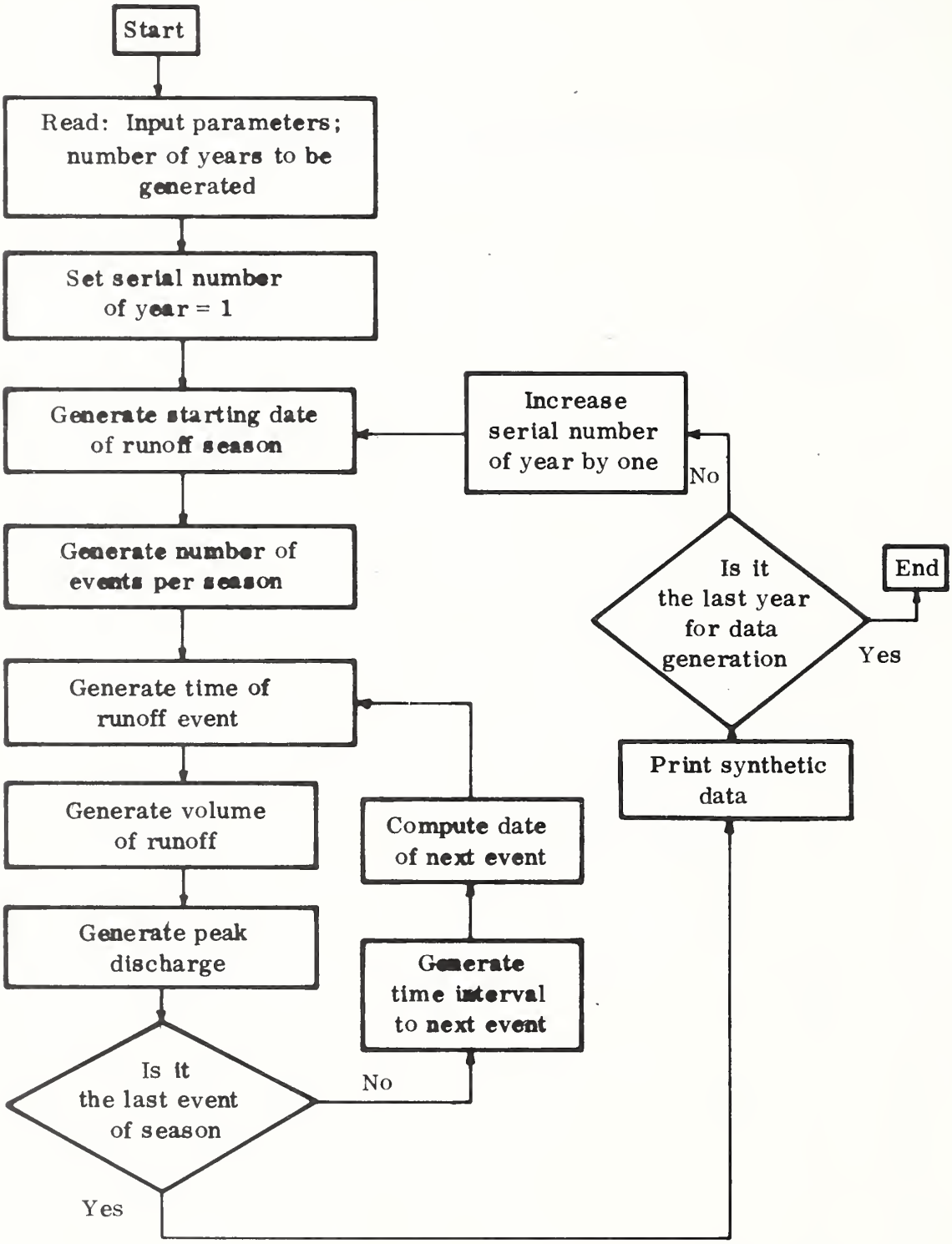

Fig. 9.--Flowchart of stochastic model for runoff events.

where $\overline{S}$ and σ_S are the mean and standard deviation of the starting date being generated, as given in Table 1.

The number of events N is generated with the aid of the correlation found between the number of events and the starting date S. A random deviation, normally distributed with mean zero, was added to values computed by the regression line. The generating equation used was

$$N = 59.0 - 0.24\,S + \varepsilon_n \qquad (2)$$

where ε_n is the deviation computed from a value of the reduced normal variate Z by

$$\varepsilon_n = 2.46\,Z \qquad (3)$$

2.46 being the root mean square deviation from the regression line.

With the number of events N generated, the program now generates for each event the time of day of the event. The values are generated with the aid of the reduced normal variate subroutine

$$T = Z \cdot \sigma_t + \overline{T} \qquad (4)$$

where $\overline{T}$ and σ_t are the mean and standard deviation given in Table 1. The starting date and the number of events per season are rounded to the nearest integer, and a check is made to ensure that the number of events is at least one. The time of start of the runoff event is checked and if it happens to be larger than 24.0 hours, a value of 24 is subtracted from the computed time, and the date of the event is advanced by one. The time is then converted from a decimal value to a value expressed in hours and minutes.

The next item to be generated is the volume of runoff of each event. As mentioned above the distribution of the logarithms of volumes of runoff appears to be double-peaked, and the cumulative curve is therefore not a straight line on normal probability paper (Fig. 8). The method adopted for generation of this distribution was by approximating the curved cumulative distribution by two straight lines as shown in Figure 8. Each of these two lines is specified in terms of two parameters corresponding to a mean and a standard

deviation. A reduced normal variate Z was generated by the subroutine mentioned above and was converted to a value of the logarithm of the volume (expressed in 10^{-6}-inch units) by one of the following two equations:

$$L = 1.27Z + 3.30 \quad (5)$$

or

$$L = 0.60Z + 4.00 \quad (6)$$

depending on whether the probability of the reduced variate Z was less than or greater than 0.84.

Values of peak discharge for each runoff event were computed from the value of logarithm of volume of runoff generated in the previous step and the regression equation developed for the relationship between this variable and the peak discharge P,

$$P = 17000\ V^{0.90} \quad (7)$$

where P is in cfs and V is in inches. A random deviation between observed and computed data was also included so that the equation used in the program was

$$\log P = 4.23 + 0.90 \log V + \varepsilon_p \quad (8)$$

where ε_p is the random deviation term generated from the reduced normal variate Z by

$$\varepsilon_p = 0.21Z \quad (9)$$

The constant 0.21 used is the standard deviation of the logarithms of the peak about the regression line.

The final step in the computations for each year is to generate for each event, except the last of the season, the interval in days until the next runoff event. The interval is generated from the negative exponential distribution, using, for the parameter of the

distribution, the value of

$$\lambda = 1/5.38 \qquad (10)$$

which is the reciprocal of the mean interval between events. The values obtained are rounded to the nearest integer. This rounding includes assigning a value of zero if the value generated was less than 0.5. If the interval between events is zero, there is a provision in the model to make sure that the time of start of the two runoff events falling on the same day are separated by at least 3.0 hours.

After completion of a series of computations for one year, the program prints the synthetic data for the current year, checks if it is the last year for which synthetic data are required, and if it is not, starts a new cycle of computations by computing the starting date of the new season of runoff.

RESULTS

A typical example of the data generated by the model is shown in Figure 10. The data presented are for a seven-year period which is the same number of years shown in Figure 2. It is, of course, not expected that a one-to-one correspondence exists between the data in the two figures, but the general appearance of the data is similar.

As a test of the adequacy of the model, it was used to generate a number of sets of data for 7-year periods, comparable to the original seven years of data available. The parameters of the synthetic data thus generated were computed and compared to the corresponding parameters of the original data. The results are shown in Table 2. As expected, the values obtained from any one such set of synthetic data are not exactly equal to the original values of the parameters, but the range of values obtained is in good agreement with the original data.

Included in the table are also two parameters that were not used in the generation of synthetic data. These are the mean length of the runoff season and the mean yearly volume of runoff. Values given are the means for the seven years of record, as well as the means for each of the seven years of synthetic data generated by the model.

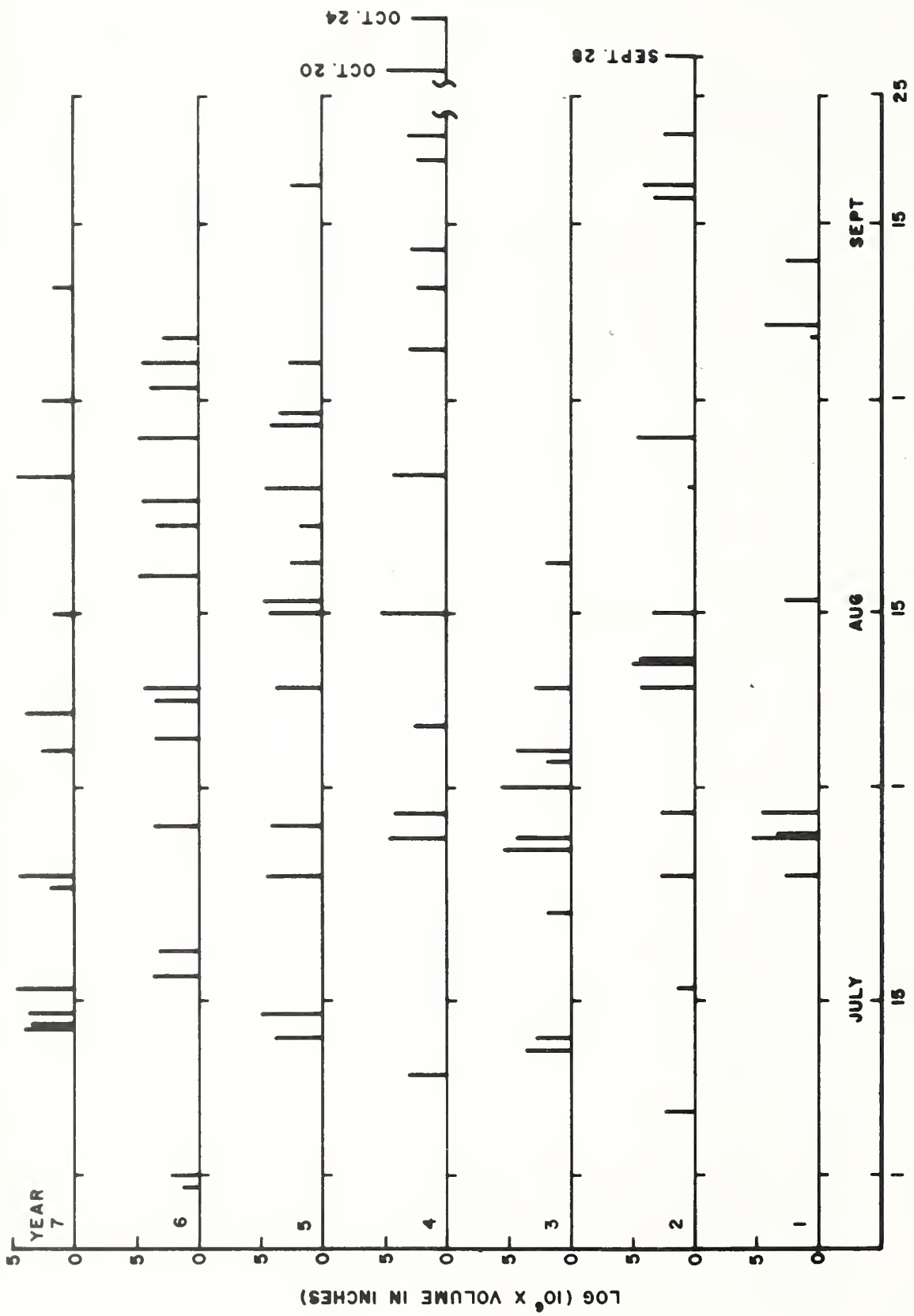

FIGURE 10. TIME DISTRIBUTION OF RUNOFF VOLUMES, SYNTHETIC DATA FOR WATERSHED 6.

TABLE 2.--Comparison of parameters for 7 years of actual data and five 7-year periods of synthetic data

Variable	Parameters	Data set					
		Observed	F-1	F-2	F-3	F-4	F-5
S [1/]	mean	196.0	201.3	200.7	195.7	191.9	194.9
	s.d. [2/]	8.70	7.57	6.18	7.45	7.65	8.80
N	mean	12.0	12.6	11.1	13.7	12.3	10.4
	s.d.	3.06	3.46	1.57	3.77	2.50	2.07
T (hours)	mean	18.0	18.0	18.5	17.7	17.4	18.0
	s.d.	3.53	3.92	3.66	3.43	3.57	3.78
V (inches)	mean	0.025	0.029	0.034	0.015	0.024	0.016
	s.d.	0.050	0.099	0.090	0.035	0.062	0.031
L(10^{-6}inches)	mean	3.30	3.39	3.17	3.25	3.37	3.23
	s.d.	1.27	1.11	1.34	1.09	1.17	1.30
P (cfs)	mean	562.	668.	803.	518.	705.	514.
	s.d.	1165.	1655.	1999.	1107.	1776.	991.
D (days)	mean	5.38	5.20	5.42	5.84	6.00	5.29
	s.d.	6.10	4.76	5.33	5.11	5.39	5.23
Mean annual volume (inches)		0.300	0.367	0.380	0.209	0.298	0.168
Mean length of season (days)		59.1	60.1	55.0	74.3	67.7	49.9

[1/] Variables defined in Table 1.

[2/] s.d. = standard deviation.

Two other comparisons between synthetic data and the original data are given in Figures 11 and 12. Figure 11 shows the cumulative yearly volume of runoff for the seven years of record compared to corresponding cumulative curves for the 5 sets of 7-year periods of synthetic data. Figure 12 gives plots of values of maximum yearly peak discharge on Gumbel's extreme value probability paper. The lines shown are for the seven years of record and the enveloping lines for the annual peak distributions for 5 sets of 7 years of synthetic data.

CONCLUSIONS

Runoff data in southeastern Arizona and in other semiarid regions where runoff events are intermittent and independent of each other may be generated with the aid of a stochastic model described herein. The model starts by generating the starting date of the season. Using this value, the number of events per season is generated using a correlation between the two variables. For each event, the model generates independently the time of occurrence of the event, the time interval to the next event, and the volume of runoff. The peak discharge of the event generated is based on the correlation between the peak and volume of runoff.

The time distribution of runoff or the shape of the hydrograph was not included in the present model. The main reason for this omission is the short duration of the runoff events in the watershed concerned. Runoff events in the watershed last usually less than 6.0 hours and, in many cases, less than 4.0 hours with the discharge reaching a peak value some 0.3 to 0.6 hours after the start of flow in the previously dry channel.

Future improvements of the model will include some considerations of the time element of the hydrograph. Another development considered is to apply models of a similar structure to other watersheds in southeastern Arizona so as to obtain the changes in the parameters with the size of the watersheds and other characteristics which may be significant. This type of investigation can lead to a regional stochastic model of runoff in semiarid areas which may be used for generation of synthetic data in ungaged watersheds.

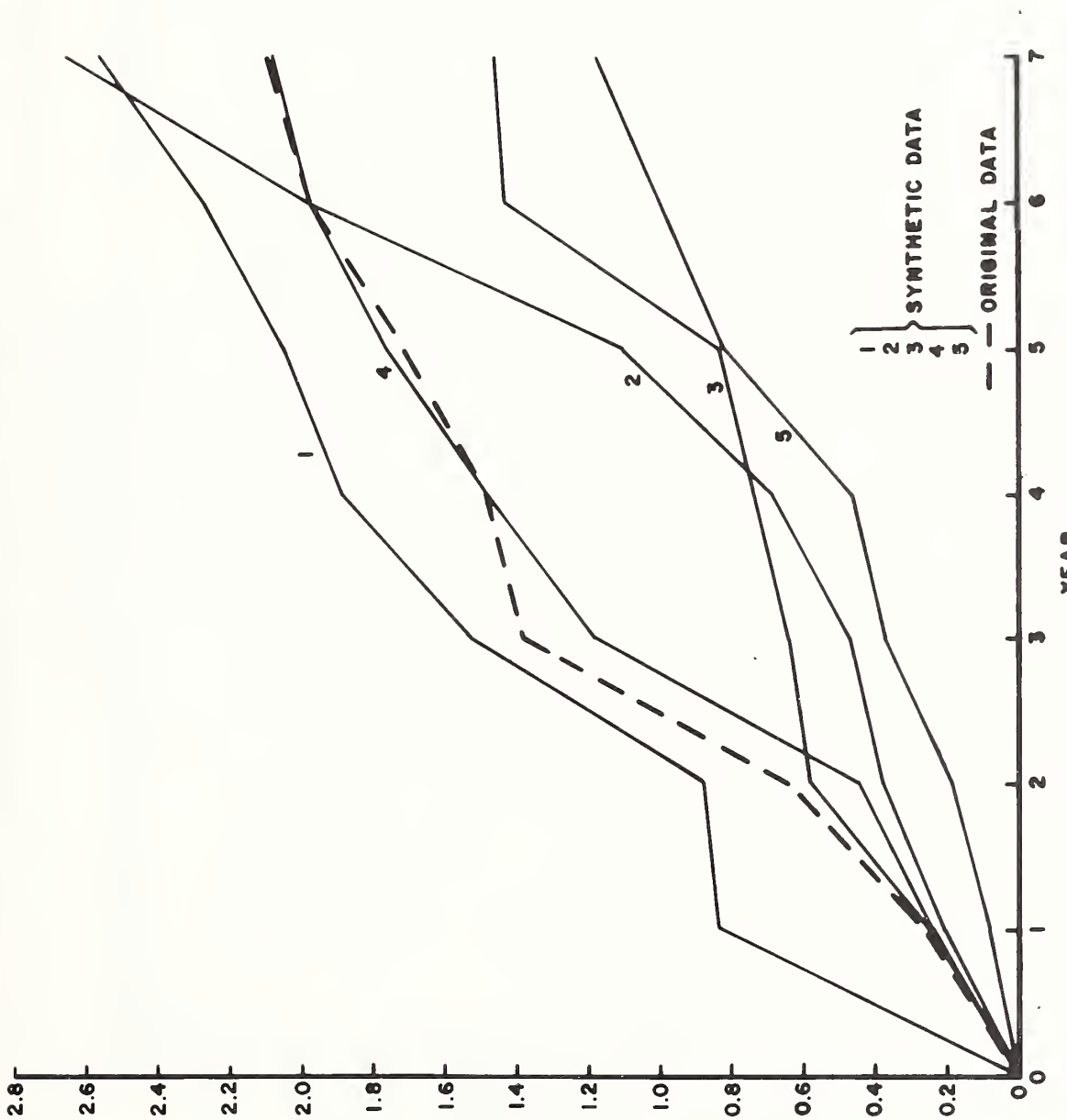

FIGURE 11. ACCUMULATIVE VOLUME OF RUNOFF FOR HISTORIC AND SYNTHETIC DATA.

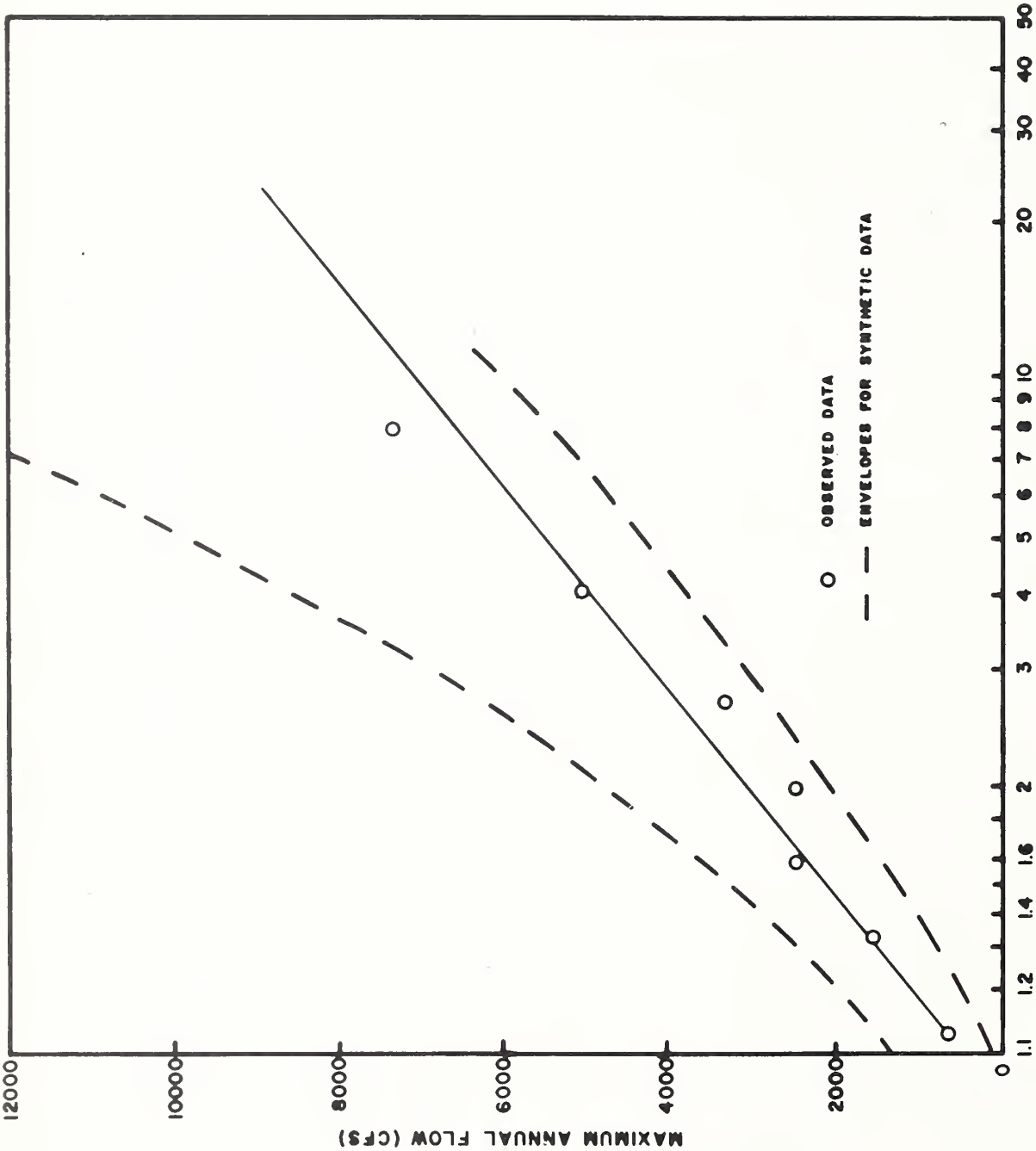

FIGURE 12. DISTRIBUTION OF MAXIMUM ANNUAL DISCHARGE FOR HISTONIC AND SYNTHETIC DATA.

The stochastic model described herein will also be related to a stochastic model of convective precipitation now under development at the Southwest Watershed Research Center in Tucson, Arizona.

REFERENCE CITED

Gwinn, W. R. Walnut Gulch supercritical measuring flume. Trans. ASAE 7(8):197-199, 1964.

RAINFALL-RUNOFF RELATIONSHIPS FOR NATURAL AND LINED-CHANNEL WATERSHEDS[1/]

by

Keith R. Cooley[2/]

INTRODUCTION:

Several methods have been proposed in recent years to supply the additional water required because of increased population. One method on which research has been in progress for several years at the U. S. Water Conservation Laboratory in Phoenix, Arizona, is water harvesting. Water harvesting is defined as the process of collecting and storing precipitation from land that has been treated to increase runoff of rainfall or snowmelt (Myers, 1964). Water harvesting is not a new idea, but was used by farmers in the Negev Desert (Evenari, 1961) and Indians in New Mexico (Haury, 1969) many hundreds of years ago. The reasons for our investigation of water harvesting is its tremendous potential for increasing water supplies at or near a given location. For example, every square yard of land in a 10-inch rainfall zone receives 56 gallons of water per year.

The bulk of research on water harvesting to date has been aimed at developing methods and materials to treat the soil surface to obtain the maximum runoff at an economical cost. This has consisted mainly of laboratory studies on the types of materials to use, and evaluation of small field test plots. Based on this research, several field installations have been constructed to collect water for livestock or wildlife. However, most of these installations have been less than one-half acre in size and runoff data have not been collected. To evaluate a large field installation, a site was selected where several small watersheds could be studied before and after treatment, thereby providing a basis for comparison of the runoff characteristics

---

1/ Contribution from the Soil and Water Conservation Research Division, Agricultural Research Service, U. S. Department of Agriculture, Phoenix, Arizona.

2/ Research Hydrologist, U. S. Water Conservation Laboratory, Phoenix, Arizona.

of treated and untreated watersheds. This paper is a report of initial stages of the calibration tests. It consists of an analysis of the rainfall-runoff relationships observed for the study area before treatment of the watershed areas themselves, but after part of the watershed channels had been lined with asphalt.

The results reported here are the relationships between rainfall and subsequent runoff for three selected storms. The storms selected for investigation were those occurring as isolated events between monthly recording periods, since only total volume of rainfall is recorded in all but the recording weather station raingage.

DESCRIPTION OF SITE AND INSTRUMENTATION:

The study area is located on the San Carlos Indian Reservation approximately 40 miles east of Globe, Arizona. It consists of about 80 acres above an existing earth reservoir which has a storage capacity of 13-15 acre feet. About 20 acres of the area is fenced and encloses three separate watersheds ranging in size from 4 to 8 acres. A fourth watershed of about 15 acres extends outside the fenced area (Figure 1).

On two of the watersheds (1 and 4), the runoff water flows down the natural channel to the measuring point. Collection ditches approximately 800 feet long intercept a portion of the runoff on watershed 3 and all of the runoff from watershed 2 before it reaches the natural channels.

After construction, the ditches were sprayed with water to settle the dust and partially compact the soil. They were then sprayed with RC-70 cutback asphalt at a rate of 2.1 kg actual asphalt m^{-2}. About three weeks later MC-250 cutback asphalt was sprayed on the ditches at a rate of 1.9 kg asphalt m^{-2}. This asphalt remained essentially on the soil surface, not penetrating like the previous application.

Each of the four watersheds is equipped with a V-notch, critical depth flume with a capacity range of 0.1 to 80 cfs. These flumes were constructed at the Laboratory and assembled at the site. Each flume is equipped with a strip-chart waterstage recorder capable of running for 90 days unattended. Other instruments at the site are 13 storage-type raingages, one vector pluviometer and one mechanical weather station. The mechanical weather station records

wind speed, wind direction, air temperature and rainfall (as sensed by a tipping bucket raingage) on a single chart, and is able to run unattended for 30 days.

PROCEDURE:

The total volume of rainfall collected in each raingage, for each of the three isolated storms, was plotted on maps of the Monument Tank watershed area. These rainfall plots revealed considerable variation in the areal distribution of rainfall over the watershed area. This variation was taken into account when determining the average depth of rainfall over the individual watersheds by using the Thiessen Polygon method of weighted averaging.

Runoff from each watershed area was determined from the waterstage chart record, utilizing a computer program developed to convert depth of water in the critical depth flumes to volume of water flowing through the flumes. The percent of runoff from each watershed, for each storm, was determined by comparing the average rainfall over the basin to the total runoff from the basin, expressed as an equivalent depth. In the case of watersheds 2 and 3, the amount of runoff from the lined ditches was assumed to be 80 and 85 percent, respectively, of the rain falling on the lined portion. These values of percent runoff were based on observation and past experience with asphalt catchments. The volume of runoff attributed to the lined ditches was computed, and subtracted from the total runoff. The remainder was then divided by the natural watershed area and the percent of runoff for the natural surface determined by comparing this value to the average rainfall.

RESULTS:

Total rainfall recorded for the year was 274 mm, which is slightly less than the three year average of 360 mm per year.

The rainfall directional pattern for the year was determined from vector pluviometer readings. The percent of the total collected by the four pluviometer openings, for the past year, are: North - 26, East - 22, South - 15, West - 37.

Estimates of the watershed characteristics of area, channel length and difference between maximum and minimum elevation are presented in Table 1. These values were

obtained from maps based on aerial photography and may require slight revision after a field survey is conducted.

The average rainfall for each storm investigated and for each watershed, along with runoff data for each event, are presented in Table 2. Results for watershed 4 are not included since runoff did not occur from this watershed during the three storms under consideration, and raingages were not in continual operation.

The results presented in Table 2 are interesting from three standpoints: (1) response of the different watersheds to storms of different types and intensities, (2) comparison of volume and percent of runoff from natural and lined-channel watersheds, and (3) comparison of runoff from the natural portion of the three watersheds.

The three storms varied from a general and rather uniform storm of two days duration (13-15 November) to a high intensity thunderstorm of only a few minutes duration (31 October). All three watersheds experienced the greatest percentage of runoff from the storm of 31 October, even though total rainfall was only one-tenth that of the large 13-15 November storm. The high intensity storm of 31 October deposited approximately 3 mm of rain in a 6 to 8 minute period.

Percent of runoff varied among watersheds even more than among storms. The range for the different storms being: from 2 to 19 percent for the natural watershed (1), from 60 to 68 percent for the partially lined-channel watershed (3), and from 44 to 72 percent for the completely lined-channel watershed (2). The increase in average runoff produced by lining a portion, or all, of the watershed channel varied from 3.5 to 30 times, depending on the type and intensity of storm. The greatest increase occurred in the case of the longer duration, higher rainfall storms.

The runoff hydrograph for each of the watersheds for the storm of 2-3 October is presented in Figure 2. The hydrographs for watersheds 2 and 3 are seen to be very similar, but watershed 3 is more sensitive to the variation in rainfall. In this case, seven distinct showers are noted for watershed 3, while only six are indicated for watershed 2. Watershed 1 is seen to be much less sensitive in that less water runs off of the natural watershed, and the hydrograph peaks, when runoff does occur, are considerably dampened. Only three showers were recorded for watershed 1, the first

four showers being used to wet the soil and fill the watershed channel and stilling basin. For this particular storm, almost all of the runoff occurring from watershed 2 was derived from the lined channel itself. Therefore, it seems that watershed 2 would be more sensitive than watershed 3, since half of the channel on watershed 3 is unlined. Watershed 3 is steeper than watershed 2, and has a sandier soil, although the soil on both is quite shallow. The fact that the lined channel on watershed 3 is in better condition and slightly steeper may also account for the difference.

The direction of storms, as determined from the vector pluviometer, did not appear to have any effect on runoff. The distribution and intensity of rainfall were much more important.

Runoff from the natural or unlined portions of watersheds 2 and 3 was compared to runoff from watershed 1. As shown in Table 2, runoff from watershed 1 varied from 2 to 19 percent, runoff from the natural area of watershed 2 varied from 1 to 30 percent, and that from the natural area of watershed 3 varied from 34 to 42 percent. The difference in slope and soil type could account for these variations. The response of watersheds 1 and 2 was very similar for the three different storm situations; the percent runoff being greater for the 31 October thunderstorm, and much smaller for the two more general storms. Watershed 3, on the other hand, produced essentially the same percent of runoff (34 to 42 percent) for all three storms.

SUMMARY:

Data collected during the past three years indicate an average annual rainfall of 360 mm for the Monument Tank watershed area.

An analysis of the rainfall-runoff relationships for the various watersheds during three isolated rainstorms was performed. This preliminary analysis indicated considerable increase in runoff from the lined-channel watersheds. The average runoff from the watershed areas during the three storms varied from: 2 to 19 percent for the smaller natural watershed (1), 60 to 68 percent for the partially lined-channel watershed (3), and 44 to 72 percent for the completely lined-channel watershed (2). There was no runoff recorded from the large natural watershed (4) during these particular storms.

The runoff from only the untreated watershed portions of watersheds 2 and 3 can be estimated by assuming a certain percentage of the rain falling on the lined channels runs off, and then subtracting this portion from the total runoff observed. Using values of runoff from the lined channels of 80 or 85 percent, the runoff from the natural area of watersheds 2 and 3 was calculated to be 1 to 30 percent and 34 to 42 percent, respectively. These calculations indicate that watersheds 1 and 2 respond similarly and suggest that channel losses are not significantly large on watershed 1. Watershed 3 also has little channel loss. The type and intensity of the storm had little effect on the percent runoff from watershed 3. The steep slope and the soil type on watershed 3 could be the reason for the same runoff during three different storms. Watershed 3 was also found to respond rapidly to rainfall events and thus produce the most sensitive water stage trace.

REFERENCES

Evenari, M., L. Shanan, N. Tadmore, and Y. Aharoni. (1961) "Ancient Agriculture in the Negev," Science, 133, 3457.

Haury, Emil W. (1969) Personal Communication.

Myers, Lloyd E. (1964) "Harvesting Precipitation," Land Erosion, Precipitation, Hydrometry, Soil Moisture. Publication No. 65, IASH, pp. 343-351, Berkeley, Calif.

Table 1. Watershed characteristics.

WATERSHED	AREA			CHANNEL			Max. Difference in Elevation
	Treated[1/]	Natural	Total	Main	Lined	Total	
#1	-	7.6 acres	330,000 ft^2 7.6 acres	290 ft	-	1220 ft	80'
#2	8200 ft^2	173,800 ft^2	182,000 ft^2 4.2 acres	-	820 ft	820 ft	70'
#3	7500 ft^2	272,500 ft^2	280,000 ft^2 6.4 acres	380 ft	750 ft	1300 ft	106'
#4	-	15.1 acres	656,000 ft^2 15.1 acres	1440 ft	-	1870 ft	120'

1/ Refers to lined ditches.

Table 2. Rainfall-runoff data.

Date	Watershed	Average Rainfall (mm)	Average Runoff		Runoff (mm)		% Runoff	
			%	(mm)	Watershed	Channel	Watershed	Channel
2-3 Oct. 1968	1	5.90	2	.14	.14	-	2	-
	2	5.93	44	2.59	.04	4.74	1	80
	3	6.89	64	4.43	2.63	5.86	38	85
31 Oct. 1968	1	2.24	19	.41	.41	-	19	-
	2	1.99	72	1.43	.59	1.59	30	80
	3	3.40	68	2.30	1.42	2.89	42	85
13-15 Nov. 1968	1	29.97	6	1.69	1.69	-	6	-
	2	28.72	56	16.09	3.91	22.98	14	80
	3	30.90	60	18.49	10.40	26.27	34	85

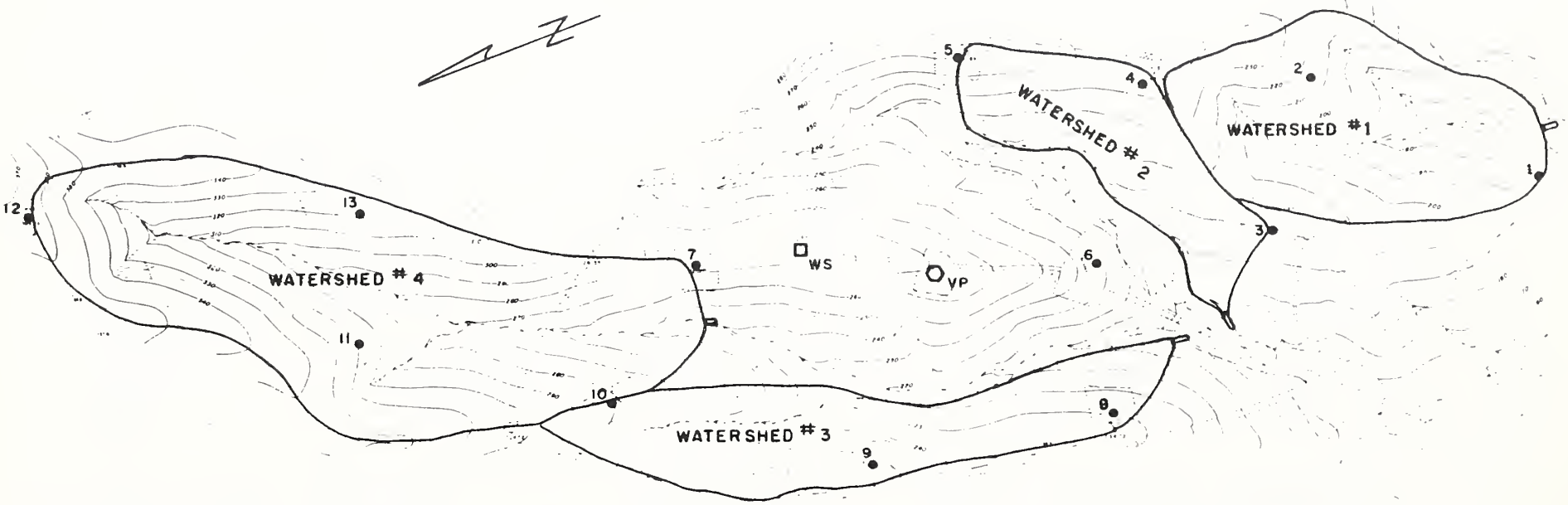

0 500' 1000 FT.

- CRITICAL DEPTH FLUME
- STORAGE RAINGAGE
- VECTOR PLUVIOMETER
- RECORDING WEATHER STATION

FIGURE I

MONUMENT TANK WATERSHED AREA
SAN CARLOS INDIAN RESERVATION
U.S. DEPARTMENT OF AGRICULTURE

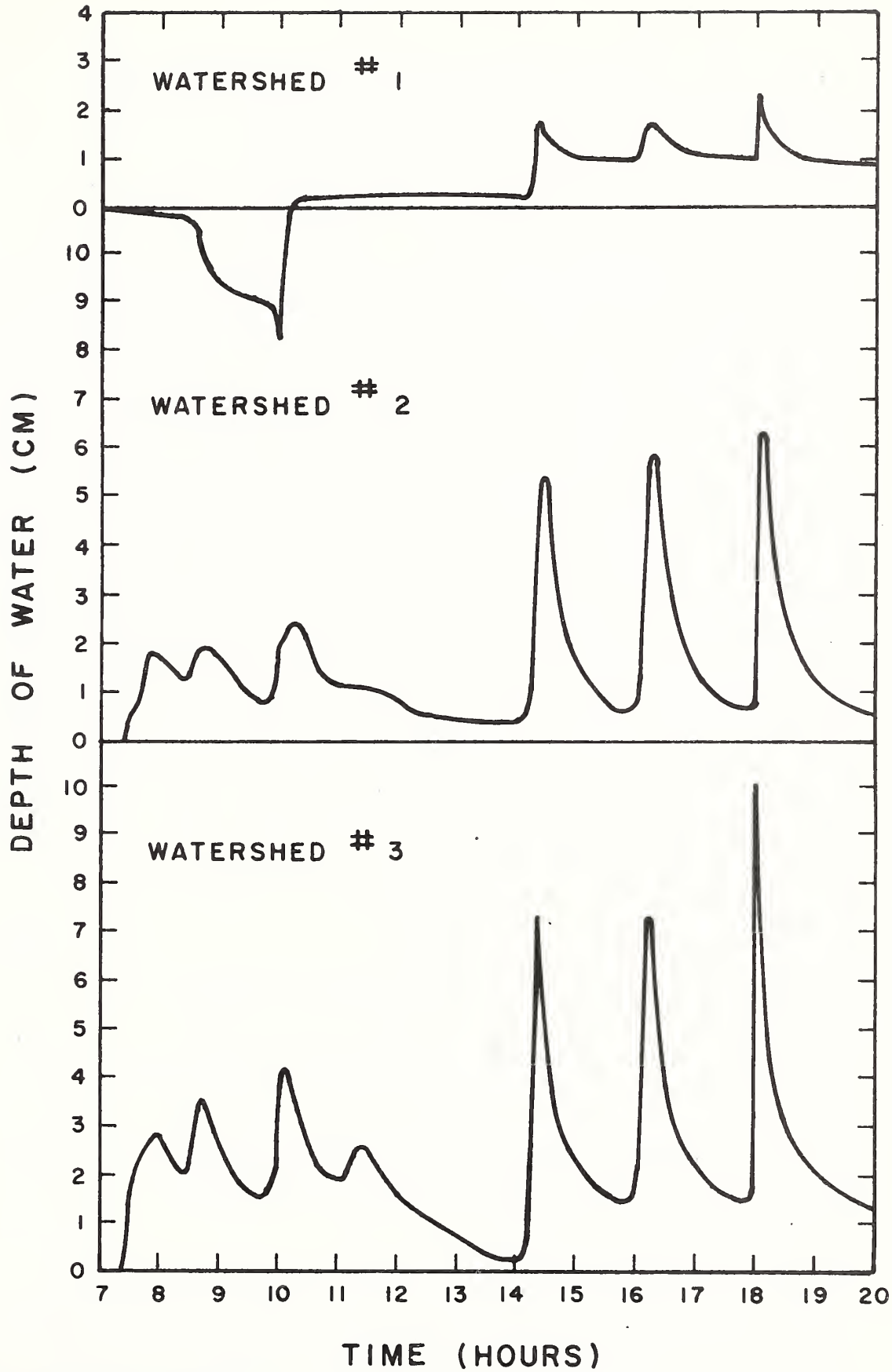

FIGURE 2. Stage vs. time for storm of Oct. 2, 1968 on three Monument Tank watersheds.

No 36

SURFACE AND SUBSURFACE ROUTING COEFFICIENTS FROM FLOW RECESSIONS[1]

By H. N. Holtan[2]

Techniques are under study in the USDA Hydrograph Laboratory for the linear segmentation of flow recessions to obtain the advantages of superposition in routing flows from dispersed hydrologic response units within the watershed. Flow from each unit is routed separately through watershed storage and summated to obtain watershed outflow. In the Hydrograph Laboratory, watersheds are subdivided into zones or hydrologic response units based upon soil depths and land capability classes. As illustrated in Figure 1, the zones give an elevation sequence of uplands, hillsides and alluviums. Rainfall in excess of infiltration is computed for these three successively, and routed into surface and subsurface flow regimes to synthesize a stream flow.

Channel flows and subsurface return flows can be routed by simultaneous solutions of the continuity equation and a storage function. Post-rainfall recession curves are plotted on semi-logarithmic paper in Figure 2 for Little Mill Creek Experimental Watershed near Coshocton, Ohio. Evapotranspiration must be eliminated if one is to obtain a true storage-flow relationship. The winter recession shows the least influence by ET and is used to derive m-values.

The equation of the recession curve is:

$$q_T = q_o e^{t/m} \qquad [1]$$

where

q_o is rate of flow at start of a period in inches per hour

q_T is rate of flow one time increment later, in inches per hour

m (computed as $t/\Delta \ln q$) is a constant for each straight-line segment of the recession curve on semi-logarithmic paper

---

[1] Contribution from the Soil and Water Conservation Research Division, Agricultural Research Service, U.S. Dept. of Agriculture, Beltsville, Maryland.

[2] Research Hydraulic Engineer and Director, USDA Hydrograph Laboratory.

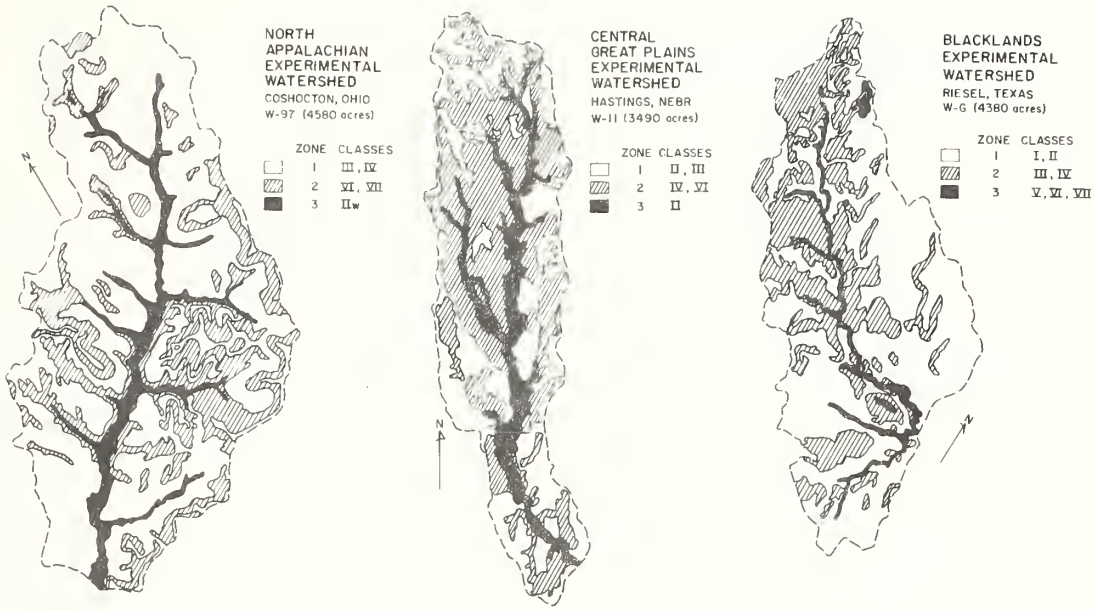

HYDROLOGIC ZONES OF LAND CAPABILITY CLASSES

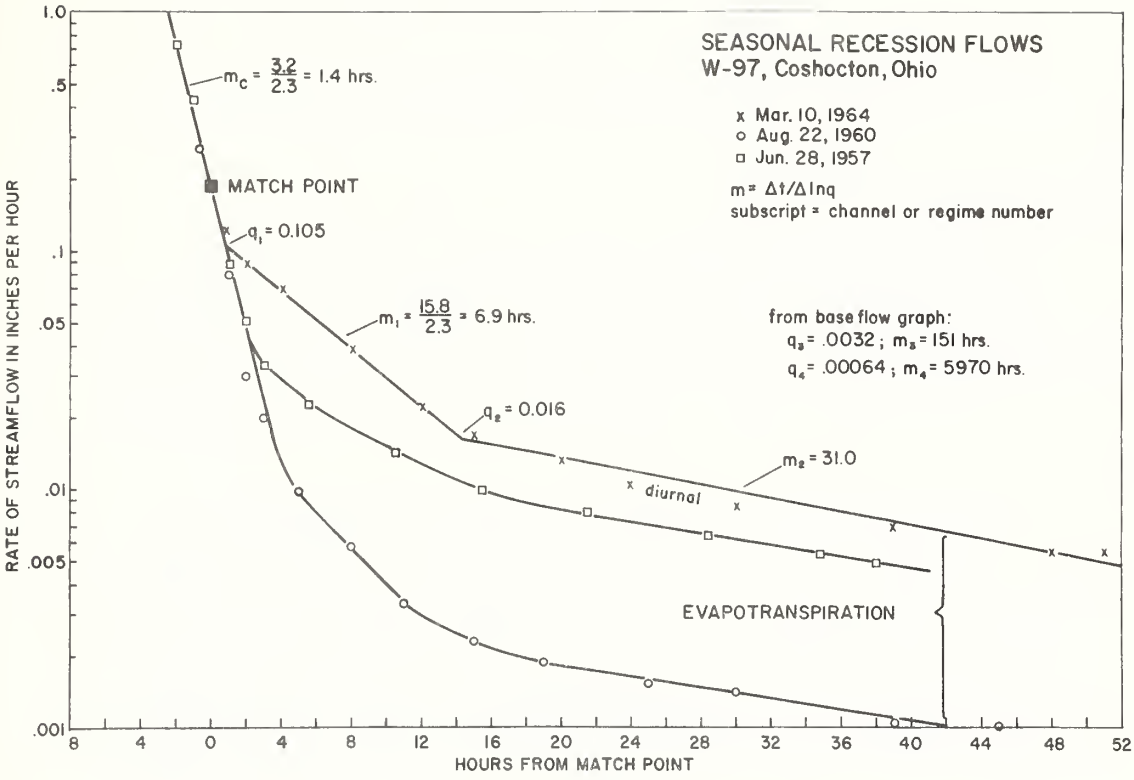
SEASONAL RECESSION FLOWS
W-97, Coshocton, Ohio
x Mar. 10, 1964
o Aug. 22, 1960
□ Jun. 28, 1957
m = Δt/Δlnq
subscript = channel or regime number
$m_c = \frac{3.2}{2.3}$ = 1.4 hrs.
MATCH POINT
q_1 = 0.105
$m_1 = \frac{15.8}{2.3}$ = 6.9 hrs.
q_2 = 0.016
m_2 = 31.0
diurnal
from base flow graph:
q_3 = .0032 ; m_3 = 151 hrs.
q_4 = .00064 ; m_4 = 5970 hrs.
EVAPOTRANSPIRATION
RATE OF STREAMFLOW IN INCHES PER HOUR
1.0
.5
.1
.05
.01
.005
.001
8 4 0 4 8 12 16 20 24 28 32 36 40 44 48 52
HOURS FROM MATCH POINT

e is logarithmic base

t is the time-increment in hours

By integration of equation [1], the storage increment, delta S, within a linear segment of the recession curve is:

$$\Delta S = m\Delta q \qquad [2]$$

Values of m and delta q are derived for each linear segment of the semi-logarithmic plotting assumed to represent successive flow regimes,[3] starting with m_c for channel flow and proceeding through a series m_1, m_2, m_3, and m_4 for successively deeper or more devious regimes of subsurface flow. Some watersheds have no return flow; hence, only m_c is defined.

At Coshocton it becomes necessary to separate flow regimes. The usual procedure has been to extend segments backward in time for subtraction from earlier regimes.[4] In our experience, and that of Kulandaiswamy and Seethorman,[5] the adjusted points never plotted as a straight line, and the resulting recession was too rapid. The author prefers to use the same procedure as is generally used for separating overlapping hydrographs of surface flows, i.e., extending the recession of the first storm forward in time for subtraction from subsequent flows.

Figure 3 is a graphical illustration of techniques suggested for separating flow regimes for input to this model. Each linear segment is extended downward to zero and subtracted from subsequent flows to get the rising hydrograph of the succeeding regime. Now, there is no question about maintaining logarithmic linearity within flow regimes. Also, the rising hydrograph fits better with the concept that return flows are less when flows in stream channels are at higher stages. The flow rates of the separated hydrograph can be

---

[3]Onstad, C. A. and Jamieson, D. G. Subsurface flow regimes of a hydrologic model. In Proc. Second Seepage Symposium, Phoenix, Arizona, U.S. Dept. Agr. ARS 41-147, pp. 46-55, 1968.

[4]Barnes, B. S. The structure of discharge-recession curves, Amer. Geophys. Union Trans. Part IV: 721-725.

[5]Kulandaiswamy, V. C. and Seethorman, S. A note on Barnes' method of hydrograph separation. Jour. Hydrol. 9(2): 222-229.

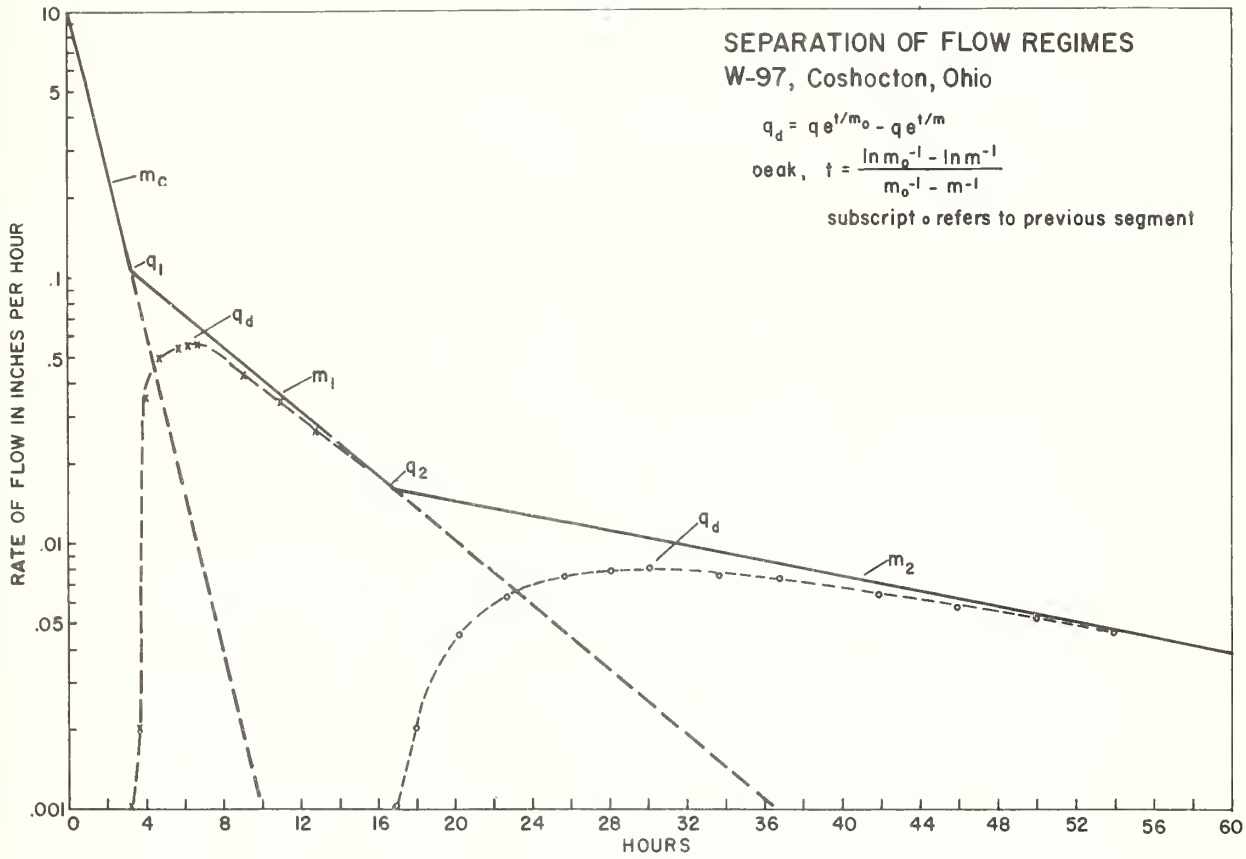
SEPARATION OF FLOW REGIMES
W-97, Coshocton, Ohio
$q_d = q e^{t/m_o} - q e^{t/m}$
peak, $t = \frac{\ln m_o^{-1} - \ln m^{-1}}{m_o^{-1} - m^{-1}}$
subscript o refers to previous segment
RATE OF FLOW IN INCHES PER HOUR
HOURS
10
5
.1
.5
.01
.05
.001
0
4
8
12
16
20
24
28
32
36
40
44
48
52
56
60
m_c
q_1
q_d
m_1
q_2
q_d
m_2

computed for successive subsurface regimes by the equation:

$$q_d = qe^{t/mo} - qe^{t/m} \quad [3]$$

wherein

q_d is the difference hydrograph in inches per hour

q is rate at intersect with previous segment of recession

m is computed as $\Delta t/\ln(q_o/q_T)$

e is base of natural logarithm

t is time from intersect in hours

and subscript $_o$ indicates m of the previous segment.

It is doubtful if equilibrium between inflow and outflow was achieved in any regime. Pending further research, the values of q at intersects are suggested in place of the peak, q_d, of the difference hydrograph. Input to the model would then be m_c, q_1, m_1, q_2, m_2, q_3, m_3, q_4 and m_4 for those watersheds having four discernable regimes of subsurface flow. The absolute value of m is readily determined as the number of hours required for the recession segment to cross one log cycle divided by 2.3, the natural logarithm of 10.0. If evapotranspiration was significant during the recession used for analyses, the values of S must be increased to include ET:

$$S = m(q + et) \quad [4]$$

and

$$m(\text{corrected}) = m(q + et)/q \quad [5]$$

wherein q and et are in inches per hour.

Maximum free-water storage is the product of m_n and q_n (in inches per hour) for each flow regime in Figure 4. The validity of the correction of m for ET during the recession can be demonstrated for Taylor Creek in Florida where records indicated that average ET in the fall of the year was essentially 0.12 inches per day, i.e. 0.005 inches per hour.

The drained soil profile in Taylor Creek is about 60 inches with about 27 per cent rapidly drained porosity, i.e., 16.20 inches of water equivalent. The summation of storage from Figure 4 is only 3.18 inches but if each m-value is corrected by adding $m_n * et/q_n$, the sum of products is 17.86 inches - more nearly equal to the porosity indicated by soils data. The new m-values, replacing those of Figure 4 for Taylor Creek are:

m_1 = 122 hours

m_2 = 575 hours

m_3 = 4,735 hours

m_4 = 171,511 hours

Equation [2], being linear, forces the routed hydrograph to peak at its crossing with the inflow hydrograph. Nonlinearity was induced on the rising side by the techniques of Holtan and Overton[6] for successive routings through one-half of indicated storage. Equations [6] and [7] are combinations of the continuity equation [2] to be solved successively for each delta t:

$$q_2' = \frac{2\Delta I}{m+\Delta t} + q_1' \frac{m-\Delta t}{m+\Delta t} \qquad [6]$$

and

$$q_2 = \frac{2\Delta Q'}{m+\Delta t} + q_1 \frac{m-\Delta t}{m+\Delta t} \qquad [7]$$

wherein

q' is theoretical rate of outflow from first half of storage in inches per hour

ΔI is increment of inflow volume in inches

m is routing coefficient in hours

Δt is increment of time in hours

$\Delta Q'$ is increment of theoretical outflow from first half reservoir in inches per hour

and subscripts $_1$ and $_2$ indicate beginning and end of delta t.

---

[6] Holtan, H. N. and Overton, D. E. Storage-flow hysteresis in hydrograph synthesis. Jour. Hydrol. 2(4): 309-323, 1965.

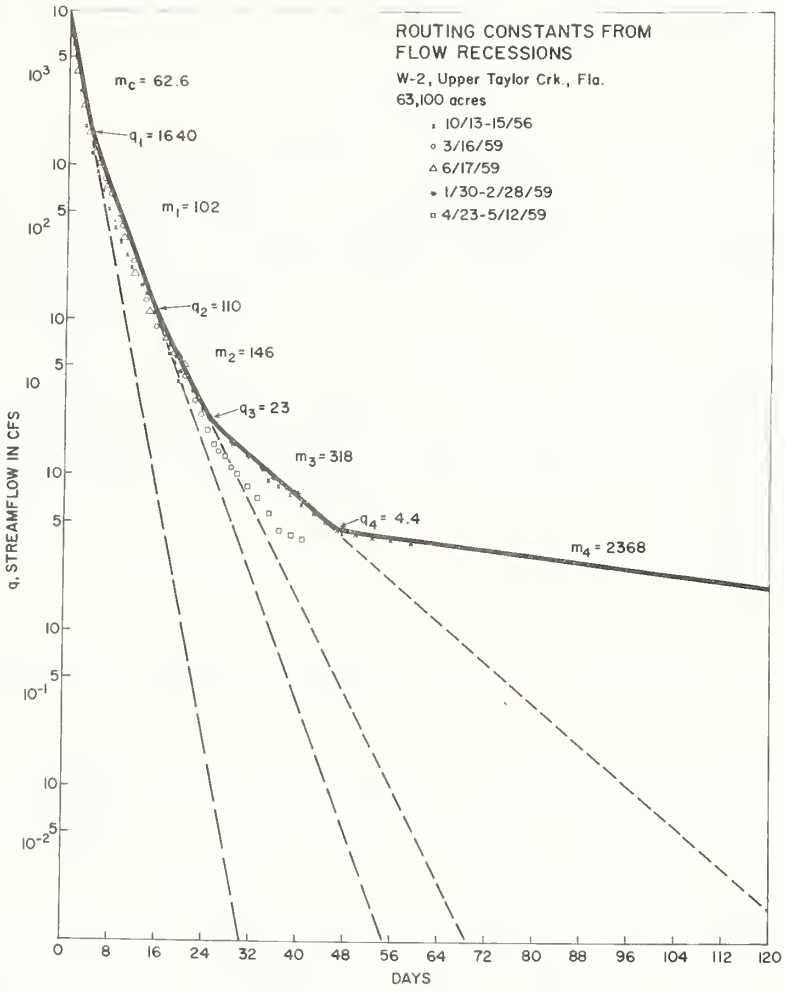
ROUTING CONSTANTS FROM
FLOW RECESSIONS
W-2, Upper Taylor Crk., Fla.
63,100 acres
x 10/13-15/56
o 3/16/59
△ 6/17/59
* 1/30-2/28/59
□ 4/23-5/12/59
m_c = 62.6
q_1 = 1640
m_1 = 102
q_2 = 110
m_2 = 146
q_3 = 23
m_3 = 318
q_4 = 4.4
m_4 = 2368
q, STREAMFLOW IN CFS
DAYS

Rainfall in excess of infiltration, summations from all zones or cascaded through overland flow, is routed through streamflow by equations [6] and [7] using m_c as the routing coefficient.

HYDROGEOLOGY

In the USDA Hydrograph Laboratory's model, infiltrated water is proportioned to downward seepage, ET, or to lateral return flow in each flow regime. Downward seepage and lateral flow are supplied by free water; hence, estimates of the seepage rate, C, and the storage coefficient, m, are needed in each flow regime.

Since subsurface flow regimes are considered sequential, seepage from the first regime is inflow to the second regime; hence maximum C_1 must be adequate to support the maximum flow, q_2, experienced in the next regime:

$$C_n = q_{n+1} + GR \qquad [8]$$

wherein n is the regime number and GR is seepage to groundwater recharge from the last regime.

Groundwater recharge from the ultimate return flow regime is estimated on a regional basis. Records of average rainfall, average ET and average streamflow yields in the vicinity can be used to derive an average annual groundwater recharge. This can be converted to the unit inches per hour, as an estimate of GR. For watersheds having no return flow, GR is estimated as equal to f_c, but the estimate for the Coshocton, Ohio watershed was 2.00 inches per year, and for the Florida watershed, GR was estimated as zero.

Total outflow from each regime is computed by substituting the increment of infiltration, delta F or the increment of seepage from above for inflow, delta I, in equation [6]. The volume of seepage subput to the next regime, is computed as the fraction C_n/C_{n-1} of outflow volume, from rates of equation [7]:

$$\Delta Q_n = (q_1 + q_2)\,\frac{\Delta t}{2} \qquad [9]$$

$$\text{Subput} = \Delta Q_n \cdot C_n/C_{n-1} \qquad [10]$$

Lateral outflow is then computed as total outflow minus subput.

Equations [6] and [7] can be applied to hydrologic response zones within the watershed using routing coefficients m_1, m_2, m_3 and m_4 and summated to compute watershed return flows. Flows from all subsurface regimes are converted to watershed units and added to rainfall excess as inflow to equations [6] and [7] for computing the channel outflow hydrograph.

Results of these techniques are demonstrated in Figure 5 by application to the experimental watershed W-2 operated by the Agricultural Research Service headquartered at Fort Lauderdale, Florida. Experience thus far indicates that the accuracy of predicting low flows is very sensitive to water yield parameters such as soil depth, root depths, ET rates and soil porosity estimates, but high flows and recessions are more sensitive to routing coefficients.

Details of the computation can be obtained from the USDA Hydrograph Laboratory in the form of a computer program entitled, *USDAHL-70 Model of Watershed Hydrology*. Research is continuing on the model, but it appears that the concepts discussed herein will continue to be useful in watershed hydrology.

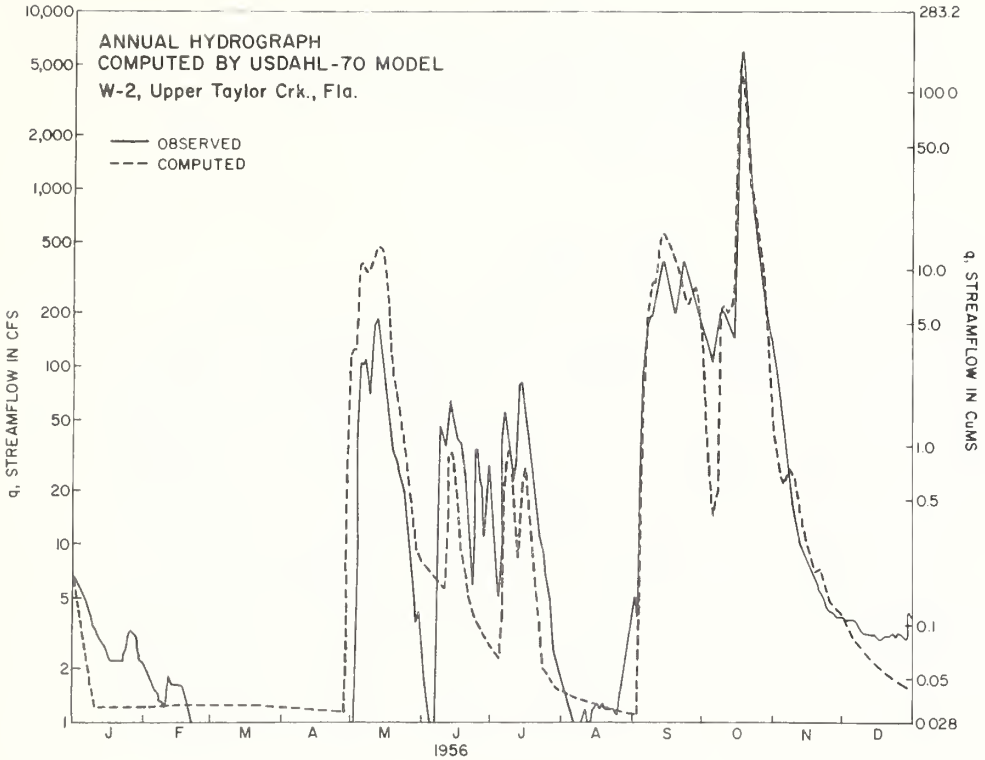
ANNUAL HYDROGRAPH
COMPUTED BY USDAHL-70 MODEL
W-2, Upper Taylor Crk., Fla.
OBSERVED
COMPUTED
q, STREAMFLOW IN CFS
q, STREAMFLOW IN CuMS
10,000
5,000
2,000
1,000
500
200
100
50
20
10
5
2
1
283.2
100.0
50.0
10.0
5.0
1.0
0.5
0.1
0.05
0.028
J
F
M
A
M
J
J
A
S
O
N
D
1956

A FRAMEWORK FOR COMPREHENSIVE MATH MODELS OF WATERSHED HYDROLOGY[1]

C. B. England[2]

INTRODUCTION

Building a truly comprehensive model of any system entails organizing knowledge from the various disciplines involved into a coherent abstraction. The degree of comprehension gained from use of the model and in its construction depends upon the fidelity with which the internal components represent their real world counterparts and on the overall structure of the model. Bouldin (2)[3] has asserted that the first and basic level of systems theory is that of the static framework, or its .....*geography and anatomy*..... He proceeds to state that .....*The accurate description of these frameworks is the beginning of organized theoretical knowledge in almost any field, for without accuracy in this description of static relationships no accurate functional or dynamic theory is possible*.....

Major emphasis in the USDA Hydrograph Laboratory has been placed on constructing a framework for a comprehensive model of watershed performance. Basic to these endeavors has been the concept that such a framework must incorporate segmentation of the system into discrete functional components to permit in-depth study of the physical processes therein. Linking of these components was to be rationally consistent with observed coupling of corresponding elements in natural watershed systems.

The lumped system approach was abandoned early in favor of the distributed system because the latter gives a truer representation of the spacial sequencing so important in regulating watershed behavior. In agriculture, we are interested in the lumped-system outflow for flood control

---

[1]Contribution from the Soil and Water Conservation Research Division, Agriculture Research Service, U.S. Department of Agriculture.

[2]Research Soil Scientist, USDA Hydrograph Laboratory, Beltsville, Maryland.

[3]Underscored numbers in parentheses refer to literature cited.

computations at some point downstream, but we are also interested in the temporal and spacial sequencing of consumptive use and water yields on each increment of land within the watershed, from the outer perimeter to concentrations of flow in streams. Watershed engineering attempts to influence these sequences for the production of food and fiber, for the reduction of flood damages and for the stabilization of water yields downstream.

WATERSHED LAND EVALUATION

Basically, any watershed consists of *land*. Regardless of how simple it sounds, land is a very specific term which refers to all the natural as well as man-made features of a portion of the earth's surface. The evaluation of land for various purposes has constituted a vital activity of man ever since he emerged from his cave. In recent years, interest in this subject has engendered an interdisciplinary scientific field called *Land Evaluation* which is concerned with the assessment of suitability of land for various uses and prediction of its response to them. Evidence of this interest was the International Symposium on Land Evalution held in 1968 (7).

The three fundamental features with which Land Evaluation is concerned are soils, vegetation and landforms. Combinations of different kinds of each of these constitute land types (1) or land units which are homogeneous with respect to the classification criteria selected. Selection of the individual units and adoption of an approach to use in their systematic classification are the two main problems in Land Evaluation. As discussed by Mabbut (5) perhaps the most widely discussed approach is called the *inductive-parametric* approach, in which individuals are identified objectively from one or more measurable parameters and these individuals are grouped into classes having narrow ranges of the parameters.

Hydrologic soil grouping is a special form of Land Evaluation in which we attempt: (a) to objectively identify individual hydrologic units which are homogeneous with respect to the soil, vegetative and landform factors which determine their role in the hydrologic cycle, and (b) to group the individual units to form a classificatory framework within which to assess the hydrologic performance of the entire watershed. Many different approaches have been suggested for selecting and

hydrologically grouping units within agricultural watersheds; many of these were included in an excellent review by A. K. Turner (8).

Soil series, soil types, soil associations, and Great Soil Groups have been used as hydrologic units. Groups of soils based on slope, surface texture, infiltration rates and other hydrologic criteria also have been used for hydrologic investigations with some success in those cases where areas were small enough for detailed consideration and where sufficiently detailed information was available. In the usual case, limitations of time, money or computer time preclude the degree of refinement required in characterizing and considering the multitude of individual soils normally occuring on agricultural watersheds. Also, rarely is there enough information on infiltration rates and moisture characteristics of the individual soils to use them as computational units, even in experimental watershed investigations.

GEOMORPHIC GROUPING OF WATERSHED SOILS

In the Hydrograph Laboratory, we have reviewed the work of many researchers who studied the interdependencies of slopes, vegetation, microclimate, landform and soil characteristics, and we drew upon these to derive a system of geomorphic grouping of soils (3). The key to this system is that soil hydrologic properties such as topsoil depth, upper-level storage capacity and drainage characteristics are related to topographic position. This results from the fact that relief and microclimate are important local soil-forming factors, and reciprocally, soil physical properties are influential in landform genesis. Thus, soils occurring on various facets of the landscape are unique with respect to many hydrologic qualities. The areal and elevational distribution of these landform units governs watershed response to storm rainfall. Maximum runoff, for example, occurs on landforms that are steep, shallow, wet or that otherwise have a low retention capacity. If a large area of such land is located near stream channels, the resultant high flows are predictable. If, on the other hand, the flows are generated from such lands occurring at higher elevations, to cascade over subjacent high capacity lands, streamflows would be minimized. Computational routing of flows cascading over or through zones of diverse capacity from ridgetop to stream channel is thus simplified. The influence of this important process on watershed runoff production cannot be predicted by considering the watershed as a lumped system.

LAND CAPABILITY GROUPS

With extensive experience in using this system of hydrologic soil grouping as a framework for the Hydrograph Laboratory model, it was noted that there was an apparent correspondence between the areal distribution of our *hydrologic response units* and that of the land capability classes mapped by the Soil Conservation Service (4). This relationship was verified by graphical comparison of the two types of mapped distributions on several ARS experimental watersheds. The watersheds selected represent almost a national sample of diverse physiography, climate, and soils in Wisconsin, Virginia, Ohio, Nebraska, Iowa, New York, and Texas.

The observed compatibility of the two grouping systems is logical, since they are based on essentially the same soil-landform qualities. The land capability classes are defined on the basis of physical features of the land which determine its suitability for sustained crop production and its response to management required to protect it from erosion and other hazards. These features include depth and texture of topsoil, land slope, drainage (a function of internal permeability and topographic position), rockiness, and other crop production factors. The classes are mapped from SCS standard soil surveys of individual farms and watersheds and are rapidly becoming available for most of the watersheds in the United States.

Three levels of classification are used in the SCS land capability system: capability units, classes and subclasses. Eight classes are defined on their general adaptability for agricultural use. These range from Class I soils suited for intensive cultivation to Class VIII lands which are suited only for recreation or wildlife. Progressive degrees of limitations due to erosion or water hazards are found in the higher classes.

A good example illustrating the use of land capability classes is presented in Figures 1 and 2, soil and capability maps, respectively, of Little Winns Creek Experimental Watershed in Halifax County, Virginia. Soils of this area, predominately the Cecil and Appling series, represent those occurring throughout the extensive Piedmont Plateau of the Southeastern states. Figure 1 shows the complexity of soil delineations in this detailed soil survey. Separations are evidently too numerous for individual consideration for hydrologic purposes.

Figure 1--Soil Map, Little Winns Creek Experimental Watershed, Halifax County, Virginia

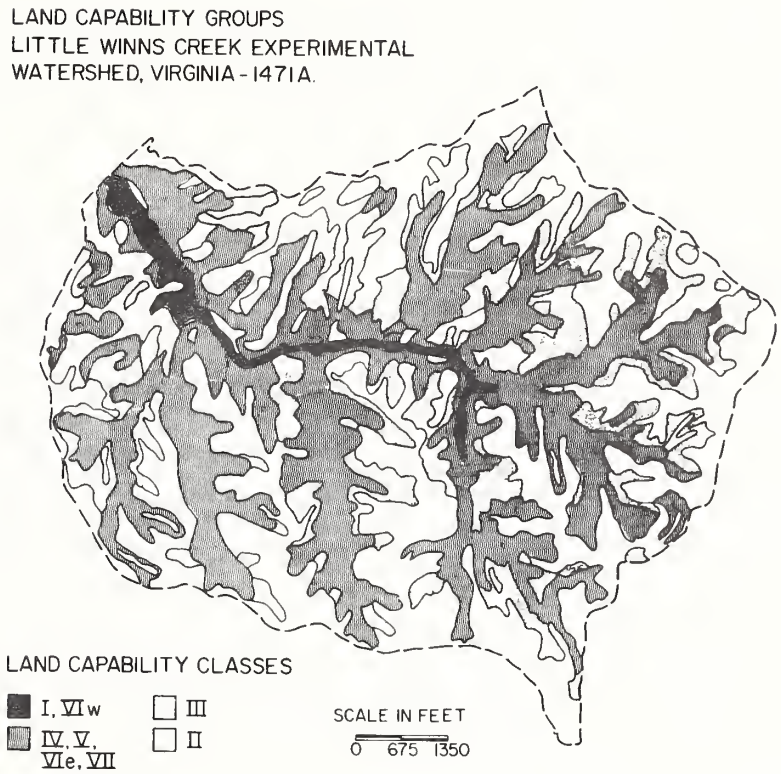

In Figure 2, the soil mapping units have been grouped into land capability classes, of which seven are represented in this watershed. A large part of the area consists of nearly level to gently sloping Class II uplands which consistently occur at the higher elevations around the perimeter. These soils are relatively uneroded and thus have deep topsoils with a high capacity for rainfall retention. These are the best lands for cultivation and land use consists of row crops, corn and tobacco.

In the next lower elevation zone are the Class III lands which occur on steeper slopes and which have lost a good portion of the topsoil reservoir. Land use is confined to close-growing crops, hays, small grains and pastures. Because they have been eroded, their infiltration and water storage capacities are much less than the Class II lands above them.

Below these two zones lie the very steep Class IV, V, VI, and VII soils on hillsides which have lost all of the topsoil, exposing clayey subsoils which have low infiltration rates. This area supports only a mixture of hardwood and conifer forests.

A small strip of level but poorly drained bottomland follows the narrow floodplain throughout its extent. Because the water retention capacity of these soils is satisfied throughout most of the year by surplus water, they can be expected to shed most of the water impinging on them either directly from rainfall or from overland and subsurface flows generated on lands above them.

This illustration provides a visual *model* of the hydrologic performance of the watershed. It is easy to visualize the distribution of zones absorbing or contributing potential runoff and the pattern of flows cascading from zone to zone enroute to the channel. Computations of infiltration, runoff and evapotranspiration by any method are facilitated by this framework consisting of a minimum number of units distributed in an elevation sequence commensurate with the hydraulics of flows.

Land capability classes are distinct hydrologically in that they are based on features significant in predicting infiltration, evapotranspiration and surface flows on agricultural watersheds. As hydrologic units they also offer a means of assessing soil and water management potentials in watershed engineering. As pressure on our lands increases, the trend toward utilizing land in accordance with its capability will intensify, so that futuristic estimates of land use as well as of the hydrology of agricultural watersheds can be facilitated by the use of land capability maps.

Figure 2--Land Capability Map, Little Winns Creek Experimental Watershed, Halifax County, Virginia

RANGE SITES

In a study of soils, geology, topography, precipitation and vegetation on Reynolds Creek Experimental Watershed, Stephenson and England (6) found that range sites offer a convenient hydrologic response unit in western watersheds. Range sites, though classified according to their estimated potential for producing climax native vegetation, are based indirectly on site characteristics which distinguish them hydrologically, namely soil physical properties and topographic features.

SUMMARY AND CONCLUSIONS

In developing a comprehensive mathematical model of agricultural watershed performance, the USDA Hydrograph Laboratory has adopted a framework of soil-landform units upon which to base computations of infiltration, surface flows and evapotranspiration. The watershed is partitioned into a minimum number of zones which are internally homogeneous with respect to soil porosity, drainage characteristics and land use. The soil-landform units also occur in an elevation sequence compatible with the hydraulics of flows.

It has been found that the factors considered in placing soils into hydrologic response units are the same as those used in mapping land capability classes in the East and Midwest United States and in mapping range sites in the West. Comparisons of mapped distributions of the three types of groupings on several ARS experimental watersheds has indicated their comparability.

Although this system of grouping soils has proven to facilitate the working of the Hydrograph Laboratory model in numerical experiments attempting to predict hydrographs and water yields, it has not yet received sufficient field testing, nor has it been tried in other models. If further experiments and field testing verify the proposed system, watershed engineers will have at hand a convenient and, fortunately, already established hydrologic soil grouping for agricultural watershed lands.

ACKNOWLEDGEMENT

Grateful appreciation is extended to James B. Burford, Manager, Hydrologic Data Center, Soil and Water Conservation Research Division, U.S.Department of Agriculture, Beltsville, Maryland for furnishing the airphoto mosaic of soils in Figure 1, and for assisting in preparation of the land capability map in Figure 2.

LITERATURE CITED

(1) Beaumont, A. B.
1941. Natural land types of Massachusetts and their use. Mass. Agr. Expt. Sta. Bull. 385.

(2) Bouldin, K. E.
1969. General Systems Theory - The Skeleton of Science. In *Quantitative Disciplines in Management*, R.I. Levin and R.P. Lamone [eds.], pp. 146-149. Dickenson Publishing Co., Inc., Belmont, Calif.

(3) England, C. B. and Holtan, H. N.
1969. Geomorphic grouping of soils in watershed engineering. J. Hydrology 7: 217-225.

(4) Klingebiel, A. A. and Montgomery, P. H.
1961. *LandCapability Classification.* U.S. Dept. Agr. Handbook 210.

(5) Mabbut, J. A.
1968. Review of concepts of land classification. In *Land Evaluation*, G.A. Stewart [ed.], 428 pp. Macmillan, Melbourne.

(6) Stephenson, G. R. and England, C. B.
1969. Digitized physical data on a rangeland watershed. J. Hydrology 8: 442-450.

(7) Stewart, G. A. [ed.]
1968. *Land Evaluation.* 428 pp., Macmillan, Melbourne.

(8) Turner, A. K.
1963. Infiltration, runoff and soil classifications. J. Hydrology 1: 129-143.

DEO-1

DEVELOPMENT OF SURFACE WATER COMPONENT MODELS[1]

D. E. Overton[2]

INTRODUCTION

The following is a report of work on mathematical models of surface runoff that has been completed in the past two years by the author. The bulk of the material is from a series of reports recently completed, (references 1, 2, 3 and 4). It is recognized that flows are not easily categorized as surface and subsurface, and that overland flow seldom, if ever, occurs as a sheet flow in rural watersheds. The models of overland flow to be presented are conceptual, and data was available to test a number of these models over a wide range of inputs on impermeable surfaces. In the past, this type of research has provided the basis for components of comprehensive mathematical models of watershed performance. Any extrapolation of these results and findings for use in comprehensive models would be related to the objective of the user. The purpose of the work not only was to determine the accuracy of surface runoff models, but was to determine the accuracy sacrificed when the computational load was lessened.

Concerning channel routing models, it has been found that the Muskingum method is really a numerical solution of the classical heat flow equation. No wave action occurs in heat flow, but a wave action is induced by the Muskingum method because of an error in the numerical solution. The method is very easy to use; the computational load is light. Nevertheless, the physical meaning of the parameters is questionable and this makes the method difficult to use consistently.

---

[1]Contribution from the Soil and Water Conservation Research Division, Agriculture Research Service, U.S. Department of Agriculture.

[2]Res. Hydraulic Engineer, USDA Hydrograph Laboratory, Beltsville, Maryland.

[3]Underscored numbers in parentheses refer to literature cited.

A model of watershed surface runoff will be reported accompanied by procedures for generalization of results in terms of the geometry, roughness and input. It will be shown how this approach can be helpful in optimization, sensitivity tests and error analysis.

OVERLAND FLOW

Hydraulic Models

The momentum equation can be written as

$$\frac{Q}{Qn} = \sqrt{1 - \frac{1}{S_o}\left(\frac{\partial y}{\partial x} + \frac{V}{g}\frac{\partial V}{\partial x} + \frac{1}{g}\frac{\partial V}{\partial t} + \frac{qV}{gy}\right)} \qquad [1]$$

where

V and y are velocity and depth of flow
Q and Qn are discharge and normal discharge
g is acceleration of gravity
S_o is slope of the plane
x and t are space and time coordinates
and q is lateral inflow (rain rate)

If the sum of the terms to the right of the minus sign in the parentheses is very small relative to the slope of the plane, then discharge is essentially normal.

$$Q \approx Qn \qquad [2]$$

The dynamic effects would be negligible, and the assumption would be that flows are essentially unsteady and non-uniform. Then the mementum equation would be represented by

$$Q = ay^m \qquad [3]$$

where the exponent m would be 3/2 if the Chezy formula is used and 5/3 if the Manning formula is used. This formulation is called the kinematic wave approximation.

The continuity equation is

$$\frac{\partial Q}{\partial x} + \frac{\partial y}{\partial t} = q \qquad [4]$$

and the complete equation of motion results upon combining Equation [3] with Equation [4].

Henderson and Wooding (5) used the method of characteristics to obtain a solution for a steady rain rate

$$Q = a(qt)^m \qquad [5]$$

However, the question remained as to the circumstances under which the approximation was valid. In 1967, Woolhiser and Liggett (6) used the method of characteristics to solve the complete equations for a wide range of lengths, slopes, roughnesses and rain rates. The results were generalized in terms of the index parameter

$$k = \frac{S_o L}{H_o F_o^2} \qquad [6]$$

where L is length of the plane

$H_o F_o$ are the depth and Froude number at equilibrium at the end of the plane

All solutions were based upon a steady-uniform rain rate, and a constant Chezy - C for all space and time. They found that for values of the index parameter k greater than 10, the kinematic wave formulation was a good approximation. This would result for low rain rates on long, rough, steep planes. Their results are generalized in Figure 1.

The results of the work of Woolhiser and Liggett (6) were tested by Overton (1) using overland flow hydrographs that were collected and reported by the Corps of Engineers (7). Overland flow hydrographs were developed from simulated rainfall over three 500 foot long concrete troughs which were sloped at 1/2, 1 and 2%. To roughen the surface, an expanded metal was placed over the concrete in an attempt to simulate the natural roughness of turf (surface called simulated turf). Hydrographs were measured at the end of the troughs for lengths in increments of 84 feet and for

steady-uniform rain rates ranging from 1/2 to 8 inches per hour.

Using the Manning's n-values calculated from accompanying normal flows by the technique developed by Overton (8), the smallest value of the index parameter k was found to be 26.3. It was concluded that the dynamic terms were negligible and the kinematic wave formulation closely approximates the complete hydraulic solution for these data.

Referring back to Equation [5], the experiments of Woolhiser and Liggett (6) have shown the kinematic solution in dimension less form to be,

$$Q_* = t_*^m \qquad [7]$$

where Q_* is discharge normalized by the rain rate

and t_* is time normalized by the time to equilibrium, t_e.

where

$$t_e = \frac{L}{V_o} \qquad [8]$$

There is a considerable amount of subjectivity in determining time to equilibrium from overland flow hydrographs. In an attempt to eliminate the subjectivity, it was found that the lag time, t_L, developed by Overton (4), the time lapse between occurrence of 50% of rainfall and 50% of runoff, was related to the time of equilibrium in Equation [8] simply as

$$t_e = 1.6t_L \qquad [9]$$

The 216 equilibrium hydrographs were all normalized by, t_L, and it was found essentially that a single rising dimensionless hydrograph existed. This was found earlier by the Corps of Engineers (7). The kinematic wave solution, both Chezy and Manning, are plotted against the observed dimensionless graph in Figure 2. The predicted time to equilibrium was precisely equal to the observed. The

Manning form of the solution was more accurate than the Chezy form, but large errors resulted in the early stage of rise of both models.

Hydrologic (Storage) Models

Horton (9) and Izzard (10) and others reviewed by Overton (1) have expressed storage or average detention in terms of discharge at the end of the overland flow plane as

$$S \propto Q^{1/m} \qquad [10]$$

According to Horton (9), the exponent m should be 5/3 for fully turbulent flow and 3 for laminar flow. Horton (9) arrived at the well known hyperbolic tangent model by assuming that the exponent was equal to 2. This was for "75% turbulent" flow.

Equation [10] can be normalized as

$$S_* = \frac{S}{S_\infty} = Q_*^{1/m} \qquad [11]$$

where S_∞ is the storage at equilibrium

Equation [11] is plotted for these values of m against the average storage-flow curve (observed) for the average rising hydrograph in Figure 3. The observed curve was calculated from the continuity equation. Equation [11] is actually an integrated kinematic wave model, and as shown in Figure 3, the fit to the storage-flow curve is poor.

The fact that the laminar model (m = 3) is much closer to the observed curve may indicate that laminar flow does exist at least in the early stages of rise. However, the Corps of Engineers (7) reported that laminar flow did not occur because of the impact of rain drops. Without a direct measurement of shear stress, resistance will remain an unknown, and all models will possess various degrees of empiricism and uncertainty.

In order to achieve a good fit to the observed storage-flow curve, it would be necessary to set m equal to about 5.

The resulting hydrograph distribution would be extremely bulky. To avoid this, a simple logarithmic function was used to fit the observed curve

$$S_* = B \ln [AQ_* + 1] \quad [12]$$

where A and B are constants and are related as

$$A = e^{1/B} - 1 \quad [13]$$

in order to match the end points of the curve. Combining Equation [12] with the continuity equation, this produced the rising hydrograph

$$Q_* = \left[1 + \frac{A+1}{2} e^{-\omega T} \operatorname{csch}(\omega T)\right]^{-1} \quad [14]$$

where $\omega = \frac{A+1}{2AB}$ [15]

and $T = t/t_L$ [16]

The Horton model is

$$Q_* = \tanh^a (T) \quad [17]$$

The B-value in Equation [14] was found by least squares best fit. Equations [14] and [17] are plotted versus the observed rising hydrograph in Figure 4.

A system of computations has been developed for synthesis of the most complex rain storm on a hillslope of varying slope, length and roughness. The synthesis was accomplished by convolution (lagging and summing unit responses) and through the concept of an equivalent plot. These concepts are developed in detail by Overton (1).

Convolution: This was easily accomplished when it was realized that the lag time for a plot is related to the intensity of rainfall. This relation followed the form shown for the example in Figure 5. Each point represents a lag time for an equilibrium hydrograph.

Equivalent Plot: This concept was developed in order to transmit hydrographs because of non-uniform rainfall and/or non-uniform slopes and roughnesses. Combining Equations [8] and [9] and expressing V_o in terms of the Manning formula

$$t_L = \frac{0.58}{i^{.4}} \left(\frac{nL}{\sqrt{S_o}} \right)^{0.6} \qquad [18]$$

where i is the rain intensity in inches per hour

and n is Manning's n-value

From Equation [18] it is seen how lag time varies with rain rate, length and slope of the plot, and the resistance coefficient. Using Equation [18], a hillslope shown in Figure 6 was transformed into an equivalent plot of equivalent length, l_{1P}', where l_1', l_2' etc. are equivalent lengths of each section. The equivalent plot would have a slope and n-value equal to that of the most down slope section (P). The equivalent lag time for entire plot at a given rain intensity was derived as

$$t_L\,(l_{1P}') = \frac{0.58}{i^{.4}} \left\{ \sum_{x=1}^{P} (nl/S_o^{\frac{1}{2}})_x \right\}^{0.6} \qquad [19]$$

Suppose now that rainfall occurred only on the uppermost section of the equivalent plot as shown in Figure 7. A scheme was developed to predict the routed hydrograph at the end of the plot.

If the rain had occurred uniformly over the plot, the total plot hydrograph could be expressed as

$$LqQ_*[L] = (L-x)qQ_*[L-x] + xqR[x] \qquad [20]$$

where R[x] is the dimensionless routed hydrograph. Equation [20] states that the total plot hydrograph is the sum of the hydrograph developed between x and L plus the hydrograph developed between 0 and x after it has flowed down (routed) to L. From Equation [20], the dimensionless routed hydrograph is

$$R[x] = \left(\frac{L}{x}\right) Q_*[L] - \left(\frac{L-x}{x}\right) Q_*[L-x] \qquad [21]$$

Since the hillslope has been converted to a uniform plot as shown in Figure 6, and lag time defined by Equation [19], the hydrograph functions $Q_*[L]$ and $Q_*[L-x]$ are defined by parameter in Equation [19] after inserting the proper lengths. The lag time corresponding to $Q_*[L]$ is Equation [19], and the lag time corresponding to $Q_*[L-x]$ would be

$$t_L(l_{1P}' - l_1') = \frac{0.58}{i^{.4}} \left\{ \sum_{x=2}^{P} (nl/S_o^{\frac{1}{2}}) \right\}^{0.6} \qquad [22]$$

After the section 1 hydrograph has been routed to P, then the section 2 hydrograph is routed to P, etc. A relation for the total hydrograph was developed in the main report and will not be shown here.

To illustrate the flexibility of this mathematical model and to demonstrate the type of output which can be produced, consider the hypothetical hillslope in Figure 8 with the associated rainfall pattern. Outputs were calculated for a stationary storm (uniform), for the storm moving upslope and then downslope at 3 miles per hour. The results of these outputs are shown in Figure 9. These outputs compare favorably with the outputs from Chow's watershed model, (11).

This hydrologic model of overland flow is accurate, flexible and involves the least number of computations of any existing hydraulic or hydrologic model. Detail comparisons of accuracy and computational load were made by Overton (1).

CHANNEL FLOW

The concern here is to develop criteria for use of approximations of the momentum equation. The work of Woolhiser and Liggett (6) would also apply theoretically to a wide rectangular channel. And at this point, their criteria for simplification will be used.

Hydrologic Models

Linear models: The Muskingum method, developed by McCarthy (12), has had considerable appeal because it has been thought to account for a wave action or wedge storage. The basis of the method is that total storage in a stream reach can be related to a weighted sum of inflow and outflow as

$$S = K[XI + (1-X)O] \qquad [23]$$

where I is inflow at head of reach
O is outflow at end of reach
and X is the weighting factor
K is the reach travel time

For the special case of X=0

$$S = KO \qquad [24]$$

which is a single reservoir effect.

Cunge (13) has shown that a routing equation in the form of the Muskingum routing method results from a numerical solution of the classical heat flow and diffusion equations. He concluded that a wave action results in routing due to an error in the numerical solution, since no wave action occurs in diffusion. In independent studies by Overton (3,1) it was shown explicitly that the Muskingum method is an implicit finite difference solution of a linear channel. It was also shown that a linear channel is a diffusive process; no wave action occurs.

A linear channel, as suggested by Dooge (14), is where the stage or area-discharge relation is linear, but the coefficient in the relation could be linear with distance along the channel. The coefficient would of course be the velocity.

$$Q = V(x)A \qquad [25]$$

It was shown that

$$V(x) = \frac{L}{2KX} \left[\left(\frac{2X-1}{1-X} \right) \left(\frac{x}{L} \right) + 1 \right] \qquad [26]$$

where x is the distance from the head of the reach

and L is the length of the reach

Combining this with the continuity equation results in

$$\frac{\partial Q}{\partial x} + \frac{1}{V(x)} \frac{\partial Q}{\partial t} = 0 \qquad [27]$$

There are three solutions to Equation [27] depending upon the value of X. For X=0, and 1, steady flow is the case; velocity approaches an infinite value and therefore the flow area approaches zero. Translation occurs only for X=0.5. However, the solutions do not involve a wave action.

Although Cunge's (13) explanation for the wave action is certainly valid, it can be explained another way. The solutions to the diffusion equation will only match certain boundary conditions. There is no solution of Equation [27] for all boundary conditions. By solving the problem numerically, a wave can be routed, but because of the underlying assumptions of heat flow it should be appreciated that the routing method "works" because of errors and inconsistencies in the solution.

Non linear models: The well known Puls or Storage-indication method is really a kinematic wave model. The end areas are established by Manning's formula or by back-water computations. The flood is routed using the continuity equation and the average storage-flow relation for the reach is calculated from the rating curves upstream and downstream. The use of this method creates a number of complications and makes necessary the development of new coefficients in order to obtain good fits to the downstream hydrograph (15,16).

If this type method is to be used, it would seem much simpler to use the kinematic wave model directly. The only parameter to be estimated is Manning's -n.

A WATERSHED SURFACE RUNOFF MODEL

The kinematic wave formulation has been used by Henderson and Wooding (5), and Liggett (17) to develop a surface runoff model for V-shaped watersheds. Using the concept of lag time developed above, Overton and Brakensiek (2) applied the kinematic wave to an ARS watershed, Hastings, Nebraska, W-3. The watershed, 481 acres, was schematized as shown in Figure 10. For a steady-uniform rain rate of v_o, the overland flow and channel flow hydrographs are shown in Figure 11, where t_{eo} is the time to equilibrium of overland flow and T_{eq} is the time to equilibrium of the watershed. Overland flow is the lateral inflow to the channel.

The solution was presented in general dimensionless form as shown in Figure 12. The parameter u_* is the ratio of time to equilibrium of overland flow to the time to equilibrium of the watershed. As $u_* \rightarrow 0$ all of the lagging is due to channel flow; as $u_* \rightarrow 1$ all of the lagging is due to overland flow. The broken line represents the watershed discharge for all values of t_{eo}.

For

$0 \leq t \leq t_{eo}$ the hydrograph is below the dashed line

$t_{eo} \leq t \leq T_{eq}$ the hydrograph is above the dashed line

If the overland flow plane was represented as the three section hillslope as shown in Figure 8 rather than a single uniform plane, the hillslope can be transformed into an equivalent plot. Therefore, the solution shown in Figure 12 is extremely general.

OPTIMIZATION, SENSITIVITY AND ERROR ANALYSIS

If any of these concepts were to be incorporated into a comprehensive model of hydrologic performance of an agricultural watershed, it would, of course, not be a matter of merely plugging in the model and estimating a Manning n-value. Obviously, the models will be used under conditions for which they were not derived. Usually, only rainfall and runoff are available to evaluate watershed models. This means that no data is available to verify the overland and channel flow components of the total model. In short, the data is not complete enough to verify that overland flow even occurs. However, in the optimization procedure the estimated Manning n - value could be used as a trial value. Also, the watershed could be transformed into the simple schematic of Figure 10, and the ratio of overland flow equilibrium time to watershed equilibrium time could be calculated. If the ratio is nearly zero, then overland flow computations are not necessary and rainfall excess could be dumped directly into the channel for stream routing.

The existence of the solution shown in Figure 12 also permits a preliminary error analysis. The solution is within the confines of the ratio of equilibrium times between zero and one. Therefore, the maximum error in the watershed hydrograph due to errors in averaging geometry and estimating roughness can be bracketed. In Figure 13, the maximum error relative to the expected value of the hydrograph for the Chezy solution is shown. The error curve for the Manning solution essentially coincided with the Chezy curve. As shown, the maximum error is 16% of the steady uniform rain rate.

For this system representation, errors in rainfall or rainfall excess are linear with errors in the dimensionless watershed hydrograph. This is true because superposition can be used in synthesis once the proper lag time is calculated for each rain intensity. Therefore, the model is much more sensitive to errors in rainfall than to errors induced by averaging hillslopes and roughness coefficients.

LITERATURE CITED

(1) Overton, D. E.
1969. Mathematical Models of Overland Flow. Unpublished report, 84 pg.

(2) _____ and Brakensiek, D. L.
1970. A Kinematic Model of Surface Runoff Response. To be presented at Internatl. Symposium on Representative and Experimental Basins, Wellington, N. Z., Dec. 1-8.

(3) _____
1970. Hydraulics of Linear Storage Routing. Unpublished report, 24 pp.

(4) _____
1970. Route or Convolute?, to be published in Water Resources Research, Feb. issue.

(5) Henderson, F. M. and Wooding, R. A.
1964. Overland Flow and Groundwater from a Steady Rainfall of Finite Duration, J. Geophys. Res., Vol. 69, No. 8, pg. 1531-1540.

(6) Woolhiser, D. A. and Liggett, J. A.
1967. Unsteady One-Dimensional Flow Over a Plane - The Rising Hydrograph, Water Res. Research, Vol. 3, No. 3, pg. 753-771.

(7) Corps of Engineers, U.S. Army
1954. Data Report, Airfield Drainage Investigation, Los Angeles District, Office of Chief of Engrs., Airfields Branch Engr. Div., Military Construction.

(8) Overton, D. E.
1967. Flow Retardance Coefficients for Selected Prismatic Channels. Trans Am. Soc. of Agric. Engrs., Vol. 10, No. 3, pg. 327-329.

(9) Horton, R. E.
1938. The Interpretation of Runoff Plot Experiments with Reference to Soil Erosion Problems. Soil Science Society of America Proceedings. Vol. 3, pg. 340-349.

(10) Izzard, C. F.
1946. Hydraulics of Runoff from Developed Surfaces. Proc. 26th Annual Meeting of Highway Res. Bd. Wash., D. C. pg. 129-150.

(11) Yen, B. C. and Chow, V. T.
1968. A Study of Surface Runoff Due to Moving Rainstorms. Civil Engr. Studies Hydraulic Engr. Series No. 17, Univ. of Illinois, Urbana, Ill.

(12) McCarthy, G. T.
1938. The Unit Hydrograph and Flood Routing. Unpublished paper, presented at a conference of North Atlantic Div. of Corps of Engrs. War Dept.

(13) Cunge, J. A.
1969. On the Subject of a Flood Propagation Method (Muskingum Method), J. Hydraulic Res. 7(2): 205-230.

(14) Dooge, J. C. I.
1959. A General Theory of the Unit Hydrograph. J. Geophys. Res. 64(2).

(15) Overton, D. E.
1966. Hydraulics in Synthesis of Upland Runoff Hydrographs 9(4): 543-549.

(16) Williams, J. R.
1969. Flood Routing with Variable Travel Time or Variable Storage Coefficients. Trans. Amer. Soc. of Agric. Engrs. 12(1): 100-103.

(17) Liggett, J. A.
1967. The Use of Shallow Water Equations in Runoff Computation. Proc. of the 3rd Annual Amer. Water Res. Conf., San Francisco, Calif.

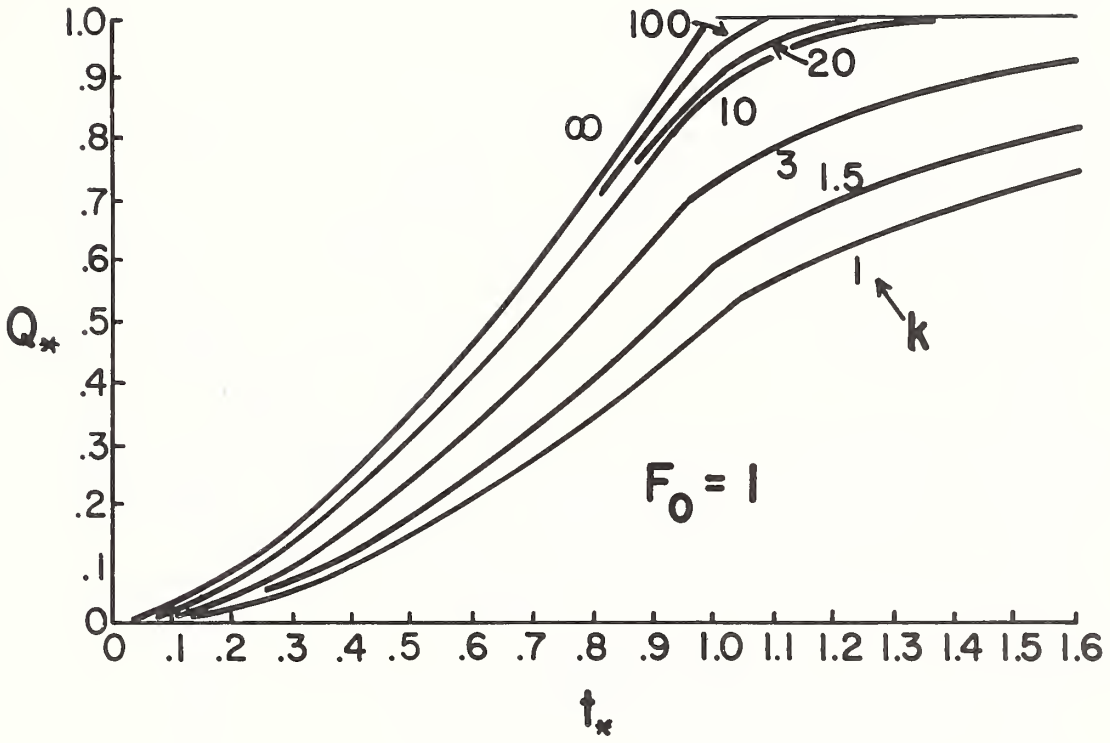

Figure 1. Results of the work of Woolhiser and Liggett.

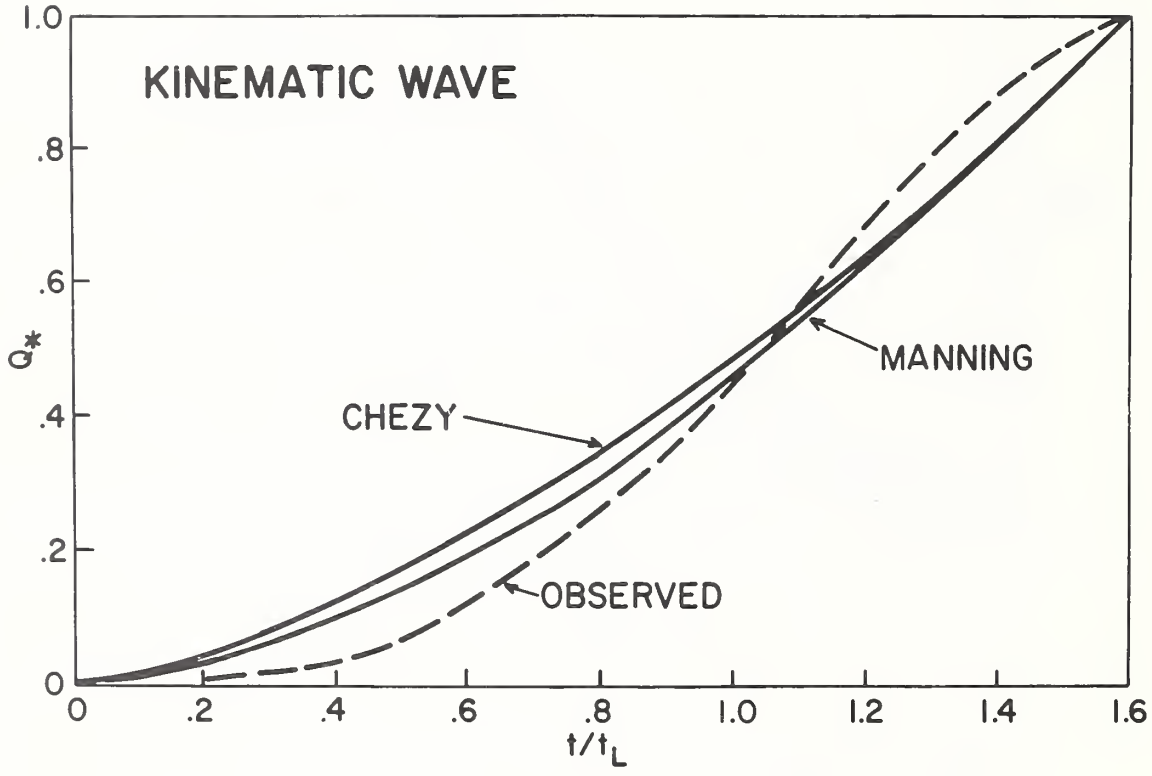

Figure 2. Kinematic Wave Solutions Versus the observed rising hydrograph.

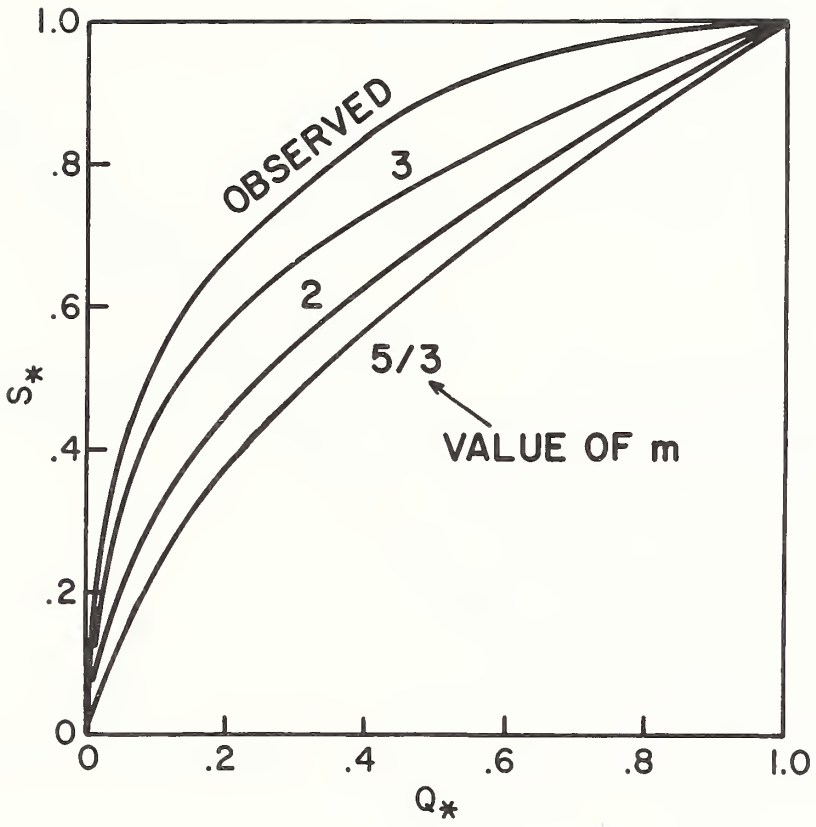

Figure 3. Equation [11] Plotted Versus the Observed Storage Flow Curve.

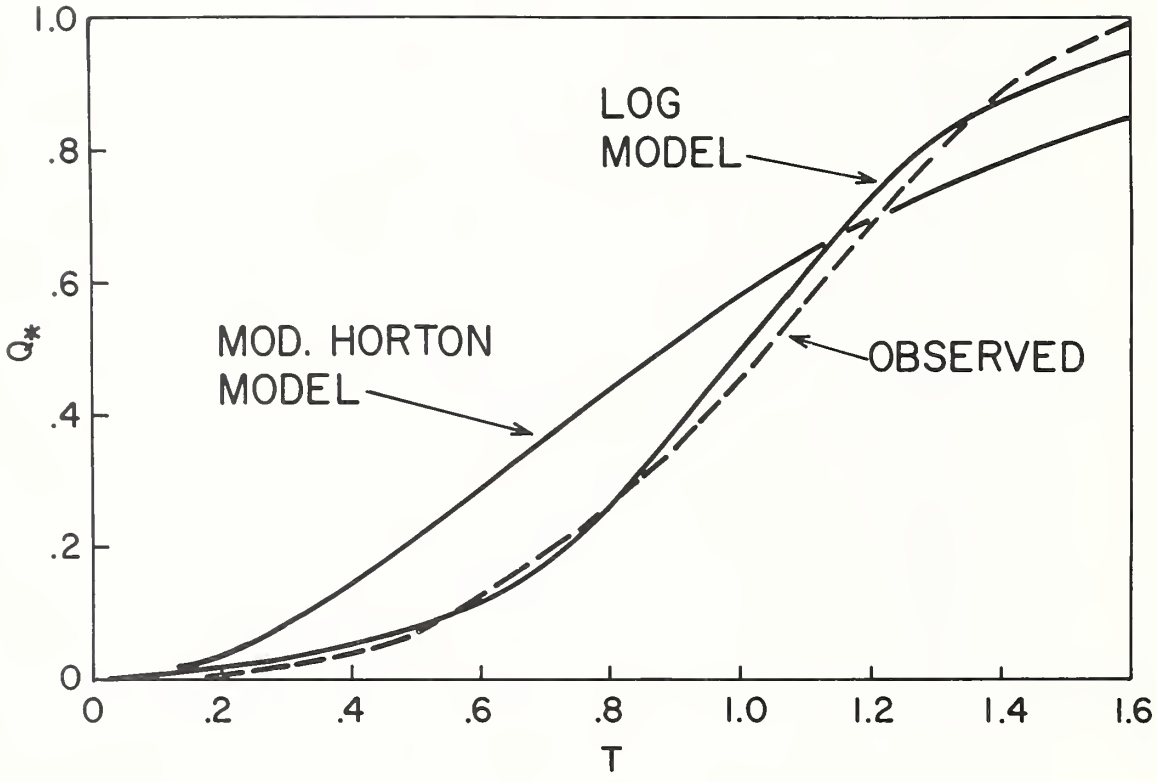

Figure 4. Log Model and Modified Horton Model Versus the Average Rising Hydrograph.

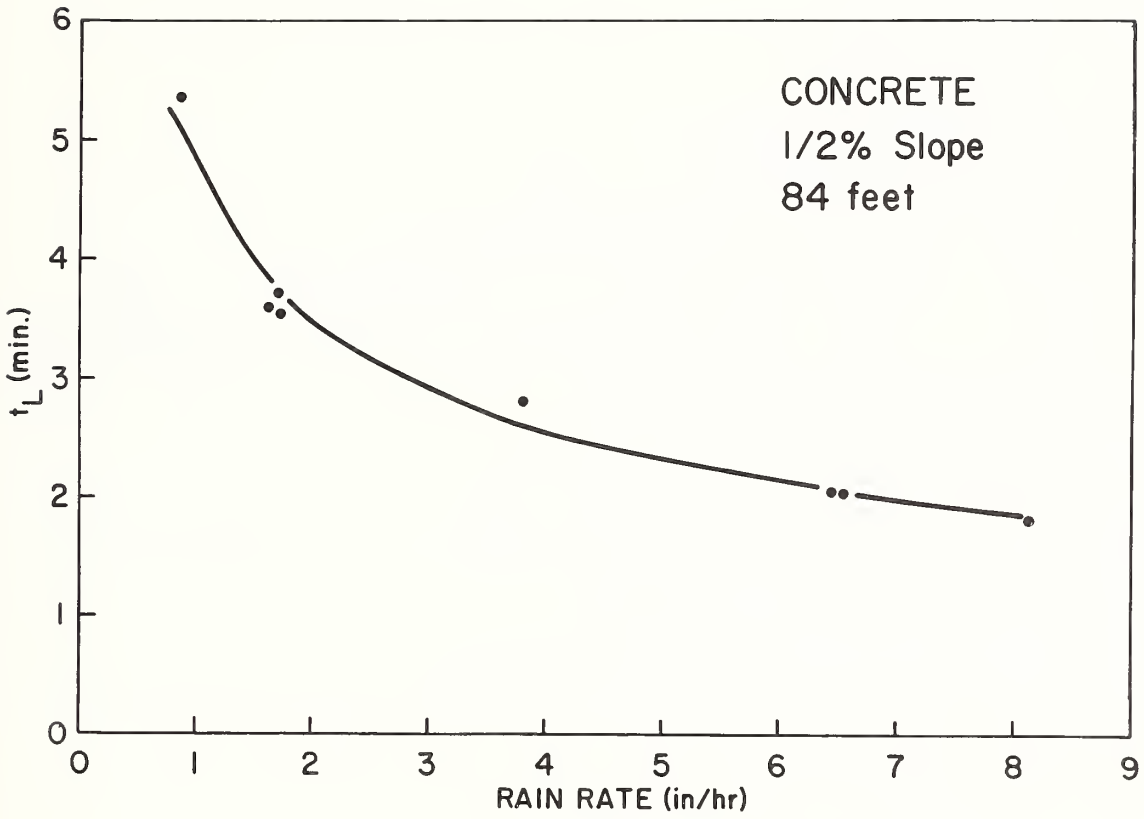

Figure 5. Variability of Lag Time with Rain Rate for a Concrete Plot.

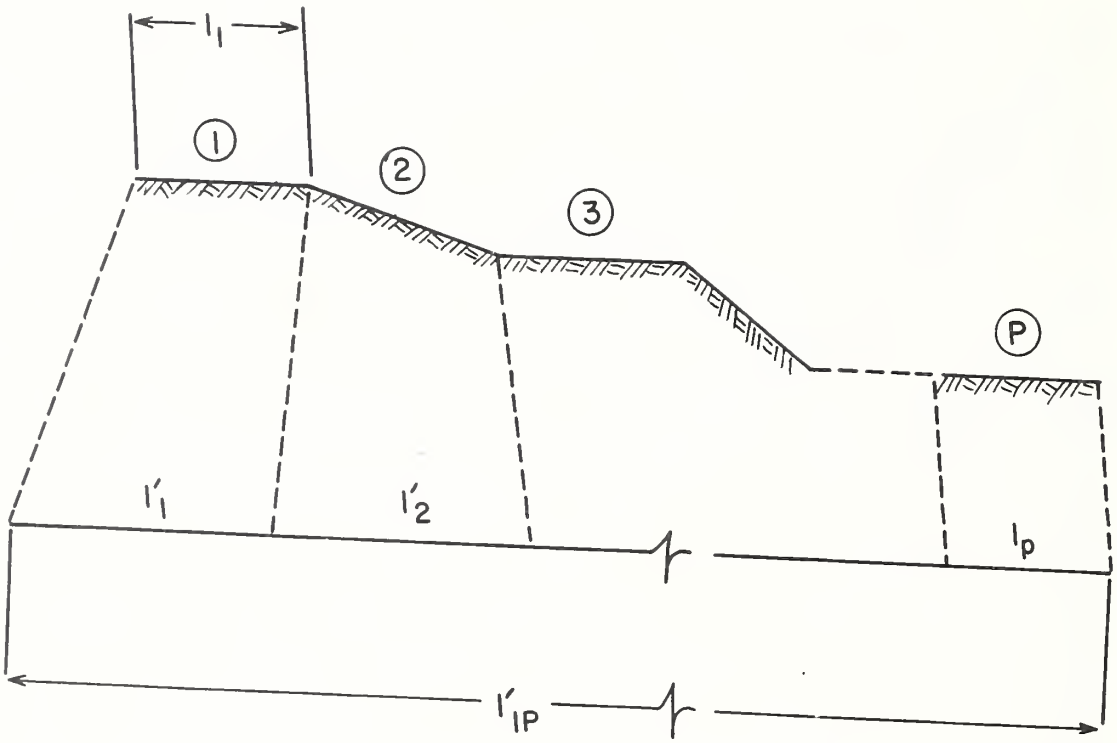

Figure 6. A Hypothetical Hillslope.

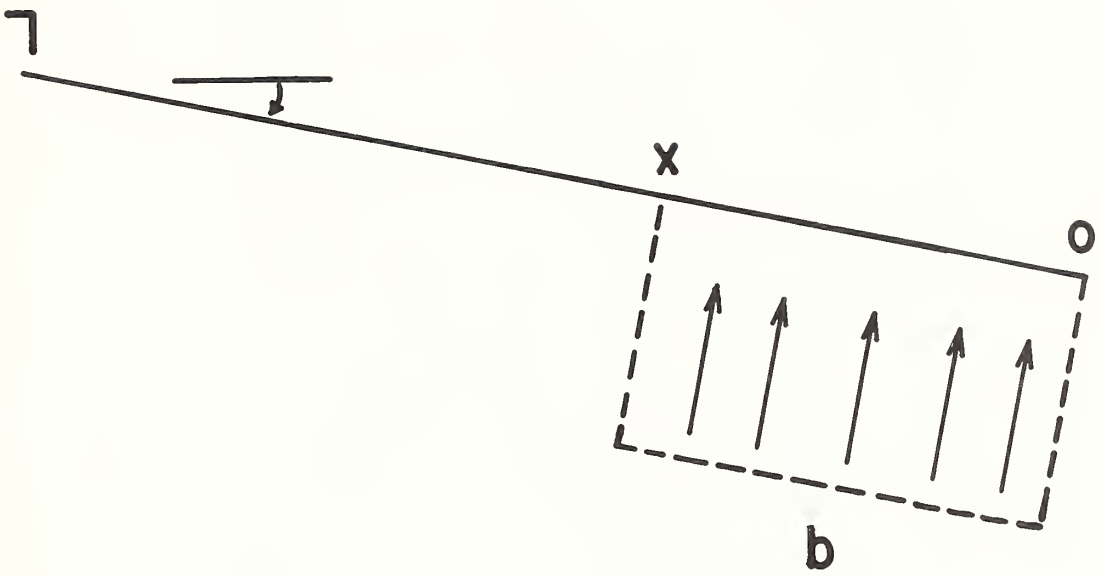

Figure 7. Rainfall Occurring only on Uppermost Section of Plot.

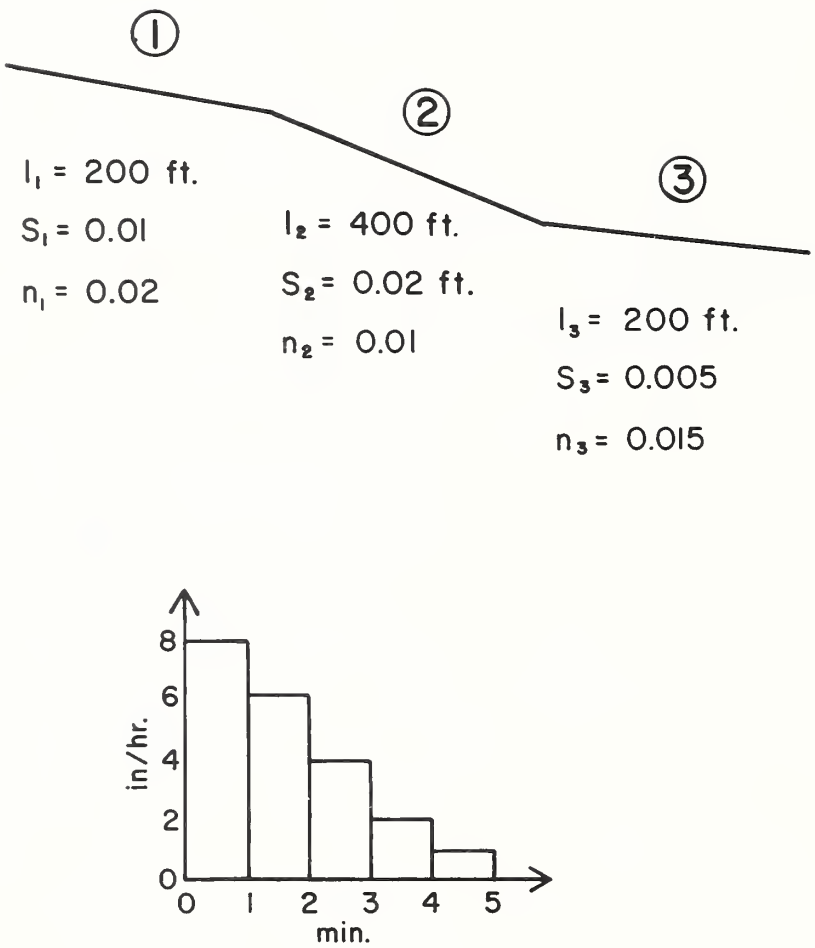

Figure 8. A Hypothetical Hillslope with Unsteady Rainfall.

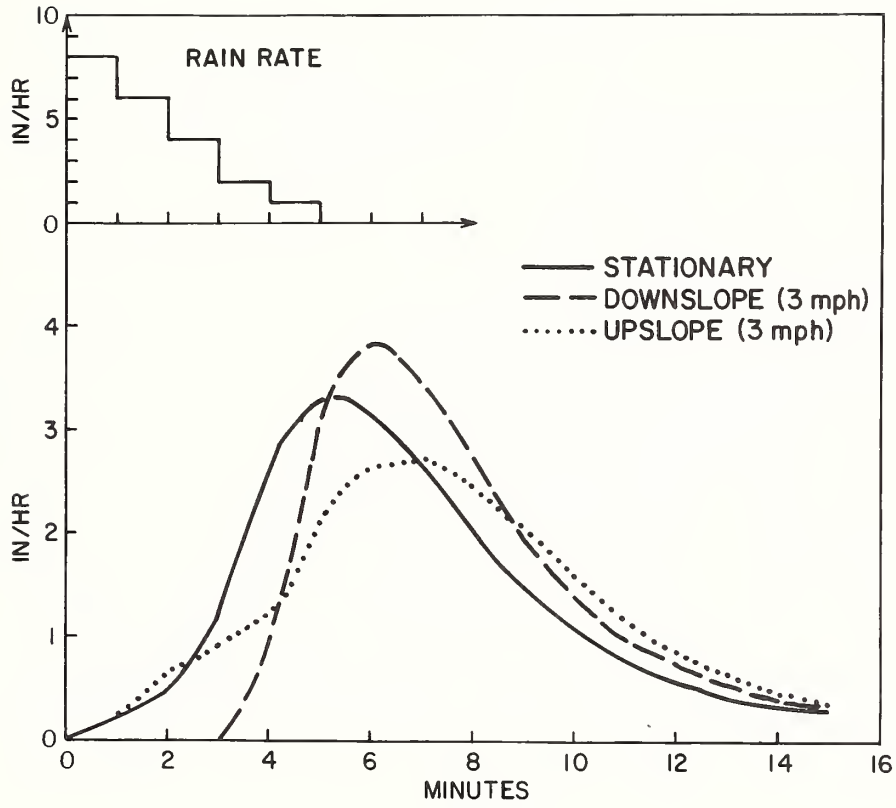

Figure 9. Output from Hillslope in Figure 8 with Stationary and Moving Rain Storms.

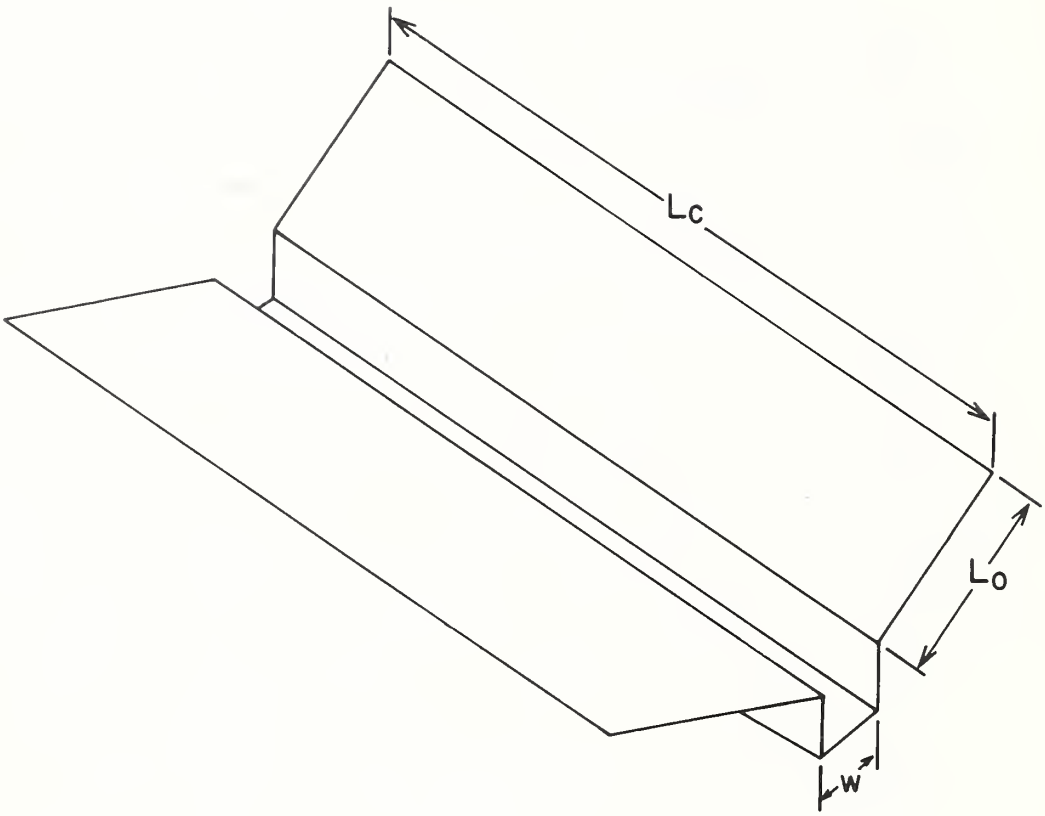

Figure 10. Schematic of Hastings W-3 (ARS).

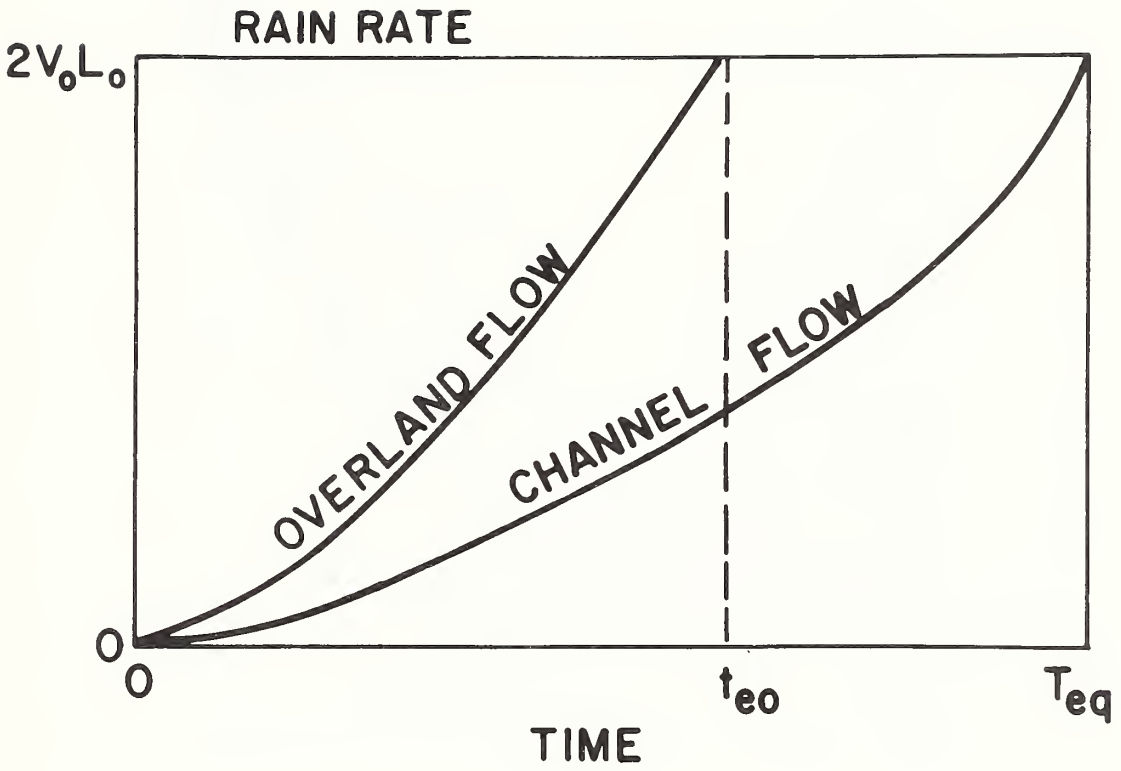

Figure 11. Output from Hastings W-3 for Steady Uniform Rain Rate.

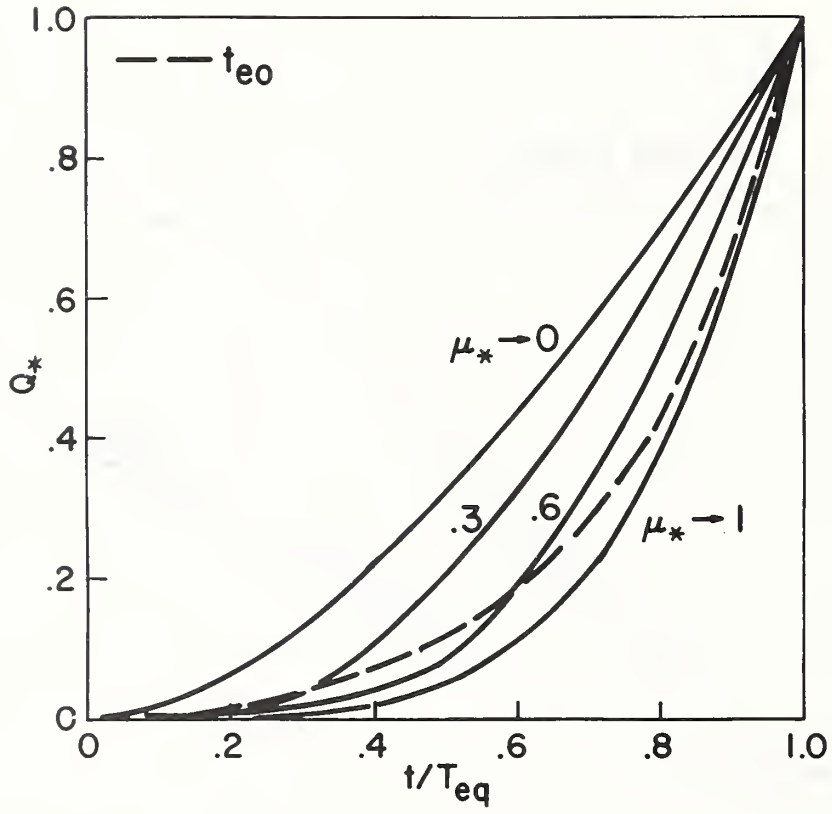

Figure 12. Generalized Dimensionless Kinematic Wave Solutions for Hastings W-3.

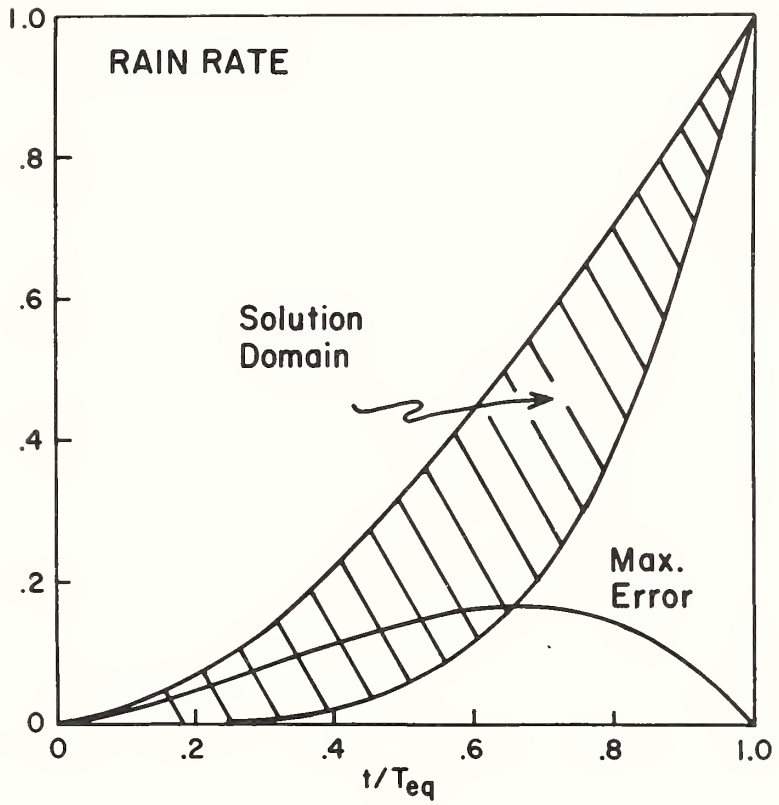

Figure 13. Solution Domain and Maximum Expected Error for Kinematic Formulation.